IDENTIFICATION AND PRE-CLINICAL DEVELOPMENT OF TUMOUR-REACTIVE T-CELL RECEPTORS FROM TUMOUR INFILTRATING LYMPHOCYTES

A thesis submitted to The University of Manchester for the degree of Doctor of Philosophy in the Faculty of Biology, Medicine and Health

2020

NATASHA L. OPPERMANS

SCHOOL OF MEDICINE, DIVISION OF CANCER SCIENCES

Table of Contents

Word count: 59957

List of Abbreviations

210M	gp100: 209-217
ACT	Adoptive cell therapy / Adoptive cell transfer
AICD	Activation-induced cell death
ALL	Acute lymphoblastic leukaemia
ANOVA	Analysis of variance
APC	Antigen-presenting cell
APC (antibody)	Allophycocyanin
CAR	Chimeric antigen receptor
CAPED	Cancer Antigen Peptide Database
CCL5	C-C motif chemokine ligand 5
CCR4	C-C motif chemokine receptor type 4
CCR5	C-C motif chemokine receptor type 5
CD	Cluster of differentiation
CD228	Melanotransferrin
cDNA	Complementary DNA
CDR3	Complementary determining region 3
CLL	Chronic lymphocytic leukaemia
CR	Complete response
CRISPR	Clustered Regularly Interspaced Short Palindromic Repeats
CST	Chronic sun damaged
CT	Cancer/testis
C_T	Cycle threshold
CTLA-4	Cytotoxic T-Lymphocyte Antigen 4
CXCL1	Chemokine (C-X-C motif) ligand 1
DMEM	Dulbecco's Modified Eagle Medium
DMSO	Dimethyl sulphoxide
DNA	Deoxyribonucleic acid
DOPA	3,4-dihydroxyphenylalanine
DR	Double responder

EBV	Epstein-Barr virus
ECM	Extracellular matrix
EDTA	Ethylenediaminetetraacetic acid
ELISA	Enzyme-linked immunosorbent assay
E: T	Effector: target
FACS	Fluorescence-activated cell sorting
FCS	Foetal Calf Serum
FDA	United States Food and Drug Administration
FITC	Fluorescein isothiocyanate
FMO	Fluorescence minus one
FOXp3	Forkhead box protein 3
Gal9	Galectin 9
GAPDH	Glyceraldehyde 3-phosphate dehydrogenase
GEM	Gel Bead-In Emulsion
GEX	Gene expression
GMP	Good manufacturing practice
Gp100	Glycoprotein 100
GRO-α	Growth-Regulated Oncogene-alpha
Gy	Gray
HEPES	4-(2-hydroxyethyl)-1-piperazineethanesulfonic acid
HLA	Human leukocyte antigen
HPV	Human papillomavirus
HRP	Horseradish peroxidase
HS	High sensitivity
IDO	Indoleamine 2,3-dioxygenase
IC50	Half maximal inhibitory concentration
ICOS	Inducible T-cell costimulator
IFNγ	Interferon gamma
IMDM	Iscove's Modified Dulbecco Media
IL-10	Interleukin 10

IL-12	Interleukin 12
IL-2	Interleukin 2
IP	Infusion product
IU	International Units
kDa	Kilodalton
LAG3	Lymphocyte activation gene 3
LAMP-1	Lysosomal-associated membrane protein 1
mAb	Monoclonal antibody
MAGE	Melanoma Antigen Gene protein
MAIT	Mucosal-associated invariant T-cells
MART-1	Melanoma-associated antigen recognized by T-cells 1
MCSP	Melanoma-associated Chondroitin Sulphate Proteoglycan
MFI	Mean fluorescence intensity
MHC	Major histocompatibility complex
MHRA	Medicine and Healthcare products Regulatory Agency
MIC	MHC class I chain-related protein
MR1	Major histocompatibility complex class I-related gene protein
mRNA	Messenger RNA
mTCR	Murine-constant TCR
NBC	Normal buffy coat
NHSBT	National Health Service Blood and Transplant
NK	Natural killer
NSCLC	Non-small cell lung cancer
NT	Non-transduced
NY-ESO-1	New York Esophageal Squamous Cell Carcinoma-1
ORR	Objective response rate
OSCC	Oesophageal squamous cell carcinoma
PBL	Peripheral blood lymphocytes

PBS	Phosphate-buffered saline
PBMC	Peripheral blood mononuclear cells
PCR	Polymerase chain reaction
PD	Progressive disease
PD-1	Programmed death protein 1
PD-L1	Programmed death protein ligand 1
PE	Phycoerythrin
PEF	Phosphate buffered saline, Ethylenediaminetetraacetic acid, Foetal calf serum
PerCP	Peridinin-Chlorophyll-protein
PFA	Paraformaldehyde
PHA	Phytohaemagglutinin
PI	Post-infusion
pMHC	peptide-MHC
PR	Partial response
P/S	Penicillin/Streptomycin
qRT-PCR	Quantitative real-time polymerase chain reaction
RACE	Rapid amplification of cDNA ends
RECIST	Response evaluation criteria in solid tumors
REP	Rapid expansion process
RIPA	Radioimmunoprecipitation assay
RNA	Ribonucleic acid
RPM	Revolutions per minute
scFv	Single-chain antibody fragment
SD	Stable disease
TAP	Transporter associated with antigen processing
TBI	Total body irradiation
TCR	T-cell receptor
TGFβ	Transforming growth factor beta
TIL	Tumour-infiltrating lymphocytes

TIM3	T-cell membrane protein 3
TMB	3,3',5,5'-Tetramethylbenzidine
TNF	Tumour necrosis factor
TRBV	T-cell receptor beta variable region
T-regs	T-regulatory cells
TU	Transforming Units
UV	Ultraviolet
Vβ	Variable beta region
V(D)J	Variable, (diversity), joining regions
WST-1	Water-soluble tetrazolium salt 1
WT1	Wilms Tumour 1

Patient tumour lines were labelled CTXM, for 'Cellular Therapeutics X Melanoma', where X refers to the type of tumour, e.g. C = cutaneous, A = acral, U = Uveal

All units of measurement are recognised by the International System of Units, unless stated otherwise.

List of figures

List of tables

Abstract

The past decade has seen many advances in the field of cancer immunotherapy, with increased research efforts into optimising adoptive cell therapies. This has been particularly successful in the setting of metastatic melanoma, where both TIL and TCR T-cell therapies have had promising clinical trial results. However, researchers are yet to fully elucidate the reactivity profile of TIL products, and best identify and characterise the tumour-reactive portion of TIL. In the work for this PhD thesis, several different models were explored to best identify the tumour-reactive population within final melanoma TIL products. Through optimisation, a model was chosen where final TIL was co-cultured with autologous patient-derived tumour cell lines and CD137 was selected as a marker of tumour-reactivity to isolate and characterise the tumour-reactive TCRs. Through this approach, several TCRs were identified and a few were chosen for validation, which indicated they were HLA-A*0201-restricted, melanoma-reactive TCRs.

In the second part of the project, pre-clinical validation of gp100-reactive TCRs isolated from a single patient TIL product was conducted in a series of flow-cytometry based assays. Through using different model systems to validate and compare the TCRs, an optimal candidate gp100 TCR was identified. This TCR was then directly compared to a control TCR originally isolated from a transgenic mouse model and previously used in gp100 TCR T-cell therapy in the clinic. Comparison with the TIL-derived gp100 TCR showed the two TCRs were comparable with regards to tumour-reactivity in the CD8+ T-cell population, however the TIL-derived TCR was considerably less cross-reactive than the control TCR.

Collectively, the work in this PhD thesis demonstrates the safety benefit that TIL-derived TCRs can confer, while proposing an optimised model of identifying and pre-clinically validating tumour-reactive TCRs from TIL products.

Declaration

I, Natasha L. Oppermans, declare that no portion of the work referred to in the thesis has been submitted in support of an application for another degree or qualification of this or any other university or other institute of learning.

Copyright statement

Acknowledgements

First of all, I would like to thank the MRC and EPSRC for funding my PhD studentship, and the leaders of the Regenerative CDT PhD programme for giving me the opportunity to carry out this work. I would also like to acknowledge Instil Bio UK for welcoming me into the company and supporting me throughout my PhD.

On that note, a special acknowledgement goes to my supervisor Dr. John Bridgeman. John has given me the perfect balance between helping me understand TIL and TCR therapies, whilst also encouraging me to think for myself and answer my own questions. More than being a fantastic supervisor, he has been a true friend to me over the last four years. I will sorely miss our morning catch ups, especially now I have perfected how he likes his tea!

Another special acknowledgement goes out to my family and friends, who have been really supportive throughout my PhD. My parents in particular have even tried to understand what it is I have been working on and always asked after my 'cell-babies' and asked how my experiments were going.

Finally, I want to acknowledge and thank my husband for all his support throughout these last four years, especially in the last six months when the world as we know it has been turned upside down. He has been there for me through all the highs and lows, and even let me plan and have a wedding whilst doing my PhD, which many people have called me crazy for.

Preface

The author of this thesis, Natasha Oppermans, achieved a BSc in Biomedical Science from Durham University in 2015, before being awarded an MRC scholarship for an MRes in Biomedical Research in the Personalised Healthcare stream at Imperial College London. This consisted of two 5-month research projects, one with Dr. Simak Ali and the other with Dr. Vania Braga. After this MRes, she was awarded an MRC and EPSRC-funded PhD studentship on the Regenerative Medicine CDT programme, which started in 2016, the work for which is presented in this PhD thesis.

1.0 Introduction

1.1 The Origins of Cancer

Cancer arises when a healthy cell in the body undergoes irreversible changes through accumulation of genomic aberrations, which leads to a malignant phenotype. This cancer phenotype has been defined by the six hallmarks of cancer that lead to tumour development; these are i) evading growth suppressors, ii) sustaining proliferative signalling, iii) resisting cell death, iv) enabling replicative immortality, v) inducing angiogenesis, and iv) activating invasion and metastasis (Hanahan and Weinberg, 2011). These changes often arise from mutations in multiple different signalling pathways, that when under tight control allow the cell to carry out its normal function, but when dysregulated, become a catalyst for further downstream changes. It is the gradual accumulation of these changes and dysregulation that leads to a cell becoming cancerous and the initiation of tumour formation.

Different types of cancer are typically named after the cell of origin. For example, melanoma cells begin life as melanocytes, which are skin cells responsible for producing the pigment melanin and are found at the basal epithelium of skin, at a ratio of roughly one melanocyte to every five keratinocytes (Haass et al., 2005). Cancerous changes can arise by multiple mechanisms, all ultimately leading to deoxyribonucleic acid (DNA) damage. Examples of these mechanisms include radiation-inducing ultraviolet (UV) rays, carcinogens such as asbestos and spontaneous DNA mutation. Cells have inbuilt mechanisms to either prevent or repair DNA damage, or to induce cell suicide known as apoptosis if the damage is irreparable (Lowe and Lin, 2000). However, if DNA becomes damaged in such a way that the cell cannot repair or kill itself, the cell may progress to a cancerous phenotype. Some genomic aberrations also appear to be invisible to control by the checkpoint proteins, which are responsible for making sure the cell does not multiply if it is unhealthy (Smith et al., 2007). If cell cycle arrest is not observed, the resulting uncontrolled cell division allows the rapid build-up of cancerous cells and the development of a cell mass known as a tumour.

1.1.1 Tumour development and metastasis

Other inherent changes in the cancer cell allow the cell to transform from a typically epithelial phenotype, to a mesenchymal phenotype, a process known as epithelial-mesenchymal transition (Seyfried and Huysentruyt, 2013). These changes include loss of cell-cell adhesion molecules, such as E-cadherin, and cell-matrix interactions, which results in the cancer cell being able to intravasate into the lymphatic system or blood stream to migrate to different parts of the body. After travelling to another part of the body, the cell then extravasates and transitions back to an epithelial phenotype, where it can replicate to establish a secondary tumour. This whole process is known as metastasis, and the secondary tumour is also termed a metastasis. The secondary tumour is named after the original tumour origin, as the tumour cell type is inherently the same as the primary tumour type. For example, if a melanoma cell metastasises to the liver and establishes a secondary tumour there, the metastasis is still classed as melanoma, as opposed to liver cancer. Tumours can be graded in many ways, with the TNM grading system being the most widely used (Sobin, Gospodarowicz, and Wittekind, 2017); The 'T' refers to primary tumour size and progression, 'N' refers to the spread of cancerous cells to local lymph nodes, and the 'M' refers to the metastatic status of the cancer. For ease of use, these classifications can be further grouped into stages 0 through to 4, with stage 0 describing carcinoma in situ (localised, abnormal cells), and stage 4 signifying that the cancer has metastasised to distant locations in the body. Common locations of tumour metastases include the lymph nodes, where up to 50 % of cancer metastases are found, as well as lungs, liver, bone and brain (Meier et al., 2002; Zbytek et al., 2008).

As a tumour forms and develops, other structures are laid down by the cancer cells to support the growing tumour, such as extracellular matrix (ECM) structures and blood vessels (Hanahan and Weinberg, 2011). In healthy tissue, the role of the ECM is to provide biophysical support, as well as utilise biochemical signals to maintain tissue homeostasis (Mammoto and Ingber, 2010). This is also the case in tumours, and the deposition of cancer-associated ECM is an integral part of tumour development. Normally, the ECM is actively remodelled to tightly control the tissue it supports and allow for controlled development. Tumours are known to undergo desmoplasia, a process by which there is increased deposition of ECM proteins, which leads to a highly

fibrotic, disorganised structure; this deregulation of ECM generation and remodelling is a key factor in tumour growth and behaviour (Pickup, Mouw and Weaver, 2014). Much like normal tissues, tumours also require various nutrients to facilitate cell growth, as well as a way of exchanging critical gases oxygen and carbon dioxide. By producing new blood vessels in a process known as angiogenesis, the tumour can draw blood from the normal vasculature system, to facilitate continued expansion of the tumour.

1.1.2 Cancer and the immune system

In addition to tumour cells and tumour-associated ECM, cells of the immune system can be found inside some tumours (Gajewski, Schreiber and Fu, 2013). These cells are likely to be able to infiltrate the tumour from the new vasculature formed that connects the tumour to the body. The immune infiltration of tumours is likely a response of the immune system to phenotypic changes and acquisition of genomic aberrations induced by the hallmarks of cancer, described above. The immune system can be separated into adaptive immunity and innate immunity. While innate immunity is the first line of defence against harmful pathogens, the response is generally non-specific, immediate and short-lasting. Innate immunity is commonly associated with response to injury and the process of inflammation. It has been observed that tumour-associated chronic inflammation can support tumorigenesis and in certain cancers such as gastric and colon cancers, can indicate a bad prognosis (Pagès et al., 2010). Conversely, the presence of cells from the adaptive immune system can be associated with a good prognosis for some cancers, such as has been shown in oesophageal squamous cell carcinoma (Sudo et al., 2017). While tumour cells have developed some mechanisms to avoid detection and elimination by the immune system, which will be discussed further in this chapter, the presence of immune cells in tumours underpins a new branch of cancer treatment known as immunotherapy. Before this is described in more detail, a basic understanding of the adaptive immune system and the key characteristics which can be utilised to target cancer cells for destruction should be explored.

1.2 The adaptive immune system and the anti-cancer response

1.2.1 Adaptive immunity

The adaptive immune system is comprised of T-cells and B-cells, which recognise foreign cells invading the body. Foreign cells are typically detected by the presence of tumour antigens, which can be recognised directly on the surface of tumour cells or as short, processed peptide regions, or epitopes, presented by antigen-presenting cells (APCs) (Murphy, 2012). APCs have the ability to engulf pathogens or tumour cells and digest them to create the fragments for presentation to other immune cells. T-cells of the adaptive immune system are capable of recognising these presented antigens through protein complexes embedded in the T-cell membrane, which are called T-cell receptors (TCRs). In humans, the majority of TCRs can only recognise the antigen if it is processed and presented properly, often in the context of the human leukocyte antigen (HLA) complex, encoded by the major histocompatibility complex (MHC) genes. Once a T-cell encounters the specific antigen it recognises, also known as its cognate antigen, it is stimulated to proliferate and differentiate into an effector T cell, whose functions vary depending on the variety of T-cell, but generally promote or carry out pathogen removal.

T-cell development occurs in a lymphoid organ known as the thymus, where naïve T-cells are exposed to millions of different 'self' antigens, which would normally be expressed by healthy cells, to prime the T-cell population. Typically, if a T-cell shows reactivity to a native, self-antigen while it is in the thymus, it is deleted in a process known as thymic selection, a key aspect of central tolerance (Murphy, 2012). This occurs in order to prevent T-cells from attacking and destroying healthy tissues, which can be described as an auto-immune response. The resulting T-cell repertoire is honed towards recognising foreign antigens that could be residing in peripheral lymphoid tissues in the body (Marrack et al., 1988). When a naïve T-cell first comes into contact with its cognate antigen through peptide-MHC-TCR interaction, the T-cell differentiates into different T-cell types with identical antigen specificity to the original T-cell (Murphy, 2012). Two subset of T-cells that can be formed are central memory T-cells, which reside in the secondary lymphoid organs, and effector memory T-cells, which remain at the site of antigenic stimulation (Golubovskaya and Wu, 2016). Upon re-exposure to the antigen at a later date, the memory T-cells facilitate a rapid, vast

response by expanding into effector T cell clones which are able to elicit a variety of different effector responses.

There are various types of T-cells that carry out effector responses. These are broadly categorised as cytotoxic T-cells, T-helper cells and T-regulatory cells (T-regs), which all have different actions which shape the immune response to a given situation. T-cells can be categorised by the cell-surface markers they possess, and can be sorted into different populations *in vitro* based on marker expression. CD8 is a glycoprotein that acts as a marker of cytotoxic T-cells, which can induce cell death of target cells by releasing specific cytotoxins and cytokines. CD4 is a glycoprotein which is generally associated with T-cells that exhibit helper functions, including supporting the expansion of CD8 cytotoxic T-cells (Hwang, Lukens and Bullock, 2007). Most importantly, CD4 and CD8 are both co-receptors for peptide-MHC (pMHC) interactions, with CD8 and CD4 recognising MHC class I and MHC class II molecules respectively (Gao, Rao and Bell, 2002). T-regs are a subpopulation of T-cells that are typically identified by elevated CD25 expression and other markers such as forkhead box P3 (FoxP3) or interleukin 10 (IL-10) (Zou, 2006; Curiel, 2008). In normal immunity, they are produced either by the thymus to circulate the body, or through T-cell conversion in the peripheral blood (Zou, 2006). T-regs have a leading role in peripheral tolerance to help prevent autoimmune reactions from occurring.

Scientific groups are constantly attempting to use different cell-surface markers to characterise potentially important cell populations. For example, when tumours are dissected, a heterogenous population of T-cells can be found, which have infiltrated the tumour. By identifying the cell types present in these populations, it gives vital information regarding the attempted immune response that the body mounts in response to cancer, and how best to utilise these cells to destroy the cancerous tissues.

1.2.2 T-cell Receptors

T-cells can be broadly classified depending on the type of TCR they possess. TCRs are heterodimers comprising of two transmembrane glycoproteins, with 90 % of TCRs consisting of an α and a β chain (known as αβ TCRs), and a minority being made of

alternative polypeptides referred to as γ and δ chains (known as γδ TCRs) (Davis and Bjorkman, 1988). The genetic components of αβ TCRs can be described by a variable (V) region, diversity (D) region, joining (J) region and a constant (C) region. It is the splicing and rearrangement of these corresponding gene segments that generates a substantial repertoire of potential TCRs (Garcia et al., 2010). Each TCR expressed by T-cells is capable of recognising a specific antigen, typically presented by as a pMHC complex. Over the years, the crystal structures of several pMHC-TCR complexes have been resolved, increasing our knowledge of the components involved in this interaction. As shown in figure 1.1, the α and β chains of the receptor are linked by a disulphide bridge, originating from a cysteine residue in the short stalk region of each chain, which extends across the plasma membrane and ends as a short, cytoplasmic tail (Murphy, 2012; Wucherpfennigs et al., 2010). In addition, the TCR complex also contains CD3 chains, which typically consist of δ, ε, γ, and ζ subunits, and the presence of these subunits is crucial for signal transduction and surface receptor stability at the plasma membrane (Rudolph, Stanfield and Wilson, 2006).

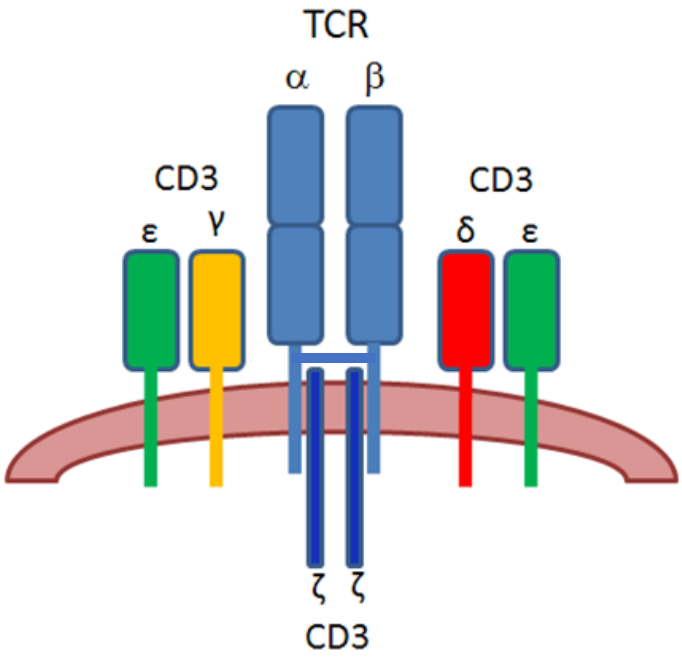

Figure 1.1. T-cell Receptor. Diagram demonstrating the structure of a typical αβ TCR. Blue units represent the variable and constant domains of the alpha and beta chains, linked by a disulphide bridge. Green units represent the epsilon subunits of the CD3 chains, which are completed with a gamma subunit (yellow unit) or delta subunit (red unit), and intracellular zeta subunits. Adapted from Lin et al., 2015.

1.2.3 T-cell co-receptors

For an optimal T-cell response mediated through TCR-pMHC interaction, the engagement of different co-receptors is required. The most noteworthy, CD4 and CD8, have been studied extensively to elucidate their role in the T-cell response and it has been found that the CD8 and CD4 co-receptors bind to invariant regions of MHC class I and MHC class II, respectively (Bridgeman et al., 2011). The co-receptors help to stabilise the TCR-pMHC complex, as well as contributing to initiation of signalling cascades by recruiting protein tyrosine kinases such as Lck to the immunological synapse. After this initial binding event, there is further interaction between the T-cell and APC through other receptors associated with co-stimulation and adhesion, notably CD2, CD28, CD58 and CD80. This additional binding encourages multiple signalling cascades to be initiated and also prolongs the contact and therefore the activation of

the T-cell. For an effective T-cell response, T-cells respond to co-stimulatory signals produced by antigen-presenting cells. This includes the binding of ligands B7-1 (CD80) and B7-2 (CD86), whose cognate receptor CD28 can be found on T-cells, and this binding induces signalling cascades that increase interleukin 2 (IL-2) production and stimulate proliferation in activated T-cells (Driessens, Kline and Gajewski, 2009). In the cancer setting, tumour cells do not typically present co-stimulatory ligands, however they do present tumour-associated antigens via MHC molecules.

To understand the role of T-cells in an anti-cancer response, it is important to consider how T-cells can detect cancer cells, the process by which they infiltrate the tumour and ultimately, how this leads to cancer cell elimination, which shall be covered in the rest of this chapter.

1.3 The Immune Response to Cancer

It is well documented in a variety of solid cancer types, such as pancreatic, melanoma and gastric cancers, that immune infiltration correlates positively with prolonged survival (Nakakubo et al., 2003; Erdag et al., 2012; Ino et al., 2013; Kim et al., 2016). The degree of this correlation and whether it can be used to predict overall survival has been investigated in greater detail for a few immunogenic cancers, such as colorectal cancer (Galón et al., 2006). After several years of validation and comparison with current tumour staging and prognostic methods, the degree of immune cell infiltration has shown to be a better prognostic factor than current methods such as microsatellite instability for some cancers (Galón et al., 2014; Mlecnik et al., 2016).

In a review by Chen and Mellman, and illustrated in figure 1.2, the process by which an immune response can be raised against a tumour is described (Chen and Mellman, 2013). When tumours grow to a certain size, the inner cell mass of the tumour becomes necrotic and the cells die. This can be one of the triggers that cause tumour-specific antigens to be released into the surrounding microenvironment, which are digested and presented by APCs. As with other types of infection, naïve T-cells that recognise the presented antigen are stimulated to proliferate and migrate out of the lymph nodes and to the site of the tumour. When they extravasate at the tumour site, they can then recognise tumour cells presenting the specific antigen they are primed to respond to. Upon recognition of the tumour, the cytotoxic T-cells are further stimulated to proliferate and kill the tumour. Since the first stage of this process is the release of cancer antigens, the types of antigens recognised by tumour-reactive TCRs will be explored in the next section.

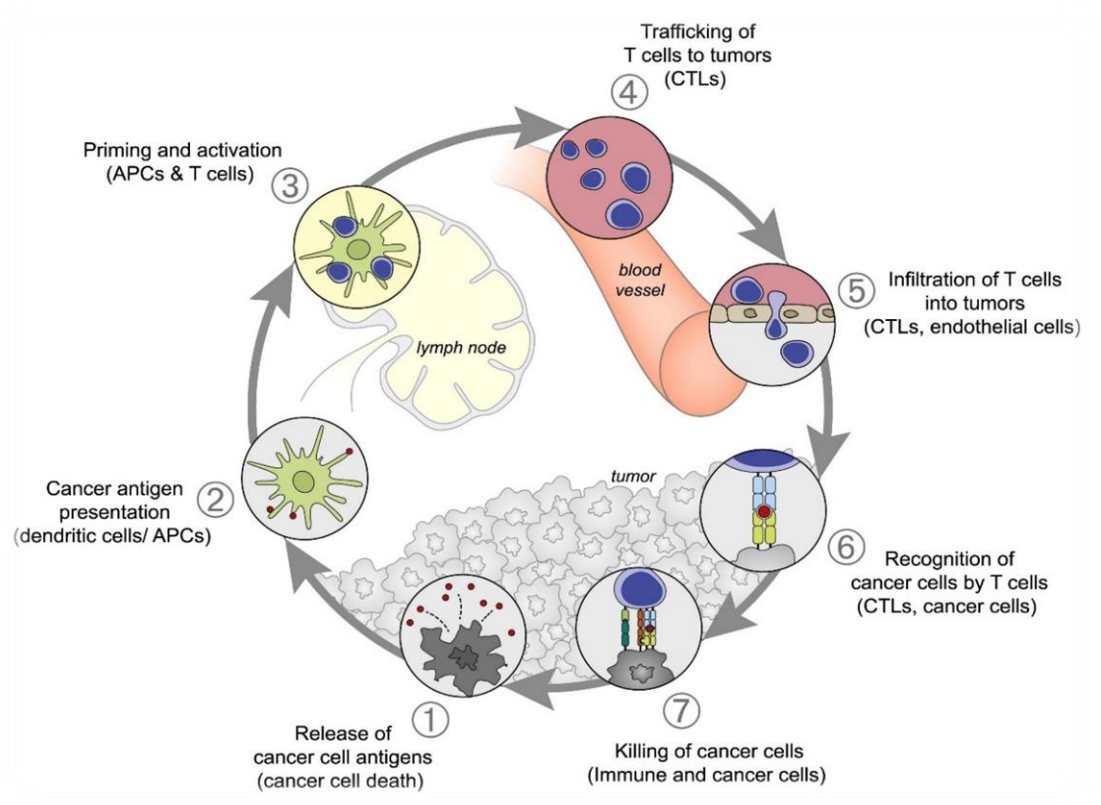

Figure 1.2. The immune response against cancer. Diagram illustrating the various stages of the immune response to a tumour. Stage 1 shows cancer antigen release after cancer cell death. Stage 2 shows the cancer antigen presentation by dendritic cells/APCs. Stage 3 shows the priming and activation of T-cells in the lymph node, which occurs following antigen presentation and trafficking of APCs to the lymph node. Stage 4 shows the trafficking of activated tumour-reactive T-cells to the tumour via the blood vessels. This is followed by stage 5 which shows the T-cell infiltration into the tumours from the blood vessels. Stage 6 illustrates the recognition of cancer cells by T-cells through the TCR complex. Lastly, stage 7 shows the killing of the cancer cells by the T-cells. Taken from Chen and Mellman, 2013.

1.3.1 Cancer peptides

Several different types of antigens can be found within tumours and are defined by the Cancer Antigen Peptide Database (CAPED) in the following categories: Unique, tumour-specific, differentiation, and over-expressed (CAPED, accessed on various dates in 2019-2020). These different categories are highlighted by figure 1.3, and described below.

Unique antigens, also commonly known as mutation or neoantigens, are tumour-specific antigens that are very rarely shared between patients, and tend to arise from

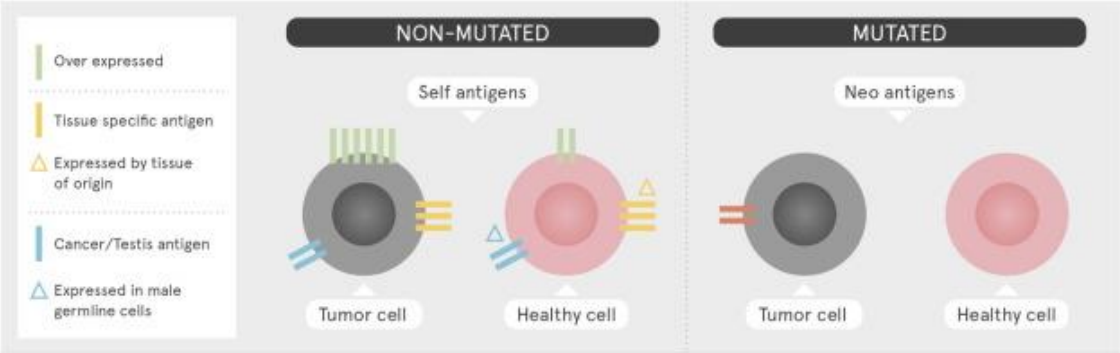

Figure 1.3. Cancer-associated antigens. Diagram depicting the different categories of cancer-associated antigens and their expression on mutated and non-mutated cells. Taken from Ophir et al., 2016.

mutations in the coding region of a gene (Lu and Robbins, 2016). They are widely considered to be the best immunotherapeutic targets with regard to the restriction of their expression, however since they are not commonly shared between patients, they are harder to identify and target. In order to identify neoantigens that are therapeutically relevant, extensive *in vitro* and *in silico* data using next-generation sequencing and mathematical modelling approaches are required (Nonomura et al., 2019). This makes the task possible but complex and expensive. Additionally, not all mutated peptides are ably presented by MHC molecules, with approximately 70 % of mutated self-antigens not being able to be presented, and therefore, not detectable by T-cells (Brown et al., 2019).

Shared tumour-specific antigens are the next most appealing antigen class to target, as they are defined as antigens that can be found across multiple patients, and cancer types, but are not normally found expressed by healthy tissue. A large group of antigens in this class are known as cancer-testis (CT) antigens, as their expression is restricted to cancer cells, and male germline cells. Since germline cells do not express MHC class I molecules, they cannot be targeted by cytotoxic TCR-presenting T-cells and are therefore protected against a potential autoimmune response. One CT antigen that has garnered a lot of interest in the field of immunotherapy is New York Esophageal Squamous Cell Carcinoma-1, commonly known as NY-ESO-1. Its popularity is warranted, as it is expressed across a wide range of cancer types, and this presence on tumours has been shown to be related to a correlating immune response (Thomas et al., 2018).

Differentiation antigens are a class of antigens typically expressed by tumour cells as well as the cell type the tumour originated from. The first tissue-specific antigen to be identified was the tyrosinase antigen, encoded by the gene for tyrosinase, a melanocyte-specific enzyme that catalyses 3,4-dihydroxyphenylalanine (DOPA) synthesis and a precursor for melanin (Brichard et al., 1993). In 1994, Kawakami et al. released two papers which described the identification of glycoprotein 100 (gp100), and Melanoma-associated antigen recognized by T-cells 1 (MART-1), as melanocyte-specific antigens that were also found in secondary tumours from a patient with metastatic melanoma (Kawakami et al., 1994a; Kawakami et al., 1994b). Whilst expression on tumour cells tends to be far greater than expression on healthy cells for this class of antigens, targeting them comes with the increased risk of an autoimmune reaction to healthy tissue. This group of antigens have seen a lot of therapeutic interest due to the high expression across target tumours, and between multiple patients of the same tumour type.

The final class of antigens is over-expressed antigens, which are typically found at low levels of a wide variety of healthy cells, as well as tumour cells. One example of antigen in this class is Wilms Tumour 1 (WT1), which is over-expressed in a range of different tumour types, making it an attractive pan-cancer therapeutic target (Inoue et al., 1997; Oji et al., 2002; Ueda et al., 2003). While the threshold level of expression for an immune response to be initiated against these antigens is often not reached in healthy tissues, they do carry the most risk for targeting compared with other antigens, as an autoimmune reaction could affect many different tissues throughout the body.

1.3.2 Thymic selection – an imperfect process

Immune cells that recognise cancer-associated antigens can be found both in the tumour and the bloodstream. Since tumour cells are not foreign cells, most cancer-associated antigens that are presented to T-cells are the same as those present on healthy cells, for the antigens classed as differentiation and over-expressed antigens. This presents a problem to the adaptive immune system. Thymic selection is a very important process to prevent autoimmunity, but in turn this means that T-cells that

have the ability to recognise cancer are destroyed before they get a chance to develop. However, if thymic selection is in place, why are immune cells found within tumours?

The answer lies in the fact that thymic selection is not a perfect process. Occasionally, the thymus misses or ignores a self-reactive TCR and the T-cell is allowed to proceed into the body's circulatory system. This is one way in which autoimmune diseases can occur, particularly as the body ages and becomes less efficient at immunosurveillance and tolerance as a result of thymic involution; one common age-related auto-immune disease being rheumatoid arthritis, which is reasonably prevalent in elderly populations (Yazici and Paget, 2000). It is through this immune escape that T-cells capable of recognising cancer-associated antigens are not all destroyed, and able to circulate the body. For a T-cell that is reactive to a self-antigen to be present in the bloodstream, it is likely that the T-cell interaction with the antigenic peptide is a weak, or low-affinity interaction (Bouneaud et al., 2000). Low-affinity TCR-pMHC interactions are known to be less effective at activating T-cells, and inducing important effector functions due to the weaker binding between the two cells (Kalergis et al., 2001; Corse, Gottschalk and Allison, 2011). It has been shown that the affinity of TCR-pMHC interactions has a direct impact on the degree of tumour eradication (Engels et al., 2013). The group found that only TCRs exhibiting pMHC interaction with half maximal inhibitory concentration (IC50) values of less than 10 nM showed tumour eradication in *in vivo* models, compared with intermediate and low-affinity TCR interactions. It has been demonstrated that several components of anti-tumour T-cell immunity, including tumour infiltration, T-cell survival and cytotoxicity are all affected by the strength of the TCR-pMHC interaction (Bos et al., 2012). This might explain why some tumours are still able to grow even though immune cells are present within the tumour; the level of response raised by the infiltrating T-cells is not sufficient to cause large-scale tumour cell death. However, there are several other factors to consider regarding cancer growth despite recognition by the immune system.

1.4 The cancer defence system

There are many reasons why an anti-tumour immune response can fail. In order for T-cells to exert an anti-tumour effect on the tumour they must first leave the thymus, traffic to the tumour, leave the circulation and enter the tumour microenvironment, identify the cognate antigen presented on the relevant tumour cells via MHC and have retained the ability to exert effector functions once activated. Even if all of these events occur, there are a number of ways in which tumours can have immunosuppressive effects on T-cells to prevent them from carrying out tumour killing. In a review by Liu and Cao, several mechanisms of immunosuppression were identified, some of which will be discussed below (Liu and Cao., 2016).

It is sometimes observed in patients treated with autologous anti-tumour T-cells, that there is an immunological response in the peripheral blood system, but the tumour is not rejected. It is theorised that some effector T-cells cannot effectively traffic to the tumour, which could be due to a lack of chemotactic signals released by tumours to aid localisation. Indeed, some chemotactic signals that have previously been shown to be produced by melanoma cell lines are not recognised by tumour-infiltrating lymphocytes (TIL), including Growth-Regulated Oncogene-alpha (GRO-α), and Chemokine (C-X-C motif) ligand 1 (CXCL1) (Kershaw et al., 2002). For the cells that do manage to infiltrate the tumour, the tumour microenvironment itself is reported to be very immunosuppressive, through a number of different means, some of which are discussed below.

1.4.1 Immune suppression through inhibitory ligands

There are a number of inhibitory ligands expressed by tumour cells, which cause inhibition of T-cell activity by binding to receptors on the surface of T-cells. T-cells express both co-stimulatory and co-inhibitory receptors on their cell surface to provide tightly regulated immune responses to pathogens, and to prevent auto-immune reactions (Pardoll, 2012). Sometimes, these co-receptors are expressed as pairs that bind to the same ligand. For example, CD28, a co-stimulatory receptor, and cytotoxic T-lymphocyte-associated antigen 4 (CTLA-4), a co-inhibitory receptor, both bind CD80 and CD86, expressed by antigen-presenting cells (Buchbinder and Desai, 2016). This

action occurs early in the T-cell activation pathway, typically after TCR binding to pMHC occurs in the lymph nodes. It is thought that the relative ratio of co-stimulatory signals to co-inhibitory signals determines whether the T-cell experiences further activation or anergy. Another co-inhibitory receptor which operates through a different mechanism is programmed death protein 1 (PD-1), which binds to programmed death protein ligand 1 or 2 (PD-L1 or PD-L2), inhibitory ligands on the surface of tumour cells. Being localised to peripheral tissues and tumours, T-cell inhibition through the PD-1 receptor occurs as a separate and later event to CD28/CTLA-4 interactions. The expression of PD-1, like CTLA-4, is triggered by TCR engagement, and once bound to one of the cognate ligands, several effector functions of the T-cell are inhibited, such as proliferation and cytokine production (Buchbinder and Desai, 2016). Some other co-inhibitory receptors and their cognate ligands which have also been studied with respect to cancer are lymphocyte activation gene 3 (LAG3), which binds directly to MHC class II molecules, and T-cell membrane protein 3 (TIM3), the ligand of which is Galectin-9 (Gal9) (Grosso et al., 2007; Zhu et al., 2005). The increased expression of PD-L1, Gal9 and MHC class II molecules on the surfaces of tumour cells, and the co-expression of their respective receptor molecules have identified them as targets for immunotherapeutic intervention, which will be expanded on later in this introduction (Pardoll, 2012).

1.4.2 Immunoediting of tumours by the immune system

The composition of tumours is often shaped by the immune response, and the inability of the immune system to control a tumour leads to a natural selection of cells that have escaped death by immune cells; this effect is known as immunoediting (Beatty and Gladney, 2015). A number of genetic mutations that upregulate or downregulate different genes can have a potent effect on how recognisable the tumour cells are to the immune system. One way in which tumours evolve and escape the immune system is through loss of antigenicity, which occurs through the clonal expansion of tumour cells that are not recognised and targeted by T-cells. One mechanism of reducing antigenicity is the literal downregulation of antigen presenting molecules, such as MHC class I molecules, which has been reported as between 20 and 60 % in several solid tumours, including melanoma and lung cancers (Campoli and Ferrone, 2008). In

theory, a tumour made up of a heterogenous mixture of cells with different antigenicity. If cytotoxic immune cells target and eradicate only the highly antigenic cells that make up a portion of the tumour, this can result in a selection pressure allowing the growth of the non-antigenic tumour cells the T-cells have difficulty recognising. This might explain why some patients who receive targeted immunotherapy against specific antigens have an initial partial response but later relapse. For a complete response with this type of immunotherapy, every cancer cell would need to present the target antigen at a high enough level for efficient tumour eradication to occur. Unfortunately, even if this were the case, there are other ways in which the tumour can suppress the immune system to escape an anti-tumour response.

1.4.3 Recruitment and conversion of T-regs

The abundance of the immune-inhibitory T-cell population known as T-regs in different tumours has been associated with poor prognosis for a variety of cancer types, including melanoma and breast cancer (Shang et al., 2015). As previously mentioned, there are different populations of T-regs in the body, and researchers attempt to identify specific T-reg populations through a number of surface markers and functional assays; a common though not comprehensive phenotype for tumour-associated T-regs is CD4+ CD25+ FOXP3+ (Curiel, 2008). T-regs contribute to immune suppression in the tumour microenvironment through different mechanisms, including the sequestration of IL-2, production of immunosuppressive cytokines such as IL-10 and transforming growth factor beta (TGFβ), and expression of inhibitory markers such as CTLA-4 and inducible T-cell costimulator (ICOS) (Ward-Hartstonge and Kemp, 2017). It has also been shown that tumour cells can influence the balance of immune regulation by directly secreting soluble factors such as TGFβ and IL-10, which can inhibit the function of normal T-cells, and in the case of TGFβ, stimulate the body to produce more inhibitory T-regs (Steinbrink et al., 1999; Peng et al., 2004). For example, in the ovarian cancer setting, it has been shown that TGFβ production stimulates the conversion of CD4+CD25+ cells from peripheral CD4+CD25- cells, thereby increasing the population of inhibitory T-cells (Li et al., 2007). In addition to direct conversion of T-cells into T-regs, tumour cells show elevated levels of the chemokine C-C Motif Chemokine Ligand

5 (CCL5), which facilitates the recruitment of immune cells which express C-C chemokine receptor type 5 (CCR5), including T-regs (Wang et al., 2017). It is likely that a combination of T-reg conversion and recruitment shifts the balance towards immune system inhibition in certain cancers.

1.4.4 Upregulation of immunosuppressive factors linked to presence of CD8+ T-cells

While the presence of cytotoxic CD8+ T-cells has been thought to be beneficial to help weaken and eradicate tumours, more recent evidence indicates that it is a more complex problem than first anticipated. Experiments using transgenic mouse models have shown that the presence of CD8+ T-cells is directly linked with increased expression of indoleamine 2, 3-dioxygenase 1 (IDO) and PD-L1, driven by the cytokine interferon gamma (IFNγ) (Spranger et al., 2013). CD8+ T-cells also increased the recruitment of inhibitory T-regs through the production of C-C chemokine receptor type 4 (CCR4)-binding chemokines. While these data could be discouraging, the use of checkpoint inhibitors such as anti-PD-1 and anti-CTLA-4 are being utilised to counteract these effects. In fact, there is evidence that indicates that the infiltration of T-cells is critical to the success of checkpoint inhibitors (Tang et al., 2016). It is likely that the future of immunotherapy will lie in approaching treatment with a multi-faceted, combinatorial approach to tumour eradication. Fortunately, there are many different immunotherapies that have been developed for the treatment of cancer, and significant work in this field has helped to shape and improve these therapies into powerful weapons in the war against cancer.

1.5 Harnessing the power of the immune system

In modern day medicine, there are several different types of immunotherapeutic approaches both in clinical trials and being actively used for treating cancer, which are illustrated in the diagram in figure 1.4.

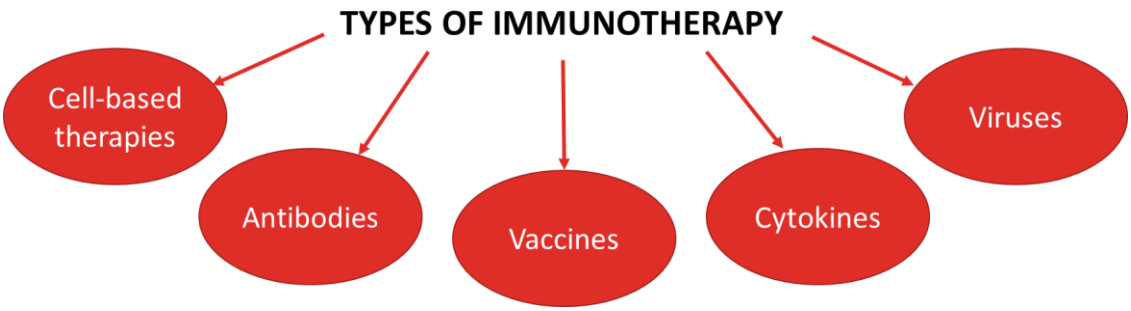

Figure 1.4 Types of immunotherapy. Schematic showing the different types of immunotherapies currently being investigated for the treatment of cancer.

1.5.1 Cytokine therapies

One immunotherapeutic approach which has been adopted is treatment with recombinant cytokines such as IL-2. IL-2 is a 15.5 kilodalton (kDa) glycoprotein that stimulates T-cells to survive and proliferate, and high-dose IL-2 therapy is thought to work by promoting further growth and differentiation of activated T-cells that have infiltrated the tumour (Kammula, White and Rosenberg, 1998). In a clinical trial of 270 patients over an eight-year period, the treatment of high-dose recombinant IL-2, was evaluated in a paper by Atkins et al., showing an objective response rate (ORR) of 16 %, including a few cases of complete responses, and was deemed a safe and beneficial treatment for metastatic melanoma (Atkins et al., 1999). Another cancer setting that has seen significant benefit from high-dose IL-2 therapy is renal cancer, which is not considered a highly immunogenic cancer; in a study of 255 patients with metastatic renal cell carcinoma, the response rate for IL-2 therapy was recorded as 14 % ORR (Fyfe et al., 1995). High-dose intravenous IL-2 therapy was approved for use by the United States Food and Drug Administration (FDA) in 1999 and is still used today. However, there are significant drawbacks to this therapeutic option. There are major toxicities associated with high-dose IL-2 therapy, which include thyroid dysfunction, fever, nausea, increased capillary permeability and cardiac arrhythmias (Krouse et al.,

1995; Bhatia, Tykodi and Thompson, 2009). To identify correlating factors between IL-2 treatment responders, Smith et al. conducted a retrospective study of 684 patients with metastatic melanoma who received high-dose IL-2 alone, or in conjunction with a melanoma vaccine against gp100 (Smith et al., 2008). Unfortunately, no pre-treatment factors could be strongly associated with increased chance of responding to the high-dose IL-2 regimen. In the patient group treated with IL-2 in combination with melanoma vaccine, there was an increased ORR for patients where the tumours were restricted to cutaneous/sub-cutaneous sites, and had 10% higher ORR than those treated with IL-2 alone.

1.5.2 Cancer vaccines

One of the biggest success stories utilising anti-cancer vaccine is human papillomavirus (HPV) vaccination for cervical cancer. After the discovery that the majority of cervical cancers contained HPV DNA, development and widespread administration of HPV vaccines has resulted in a significant decrease in incidence of cervical cancer in the treated population (de Sanjose et al., 2010; Guo, Cofie and Berenson, 2018). Due to the advancement of genetic sequencing and advanced mathematical modelling, there have been a number of other cancers identified which could be viral in origin, and therefore potentially good targets for vaccination; these include HPV-related head and neck cancers, HPV-related bladder cancer and some breast cancer (Lawrence et al., 2013).

There have been a variety of different vaccines developed for melanoma, which can be separated into different categories: short peptides (8-10 amino acids long), long peptides (around 30 amino acids long), ribonucleic acid (RNA), DNA, or whole protein (Ophir et al., 2016). These cancer vaccines work by attempting to stimulate the existing tumour-reactive cytotoxic T-cells, to form an attack against the tumour. As discussed in section 1.4, sometimes the presentation of antigens by tumour cells gets downregulated, or the immunosuppressive microenvironment prevents a response from being effective against the tumour. By presenting tumour antigens to the T-cells in a different context, proliferation of the cytotoxic T-cells can occur independently of tumour localisation to increase the chances of the immune response being large

enough to overcome the tumour's defences. The approach of immunisation with melanoma-associated peptides has been investigated by several groups, showing moderate success, and this success has been increased when in combination with cytokine or antibody therapies (Blanchard, Srivastava and Duan, 2013). For example, Schwartzentruber et al. describe a phase III clinical trial for a gp100: 209–217 (210M) peptide in combination with high-dose IL-2, which showed that when compared with high-dose IL-2 alone, the short gp100 peptide vaccine conferred better ORR and progression-free survival (Schwartzentruber et al., 2009). Side effects were noted as being the same severity as high-dose IL-2 administered alone.

A phase I/II clinical trial investigating the safety and clinical outcome following direct injection of messenger RNA (mRNA) encoding melanoma-associated antigens is a key example of how genetic constructs can be used therapeutically as anti-cancer vaccines (Weide et al., 2009). The protamine-stabilised mRNA was injected intradermally into patients, a different type of application compared with the intravenous applications of other vaccines and immunotherapies. The trial reported a decrease in CD4+ regulatory T-cells, increased numbers of T-cells responsive to the vaccine in a subset of patients, and one patient showed a complete response. This demonstration of safe and tolerable mRNA vaccination provided a framework for future work into protamine-formulated mRNA vaccine system, RNActive®, which was shown to be well tolerated in phase I/II clinical trial (Sebastian et al., 2019). Vaccines, and as well as other immunotherapies against melanoma differentiation antigens like gp100, are not tumour-specific, but often the tissue-specific side effects are tolerable as well as reversible. For example, vitiligo is a depigmentation condition that has been associated with favourable prognosis both prior to diagnosis as well as following treatment for metastatic melanoma (Nordlund et al., 1983; Hua et al., 2016).

1.5.3 Antibody therapies

Antibody-based therapies have seen a great deal of success as an immunotherapy. One of the first immunotherapy interventions for metastatic melanoma was Ipilimumab, a human monoclonal antibody vaccine against the checkpoint inhibitor CTLA-4 (Bhatia, Tykodi and Thompson, 2009). By blocking CTLA-4, Ipilimumab prevents the co-inhibitor

expressed by activated T-cells from binding CD80 or CD86. As a result, the activated T-cell population is better situated to carry out cytotoxic T-cell responses against the tumour. In a phase III clinical trial of 676 patients, Ipilimumab was shown to result in improved patient survival compared to a gp100 vaccine (Hodi et al., 2010). As the expression of CTLA-4 is not restricted to tumour cells, the side effects were reported to be fairly severe, but reversible with careful treatment. However, this drug is likely to only be effective if there are already significant immune infiltrates in the tumour, a phenomenon which is not observed in all cancers or metastases (Pagés et al, 2010).

Another antibody therapy which has attracted a lot of attention within the cancer immunotherapy field recently is anti-PD-1. As mentioned previously, the ligands for PD-1, called PD-L1 and PD-L2, are expressed on tumour cells, and interact with PD-1 on T-cells to suppress T-cell function. An anti-PD-1 monoclonal antibody therapy, Nivolumab, has been approved for use post-surgery in the UK for melanoma since 2018, having given promising results in different clinical trials regarding safety and efficacy, with tolerable side effects (Topalian et al., 2014; Robert et al., 2015a). Another anti-PD-1 therapy which is approved for use in the UK is Pembrolizumab. Clinical trials have demonstrated the effectiveness and safety of Pembrolizumab, as well as showing a superior clinical response and toxicity profile when compared to Ipilimumab (Ribas et al., 2015; Robert et al., 2015b).

In recent years, clinical trials have investigated the combination of different antibody immunotherapies such as Nivolumab and Ipilimumab. In a study of 142 previously-untreated metastatic melanoma patients, the combination of Nivolumab and Ipilimumab resulted in an ORR of 61 %, compared with 11 % ORR in the group treated with Ipilimumab plus placebo (Postow et al., 2015). In a separate study, a two-year follow up report of phase II and III clinical trials for treatment of patients with advanced melanoma with a combination therapy of Nivolumab and Ipilimumab revealed favourable results for the combination therapy over ipilimumab alone (Hodi et al., 2016). The two-year overall survival rates for the combination therapy were 63.8%, compared to 53.6% for ipilimumab alone. A trade-off for this higher survival rate was that the incidence rate of treatment-related adverse events for the combination therapy was significantly higher (56% compared to 20%) than the ipilimumab treatment. However, it is still a promising result for the future of anti-PD1

therapy in combination with other immunotherapies, the synergistic effect of which can lead to tumour reject, recently demonstrated by combination with Fc-Optimized anti-CD25 (Arce Vargas et al., 2019).

1.5.4 Adoptive cell therapies

Adoptive cell therapies (ACT) are a group of different therapies which can utilise immune cells to target cancer, as illustrated below in figure 1.5. The majority of cell therapies for cancer are autologous, where the immune cells are isolated from the patient's blood or tumour, but there is a drive to generate allogenic products to increase the throughput and standardise the procedure (Geller et al., 2011; Besser et al., 2013). Autologous ACT forms the basis of the work in this PhD, so will be the focus of the rest of the introduction.

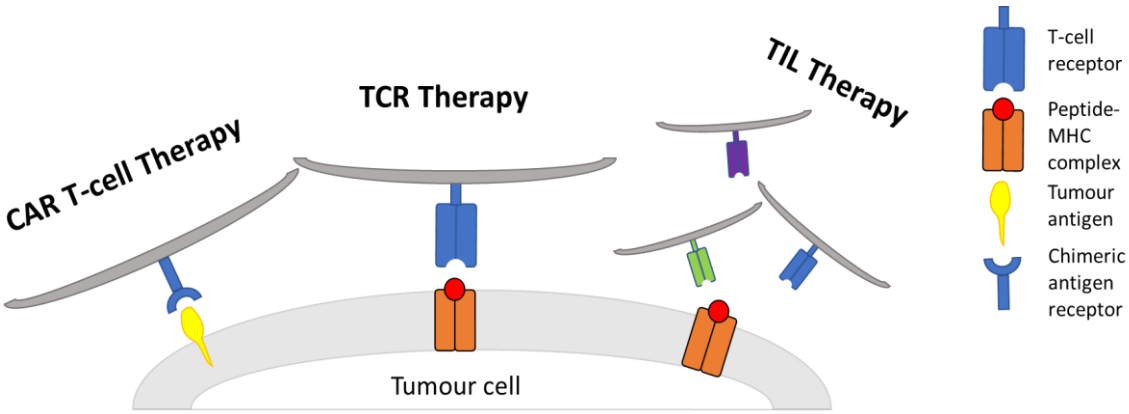

Figure 1.5 - Adoptive cell therapies for cancer. Diagram depicts the three main ACTs that use T-cells to target tumour cells.

A lot of interest in the field of immunotherapy ACTs has been garnered in the innovative chimeric antigen receptor (CAR) T-cell therapy. In CAR T-cell therapy, patient T-cells are commonly used, by isolating them from the blood and then transducing them with the CAR in question. The CAR-transduced T-cells are then re-infused back into the patient, now with the potential to recognise and attack tumour cells. The mode of action for CAR T-cells is based upon antigen recognition independent of HLA expression, since they are composed of an antigen-recognition domain from a single-chain antibody fragment (scFv) which is attached to an intracellular signalling domain (Srivastava and Riddell, 2015). As CAR T-cells have been developed, successive generations have incorporated costimulatory receptors such as

CD28 or CD137 (4-1BB) to provide additional signalling to the CAR T-cells when stimulated (Kowolik et al., 2006; Bridgeman et al., 2010; Song et al., 2011). One area where CAR T-cells have proven highly successful is in the treatment of B-cell malignancies, such as chronic lymphocytic leukaemia (CLL) and follicular lymphoma (Brentjens et al., 2013). In the Brentjens et al. study, five patients with relapsed acute lymphoblastic leukaemia (ALL), were treated using autologous, CD19-engineered CAR T-cells. All five patients achieved complete remissions with no evidence of minimal residual disease, with cytokine elevation consistent with previous reported levels. In 2016, a larger clinical trial reported 31/33 (94%) with ALL showed complete remission with CD19 CAR T-cell therapy, with 84% and 50% complete remissions in Non-Hodgkin's Lymphoma and CLL respectively (Turtle et al., 2016). One restriction with CAR T-cells is that the antigen needs to be present on the surface of the target cell to be recognised, limiting their uses to exclude intracellular antigens. Whilst there have been several clinical trials of CAR T-cells against a variety of different cancers showing reasonable success, there have been concerns over safety, with reports of adverse side effects related to a phenomenon known as cytokine storm (Brentjens et al., 2010; Morgan et al., 2010). Along with the success of the therapy in certain cancer types, there has been a lack of success in solid cancers, the reason of which is not currently known and a topic of continued scientific research (Newick et al., 2017).

TCR T-cell therapy is another type of ACT which uses T-cells transduced with a TCR recognising a known cancer-associated antigen to target a patient's tumour. Like with CAR T-cell therapy, the T-cells are typically isolated from the patient's blood, then transduced to express the anti-cancer TCR before re-infusion. TCRs have been identified and developed for a number of different antigens of all types. There have been over 100 clinical trials using TCR T-cell therapy, with some great successes, as well as some important failings, which have been reviewed previously (Oppermans et al., 2020). In the review, it is highlighted that melanoma is the most targeted cancer type by currently recruiting and completed trials, for which the majority of TCRs utilised recognise differentiation antigens such as gp100 and MART-1. Despite this, there is a dominance of TCRs directed against NY-ESO-1, the tumour-specific CT antigen expressed by a wide variety of tumour types. Over 50 % of the clinical trials identified were in phase I, and no clinical trials were listed as phase III, illustrating that

there are still important safety and efficacy targets to be met before a large-scale clinical trial can be planned. The majority of the trials in the clinic involved TCRs restricted by HLA-A*0201, one of the most prevalent HLA haplotypes in the Western world, however this limits the number and diversity of the participants that can enrol on these clinical trials. One advantage of TCR T-cell therapy over CAR T-cell therapy is that is has shown success in a variety of cancers, both haematological and more notably, solid cancers. It has also been associated with fewer instances of cytokine storm, although unexpected instances of off-tumour on-target reactivity leading to patient death has been a cause for concern in the progression of TCR T-cell therapies in the clinic. From past clinical trials and subsequent literature, there are a number of key successes and failings discussed in the review; some of these will be discussed as part of an introduction to chapter 4.

The final ACT immunotherapy, and the foundation of the work in the thesis, is tumour-infiltrating lymphocyte (TIL) therapy, which shall now be discussed in more detail in the next section.

1.6 TIL Therapy

TIL therapy harnesses the power of thymically-selected T-cells that have trafficked to and infiltrated the tumour. T-cells are isolated from the patient through surgical removal of the tumour, and the T-cells grown out and expanded *ex vivo* through a process known as a rapid expansion protocol (REP) (Dudley et al., 2003). This is the process by which outgrowth TIL are put into a large-scale culture with irradiated peripheral blood mononuclear cells (PBMC) feeder cells typically at a ratio of around 200: 1 feeder cells to T-cell, as well as an activating agent such as an anti-CD3 antibody (e.g. Muromonab-CD3, clone: OKT3) or phytohaemagglutinin (PHA), and IL-2. The cells are expanded for up to 14 days, with media exchanges and addition of more IL-2 during the culture to promote cell proliferation. After expansion, the cells are reinfused back into the patient where the TIL can circulate the body and infiltrate remaining tumours in the patient.

TIL therapy has been reported to produce ORR of around 50 % consistently across multiple clinical trials, and often in patients who have previously failed on multiple different first-line therapies (Radvanyi, 2015). A key benefit of this therapy is that the use of autologous cells negates any graft vs host effect that other therapies using allogenic cells are troubled with. There is also no evidence from current and previous clinical trials of serious adverse side-effects such as cytokine storm, that are seen with other immunotherapies such as CAR T-cells and TCR therapy. TIL therapy has gathered a lot of interest from scientists and clinicians in the field. It is a comparatively simple therapy, as specific antigens or T-cells do not need to be identified as part of the manufacturing process, and the ORRs have been some of the most favourable from cancer immunotherapies in the clinic to date. TIL therapy is currently offered as a ‘specials’ treatment in the UK on a compassionate basis, and is not yet licensed for use by the National Health Service. To be permitted to be treated by TIL therapy in the UK, the patient must have tried all other therapeutic options before TIL therapy, which usually includes chemotherapy, checkpoint inhibitor blockade or radiotherapy.

1.6.1 The development of TIL therapy: A brief history

The first evidence that TIL therapy might be a viable therapeutic immunotherapy coming from Rosenberg et al. back in 1986, and was first used to treat patients in 1988 (Rosenberg, Spiess and Lafreniere, 1986; Rosenberg et al., 1988). The TIL therapy process was first reviewed in 1994, after 86 patients with advanced metastatic melanoma were treated with TIL plus high-bolus IL-2 (Rosenberg et al., 1994). At this early stage, not all patients were pre-treated with the chemotherapeutic agent cyclophosphamide, so the addition of this in the treatment regime was also analysed. They observed a 31 % ORR in patients treated with TIL plus high bolus IL-2, and 35 % ORR in the treatment group who also received cyclophosphamide prior to TIL infusion. Some of the factors that were statistically shown to be correlated with improved patient response included TILs with shorter doubling times, TILs from younger cultures, and TIL that exhibited lysis to autologous tumour *in vitro* (Rosenberg et al., 1994). This led to an adaption in the protocol of TIL therapy, with patients only progressing to treatment if the TIL showed tumour-reactivity during the outgrowth stage. Even today, there is little variation in TIL generation protocols across different groups globally, except for some groups opting for dissecting tumour into chunks for the outgrowth phase, and others choose to use chemical and mechanical disaggregation methods to digest the tumour collectively for the outgrowth stage; both methods have proven successful for TIL generation (Dudley et al., 2003; Baldan et al. 2015).

For TIL therapy, and other ACT immunotherapies, the patient's existing T-cells are typically depleted with pre-conditioning lymphodepletion chemotherapy, and when TIL are re-administered, a regime of IL-2 is given to support the T-cells *in vivo*. The extent of pre-conditioning chemotherapy, as well as the dose of IL-2 given, has been fine-tuned by various groups over the years. Dudley et al. compared response rates of patients given TIL therapy following two different myeloablative chemotherapy regimens, and showed that using 12 Gray (Gy) total body irradiation (TBI) rather than 2 Gy increased the response rate by 20 % (Dudley et al., 2008). This key paper helped solidify the role of lymphodepletion as a crucial part of the TIL treatment in order to achieve the best responses. This clinical trial was expanded, analysed retrospectively, and long-term follow up of the patients was carried out. In the three treatment groups (non-myeloablative chemotherapy only, or with 2 Gy or 12 Gy TBI), the response rates

were reported as 49 %, 52 %, and 72 %, and the complete responses were 12 %, 20 %, and 40 %, respectively (Rosenberg et al., 2011). It could be hypothesised that the rate of complete responders is directly correlated with the degree of TBI administered prior to TIL transfer. This hypothesis was addressed in a randomised clinical trial where 101 patients with metastatic melanoma received TIL therapy with or without 12 Gy TBI (Goff et al., 2016). In both trial groups, the rate of complete responders was 24 %, and the objective response rates was also comparable. By combining the patient data, there was no statistical significance observed in the responses related to age, gender or prior treatment, which are all factors that have previously been suggested could influence response (Joseph et al., 2011). Another important observation was that the reactivity of TIL when co-cultured with autologous tumour, measured by IFNγ release, was not predictive of *in vivo* response. This supported the notion that all patients should be treated with TIL therapy if eligible, regardless of the *in vitro* TIL response to tumour.

Another pivotal development in TIL therapy was the research that led to the attenuation of the IL-2 regime that accompanies TIL treatment. While a crucial part of the therapy in order to support and sustain the T-cells upon re-infusion, high dose IL-2 is known to be particularly toxic and lead to serious adverse side effects (Kammula, White and Rosenberg, 1998). While these side effects are not long-lasting and can be treated, the high dose IL-2 is considered as the hardest part of the therapy for the patients. In Denmark, a small-scale clinical trial was conducted with just 6 patients, where instead of intravenous high-dose IL-2, subcutaneous injections of low-dose IL-2 was used following ACT (Ellebaek et al., 2012). They reported that two patients had complete response to the TIL therapy, two had stable disease and the other two had disease progression. Across all the patients, significantly lower and more manageable adverse events were experienced as a result of the low dose IL-2 treatment. This feasibility study paved the way for a larger phase I/II trial in which 25 patients were enrolled, where patients were treated with TIL therapy accompanied by a gradually decreasing IL-2 regime given intravenously (Andersen et al., 2016). Of the 25 patients treated, 3 had complete tumour remission and 7 more had partial responses, giving an objective response rate of 42 %. This is comparable with the current regime of TIL therapy with high-dose IL-2. One of the key benefits of this attenuated IL-2 regime was

that due to the reduced severity of the IL-2-related side effects, the patients could be treated for the adverse side effects in the cancer ward rather than having to transfer to an intensive care unit. This has lower cost implications as patients can receive the TIL reinfusion and IL-2 regime as outpatients.

1.6.2 TIL therapy is a viable treatment for multiple cancer types

TIL therapy has been shown to be a viable treatment option for a variety of cancer types to date. The first hurdle in determining if TIL therapy could be beneficial for a given cancer is to see if TIL can be grown *ex vivo* from resected tumour. This has been shown to be possible for some cancers which do not have very good current treatment options, such as pancreatic cancer (Hall et al., 2016). In non-small cell lung cancer (NSCLC), TIL therapy showed an improved clinical benefit with increased stage of cancer, and retrospective studies have shown the presence of TIL in this cancer type is a good prognostic marker (Ratto et al., 1996; Zeng et al., 2016). The type of cancer most commonly treated with TIL therapy is advanced metastatic melanoma. One reason it is suspected that TIL therapy works so well in the melanoma setting is the immunogenicity of the cancer. As illustrated in figure 1.6, melanoma has the highest prevalence of somatic mutations compared with other cancer types, likely due to the type and extent of DNA damage induced by UV radiation (Alexandrov et al., 2013).

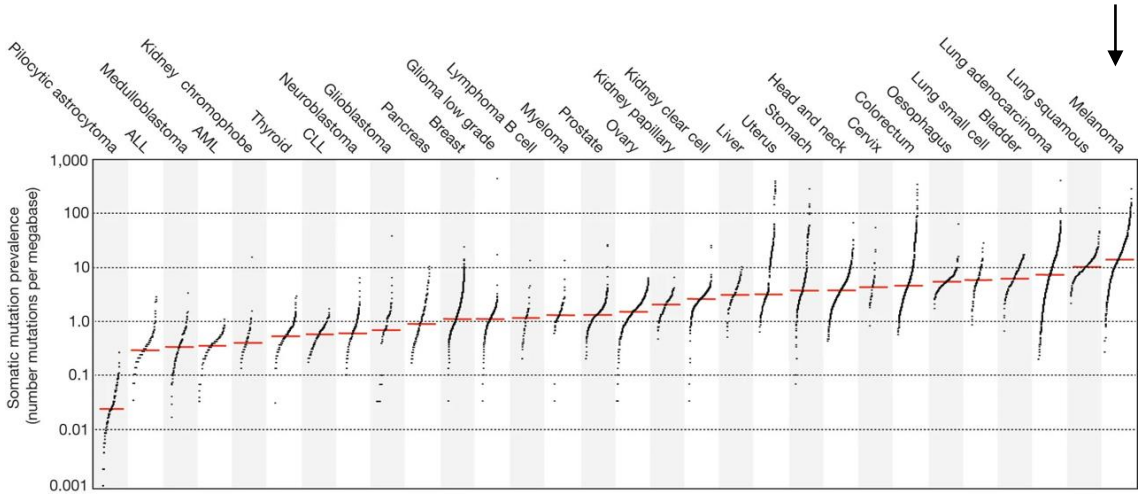

Figure 1.6. Mutational burden of different cancers. Number of somatic mutations on the *y* axis, plotted for several different cancer types. The arrow indicates melanoma as the cancer type with the highest prevalence of somatic mutations. Adapted from Alexandrov et al., 2013.

Interestingly, not all melanomas behave in the same way, and the high mutational burden described by Alexandrov et al. is more specifically restricted to cutaneous melanoma, the most common type of melanoma that arises from mutated melanocytes in the skin. However, melanocytes can also be found in other tissues, including several parts of the eye such as the choroid, ciliary body and iris (Chattopadhyay et al., 2016). Tumours arising from melanocytes in the eye are referred to as uveal melanomas are a rarer type of melanoma, approximately 5 % compared with cutaneous melanoma which makes up around 90 % of all melanomas (Chang, Karnell and Menck, 1998). There are several other differences between these tumour types. Mutations that are often found in cutaneous melanoma, such as *BRAF* and *NRAS*, are seldom found in uveal melanoma, and conversely, mutations like *GNAQ* and *GNA11* are highly prevalent in uveal melanoma but not cutaneous melanoma (Malaponte et al., 2006; van Raamsdonk et al., 2009; van Raamsdonk et al., 2010). While there are a few options for localised treatment of the primary lesion, once metastasised, several systemic therapeutic options that are generally successful for cutaneous melanoma have proven ineffective for uveal melanoma (Dorval et al., 1992; Carvajal et al., 2014; Algazi et al., 2016). These results have led to widespread belief that uveal melanomas are immunologically naïve and immunotherapies would not be effective treatment options, and several groups have sought to understand the immunological landscape of uveal melanomas. Research has since shown that uveal melanoma is immunologically different from other melanoma; while there are no differences in the number of CD8+ T-cells found in the tumours, the levels of PD-1 on CD8+ T-cells and corresponding PD-L1 found in the uveal melanomas was significantly lower than those found in cutaneous melanomas (Qin et al., 2017). The presence of TIL within uveal melanomas shows that there is hope for immunotherapies for this cancer type, and this appears to be the case with the successful treatment of several uveal melanoma patients using TIL therapy (Chandran et al., 2017). It is possible that the TIL found in uveal melanomas could be reactive to common melanoma antigens also found in cutaneous melanomas such as gp100, MART-1 and tyrosinase, due to the presence of these antigens (De Vries et al., 1998).

Other types of melanoma include mucosal, which arise from mucosal melanocytes in the body which can be found in the paranasal sinuses, oropharynx or anogenital

tissues, and acral melanoma, which arise from the non-hair-bearing skin such as that found on the palms of the hand or soles of the feet (Kaunitz et al., 2017). Another subgroup of melanomas is referred to as chronic sun damaged (CSD), and these are often located on the head and neck regions of older patients. In work carried out by Kaunitz et al., the prevalence of PD-L1 expression in different melanoma subtypes was explored, and found to be 31 % for acral, 44 % for mucosal, 10 % for uveal and 62 % for CSD; for comparison, PD-L1 expression in cutaneous melanoma was referenced as 35 %. They also found that the presence of PD-L1 in tumour subtypes correlated geographically with the presence of CD8+ T-cells. This finding was in line with work from other groups showing that the presence of TIL was associated with more favourable prognosis in acral melanoma, and a reduced risk of metastasis in mucosal melanoma (Lee et al., 2013; Song et al., 2015).

1.6.3 Challenges and the optimisation of the TIL therapy process

TIL is a personalised therapy approach, which means that the generation of TIL has to be conducted on a patient-by-patient basis and the resulting outputs are time- and resource-demanding. The associated cost of treating a patient with TIL therapy can be considered significantly higher than treatment by a non-personalised therapy such as checkpoint inhibitor blockade and, in many cases, a decision has to be made whether it is financially and medically viable to opt for personalised ACT treatment. In order for a patient to be eligible for treatment by TIL therapy, a number of conditions have to be met. Firstly, and most obviously, TIL has be grown out from the tumour. There are a few reasons why this might not be possible, such as a distinct lack of T-cell infiltration, or bacterial contamination of the tumour biopsy. While the lack of T-cell infiltration in some cancer types could prove challenging in future TIL generation, for melanoma, TIL products of over 1×10^{10} cells can typically be generated, especially with the more recent application of bioreactor technology (Sadeghi et al., 2011). The issue of TIL contamination is rare in melanoma, and typically associated with attempting to grow out TIL from tumours resected from sites of the gastrointestinal regions such as tumours of the colon (Marchesi et al., 2011). Since bacterial contamination can be combated with antibiotic treatment, this is also of low concern.

Another challenge to overcome in TIL therapy is the timescale of TIL product generation. Initial protocols of TIL production took as long as 51 days, and in some unfortunate cases, the continued decline in patient health led to death before TIL administration, or the patient being too weak to receive pre-conditioning chemotherapy and the particularly toxic but crucial IL-2 regime that accompanies TIL treatment. The patients eligible for TIL therapy are often the most ill, since their cancers have progressed to late-stage metastatic disease, and have often failed treatment by other means. At this stage, this is still an unavoidable challenge. However, there has been a lot of progression within TIL therapy, with different groups developing more efficient, scalable and effective methods of TIL extraction and expansion. In particular, considerable efforts have been made universally to shorten the *in vitro* expansion stage of TIL generation with minimally cultured TIL products, termed 'young' TIL.

1.6.4 Minimally-cultured TIL

There have been several groups who have championed the use of 'young' TIL, with the aim of cutting down the time between tumour acquisition and TIL administration, as well as sidestepping the issue of failed TIL generation for some patients. Tran et al. describe the protocol for minimally cultured TIL generation, which was investigated due to early data suggesting that younger TIL was associated with better response rates in patients (Rosenberg et al., 1994; Tran et al., 2008). After initiation, TIL were cultured for just 10-18 days, which was considerably shorter than the standard TIL protocol of 21-36 days. After this initial outgrowth stage, both the 'young' and standard TIL were put into REPs following the standard 14-day REP protocol, described previously (Dudley et al., 2003). Substantial evidence had been previously generated to investigate why minimally cultured TIL might result in better patient responses. In animal models, it was shown that the transfer of naïve, early effector T-cells was more effective at eradicating tumours than more differentiated effector T-cells (Gattinoni et al., 2005a). This was partly attributed to the expression of costimulatory receptors CD27 and CD28 on early effector cells, which are associated with enhanced proliferation and better persistence in the patient (Huang et al., 2005). This suggested that their full characterisation as effector memory cells, with the profile CD27+ CD28+

CD62L- CCR7-, could help contribute to better *in vivo* persistence as well as long-term tumour immunity (Powell et al., 2005). These early phenotype T-cells were also noted to have longer telomeres than their late-stage counterparts, and clones which had longer telomeres upon reinfusion to the patient tended to be the ones that persisted longer and exhibited clinical response (Shen et al., 2007).

Another group who carried out a comparison of young TIL and standard TIL treatment reported the most notable difference was in the number of patients who were treated with TIL therapy, as a result of the shorter culture phase and wide inclusion criteria; only 21 out of 33 patients enrolled on the standard TIL protocol were treated due to either lack of *in vitro* TIL activity or clinical progression prior to receiving the therapy (Besser et al., 2009). Dudley et al. continued their work into optimising TIL therapy, showing successful results in patients treated with CD8+ enriched young TIL compared with standard TIL (Dudley et al., 2010). After treatment, the CD8+ enriched young TIL were tested *in vitro* for tumour reactivity, as this was not a part of the young TIL generation process. Out of the examinable CD8+ young TIL samples, 69 % exhibited autologous tumour recognition. Perhaps more interestingly, 37 % of patients had objective response rates who were treated with young TIL which did not exhibit specific tumour recognition *in vitro*. The significance of this result is that under previous inclusion criteria, if TIL did not exhibit autologous tumour recognition, the corresponding patients would not have received the TIL product. This led to the incorporation of young TIL in large scale expansion for treating patients using this method, although the objective response rates of patients treated by this group was reported as 48 %, which is not significantly higher than previous response rates reported for standard TIL treatment (Itzhaki et al., 2011).

One observation that has been made about young TIL is the ratio of CD4 to CD8 cells – it has been shown by some TIL researchers that good clinical response can be linked to a higher proportion of CD8 cells in the final TIL product (Radvanyi et al., 2012). Young TIL are predominantly CD4 in composition, so how does this impact the resulting TIL product and patient response? The answer is more complex than it seems, as there are several contradictory data which has led groups to question the role of CD4 cells in the TIL product, and their importance to the overall clinical response.

1.6.5 CD4 T-cells – a help or a hindrance?

As mentioned in section 1.2, CD4 is a co-receptor that has also been used as a marker of T-helper cell and T-reg cell populations. Antony et al. recognised that the tumour-reactive CD4+ T-reg cells present in TIL populations may be hindering the effectiveness of TIL therapy, and conducted a series of *in vivo* experiments in mice to investigate this cell population (Antony et al., 2005). Not only did the CD4+ T-reg cells prevent CD8+ T-cells from establishing an immune response against the tumour, they greatly impaired the ability of CD4+ helper T-cells in assisting their CD8+ T-cell counterparts. They also showed that depleting the CD4+ T-reg population was not sufficient for tumour suppression, for which anti-tumour CD8+ T-cells are required. Another crucial result shown in this paper was that the action of the CD4+ T-reg population was IL-2 dependent. This was previously proven by Papiernik et al., who showed that IL-2-/- mice did not have a CD4+ CD25+ T-reg population (Papiernik et al., 1998). This has greater implications in the treatment of metastatic melanoma, for which high dose IL-2 is being used both as an independent treatment and a part of the TIL therapy regime. Collectively, these results gave support to the idea that endogenous CD4+ T-reg cells can greatly hinder treatment with TIL therapy, and help to explain why the lymphodepletion regime that patients are given prior to TIL infusion can result in better prognosis.

In contrast to the immune-inhibitory effects of the CD4+ T-reg population, other CD4+ populations have been shown to contribute in a positive way towards the anti-tumour response. In one such investigation, researchers depleted the CD8+ cells from melanoma TIL samples and investigated the resulting population for responses to autologous tumour cells (Friedman et al., 2012). They demonstrated IFNɣ production in response to tumour cells for 9 out of the 44 CD8-depleted TIL samples, with subsequent analysis showing that the majority of these tumour-reactive populations had high CD4 expression. In addition, they provided an example where a patient with highly metastatic disease was treated with TIL harbouring T-cells with MHC-class II-restricted tumour reactivity, and regression of metastases in the liver and spleen was observed. This highlights that CD4+ TIL populations can mediate cytotoxic anti-tumour responses and contribute to the overall cytotoxicity of TIL.

1.6.6 Alternative TIL selection protocols

In standard TIL therapy, the T-cells are usually unmodified and unselected, although in early TIL trials in the US, the Rosenberg group historically championed TIL treatment where TIL is only administered for patient when the TIL cultures showed tumour-reactivity during the outgrowth phase (Dudley et al., 2003). In a large retrospective analysis of metastatic melanoma patients treated with TIL therapy over a five-year period, 107 out of a possible 402 patients (27 %) were treated. Of the 402 patients, TIL were able to be grown for 376 patients (94 %), and only 269 showed reactivity to tumour (67 %); only 107 of these 269 patients received the therapy, with the non-treated patients being excluded for clinical or technical reasons (Goff et al., 2010a). This demonstrates the use of initial selection measures, albeit without manipulation of the cultures, but does come with the caveat that if TIL does not exhibit tumour-reactivity, the treatment does not go ahead.

One method of improving TIL therapy that has been explored in the clinic is intentionally selecting for cytotoxic T-cells during the *ex vivo* phase of TIL generation, through CD8 selection. As it is generally accepted that a CD8-dominant TIL product is therapeutically superior, some groups have investigated enhancing the TIL product further by combining the young TIL generation protocol with a CD8+ T-cell selection. One such group showed data which demonstrated increased tumour-reactivity by IFNγ production in CD8+ young TIL compared with the unselected young TIL, including induction of tumour-reactivity in 38 % of samples that was previously unmeasurable (Prieto et al., 2010). However, data from a different group seemed to convincingly prove that CD8+ selected young TIL carried no therapeutic benefit from unselected young TIL through a robust, randomised clinical trial (Dudley et al., 2013). They demonstrated that 35 % of the unselected TIL treatment arm showed a clinical response, compared to only 20 % of the CD8-selected TIL arm. Since the CD8+ T-cell selection process required more time and resources, this group suggested that it is an unnecessary process that should not be pursued in research. This put back into question the importance of CD4+ TIL cells in the final TIL product, suggesting that there might be a critical ratio of CD4 to CD8 cells where the CD4+ cells provide optimal support and the CD8+ cells are abundant enough to instigate a strong clinical response.

An interesting peptide-based expansion method was described more recently in 2016 by Theaker et al., who used CD3/CD28 microbeads to expand polyclonal T-cell populations in a 96-well format, before reactivity against a library of different known peptides was tested (Theaker et al., 2016). Reactive clones were then expanded using cytokines prior to *in vitro* validation, a process that took less than 6 weeks from start to finish. This process would theoretically work well for patients who have tumours expressing a known melanoma antigen such as MART-1 or gp100. Considering TIL populations are greatly polyclonal, a method which allows the isolation of minor clonotypes which might be highly tumour-reactive has promise. However, as this is a library-based selection method, TIL populations which recognise neoantigens and could be highly effective tumour-killing cells, would not be selected using this protocol.

Certain desirable features such as *in vivo* persistence and anti-tumour activity have been associated with the subpopulation CD8+ effector memory T-cells, and many groups have tried to implement strategies during TIL expansion to manipulate cultures towards this desired phenotype. One successful method of this TIL selection is the addition of anti-CD137 agonist into the cell cultures (Chacon et al., 2013). CD137 is a member of the tumour necrosis factor (TNF) receptor family, and upregulation of CD137 on T-cells leads to downstream proliferation, increased production of IL-2 and reduced susceptibility to apoptosis (Sanchez-Paulete et al., 2016). This group found that during the REP stage, CD137 is upregulated in the first 24-48 hrs of T-cell expansion, but the corresponding ligand CD137L is not expressed highly by irradiated feeder cells or the TIL themselves. The group theorised that if the TIL had continued activation of CD137 through exogenous monoclonal antibody (mAb) agonist, the phenotype associated with CD137 expression could be preserved. They optimised the addition of CD137 agonist to the REP process and showed a dose-dependent increase in CD8+ T-cells, that could be specifically attributed to the CD137 mAb agonist. They also demonstrated that growing TIL in the presence of CD137 agonist antibody protected the TIL from loss of CD28, which preserved the desirable effector-memory phenotype of the TIL. This also correlated with a higher resistance to activation-induced cell death (AICD) upon re-stimulation with melanoma antigen MART-1 when presented by APCs. The TIL that had been expanded with anti-CD137 mAb exhibited enhanced cytokine production when measured for TNFα, IFNγ and IL-2. Finally, when

stimulated with HLA-matched and HLA-mismatched tumour lines, the anti-CD137 expanded TIL showed enhanced, specific, tumour-killing capabilities, and it was confirmed that this was not as a result of the outgrowth of a specific melanoma-reactive clone. The data presented in this paper is a robust and convincing demonstration of the important role CD137 plays concerning retention of many desirable TIL properties. It is supported by further work which confirmed the theory that the combinatorial effect of using CD137 agonist combined with IL-2 during the first stage of the REP process resulted in a higher proportion of CD8+ TIL and enhanced reactivity to the matched patient tumour, for both cutaneous and uveal melanomas (Tavera et al., 2018). The work in this paper also utilised OKT3 during the first stage of REP to stimulate T-cell activation through the TCR, which is referred to as signal 1, with anti-CD137 antibody providing signal 2 stimulation and IL-2 supporting the T-cells with signal 3. The combination of activating T-cells using all three signalling pathways resulted in therapeutically superior TIL than those which were generated by just activating one or two of these pathways.

Fluorescence-activated cell sorting (FACS) is a technique which involves tagging specific populations of cells using fluorescently-labelled antibodies and isolating the population of interest with a flow cytometry-based sorting device. It has been utilised in recent years as a selection method for isolating specific populations of TIL from tumour digest or post-outgrowth TIL, to more robustly select T-cells with a desired phenotype. One example of this was the selection of CD8+ PD-1+ TIL from melanoma tumour digest material, which researchers showed resulted in higher IFNɣ production in response to tumour when compared to CD8+ PD-1- TIL (Inozume et al., 2010). Another example of TIL selection using FACS in recent years is the isolation of CD8+CD137+ TIL from melanoma tumour digest, which was used to interrogate the tumour-reactive TCR repertoire of TIL (Parkhurst et al., 2017). The researchers were able to show that CD8+ CD137+ TIL from 6 melanoma patients collectively harboured 27 neoantigen-specific TCRs, validating this selection method as a way of isolating and identifying neoantigen-specific TIL for enhanced patient-specific ACT. Other researchers have also sought to isolate CD137+ TIL through the use of magnetic bead capture, where instead of fluorescent labelling, the antibody of interest is bound to a magnetic bead and the population of interest can be isolated from bulk T-cells using magnetic separation. This

technique was utilised for CD137+ TIL isolation by Ye et al., who were also able to demonstrate that the CD137+ population of TIL accurately identifies tumour-reactive cells in ovarian and melanoma TIL samples (Ye et al., 2014). Taken together, these findings suggest that isolating CD137+ TIL could be a valuable strategy for improving TIL therapy in the melanoma setting, and possibly for other cancer settings as well.

1.6.7 Genetically-engineered TIL

Genetic engineering of TIL is an attractive option to help enhance TIL therapy and develop a superior ACT product for immunotherapy. There are some key considerations to keep in mind when discussing genetic engineering of TIL products. Firstly, genetically manipulating a cell population can require significant *in vitro* optimisation to produce a cell product that is homogenous for the introduced manipulation. If the aim is to knock out or transduce in a receptor, for example, the efficiency of knock out/transduction might initially be low and optimisation can be time-consuming. Another key consideration is the cost associated with producing genetically-engineered TIL, which is much greater than unmodified TIL due to the additional resources and skill required. However, since TIL therapy holds such promise for many solid cancer types, it could be possible that through genetic engineering, TIL therapy can be even more potent, more accessible and treat a wider variety of cancer types.

An example of a genetic manipulation approach used by one group is PD-1 knock down of TIL through the use of directed zinc finger nuclease technology (Beane et al., 2015). They reported the knock down resulted in a 76 % decrease in PD-1 surface expression overall, and in two of the three TIL they tested, there was a significant increase in cytokine production *in vitro.* In all donors, the cells expanded between 500- and 2000-fold, and all the cells exhibited an effector memory phenotype. This provided a basis and pre-clinical evidence that genetically engineered TIL through PD-1 knockdown may result in longer persistence *in vivo* as well as having an enhanced tumour-reactive phenotype.

Another example of genetically-engineered TIL came from the same research group, but rather than knocking down genes, they genetically engineered TIL to increase IL-2

production by transducing them with a retrovirus containing the IL-2 gene (Heemsherk et al., 2008). Their hypothesis was that through continued exposure to IL-2, the TIL would persist better *in vivo*, based on evidence that TIL survive significantly longer *in vitro* after IL-2 withdrawal. However, when 7 patients were treated with the IL-2-transduced TIL, without post-infusion supplementary IL-2, partial response was only seen in one patient. A further five patients were then treated with the genetically-engineered TIL, with post-infusion IL-2 was given as an additional measure; only one of these five patients had a partial response. It was concluded that genetically manipulating TIL to produce IL-2 did not result in increased persistence *in vivo*, potentially due to the TIL having shorter telomeres as a result of extended culture time required for this protocol. Some years later, the group attempted an alternative strategy of genetically engineering TIL to express an inducible single chain interleukin 12 (IL-12) receptor, with the theory that IL-12 production by these cells would support the TIL *in vivo*, negating the use for additional exogenous IL-2 (Zhang et al., 2015). In a trial of 17 patients, one patient had an objective response when infused with a lower number of transduced TIL, and when the TIL 'dose' was increased, 10 out of the other 16 achieved objective responses, without supportive IL-2 administration. However, there were moderate toxicity side effects, attributed to the elevated IL-12 levels, which included "liver dysfunction, high fevers, and sporadic life-threatening hemodynamic instability". The responses were also short-lived, often not lasting more than one month, which was a disappointing result, and highlighted some of the benefits of using a supportive IL-2 regime. However, it appears as though this group have since put considerable efforts into developing this IL-12 model, as a recent paper describes a new approach they have taken, swapping the activation-induced IL-12-producing system for membrane anchored IL-12 (Zhang et al., 2020). Theoretically, this would reduce the amount of released IL-12 found in the serum and give greater control and localisation to the interaction with IL-12. They demonstrated that this new anchored IL-12 improved T-cell therapies in both murine and xenograft models, taking promising steps towards a future clinical trial using this form of genetic engineering for ACTs.

1.6.8 Combination of TIL therapy with checkpoint inhibitor blockade

Another direction to investigate regarding improvement of TIL therapy for treatment of metastatic disease is combinatorial immunotherapy, for example combining checkpoint inhibitor blockade with TIL therapy, and this is starting to be seen in clinical trials (Mullinax et al., 2018). In the aforementioned paper, a clinical trial was conducted which combined the anti-CTLA-4 monoclonal antibody Ipilimumab with TIL therapy, with the aim of reducing TIL therapy attrition due to disease progression during the *ex vivo* TIL expansion phase. Patients were given Ipilimumab two weeks before tumour resection, 1-week post-resection, then again 2 and 5 weeks after the standard treatment with pre-conditioning chemotherapy and TIL infusion plus IL-2. The trial results showed that all patients received the first two doses of Ipilimumab, with 93 % (12 out of the 13 patients) then proceeding to be given TIL therapy, which as considerably improved from the 32 % attrition rate previously experienced by the institute. The ORR, measured as a secondary endpoint, and was 38 % after 12 weeks, with a 31 % ORR after 1 year, demonstrating the combination of Ipilimumab and TIL therapy was well tolerated and decreased attrition due to disease progression. This was compared to This was the first published example of combining TIL therapy with checkpoint inhibitor blockade, and this approach appears to have been adopted by other researchers, through details of clinical trials combining TIL therapy with anti-PD-1 (Chesney et al., 2019; Kverneland et al., 2020).

1.6.9 Current landscape of TIL therapy clinical trials

The majority of TIL clinical trials follow the standard TIL generation protocol, preceded by lymphodepleting chemotherapy and in conjunction with post-infusion IL-2. However, a number of trials across different countries are adopting some well-reported adaptations to standard TIL therapy, such as the Tran et al. 'young' TIL protocol or attenuated IL-2 dose described by Andersen et al. (Tran et al., 2008; Andersen et al., 2016). As previously mentioned, to date, TIL therapy for advanced melanoma has not been licensed as a medicinal product and is only available through clinical trials or at some facilities which manufacture it on a compassionate basis, such as a specials treatment licensed by the Medicine and Healthcare products Regulatory

Agency (MHRA) specials treatment in the UK. A list of clinical trials utilising TIL therapy can be found in table S1 in the supplementary section.

To summarise table S1, there are currently 57 ongoing clinical trials involving TIL therapy globally, as identified through a search of the clinical trials database. Over half (30 out of 57) of these are being conducted in USA, but other key centres for TIL therapy trials include China (9), Israel (4), Denmark (6), Canada (4), France (5), the UK (3), Switzerland (6) and the Netherlands (4). The majority of these clinical trials (38 out of 57) are in or are planned to progress to phase II, however there is only one trial in phase III, which highlights the need for reliable phase II data and further TIL therapy research to really progress this immunotherapy. Regarding the types of cancer being targeted, 27 out of 57 specifically mention melanoma in some form, which is unsurprising given the previous promising clinical data in this indication. However, it is encouraging to see a variety of other cancer types being targeted, especially considering the poor prognosis and lack of current therapeutic options for some of those cancer types, such as pleural mesothelioma and glioblastoma (Tsao et al., 2009; Armocida et al., 2019). There are also a mix of different types of treatment, with several trials investigating the effect of previously-validated 'young' TIL or low-dose IL-2 in different disease settings, while others are bringing novel, transgenic TIL into the clinic. The variety of different TIL treatments in different cancer disciplines is very promising for the field of cancer immunotherapy and paves an exciting road ahead for this adoptive cell therapy.

1.7 Elucidating the tumour-reactivity of TIL; a challenge for improving TIL therapy

In order to investigate optimising TIL therapy, it is important to look at the proportion of cells which actively respond to the tumour, as well as what the tumour-reactive cells are recognising. With most research in the field of TIL therapy focussing on how to increase persistence and abrogate the immunosuppressive tumour microenvironment, questions remain regarding the innate tumour-reactivity of different TIL. Part of this question comes in the form of identifying what antigens tumours are expressing and whether this changes over time or between different metastases, which in turn might affect the choice of immunotherapy used.

1.7.1 TIL recognition of shared antigens

One of the reasons underpinning the success of TIL therapy is that it contains T-cells reactive to a broad spectrum of antigens. However, there has been little work done towards investigating and interrogating the tumour-reactive population of T-cells across multiple different patients. Could it be that the type of antigens being targeted by the T-cells within TIL has a correlation with patient outcome? A series of experiments investigating the relative tumour expression of a number of melanoma-associated antigens was carried out by Barrow et al., with the aim of finding links between antigen expression and potential prognostic factors (Barrow et al., 2006). They selected six, frequently expressed, melanoma-associated antigens and evaluated their expression in 586 primary or metastatic melanoma samples from 426 patients, with multiple samples taken from 86 patients to study expression over time. Out of the six antigens, three were associated with differentiation (gp100, MART-1 and tyrosinase), and three were CT antigens (members of the Melanoma Antigen Gene (MAGE), MAGE-A1 and MAGE-A4, and NY-ESO-1). Previous studies tended to evaluate the different groups of antigens separately, however the authors pointed out that polyvalent vaccines could be developed incorporating more than one antigen, hence the relevance of investigating them side-by-side. The prevalence of the CT antigens in primary tumours was 20 %, 9 %, and 45 %, respectively. A key observation they noted was that the expression of the MAGE antigens increased with tumour staging, rising to 51 % and 44 % respectively in distant metastases. This result was not observed for the

differentiation antigens, whose expression remained high (93-95 %) regardless of tumour stage or location. For the differentiation antigens, all three antigens were co-expressed in 94 % of primary melanomas, with 89 % of metastases also presenting all three antigens. From this data, one might conclude that there is a high chance of TIL harbouring TCRs reactive to differentiation antigens, due to their higher expression. However, there is evidence to the contrary shown by Kelderman et al., who showed that unmodified TIL had a low recognition rate of these antigens, an observation first made by Kvistborg et al. (Kelderman et al., 2016; Kvistborg et al., 2012). However, they sought to enhance the TIL by selectively expanding TIL with shared-melanoma antigen reactivity. This approach was successful, increasing the reactivity of the TIL to the matched tumour from 7 % to 48 % in clinical-grade TIL. However, it is right to include the caveat that tumours have to be shown to harbour these specific melanoma-associated antigens for the TIL to be effective. Part of the appeal of TIL therapy is that TIL are reactive to multiple different epitopes, particularly neoantigens which are optimal antigens for TCR targeting due to their tumour-restricted expression.

In a more comprehensive study of antigen-specific responses in TIL generated for metastatic melanoma, Andersen et al. developed a high-throughput screen of 175 melanoma-associated epitopes to test the reactivity of different TIL populations (Andersen et al., 2012). Their results showed that heterogenous TIL populations contained both high frequency populations and a range of different low frequency, antigen-specific populations. The antigens which had the most responses were differentiation antigens gp100 and MART-1, which bound to the HLA class I proteins with relatively low affinity. When drawing conclusions from their experiments, they were clear to acknowledge that the current repertoire of known melanoma-associated antigens is not sufficient to provide conclusive answers about tumour reactivity in melanoma TIL populations. Some of the populations not identified by the screen developed by this lab might include T-cells specific to neoantigens, representing a more patient-specific population of cells.

An interesting new study has sought to delve deeper into tumour antigen reactivity of TIL to shared melanoma antigens through the use of novel peptide-exchangeable peptide-HLA multimers (Murata et al., 2020). The artificial antigen-presenting cells they used covered 25 different MHC class I alleles and more than 800 peptides to more

comprehensively map the reactivity to shared melanoma epitopes for eight melanoma patient TIL products. This approach is exciting as previous efforts to investigate reactivity to known antigens were largely restricted to HLA-A*0201, since it is one of the most prevalent HLA class I alleles in the Western population. They showed that over 12 % of the TILs recognised a mean of 3.1 shared antigens from HLA-A, -B and -C. Not only does this confirm that shared antigens are widely expressed between patients but that research restricted to HLA-A*0201 epitopes could be missing out key tumour-reactive TCRs with alternative HLA allelic restrictions, which could be greatly beneficial for treating a wider proportion of melanoma patients.

1.7.2 TIL recognition of neoantigens

Identifying and pre-clinically validating TIL which are reactive to neoantigens is a more complex challenge than the previous approaches using shared-melanoma antigens as the antigen sequence and TCR haplotype are often both unknown. However, advances in next generation sequencing techniques have allowed researchers to begin to dissect TIL responses to such patient-specific antigens. As previously mentioned, a high number of somatic mutations can correlate with the immunogenicity of a tumour. In a recent, meta-analysis study by Brown et al., it was shown that cancers with a greater number of exomic, missense mutations have much higher numbers of infiltrating CD8+ lymphocytes, which also correlated with higher patient survival rates (Brown et al., 2014). The approach taken involved analysing RNA sequence data of 515 patients, taken from The Cancer Genome Atlas. The data generated here could be a useful tool for predicting which therapeutic option is best for a given patient, bringing a more personalised approach to cancer treatment; the more somatic mutations present, the greater the likelihood of immunotherapy being a valid option for treatment.

In a study using human patient data, Robbins et al. used whole exome sequencing data of metastatic melanoma and matched normal DNA, combined with a pMHC binding algorithm, to identify candidate neoantigens for three patients (Robbins et al., 2013). From the three patient melanoma samples tested, which were HLA-A*0201, HLA-A*0101 and HLA-A*2601 restricted, they found 62, 56 and 50 candidate epitopes respectively. Using algorithms to identify the peptides predicted to bind with high

affinity to the relevant HLA complex, they narrowed the selection to a few candidate neoantigens per patient, to be taken forward for further validation (Nielson et al., 2007). When the candidate neoantigens were screened for reactivity against matched patient TIL, they were shown to be recognised by T-cells within the TIL, demonstrating that TIL harbour neoantigen-specific TCRs and detailing a method by which these neoantigens can be identified. They suggest that this is a more accessible approach to identifying mutated tumour-specific antigens compared with other efforts which involve establishing a complementary DNA (cDNA) library to use for screening tumours.

Another paper reporting neoantigen recognition by melanoma TIL describes a discordance between TIL reactivity and antigen presentation through pMHC complexes (Wickström et al., 2019). The researchers carried out exome sequencing and HLA-A*0201 epitope prediction for cell lines from two melanoma TIL patients where the TIL showed a high degree of tumour reactivity. The candidate neoantigens were tested for reactivity by matched TIL, as well as presentation by MHC class I molecules. They found that the patient TIL only recognised 5/181 or 3/49 neoantigens respectively, and that only one of those neoantigens was presented efficiently by MHC class I for each patient (for the second patient, this was only observed after treatment with IFNɣ). These results indicate that despite advancements in sequencing technologies and mathematical modelling to predict neoantigens, there are more complex issues surrounding the efficient presentation and recognition of those neoantigens by MHC molecules and TIL respectively.

1.7.3 Presence of 'bystander' T-cells in TIL

Some researchers investigating tumour-reactivity of TIL have found that large populations of non-reactive cells can be found within TIL populations. For example, an interesting finding by Li et al. was that along with great success of TIL therapy for patients with locoregionally advanced nasopharyngeal cancers, there was specific clonal expansion of Epstein-Barr virus (EBV)-reactive T-cells in the plasma of patients, accompanied by clearance of EBV particles in the patient post-treatment (Li et al., 2015). This offers an exciting alternative therapy option for patients with this cancer

type, which is important since EBV-specific TCR T-cell therapy has proven to have only partial responses, potentially due to the evolution of EBV antigens in the tumour. However, it has also been evidenced that T-cells reactive to bacterial or viral antigens can be found in tumours that do not harbour these epitopes (Simoni et al., 2018). The reason for the presence of these 'bystander' CD8+ T-cells in tumours is unknown, but if they are isolated and expanded along with tumour-reactive T-cells, then the overall proportion of tumour-reactive cells in the final TIL product will be affected.

1.7.4 Breadth of TIL repertoire plays a role in tumour-reactivity

The breadth of the TIL repertoire is an interesting topic, and one which has not been explored fully to date. A popular approach to defining the TCR repertoire of a population of T-cells has been the use of flow-cytometric approaches, through antibody staining the variable beta (Vβ) regions of TCRs. Sometimes this is combined with more in-depth molecular approaches, such as spectratyping, which analyses the lengths of the TCR-CDR3 regions (Pilch et al., 2002). An early report analysed the TCR repertoire of melanoma TIL products used to treat patients, with the first observation being that HLA-A2-restricted, melanoma-reactive TCRs can react to different HLA-A2 matched patient tumours, giving evidence that there are TCRs raised against shared melanoma antigens present in TIL (Nishimura et al., 1994). A further observation was that the repertoire of these TIL tended to be quite broad, with approximately 11 (+/- 6) of the 23 measured Vβs identified in the TIL products. The paper did note that there was no particular Vβ that was associated with clinical response, indicating that melanoma-specific TCRs are not restricted to specific Vβ expression, and that clinical response is unlikely to arise from a single, large clonal expansion.

There have been many studies which investigate the breadth of the TCR repertoire with respect to the ensuing anti-tumour response of TIL. This follows the idea that the TIL harboured by tumours are reactive to multiple different antigens, as opposed to only a few known antigens. In a comparison of TCR diversity of tumour-infiltrating T-cells from colorectal cancer and adjacent mucosal tissues, it was found that the TIL TCR repertoire was broader in the colorectal cancer setting than healthy mucosa (Sherwood et al., 2013). Another study by the same group using ovarian TIL

demonstrated that the TCR repertoire showed a high degree of homogeneity between different samples of the same tumour, and that this repertoire was distinct from that seen in peripheral blood T-cells (Emerson et al., 2013). A correlation has also been observed between TCR Vβ diversity and age, with the diversity of TIL but not peripheral blood lymphocytes (PBL) decreasing as age increases; TIL samples were from patients with lung, colon or liver cancer, showing that this phenomenon is not restricted to a particular cancer type (Shao et al., 2014). Another study has shown that the synergistic effect of combining two different therapies, radiotherapy and anti-CTLA-4, leads to tumour eradication in a melanoma mouse model, and the TCR repertoire of the TIL isolated from the tumour after treatment with this combination is broader than just anti-CTLA-4 therapy, while still allowing oligoclonal expansion (Rudqvist et al., 2018).

One study carried out for oesophageal squamous cell carcinoma (OSCC) using next-generation sequencing techniques effectively demonstrated that the TCR repertoire of TIL is distinct to the repertoire of T-cells in nearby tissue, corroborating the results seen by Sherwood and Emerson (Chen et al., 2016; Sherwood et al., 2013; Emerson et al., 2013). This illustrates that TIL likely infiltrate tumour in response to antigenic stimulation, and have an innate enhanced ability to do so, compared with peripheral lymphocytes that do not possess TCRs directed against tumour antigens. Secondly, they analysed the TCR repertoire of TILs from different segments of the same tumour, to investigate the breadth of the repertoire across a whole tumour sample. They found that approximately 25 % of the top 100 TCRs were shared between different tumour sections. The most prevalent TCR clone was ubiquitously found in all of the tumour segments, whereas other TCR clones were just found distinctly in one segment. It is likely that the TCR clones that were shared between different tumours were reactive to mutations present across the whole tumour, whereas locally-restricted clones are likely to be reacting to mutations that are confined to one area of the tumour. It is important to consider if these findings are shared between TIL from other tumour types, or purely characteristic of OSCC. Research previously carried out repertoire analysis using TCRβ sequencing methods for other tumour types found that TIL from renal cell carcinomas were highly heterogenous, whereas TIL from ovarian cancer was much more homogenous (Gerlinger et al., 2013; Emerson et al., 2013). This could be

explained by referring back to figure 1.6 and comparing the mutational load of these different tumours. The figure shows that oesophageal cancers have a higher number of somatic mutations than ovarian cancer, and while not all the specific cancer types are shown in this figure, the mutational load of other cancers of the kidney are generally higher than ovarian cancers. On this basis, it is likely that melanoma would have the broadest, most heterogenous TIL population of all cancer types.

1.7.5 Does TIL repertoire change during ex vivo expansion?

In order to ensure a consistent, optimal and therapeutically beneficial TIL product, it is a good idea to question how the TIL generation process, including outgrowth and REP phases, alters the repertoire of the resulting TIL product. Efforts have been made by some researchers to directly study the diversity of TIL, prior to expansion. One such evidence of TIL diversity observed in this was came from a 1992 paper, where polymerase chain reaction (PCR) was used to detect TIL from a melanoma metastasis directly, to avoid any bias introduced through *in vitro* culture, and 266 β-chain transcripts were found (Ferradini et al., 1993). They were able to identify TCR-β transcripts that appeared to have clonally expanded within the tumour site, likely as a result of antigenic stimulation.

More recently, studies on TIL generation have focused on the phenotype of the final TIL products, and changes have been implemented to produce functionally optimal TIL, such as increasing the proportion of CD8+ effector memory TIL, without considering the diversity of the resulting repertoire. If it is evident that the breadth and reactivity of TIL changes during this stage, does this result in a narrower TCR repertoire, and more importantly, is this functionally beneficial or detrimental to the reactivity to autologous tumour? If it is shown to be detrimental, changes could be made to the process to result in a broader repertoire, providing the functionality of the TIL remains optimal. These are questions that have been addressed by a few researchers in recent years. Firstly, it was shown that in both pancreatic ductal adenocarcinoma and metastatic melanoma TIL, the frequency of clones which were dominant in the tumour was considerably reduced after *in vitro* cell culture (Poschke et al., 2020). In fact, in several patients, all of the top 25 TCRs were lost after *in vitro* TIL expansion, which was

accompanied by expansion of other TCR clones typically present at very low frequencies in the tumour samples. Through the use of duplicate or triplicate TIL cultures using cells from the same tumour fragment or metastasis, they demonstrated the reproducibility of this TIL expansion, noting the same TCR clones were expanded in each culture, and the clonal hierarchy was very similar. This implies that there is an intrinsic capacity of particular clones to greatly expand *in vitro*. Another observation regarding changing clone frequencies during TIL expansion made by Andersen et al. was that post-REP TIL showed a decrease in tumour-specific T-cells and an increase in viral-specific T-cells (Andersen et al., 2012). This highlights one of the drawbacks about using a REP to expand T-cells *in vitro*; the potential expansion of non-tumour-reactive T-cell populations, such as the 'bystander' T-cells mentioned previously and likely observed in this study also.

1.7.6 Investigating the prevalence of tumour-reactive clones

Whilst a broad TIL TCR repertoire might be beneficial in capturing tumour-reactive clones against a large range of different mutated and non-mutated antigens, the frequency of tumour-reactive clones in the final TIL product is likely to also be important. We know from various past studies discussed earlier that TIL products are seldom ever fully tumour-reactive, potentially as a result of anergy, exhaustion and T-cell inhibition. From a previous theory that CD8+ PD-1+ TIL represent the most tumour-reactive cells in the repertoire, one study investigated the TCR repertoire and reactivity of this population prior to *in vitro* culture to look at the clones present in the tumour (Pasetto et al., 2016). The rationale behind focussing on this population was to investigate if antigen encounter *in vivo* resulted in oligoclonal expansion of tumour-reactive clones, meaning that most prevalent TIL clones found in TIL would also likely be tumour-reactive. They found that the most abundant TCR clones from TIL analysed from 12 metastatic melanoma patients shared the CD8+ PD-1+ phenotype. From these, 7 out of the 12 top TCRs from the 12 TIL samples also recognised autologous tumour, and in 11 out of 12 TIL samples, up to 5 tumour-reactive TCRs were identified from the top 5 most abundant clones. This data allows us to draw some important conclusions. Firstly, it confirms that CD8+ PD-1+ T-cells are largely tumour-reactive. Secondly, that the relative abundance of TCRs in this population has a degree of

correlation with tumour-reactivity. But also, it was not always the case that the most abundant clone was tumour-reactive. In this paper, they address this in the discussion by highlighting that incorrect pairing could have been a factor in these results, along with errors arising from the PCR method used. This result, and the considerations around it, is an important caveat which should be considered when drawing conclusions. If the most abundant TCRs in a given TIL population are likely to be tumour-reactive, it should be possible to identify and selectively expand tumour-reactive clones based on their relative abundance via flow cytometry, without the need for expensive, time-consuming techniques such as next-generation sequencing. This is a theory that will be considered and addressed in this thesis.

1.8 Aims of PhD Thesis

In this PhD thesis, tools and technologies have been developed to interrogate the TIL TCR repertoire. This began with a research collaboration with an American company GigaMune Ltd. (previously known as GigaGen Ltd.), which utilised their novel paired TCR single-cell sequencing to identify the definitive TCR repertoire for a number of TIL samples (Spindler et al., 2020). This work was then furthered by development of an in-house method which was subsequently validated to show correct identification of tumour-reactive TCRs within TIL populations. As there has been significant work demonstrating the benefit of minimally-cultured TIL, the work in this thesis aimed to develop a workflow which could quickly and easily identify T-cells from TIL which have the potential to eradicate tumours, as well as isolate them for generation of an enhanced TIL product. While significant advancement in various sequencing approaches have allowed for TCR-αβ repertoire to be investigated, this approach can be both costly and time-consuming, making it unrealistic to carry out on a large-scale basis. To work around this limitation, the question of whether cheaper and time-efficient methods of T-cell analysis, based around flow cytometry, could be used to identify and characterise tumour-reactive populations, either in conjunction with TCR sequencing, or independently was also investigated.

This PhD project has been based at Instil Bio UK (formally Immetacyte Ltd.), a company who produce TIL products for the treatment of advanced metastatic melanoma patients who have progressed after treatment by other therapies. This has enabled access to, and use of frozen, excess final TIL products and matched autologous tumour cells, in the form of tumour lines grown out from patient tumour digest. This use of these valuable resources has allowed the retrospective analysis of multiple TIL products, which can be combined with the insight of whether the TIL therapy was successful *in vivo*. This aspect of the project design is quite different from previous approaches, which have tended to look at TIL repertoire prior to outgrowth. There are benefits and drawbacks to each approach, which will be taken into consideration during the project.

Questions remain in the area of TIL therapy regarding the optimal breadth of TIL repertoire, and whether this is affected by the TIL generation process. Using final TIL products, the breadth of the tumour-reactive repertoire has been investigated, with

attempts to identify patterns either regarding TCR diversity or linked gene expression which might help identify novel indicators of responders to TIL therapy. Fortunately, for some patients there was also access to follow-up blood from different time-points after TIL infusion, and this was used to compare the final TIL product with the surviving TIL to investigate whether clonal expansion *in vivo* post-treatment could be linked with tumour-reactive clones.

As discussed in the above introduction, there have been several shared melanoma antigens identified between melanoma patients, and the substantial research in this area has allowed for the development of TCR T-cell therapy. These melanoma-specific TCRs show promise, to the point where researchers have tried to manipulate TIL to selective expand these cells during TIL generation phase. As previously reviewed, some TCR T-cell therapies have failed due to unknown cross-reactivity of the TCRs used, and the way they were generated that bypassed thymic selection (Oppermans et al., 2020). With these findings in mind, the hypothesis was generated that tumour-specific TCRs harboured within TIL products would display optimal cross-reactivity profiles compared to TCRs identified from non-thymically selected populations. The work in this thesis has aimed to identify such TCRs and subsequently interrogate them in terms of antigen reactivity, cross-reactivity and tumour-reactivity. Utilising thymically-selected TCRs in TCR therapy, or selectively directing TIL product to expand these melanoma-specific clones could be promising therapeutic strategies, providing the TCRs identified show good, specific antigen and tumour-reactivity.

2.0 Materials and Methods

2.1 Tissue Culture

Table 2.1. Cell culture media and buffers used during project

Reagent	Constituents
293T media	Dulbecco's Modified Eagle's Medium (DMEM) (1X)+GlutaMAX™-I (Life Technologies™), 10 % Foetal Calf Serum (FCS) (Sigma-Aldrich), 1 % Penicillin/Streptomycin (P/S) (Sigma-Aldrich), 1 % 4-(2-hydroxyethyl)-1-piperazineethanesulfonic acid (HEPES) solution (Sigma-Aldrich)
Freezing media	FCS, 10 % Dimethyl sulphoxide (DMSO) (Sigma-Aldrich)
PEF	PBS, 0.5 % FCS, 2 mM Ethylenediaminetetraacetic acid (EDTA) (VWR Life Science)
T-cell media	RPMI medium 1640 (1X) (Life Technologies™), 10 % FCS, 1 % P/S, 1 % HEPES solution
Tumour cell media	Iscove's Modified Dulbecco Media (IMDM) (Life Technologies™), 20 % FCS, 1 % P/S, 1 % HEPES solution
Wash buffer	PBS, 0.05 % Tween® 20 (Sigma-Aldrich)

Table 2.2 TCRs used in project

Name	Reactivity	Origin	HLA-A2 restricted	Reference
Gp100-1	Gp100	Jurkat library for TIL039	Y	Spindler et al. (2020)
Gp100-2	Gp100	Jurkat library for TIL039	Y	Spindler et al. (2020)
Gp100-3	Gp100	Jurkat library for TIL039	Y	Spindler et al. (2020)
Gp100-4	Gp100	Jurkat library for TIL039	Y	Spindler et al. (2020)
Gp100-5	Gp100	Jurkat library for TIL039	Y	Spindler et al. (2020)
Gp100-c	Gp100	Transgenic mouse	Y	Johnson et al. (2009)
MART-1	MART-1	PBMCs	Y	Cole et al. (2009)
TCR1	Unknown	TIL054	Y	N/A
TCR2	Unknown	TIL054	Y	N/A
TCR3	Unknown	TIL054	Y	N/A

Table 2.3 Tumour lines used in project

Name	Origin	Type	Culture	HLA-A2
SK-MEL-5	Commercial – (lgcstandards-atcc.org)	Cutaneous Melanoma	Adherent	Y
SK-MEL-28	Commercial – (lgcstandards-atcc.org)	Cutaneous Melanoma	Adherent	N
CTCM32.1	Patient-derived	Cutaneous Melanoma	Adherent	N
CTCM39.3	Patient-derived	Cutaneous Melanoma	Adherent	Y
CTCM41.1	Patient-derived	Cutaneous Melanoma	Adherent	N
CTCM54.1	Patient-derived	Cutaneous Melanoma	Semi-adherent	Y
CTMM4.1	Patient-derived	Cutaneous Melanoma	Adherent	Y
CTAM28.1	Patient-derived	Acral Melanoma	Adherent	Y
CTAM36.1	Patient-derived	Acral Melanoma	Adherent	Y
CTUM42.1	Patient-derived	Uveal Melanoma	Adherent	Y
H508	Commercial – (lgcstandards-atcc.org)	Colorectal Adenocarcinoma	Semi-adherent	

Table 2.4 TIL products used in project

Name	Type of melanoma	Patient response
TIL001	Cutaneous	Partial response
TIL003	Cutaneous	Complete response
TIL028	Acral	Stable disease
TIL032	Cutaneous	Partial response
TIL036	Acral	Stable response
TIL037	Cutaneous	Progressive disease
TIL038	Cutaneous	Complete response
TIL039	Cutaneous	Partial response
TIL040	Cutaneous	Progressive disease
TIL041	Cutaneous	Partial response
TIL042	Uveal	Stable disease
TIL044	Blue naevus	Stable disease
TIL045	Cutaneous	Not treated, patient too ill
TIL051	Cutaneous	Stable disease
TIL054	Cutaneous	Complete response
TIL060	Uveal	Stable disease
TIL065	Cutaneous	Stable disease

2.1.1 Patient-derived tumour cell lines

Patient-derived tumour cell lines were established by Instil Bio UK prior to the commencement of this PhD project, by the following method. Patient-matched tumour cell lines were grown by plating out 500 µL of PBS-washed tumour digest material per well onto 24-well tissue culture plates in tumour cell media, before incubating overnight at 37 ˚C. After 24 h, the supernatant was removed and replaced with fresh media. Wells were observed every few days, and tumour media was changed and wells were split following the method below as necessary.

2.1.2 Culturing and splitting cells

When approximately 80 % confluent, adherent cells such as melanoma cell lines were washed with 5 mL sterile PBS before 5 mL Trypsin-EDTA Solution (Sigma-Aldrich) was added and incubated at 37 ˚C for approximately 5 min. Once detached, the cells were added to 5 mL of the relevant media and centrifuged in 15 mL polypropylene tubes at 400 *g* for 5 min. The supernatant was then removed, and cell pellets were resuspended in tumour cell media. To split by a quarter, three quarters of the resuspended cells were discarded, and the remaining cells put back into tissue culture flasks. Depending on the rate of growth, most tumour cell lines were split 1 in 4, three times a week.

For assays using the immortalised cell line J.RT3-T3.5 ATCC ® TIB-153™ Homo sapiens peripheral blood ac (lgcstandards-atcc.org) (also referred to as JRT3, or Jurkats), cells were split by pipetting off approximately 50 % of resuspended cells and adding fresh T-cell media to the cell culture flask, to give a final concentration of approximately 5 x 10^5 cells/mL. For TIL and primary T-cells, IL-2 (Proleukin®, Novartis) at 200 international units (IU)/mL was also added.

2.1.3 Freezing and thawing cells

Cells were resuspended in an appropriate volume of freezing media and aliquoted into labelled cryovials before controlled freezing at 1 ˚C per minute in a Mr. Frosty™ (Thermo Fisher Scientific) to -80 ˚C. Once frozen, cryovials were transferred to liquid nitrogen vapour phase for long-term storage until further use.

To thaw, the cryovial of cells was put in a water bath set to 37 ˚C for approximately 5 min until thawed. The cells were then added to at least 5 mL of T-cell or tumour media, centrifuged and then resuspended at approximately 1 x 10^6 cells/mL in a relevant size tissue culture flask and incubated at 37 ˚C. For TIL and primary T-cells, IL-2 at 200 IU/mL was also added.

2.1.4 Counting cells

Cells were resuspended to create a single cell suspension and 10 µL of cells was added to 10 µL Trypan Blue solution (Sigma-Aldrich) and loaded onto a haemocytometer to be counted using a microscope. In other experiments, 50 µL of cells were resuspended in 200 µL PBS-EDTA-FCS (PEF) buffer and stained using 1:200 DRAQ7™ live/dead stain (Abcam) prior to counting on the MACSQuant® Analyser 10 flow cytometer (Miltenyi Biotec).

2.1.5 Isolation of PBMCs from buffy coats

Normal buffy coat (NBC) blood from donors (provided under ethical approval from the National Health Service Blood and Transplant (NHSBT) service) was carefully layered onto Ficoll®-Paque Plus (GE Healthcare) in a 50 mL Falcon tube, or a pre-prepared 50 mL LeucoSep™ tube (Greiner Bio-One). The cells were centrifuged at 400 *g* for 20 min, with 0 deceleration. The resulting PBMC layer was removed carefully using a Pasteur pipette, and washed in 50 mL cold PEF. The cells were centrifuged at 200 *g* for 10 min to remove platelets. To remove red blood cell contamination, 2 mL of 1X BD Pharm Lyse™ (BD Biosciences) was added to the cell pellet and vortexed, before incubating at room temperature in the dark for 15 min. The PBMCs were then washed and resuspended in T-cell media with 200 IU/mL IL-2 for further use.

2.1.6 T-cell isolation from PBMCs

T-cells were isolated from PBMCs using the EasySep™ T-cell isolation kit (Stemcell Technologies) as per manufacturer's instructions. Briefly, PBMCs were resuspended in PBS at 1 x 10^7 cells/mL and transferred to 5 mL polypropylene tubes. The cells were incubated with 50 µL/mL EasySep™ Human T cell Isolation Cocktail and incubated at room temperature for 3 min. After vortexing for 30 s to resuspend, 50 µL/mL of EasySep™ Dextran RapidSpheres™ were then added to the cells and resuspended using a pipette, before topping up to 2.5 mL with PBS. The tube was incubated for 3 min on the EasySep™ magnet, during which time the non-T-cell fraction was bound to the sides of the tube and untouched T-cells were negatively selected by pouring into a 15

mL Falcon. The T-cells were then resuspended in full T-cell media with 200 IU/mL IL-2 until further use.

2.1.7 Rapid Expansion Protocol

Up to 1 x 10^6 primary T-cells or TIL were seeded into either a T25 flask, 24-well or 6-well G-Rex® plate (Wilson Wolf). Irradiated PBMC feeder cells were then added at a ratio between 1:20 to 1:200 T-cells: feeder cells, along with 1 µg/mL PHA (Merck Chemicals) and 200 IU/mL IL-2 and the REPs incubated at 37 ˚C, 5 % CO_2. After 5 days, half the media was exchanged for fresh T-cell media, and fresh IL-2 added to give a final concentration of 200 IU/mL. IL-2 was added at this concentration every 2-3 days, and another half media exchange was carried out as required. After 12 days, the cells were counted and used in assays.

2.1.8 FACS sorting of T-cells

For FACS sorting, T-cells were centrifuged at 400 *g* and resuspended in PEF buffer and labelled with the appropriate antibodies (information provided in tables 2.3 and 2.4). After incubating at 4 ˚C for 20 min, the cells were topped up to 15 mL with PEF buffer and passed through a 70 µm MACS® SmartStrainer (Miltenyi Biotec) to obtain a single-cell suspension. The cells were then resuspended in 500-2000 µL PEF buffer with DRAQ7™ and transferred to 5 mL polypropylene tubes for analysis and sorting using a BD Influx™ flow sorter (BD Biosciences). Fluorescence minus one (FMO) and BD™ CompBead particles (BD Biosciences) were used to optimise sorting.

2.1.9 Lentivirus production using 293T cells

To a Poly-D-lysine coated T75 flask (Greiner Bio-One), 6 x 10^6 293T cells were plated out the day before transfection. For transfection, HEPES-buffered serum-free DMEM (pH 7.1) and DMEM + 10 % FCS (pH 7.9) media were prepared and syringe-filtered with an *Acrodisc*® 32 mm Syringe Filter with 0.2 µm *Supor*® Membrane (PALL® Life Sciences). The following components were combined in a 15 mL falcon: 10 µg pSF.lenti

transfer plasmid (Oxford Genetics), 30 µg lenti packaging plasmid mix (pVSVg, pCgpV, pRSV.Rev) (Cell Biolabs), pH 7.1 media (to make up to 1.425 mL), and finally, 75 µL of 1 M $CaCl_2$ (Sigma-Aldrich). The mixture was vortexed and left at room temperature for 20-30 min. Media was removed from the 293T flask and replaced with 6 mL pH 7.9 media. The virus mix was then briefly vortexed and added dropwise to the surface of the media and incubated at 37 °C, 5 % CO_2. The following day, media was replaced with fresh 293T media. After 48 hrs, the supernatant from the 293T cells was collected, centrifuged at 400 *g* for 5 min, and stored at 4 °C. A second supernatant collection took place at 72 hrs post-transfection, combined with the 48-hr collection and syringe-filtered with a 0.45 µm Minisart® Syringe Filter (Sartorius). To concentrate, supernatant was mixed with Lenti-X™ Concentrator (Clontech) at a 3:1 ratio and incubated at 4 °C for at least 30 min before centrifuging at 1,500 *g* for 45 min at 4 °C, resulting in a small off-white pellet of virus. The supernatant was carefully removed, and the pellet resuspended in T-cell media at 1/10 volume, aliquoted into 500 µL aliquots and stored at -80 °C until further use.

2.1.10 Transduction of T-cells using lentivirus

T-cells were plated out in a 96-well plate, at 100,000 cells/well, and activated overnight with Dynabeads® Human T-Activator CD3/CD28 beads (Thermo Fisher Scientific) at a ratio of 10 µL per 1 x 10^6 T-cells. The following day, the supernatant was carefully removed and replaced with 100 µL neat virus, plus 4 µg/mL polybrene (Sigma-Aldrich) and 200 IU/mL IL-2, and incubated at 37 °C. After 72 hrs, cells were stained and tested for transduction levels using flow cytometry.

2.2 Assays

2.2.1 Peptide information

The gp100 peptides were acquired from ProteoGenix in lyophilised form and were reconstituted in either distilled H_2O with or without DMSO, depending on solubility, giving a final concentration of 10 mM. The peptides used in this PhD are included in the table below:

Table 2.5 Peptide sequences of key peptides used for various assays.

Peptide name	Amino Acid Sequence	Relevant assay
Gp100 signal peptide	KTWGQYWQV	Peptide titration, Cross-reactivity
Gp100 variant 1 (P1)	ATWGQYWQV	Cross-reactivity
Gp100 variant 2 (P2)	KAWGQYWQV	Cross-reactivity
Gp100 variant 3 (P3)	KTAGQYWQV	Cross-reactivity
Gp100 variant 4 (P4)	KTWAQYWQV	Cross-reactivity
Gp100 variant 5 (P5)	KTWGAYWQV	Cross-reactivity
Gp100 variant 6 (P6)	KTWGQAWQV	Cross-reactivity
Gp100 variant 7 (P7)	KTWGQYAQV	Cross-reactivity
Gp100 variant 8 (P8)	KTWGQYWAV	Cross-reactivity
Gp100 variant 9 (P9)	KTWGQYWQA	Cross-reactivity
MART-1 peptide 1 (ELA)	ELAGIGILTV	Peptide titration
MART-1 peptide 2 (T3)	ELTGIGILTV	Peptide titration
MART-1 peptide 3 (FAT)	FATGIGIITV	Peptide titration

2.2.2 Antibody information

The mouse anti-human monoclonal antibodies used to produce the work detailed in this thesis are detailed in the tables below, categorised by the assays they were used for. In addition, a hamster anti-mouse TCR β-chain antibody (BioLegend®) was used throughout the project to detect TCRs that had been constructed using a mouse β-chain constant region, such as the gp100 TCRs.

2.6 Mouse anti-human TCR-Vβ mAbs (Beckman Coulter Ltd.) used for Vβ panel screens. Antibodies were bought conjugated to either Phycoerythrin (PE) or Fluorescein isothiocyanate (FITC). The international ImMunoGeneTics information system (IMGT) was used to identify which genes the Vβ antibodies corresponded to. For Jurkat library and TIL Vβ staining, 1 x 10^5 cells/well were stained in a round-bottom 96-well plate.

Vβ	Fluorochrome	IMGT Nomenclature
1	PE	TRBV9
2	PE	TRBV20-1
3	FITC	TRBV28
4	FITC	TRBV29-1
5.1	FITC	TRBV5-1
5.2	FITC	TRBV5-6
5.3	PE	TRBV5-5
7.1	PE	TRBV4-1
7.2	PE	TRBV4-3
8	FITC	TRBV12
9	FITC	TRBV3
11	PE	TRBV25
12	FITC	TRBV10
13.1	FITC	TRBV6-5
13.2	PE	TRBV6-2
13.6	PE	TRBV6-6
14	FITC	TRBV27
16	FITC	TRBV14
17	FITC	TRBV19
18	PE	TRBV18
20	PE	TRBV30
21.3	FITC	TRBV11-2
22	PE	TRBV2
23	PE	TRBV13

Table 2.7. Mouse anti-human mAbs used for gp100 and activation assays

Name	Fluorochrome	Supplier
CD107a (LAMP-1)	PE	Miltenyi Biotec
CD137 (4-1BB)	PE	BioLegend®
CD2	Peridinin-Chlorophyll-protein (PerCP)-eFluor®710	eBioscience
CD3	Allophycocyanin (APC), FITC, PE	Miltenyi Biotec, BD Biosciences
CD4	APC	Miltenyi Biotec
CD45	FITC	Beckman Coulter Ltd.
CD62L	APC	BioLegend®
CD69	PE	BioLegend®
CD8	PE-Vio770™, FITC	Miltenyi Biotec, BD Biosciences
DRAQ7™	Far-red	Abcam
Fixable Viability Dye	eFluor®780	eBioscience™
IFNɣ	APC	BioLegend®
IL-2	PerCP-ef710	eBioscience™
TNFα	PE-Cy™7	eBioscience™

Table 2.8. Mouse anti-human mAbs used for tumour immunophenotyping

Name	Fluorochrome	Supplier
CD273 (B7-DC, PD-L2)	PE	BioLegend®
CD274 (B7-HI, PD-L1)	PE	BioLegend®
CD54	PE	BioLegend®
CD58	PE	BioLegend®
Fixable Viability Dye eFluor®450	eFluor®450	Invitrogen™ eBioscience™
Galectin-9 (Gal9)	PE	BioLegend®
HLA-ABC	VioBlue®	Miltenyi Biotec
HLA-A2	PerCP-eFluor®710	Invitrogen™ eBioscience™
Melanoma-associated Chondroitin Sulfate Proteoglycan (MCSP)	PE	Miltenyi Biotec
anti-melanoma (MART-1, Tyrosinase and gp100)	PE	Novus Biologicals
Melanotransferrin (CD228)	PE	R&D Systems
MHC class I chain-related protein A and B (MICA/MICB)	PE	Miltenyi Biotec

2.2.3 Extracellular staining for flow cytometry

If used, adherent tumour cells were detached using trypsin, as per 2.1.1. Cells were washed twice with PEF and then resuspended in 50 µL PEF and the relevant antibodies added and incubated in the dark for 20 min at 4 °C. After staining, the cells were washed twice more with PEF and resuspended in 100-200 µL PEF with 1:200 DRAQ7™ live/dead dye for flow cytometric analysis.

2.2.4 Intracellular staining for flow cytometry

Cells were first stained with eFluor®780 Fixable Viability Dye as per manufacturer's instructions (Invitrogen™ eBioscience™), before fixing in 4 % paraformaldehyde (PFA) (VWR Life Science). After fixing, the cells were then stained for intracellular cytokines by permeabilizing the cells in BD Perm/Wash™ (BD Biosciences) and staining with the relevant antibodies for 25 min at 4 °C. Cells were then washed with BD Perm/Wash™ buffer and resuspended in 200 µL PEF buffer before the samples were run on the MACSQuant® Flow Cytometer.

2.2.5 Lentivirus titration using Jurkat cells

Immortalised, TCR-ve T-cell line J.RT3-T3.5 ATCC ® TIB-153™ Homo sapiens peripheral blood ac (lgcstandards-atcc.org) (from here on termed Jurkat cells) were plated out in a 96-well flat-bottomed plate at 1 x 10^5 cells/well and transduced with 100 µL media containing virus, mixed with 4 µg/mL polybrene at the following dilutions: neat virus, 1:50 virus: media, 1:100, 1:200, 1:400, 1:800 and media without virus, also referred to as non-transduced (NT). After 3 days, fresh T-cell media was added to feed the Jurkat cells. On the fifth day, Jurkats were stained with an antibody to detect receptor expression and run on the flow cytometer. Viral titre in transforming units (TU)/mL was calculated using an appropriate dilution based on the % of transduced cells, with the optimal infection range being 1-20 % of transduced cells. Less than 1 % transduction may not be reliable for assessing accurate transduction, and over 20 % increased the chances of a single cell being transduced twice. The following equation was used to calculate viral titre: Titre = (F x C/V) x D where F = frequency of % positive

cells, C = cell number per well at the time of transduction, V = volume of inoculum in mL, D = lentivirus dilution factor that gives between 1-20 % transduced cells.

2.2.6 Peptide titration assay

Antigen-presenting 174 x CEM T2 cells (ATCC® CRL-1992™) (from here on termed T2 cells) were used for all peptide assays due to their expression of HLA-A*02 and lack of transporter associated with antigen processing (TAP) which renders them unable to present endogenous peptide. T2 cells were plated in a 96-well round-bottomed plate at 1 x 10^5 cells/well, then loaded with serial dilutions of peptide by incubating at 37 °C for 1 hr. The T2 cells were then centrifuged and resuspended in fresh media with T-cells (either Jurkat or primary T-cells) at 1:1 ratio of T-cells to T2 cells and incubated at 37 °C overnight. The following day, cells were stained for either for extracellular activation markers as per 2.2.3 or for intracellular cytokines as per 2.2.4. For intracellular cytokine assays, 1:1000 each of Monensin solution (1000X) (Invitrogen™ eBioscience™) and Brefeldin A Solution (1000X) (BioLegend®) were added during the overnight co-culture.

2.2.7 Cross-reactivity assay

T2 cells were plated in a 96-well round-bottomed plate at 1 x 10^5 cells/well, then loaded with either gp100 index peptide or peptide variant with an alanine substituted at each position in the 9-mer peptide, by incubating at 37 °C for 1 hr. The T2 cells were then centrifuged and resuspended in fresh media with T-cells (either Jurkats or primary T-cells) at 1: 1 ratio of T-cells to T2 cells and incubated at 37 °C overnight. The following day, cells were stained either for extracellular activation markers as per 2.2.3 or for intracellular cytokines as per 2.2.4. For intracellular cytokine assays, 1:1000 each of Monensin solution (1000X) and Brefeldin A Solution (1000X) were added during the overnight co-culture.

2.2.8 Tumour co-culture assay

In a 96-well round-bottomed plate, tumour cells were plated out at 1 x 10^5 cells/well. Rested T-cells (Jurkats, primary T-cells or TIL) were then added to the tumour cells at a 1: 1 ratio of T-cells to tumour cells, and incubated at 37 °C overnight. The following day, cells were stained for either for extracellular activation markers as per 2.2.3 or for intracellular cytokines as per 2.2.4. For intracellular cytokine assays, 1: 1000 each of Monensin solution (1000X) and Brefeldin A Solution (1000X) were added during the overnight co-culture.

2.2.9 WST-1 assay

Water-soluble tetrazolium salt (WST-1) is a tetrazolium salt that gets cleaved into a red dye known as formazan when in the presence of living cells (Peskin and Winterbourn, 2000). As tumour cells have an enhanced metabolic activity, a measured reduction in this capacity can be inferred as a reduction tumour cells. In a 96-well round-bottomed plate, tumour cells were co-cultured with rested T-cells (Jurkats, primary T-cells or TIL) at varying ratio of T-cells to tumour cells, and incubated at 37 °C overnight. The following day, cells were centrifuged, 100 µL supernatant removed and 10 µL Cell Proliferation Reagent WST-1 (Roche) was added to the cells. After ~30 min incubation, a yellow colour developed and 80 µL supernatant was removed to a flat-bottomed plate for analysing on the FLUOStar® Omega plate reader (BMG Labtech). T-cells alone controls were included to for normalisation of the results, to account for any T-cell dye uptake.

2.2.10 TIL tumour co-culture and sample cDNA preparation for 10x Genomics® V(D)J and 5' gene expression library construction

The 10x Genomics® Chromium™ Single Cell Controller was used to generate thousands microdroplets containing individually barcoded cells, facilitating cDNA library generation and subsequent TCR repertoire and gene expression analyses of TIL products. This single cell barcoding technology allows full heterogeneity of the TIL product to be captured and explored in detail using paired V(D)J clonotype and gene expression clustering analysis.

In a 96-well round-bottomed plate, matched patient TIL and tumour cells were co-cultured at 37 °C overnight. The following day, the cells were pooled and stained for flow sorting and both CD2+ and CD2+CD137+ cell populations were isolated (as described in 2.1.7). The cells were counted, filtered with an appropriate size cell strainer, and ~8700 cells used to create cDNA for V(D)J and 5' gene expression (GEX) library creation. Libraries were created using the Chromium™ Single Cell 5' Library & Gel Bead Kit, Chromium™ Single Cell A Chip Kit, Chromium™ i7 Multiplex Kit, Chromium™ Single Cell V(D)J Enrichment Kit for Human T Cell and Chromium™ Single Cell Controller and Accessory Kit (10x Genomics®), according to the 10x Genomics® protocol.

In summary, a 10X PCR Master mix was prepared containing the Template Switch Oligonucleotides, RT reagent B, reducing agent B and RT enzyme C, before mixing with the appropriate volume of single cell suspension and nuclease-free water. The Chromium™ Next Gel Bead-In Emulsion (GEM) Chip G was assembled, and the gel beads were vortexed before 50 µL was carefully loaded into row 2 of the assembled chip. Into row 1, 70 µL of Master mix plus cell suspension was carefully loaded. Into row 3, 45 µL partitioning oil was carefully loaded and the GEM gasket was attached to the fully loaded chip, which was then immediately run in the Chromium™ Controller. Once the run was completed, the gasket was removed and 100 µL of the GEMs were very slowly removed from row 3. Over the course of 20 sec, the GEMs were dispensed into a tube strip on ice. Reverse transcription incubation of the GEM products was then set up in a thermal cycler, according to the protocol instruction. For GEM reverse transcription clean up, 125 µL of Recovery Agent was added to the sample at room temperature, resulting in a pink, biphasic mixture of recovery agent/partitioning oil

and an aqueous phase, which was carefully removed. For preparing the Dynabeads® clean-up mix, Dynabeads® MyOne™ SILANE were vortexed and added to clean-up buffer, reducing agent B and nuclease-free water, totalling 200 µL. The Dynabeads® clean-up mix was added to the sample and incubated at room temperature for 10 min. The samples were then placed on a Magnetic Separator in the 'High' position until the solution cleared. The supernatant was removed with the sample still in the magnet and 300 µL 80 % ethanol was added to the pellet for 30 sec. The ethanol was then removed and replaced with 200 µL ethanol for 30 sec. After the ethanol was removed, the pellet was air-dried for 1 min before 35.5 µL of Elution solution I (which was prepared with EB buffer, 10 % Tween® 20 and reducing agent B) was added to the pellet. The resulting cDNA was amplified by adding 65 µL of a cDNA Amplification Reaction Mix to the sample and incubating in a thermal cycler following the cDNA amplification protocol. The cDNA was quantified using the Qubit® (see 2.1.12) before V(D)J amplification and V(D)J library construction, or 5' GEX library construction.

The V(D)J Amplification Mix was prepared and 98 µL was added to 2 µL of sample post-cDNA amplification. The sample was then incubated in a thermal cycler according to the protocol. After V(D)J amplification, 50 µL SPRIselect reagent (0.5X) (Beckman Coulter) was added to each sample and incubated for 5 min at room temperature. The samples were placed in the magnet and when the solution cleared, 145 µL supernatant was transferred to a new tube strip. At this point, 30 µL SPRIselect reagent (0.8X) was added to the sample in the new strip and incubated for 5 min at room temperature. The sample was placed in the magnet until the solution cleared and 170 µL supernatant was removed. 200 µL 80% ethanol was added to the beads on the magnet, for 30 s. The ethanol was removed and the ethanol wash repeated for a total of two washes. The remaining ethanol was removed and 35.5 µL EB buffer was added to the beads, incubating at room temperature for 2 min. The sample was placed in the magnet on the 'low' position and 35 µL sample transferred to a new test strip. The above V(D)J amplification and post-amplification clean-up was repeated to allow for double sided size selection, and the resulting sample was quantified with the Qubit® prior to V(D)J library construction.

For V(D)J library construction, 50 ng worth of the sample was made up to 20 µL with nuclease-free water. The Fragmentation Mix was prepared on ice as per the protocol,

and 30 µL added to the 20 µL of sample. The thermal cycler was pre-cooled to 4 ˚C and the sample was added to the thermal cycler following the protocol for fragmentation, end repair and A-tailing. After this step, the Adaptor Ligation Mix was made as per the protocol and 50 µL added to the 50 µL of sample. The sample was then incubated in a thermal cycler following the protocol for adaptor ligation. For post-ligation clean-up, 80 µL SPRIselect reagent (0.8X) was added to each sample and incubated at room temperature for 5 min. The sample was placed in the magnet (high) until the solution cleared, then the supernatant was removed and 200 µL 80% ethanol was added to the pellet for 30 s. The ethanol was removed and the 80 % ethanol wash step was repeated for a total of two washes. After all ethanol was removed the pellet was air dried for 2 min before adding 30.5 µL EB buffer and resuspending. The sample was placed in the magnet (low) and 30 µL sample transferred to a new test strip. For sample indexing, an appropriate set of sample indexes from the PN-3000431 Dual Index Plate TT Set A were selected to make sure that no sample indices overlapped. To the 30 µL of sample, 50 µL of Amp Mix (PN-2000047/20000103) (10x Genomics) was added, and 20 µL of the individual Dual Index TT Set A added to the sample, recording the well ID used for each sample. The sample was then incubated in the thermal cycler according to the sample index PCR protocol, and afterwards the sample was cleaned up as per the SPRIselect clean-up described above. For 5' GEX Dual Index Library construction, a similar protocol as described for the V(D)J library construction was followed, including fragmentation, end repair and A-tailing double-sided size selection, adaptor ligation, ligation clean-up, GEX sample index PCR and GEX post sample index PCR double sided size selection.

After construction, the V(D)J and GEX libraries were quantified using the Qubit® and quality was assessed by GENEWIZ® prior to sequencing. To analyse the datasets, the 10x Genomics® Cell Ranger and Loupe Browser software was used, which processes the Chromium™ single-cell RNA-seq data and performs clustering analysis. The cross-compatibility of the Cell Ranger and Loupe Browser platforms allows both V(D)J analysis and gene expression data to be correlated for comprehensive analysis.

2.2.11 Lysing cells for protein assays

Adherent tumour cells were washed twice with PBS and detached using trypsin-EDTA. The cells were then centrifuged and washed twice more with PBS. To the washed cell pellet, 500 µL of ready-to-use, cold radioimmunoprecipitation assay (RIPA) buffer (Life Technologies™) was added along with 5 µL Halt™ Protease Inhibitor Cocktail (Thermo Fisher Scientific). The cells were left to lyse on ice for 15 min, then centrifuged at 14,000 revolutions per minute (RPM) for 5 min. The supernatant was collected and stored at -80 ˚C until needed.

2.2.12 Qubit® dsDNA Assay

cDNA libraries generated from the 10x genomics assay described in 2.1.10 were quantified using the Qubit® dsDNA HS (high sensitivity) Assay Kit (Life Technologies™), according to the standard protocol. In summary, Qubit® dsDNA HS reagent was diluted 1:200 in Qubit® dsDNA HS buffer to make a working solution. To 190 µL of Qubit® working solution, 10 µL of each Qubit® standard was added to the appropriate tube. For individual samples, between 1-10 µL was diluted in between 190-199 µL working solution. All samples and standards were then incubated at room temperature for 2 min before running on the Qubit® 3.0 Fluorometer.

2.2.13 IFNɣ ELISA

For the IFNɣ enzyme-linked immunosorbent assay (ELISA), the Human IFNɣ ELISA MAX™ Standard kit (BioLegend®) was used, which included Human IFN-γ ELISA MAX™ Capture Antibody (200X), Human IFN-γ ELISA MAX™ Detection Antibody (200X), Human IFN-γ Standard and Avidin-horseradish peroxidase (HRP) (1000X). Prior to running the ELISA, the Capture Antibody was diluted in ELISA Coating Buffer (5X) (BioLegend®), and 100 µL of the Capture Antibody solution was added to each well of a 96-well flat-bottomed plate. The plate was sealed and incubated overnight at 4 ˚C. The following day, the plate was washed four times using at least 300 µL of wash buffer (as detailed in table 2.1) per well and then residual buffer was removed by tapping the plate upside down on absorbent paper. To block non-specific binding and reduce the

background, 200 µL ELISA Assay Diluent (5X) (BioLegend®) was added to each well of the plate, after which the plate was sealed and incubated at room temperature for 1 hour while on a plate shaker. During this time, standard dilutions were prepared for the assay, according to the protocol. After blocking, the plate was washed four times with wash buffer and blotted as before. To each well, 100 µL of either standard dilution or samples (supernatant from a T-cell-tumour co-cultures) were added, the plate sealed and incubated at room temperature for 2 hrs on the plate shaker. The plate was then washed four times and blotted before 100 µL of diluted Avidin-HRP solution was added to each well. The plate was sealed and incubated on the plate shaker at room temperature for 30 min. The plate was washed five times, soaking the wells in wash buffer for 30 – 60 s each time. After blotting, 100 µL of 3,3',5,5'-Tetramethylbenzidine (TMB) Substrate Solution (BioLegend®) (prepared by mixing equal volumes Substrate A and Substrate B) was added to each well and the plate was incubated at room temperature in the dark until the desired blue colour developed. After this time, the reaction was stopped by adding 100 µL Stop Solution (BioLegend®) to each well, turning the colour from blue to yellow. The absorbance was then read on the FLUOStar® Omega plate reader (BMG Labtech) at 450 nm and the standard curve generated from the assay used to determine the concentration of IFNɣ in pg/mL.

2.2.14 Real-time qPCR

Real-time PCR was used to test the relative expression of *MART-1*, *gp100* and *tyrosinase* genes in four different melanoma cell lines, when compared to a housekeeping gene, *Glyceraldehyde 3-phosphate dehydrogenase* (*GAPDH*). PCR reactions were set up to give a total of 20 µL using the TaqMan® probes (Applied Biosystems) and qScript™ XLT One-Step RT-qPCR ToughMix (QuantaBio) in the reaction mix shown in table 2.6 shown below. The use of the qScript™ XLT One-Step RT-qPCR ToughMix allows cDNA synthesis and ensuing PCR amplification to be carried out in the same reaction using an optimised thermal cycling program. The PCR reactions were run on the StepOne™ Real-Time PCR System (Applied Biosystems) using the parameters set up in table 2.7. The assay was carried out using technical triplicates and RNA-free controls were added to check for non-specific cDNA amplification. The

resulting threshold cycle values (C_T values) from the three technical replicates were averaged and gene expression calculated using the following equation:

$$\text{Expression} = 2^{(C_T \text{ (housekeeping gene)} - C_T \text{ (gene of interest)})}$$

Table 2.9 PCR reaction mix for RT-qPCR reactions.

Component	**Volume added / µL**
qScript™ XLT One-Step RT-qPCR ToughMix	10
TaqMan® probes	1
Nuclease-free water	5-8 (dependent on RNA volume)
RNA template	2-5

Table 2.10 Thermal cycler program for RT-qPCR.

Step	**Temperature /**	**Time**
cDNA Synthesis	50	2 min
Initial denaturation	95	10 min
PCR cycling (40 cycles)	95	15 s
	60	1 min

2.3 Figures and data analysis

Figures were made using GraphPad Prism 8 (GraphPad Software, LLC). Statistical analysis was also carried out using GraphPad Prism 8 software. MACSQuant® data was analysed using MACSQuantify™ software (Miltenyi Biotec). V(D)J and GEX library sequencing and cluster analysis was conducted using the 10x Genomics® Cell Ranger software.

3.0 Identification of tumour-reactive T-cells from final TIL products through an optimal model system

3.1 Background

The main aim of this chapter of work is to interrogate the tumour-reactive repertoire of TIL products, for two means: To better understand the repertoire of T-cell receptors involved in an anti-tumour response, and to potentially identify TCRs which may be therapeutically beneficial.

3.1.1 Markers of activation – phenotypic changes and cytokine production

The tumour-reactivity of T-cells is essentially a characteristic which allows the cells to identify tumour cells, become activated as a result of interaction with those tumour cells and then carry out downstream effector functions. For T-cells, this reactivity is mediated by T-cell receptors binding to cognate peptide-MHC complexes, and enhanced by involvement of co-receptors such as CD4 and CD8, which helps to amplify downstream signal transduction (Laugel et al., 2007). As discussed in the chapter 1.2.3, the CD8 co-receptor typically engages with MHC class I molecules leading to cytotoxic effector functions, whereas the CD4 co-receptor engagement occurs with MHC class II complexes and has a more complex, supportive role in immunological responses (Bridgeman et al., 2011). In the above review, Bridgeman et al. discuss several suggested models of T-cell activation where the structure and conformation of TCR-pMHC complexes have important roles, such as the induced fit model and conformational change model. Some models are now more widely accepted than others, however there tends to be agreement that TCR-pMHC affinity directly impacts the level of T-cell activation, and the downstream effector responses of the T-cell.

T-cells respond to activation by altering their phenotype and effector activity; these changes can be utilised as an inference of recent activity. There are several targets in this activation pathway which can be used to identify whether a cell is reactive to tumour. T-cells upregulate a variety of different markers upon activation, for example CD69, CD71, CD25 and CD137, some of which are more easily identifiable than others, based on the localisation of the marker either extracellularly or intracellularly (Caruso et al., 1997). In this paper, the expression of activation markers CD69, CD25, CD71 and

HLA-DR on healthy donor T-cells are compared in response to different stimuli, over the course of 8 days. The peak expression of the different markers occurs at different time points, and the strength of these responses differs depending on the stimuli used for activation. CD69 can be detected on cells just 3 hours after activation with PHA, with a peak at 15 hours which starts to drop after 4 days. The other markers, CD25, CD71 and HLA-DR all show peak activation between days 4 and 8, demonstrating a different activation kinetic than CD69. When activated by the recall antigens tetanus toxoid or influenza A virus, all activation markers showed a similar kinetic profile, with peak activation of CD69 at day 6, and the other markers peaking around day 8. This evaluation of the kinetic profiles of different activation markers in response to different stimuli demonstrates that the choice of activation marker and timepoint for measuring activation marker expression are both important variables to consider, and can vary depending on the stimuli used.

Another marker which is expressed through a phenotypic change in T-cells following activation is CD137. CD137, also known as 4-1BB or TNFSFR9, is a member of the TNF receptor family, which has been identified as an inducible co-stimulatory receptor on mouse and human CD4+ and CD8+ T-cells, which leads to downstream activation and differentiation (Vinay and Kwon, 1998). Upon stimulation with cognate antigen-pulsed presenting cells, it has been shown to reach peak expression on T-cells at around 24 hours and decreases in expression after 72 hours (Wolfl et al., 2007). In this assay, the extent of CD137 expression was markedly higher than expression of other activation-related markers, including CD69 and CD25. It was also the only marker which was absent from rested, unstimulated T-cells, which is a favourable characteristic for the separation of activated and non-activated T-cells. Expression of CD137 has been associated with tumour-reactivity, making it a target of interest for identifying tumour-reactive T-cells within TIL; indeed, successful isolation of CD137+ T-cells that are specific for known antigens has been demonstrated by different researchers (Wolfl et al., 2007; Ye et al., 2014).

Another group of targets which can be identified in T-cells following activation by tumour cells are associated with downstream effector functions such as degranulation and cytokine production. In immunology research, these effector functions are often surrogate markers for activation and are widely used as identifiable markers in a

number of different assays, including ELISAs which measure cytokine production, and flow-cytometric assays. Degranulation is the process by which lysosomes are stimulated to move towards the point of cell-cell contact with the target cell and fuse with the cell membrane to allow cytokine release (Aktas et al., 2009). After fusion of the lysosomes with the cell membrane, soluble molecules are released into the immunological synapse to exert numerous effects on other effector and target cells. A widely accepted marker for measuring degranulation is CD107a, and this is commonly used as a marker for tumour-reactivity and an indirect measure of tumour killing. CD107a appears quite soon after initial activation markers, commonly detected at a maximal level just 4 hrs after tumour cell contact (Betts et al., 2003). It can be transiently identified on the surface of activated T-cells, however only briefly before being recycled by the endocytic pathway. Its primary location during activation is intracellular associated with lysosomes, meaning that for accurate measurement, T-cells need to be immobilised through fixation and permeabilised to allow antibodies inside the cell to stain the marker at this time. However, by incorporating CD107a-specific antibodies for the duration of stimulation, CD107a can be immobilised on the cell surface after cytolytic granules are released for up to 24 hrs, which would allow for extracellular surface detection (Betts et al., 2003). As it is a marker of degranulation, naturally the expression of CD107a is predominantly restricted to cytotoxic T-cells and natural killer cells, although it is constitutively expressed on activated platelets.

Cytokines are produced in response to T-cell activation and have several functions, including continued support of T-cells and activation of other cytotoxic cells such as natural killer (NK) cells. The measurement of cytokines is another popular method for assessing tumour reactivity, and there are multiple different approaches to achieve this. A review by Kupcova Skalnikova et al., highlights the range and applications of several methods of measuring cytokines, in the context of melanoma, due to the link between prognosis and cytokine production (Kupcova Skalnikova et al., 2017). These include current proteomic analysis techniques such as mass spectroscopy approaches, as well as new and emerging techniques, involving single-cell multiplex technologies; some of the most relevant and widely-used approached are discussed below.

One of the easiest, cheapest and most commonly-used methods of measuring cytokine production is through ELISA, by which the amount of a specific cytokine produced by T-

cells can be quantifiably measured. Some popular ELISAs used for measuring T-cell activity are IFNɣ and IL-2, two cytokines that are produced downstream of T-cell activation. However, there are some critical limitations of the ELISA. Firstly, the majority of ELISA kits tend to be monochromatic, meaning only one cytokine can be measured at a time, so multiple cytokines cannot be directly assessed for the same population of cells. Some polychromatic ELISA-type assays are available, but these are more complex and expensive. Secondly, the ELISA is a population-based analytical approach, meaning differential expression between different subpopulations cannot be distinguished; for an ELISA result to therefore be clearly attributed to a specific subpopulation, the cells would first need to be sorted to ensure a pure subpopulation is being measured. Fortunately, there are other ways of detecting and measuring cytokines that are not affected by these limitations. The most popular and versatile of these approaches is flow cytometry. Due to the polychromatic nature of flow cytometry, multiple different markers of activation and T-cell subpopulations can be measured simultaneously, on a single-cell basis. Cytokines can be measured intracellularly in conjunction with other markers, typically through co-culturing the cells with brefeldin which prevents the release of cytokines into the media, retaining them inside the cell. Through the use of various fluorochrome-conjugated monoclonal antibodies and different gating strategies during analysis, multiple markers of activation including cytokines can be measured simultaneously. One key difference with ELISA is that the reading is not a direct measure of the amount of cytokine produced, rather the amount of fluorescence emitted upon antibody binding to the cytokine is measured. These are often recorded as a percentage of the cell population that is emitting a signal detected by a specific channel on the flow cytometer, or the mean fluorescence intensity (MFI) of the population of cells. This type of analysis is particularly useful for deciphering which population of cells in contributing to a particular phenotypic change or cytokine response upon contact with tumour cells.

3.1.2 Assessing breadth of the tumour-reactive population

Analysing the breadth of TCRs in a given population is a complex challenge, given that there are over 10^{15} possible αβ TCR clonotypes (Murphy, 2012). Over the years, the advancement of different PCR-based sequencing approaches has provided researchers

with the tools needed to start to elucidate TCR repertoires. There are a couple of different methods that are commonly used for this purpose. One of the first genomics approaches to TCR repertoire analysis involved analysis of complementary determining region 3 (CDR3) length distribution through techniques such as Immunoscope or CDR3 spectratyping (De Simone, Rossetti and Pagani, 2018). In these techniques, the breadth of the repertoire was predicted by analysing the expected frequency of the CDR3 lengths to fit a Gaussian distribution model, with any deviation from this model indicating clonal expansion. These techniques were improved with the introduction of nucleotide sequencing techniques such as Sanger sequencing, and then again with high-throughput sequencing of DNA of millions of cells, allowing for whole CDR3 to be read and full α and β chains to be detected.

Given that the potential variation in antigen specificity is dictated by the CDR3 region of the β chain and can be largely attributed to gene rearrangements of the V, D and J regions, sequencing the β chains of T-cells provides a great deal of information about the breadth of a TCR repertoire. Additionally, due to allelic exclusion, only one β-chain is expressed by a single T-cell, whereas multiple different α-chains can be expressed; this effectively means that sequencing the β-chains provides a unique identifier for a specific T-cell (Bergman, 1999). Previous studies have used TCR-β sequencing approaches, such as Illumina sequencing of 5' rapid amplification of cDNA ends (RACE) products or multiplex PCR of the β-chain CDR3 regions to investigate the TCR-β repertoire of different samples (Freeman et al., 2009; Hou et al., 2016). However, using these approaches, one would not be able to definitively elucidate the TCR repertoire or isolate specific TCR sequences, as no information regarding the α-chain is provided. For more comprehensive TCR-αβ repertoire to be investigated, both the α and β chains should be sequenced. This has been shown to provide much more detailed data of the most prevalent TRA and TRB genes and CDR3 regions in a given T-cell population (Fang et al., 2014). However, for even more accurate TCR repertoire analysis, scientists have made considerable efforts to either predict TCRαβ pairings through advanced rearrangement modelling (Ruggiero et al., 2015), or conduct paired TCRαβ single cell sequencing, where the α and β chain remain together throughout the sequencing process to allow for definitive TCR repertoire analysis (Kim et al., 2012; Han et al., 2014; Howie et al., 2015; Spindler et al., 2020). These techniques typically use

emulsion-based PCR techniques to partition single cells using oil-in-water, creating PCR products on a cell-by-cell basis, which greatly increases the throughput of the model (Turchaninova et al., 2013).

The most accurate and comprehensive way to elucidate the TCR repertoire of a T-cell population such as TIL is undoubtably to use TCRαβ sequencing to sequence the entire cell product. However, while this is theoretically possible, it is not practical. Firstly, the degree of throughput of high throughput single-cell sequencing methods like the 10x Genomics® Chromium™ system is up to 10,000 cells per sample (10x Genomics® protocol). For a large-scale TIL product such as those utilised in this project, there are often at least 1 x 10^9 cells given back to the patient and the vials of TIL product are aliquoted often at 1 x 10^7 cells per vial. Therefore, to fully sequence even a single vial of TIL would be virtually impossible with the given time and monetary resources. Carrying out TCR analysis of pre-REP TIL prior to large-scale expansion would be more likely to detect all the TCRs present in the final TIL product. However, in the scope of this project, the focus was on retrospective analysis of TIL product. Therefore, a degree of sampling had to take place to estimate the breadth of the TCR repertoire.

A different, non-genomic approach for assessing TCR repertoire of TIL that is widely used is flow cytometric analysis of the TCR-β variable chains (Vβ) through specific antibodies, to give an idea of the breadth of the TCR repertoire. This approach is considerably less powerful and less informative than the next generation sequencing approaches, however the ease, speed and low cost of flow cytometry is ideal for initial TCR repertoire experiments, where the full power of PCR-based sequencing is not needed. Several different companies have produced antibodies against these variable regions, and while they do not cover the full spectrum of possible Vβ regions, they can provide good insight into how the repertoire is distributed. This has been used previously in the literature to track changes in T-cell distribution in a variety of disease settings, such as autoimmune diseases like Type I diabetes mellitus and systemic lupus erythematosus (Tzifi et al., 2013). In these cases, the Vβ panel highlighted specific subpopulations of CD4+ cells that were skewed in distribution when compared to healthy controls. For this project, a panel of 24 Vβ antibodies by Beckman Coulter was selected, with 12 conjugated to PE and 12 conjugated to FITC. This panel allows samples to be stained with two Vβ antibodies simultaneously, along with other

markers depending on how many channels the flow cytometer used can detect. Other antibody suppliers use pre-mixed panels of antibodies where 3 antibodies are combined carry the benefit of requiring fewer cells, however the different antibodies cannot be used independently in this case, and there are fewer empty channels left for further staining to detect other markers.

It is common for researchers to use a combination of sequencing and flow cytometry staining to assess TCR repertoire as the two techniques give complementary results. In the context of this project, assays to assess the breadth of the TCR repertoire were mostly carried out using flow cytometry, which were supported later on in the project by highly novel, paired TCR single cell sequencing with the 10x Genomics® Chromium™ system to further interrogate the tumour-reactive repertoire.

3.1.3 Aims

With the above methodological restrictions in mind, the first aim for this PhD project was to develop a model by which the breadth and extent of the tumour-reactive population of different melanoma TIL could be most effectively assessed *in vitro*. In order to address this aim, a model system would have to include a measure of tumour-reactivity that could be combined with method of identifying specific subpopulations of cells and eventually, the specific T-cell receptors responsible for the detected tumour reactivity. Other factors that came into consideration when designing the model systems included cost of reagents, time for assays and analysis, availability of cells within the scope of this project and the degree of throughput for the model. As one of the goals of the PhD project was to retrospectively analyse patient TIL products after re-stimulation with matched tumour, the starting material of cells was limited by the number of TIL available to use and whether matched tumour lines had been established for them. Therefore, an attractive model would be one that used very few cells but could be analysed in a variety of ways. In this chapter, three different models are explored with the aim of identifying tumour-reactive TCRs from TIL products: The Jurkat Library model, the Vβ comparison model and the CD137 co-culture model.

3.2 The Jurkat Library Model

3.2.1 Establishing patient-specific Jurkat libraries of TCRs

The first model system to be explored was part of a collaboration with the American company GigaGen Ltd. (now GigaMune Ltd.), which utilised their novel single-cell paired TCR sequencing approach that was originally developed for identifying virus-specific TCRs for vaccines (Spindler et al., 2020). A flow diagram illustrating their approach can be seen in figure 3.1, which gives an overview on how their microdroplet technology was used to allow for single cell emulsion PCR to take place, with more information on the methodology detailed in the Spindler et al. paper. In summary, using emulsion technology, single T-cells, oligo(dT) beads and lysis mixture were encapsulated into microdroplets. The RNA-bound beads were then reinjected into microdroplets with RT-PCR primers to allow for amplification of TCRα and TCRβ primers, which were subsequently linked through a region of complementarity to form a single PCR product. Following this step, the emulsion was broken to release the amplicons, which were cloned into vectors using successive rounds of Gibson assembly to reconstruct full length αβ TCRs. These were then packaged into lentiviral vectors to allow for the transduction of J.RT3-T3.5 Jurkat cells, a cell line that had been genetically engineered not to express the endogenous variable β-chain of the αβ TCR from the parental E6.1 Jurkat line (Ohashi et al., 1985). The J.RT3-T3.5 cells will now be referred to as Jurkat cells for the remainder of the chapter. The lentiviral plasmids used for the transduction contained a puromycin resistance gene, to allow for downstream selection of transduced cells with puromycin. The resultant Jurkat library of cells would, in theory, accurately represent the full repertoire of TCRs harboured by the TIL product, and due to the immortal nature of the cell line, allow for extended culture to provide a continual supply of cells. At this point, the Jurkat libraries were shipped to the UK, and all subsequent optimisation and characterisation was carried out as part of this PhD project. For optimisation, activation markers commonly used for Jurkat cells, such as expression of CD69 and loss of CD62L, could be utilised to measure reactivity to matched tumour and subsequent sorting of tumour-reactive cells with the rapid and easy expansion associated with using Jurkat cells (Buckley, Kuo and Leiden, 2001). Jurkat libraries were constructed for three TIL products which had matched tumour lines: TIL032, TIL039 and TIL041. The protocol, described in context of

TIL039 in the Spindler et al. paper, used around 1.4 million TIL039 for library construction, which resulted in just over 86,000 unique clonotypes (Spindler et al., 2020).

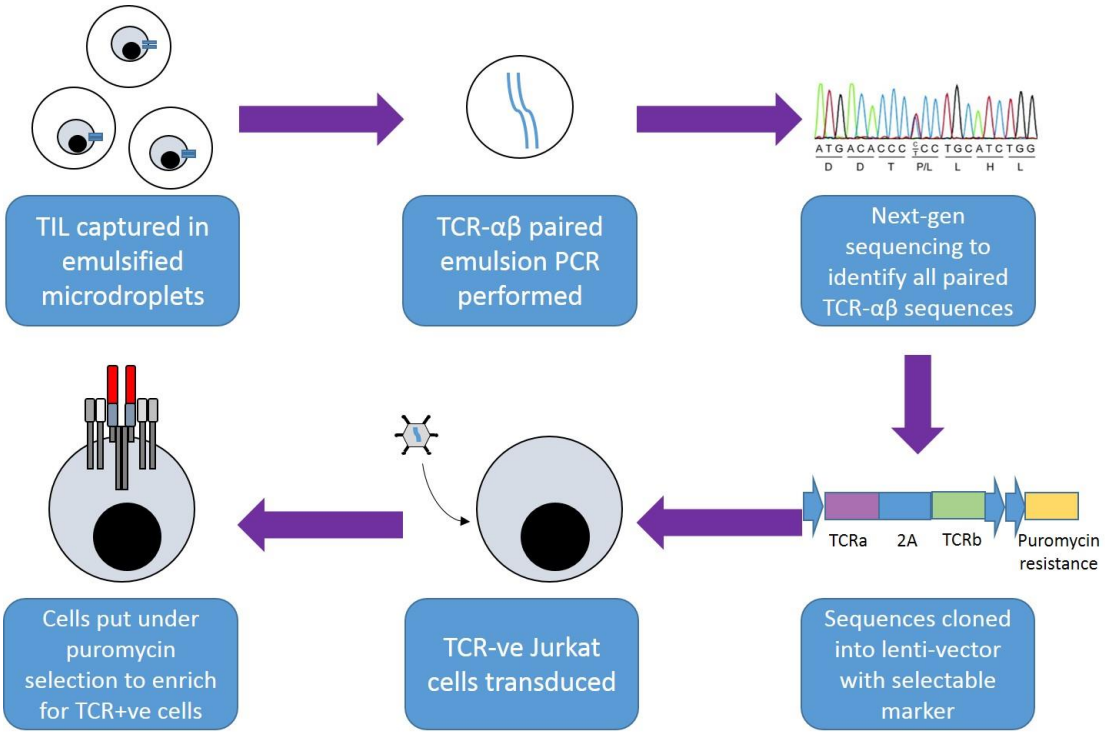

Figure 3.1. Diagram of the Jurkat library construction for the Jurkat library model. Flow diagram showing the process of construction of the Jurkat libraries carried out by GigaGen Ltd., using final TIL product supplied by Instil Bio UK. Full details can be found in the Spindler et al. paper (Spindler et al., 2020).

3.2.2 Optimisation of activation marker staining for Jurkat assays

As part of the model system development, the activation assays needed to be optimised to ascertain the optimal effector to target ratio (E: T), as well as the optimal timepoint for measuring the activation markers. To test these variables, one of the Jurkat libraries was co-cultured with the patient-matched tumour line, and subsequently the levels of activation markers CD69 and CD62L were measured. As shown in figure 3.2A and 3.2B., a 1: 1 E: T resulted in the highest activation of Jurkat cells when measured by CD69 expression, while the loss of CD62L did not change greatly between the different effector to target ratios. Using this E: T, the time course assay was then conducted, using PHA to activate the Jurkat libraries to ensure maximal response. The figure 3.2C showed that expression of CD69 gradually increased to 16

hr, and slightly dropped at 24, while CD62L was increasingly lost over time till 24 hr. It was decided that 24 hr was the optimal time point for measuring the two markers in conjunction.

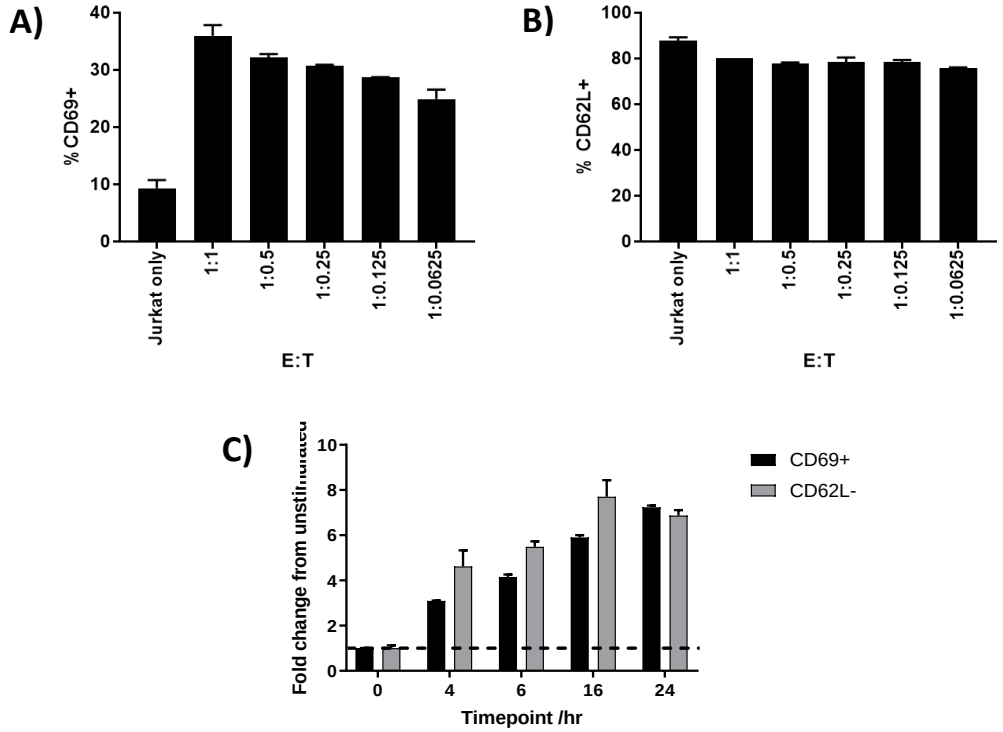

Figure 3.2. Optimisation of Jurkat library activation assays. Jurkat libraries were co-cultured with patient-matched tumour cells at varying effector: target ratios and the subsequent percentage of activated cells was identified through flow cytometry. A) Percentage of cells expressing CD69 at different E:T ratios. B) Percentage of cells expressing CD62L at different E:T ratios. C) Fold change in activation marker expression over a 24-hour time-course, when stimulated with PHA. Dotted line indicates 1-fold, which is no change from unstimulated cells. All assays were carried out once (n=1), with 3 technical replicates.

3.2.3 Vβ flow cytometry panel validation

While the Vβ assay has been used by many researchers, due to the fact that samples can only be stained with two Vβ antibodies at a time, it was necessary to investigate if any cross-reactivity occurred between the antibodies. While the best validation of this method would be to stain a positive control for each Vβ with the full panel of antibodies, a full range of positive controls would be an expensive resource. As a compromise, a few TCRs of known clonotype were transduced into Jurkat cells and then stained with the full panel of Vβ antibodies to demonstrate that when used for Jurkat library TCR repertoire analysis, the Jurkat libraries would stain as expected. As

shown in figure 3.3, the antibody staining was restricted to the Vβ of the known clonotype, and for the clone where no antibody was available to detect it (Vβ7.6), there was a lack of staining with other Vβ antibodies. This shows the assay has a good degree of specificity, and cross-reactivity of antibodies is unlikely to occur.

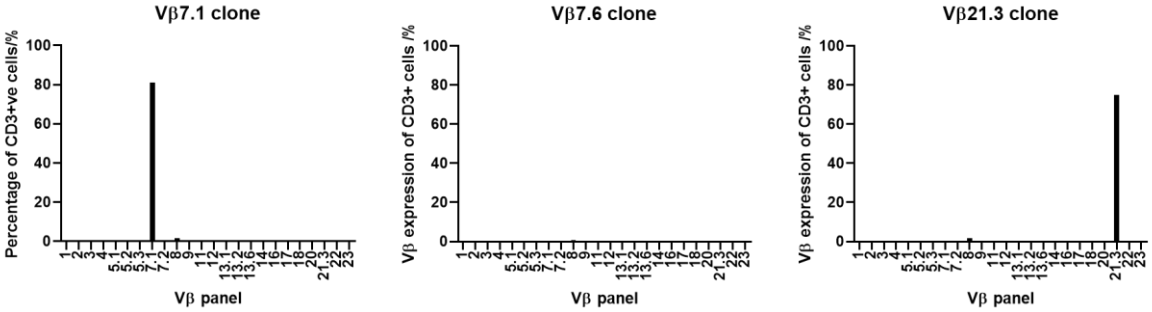

Figure 3.3. Demonstration of specificity of the Vβ panel antibodies. TCRs of known Vβ were cloned into Jurkat cells and stained with the full panel of 24 Vβ antibodies, before running on the MACSQuant flow cytometer. Graphs show the percentage of Vβ expression of CD3+ Jurkat cells expressing a TCR with a known Vβ (7.1, 7.6 or 21.3). Assays were carried out once (n=1).

3.2.4 Unexpected Vβ8 expression dominates the Jurkat libraries.

To investigate the breadth of the Jurkat library TCR repertoires, the libraries were stained with the Vβ panel. Figure 3.4A shows the Vβ expression of the three Jurkat libraries, and reveals that they were all dominated by the expression of Vβ8. If this result was observed in just one TIL library, it might have indicated the presence of a dominant clone, but the likelihood of Vβ8 dominance in multiple TIL repertoires was low. To test if the Vβ expression was accurately representative of the final TIL products, Vβ repertoire analysis of TIL032 and TIL041 was performed, within the CD4+ and CD8+ compartments, to observe the true TCR repertoire. Unfortunately, due to availability of final product TIL stocks, TIL039 could not be analysed. In figure 3.4B and C, it is shown that neither TIL032 or TIL041 show a large dominance of Vβ8. TIL041 does have a larger CD4+ population of Vβ8 cells, but the high expression of Vβ13.2 in the CD4+ or Vβ7.1 in the CD8+ population is not represented as highly as would be expected in the Jurkat library if the Vβ8 dominance were accurate. Additionally, there is no high expression of Vβ8 cells in TIL032, which led to doubts as to the overall usefulness of the Jurkat libraries moving forward.

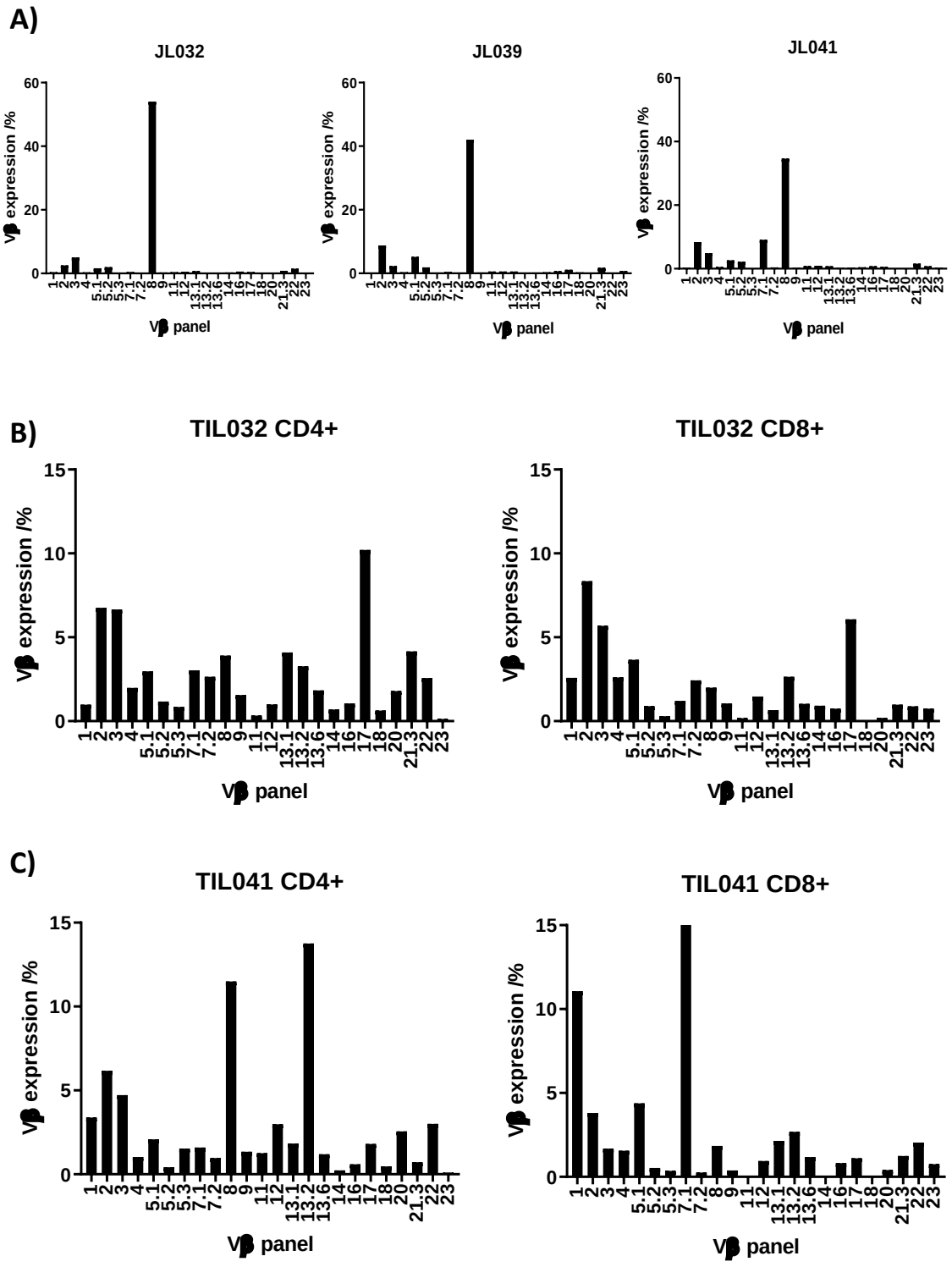

Figure 3.4. Comparison of Jurkat library and TIL Vβ expression. A) Jurkat libraries representing the TCR repertoire of TIL032, TIL039 and TIL041 were stained with the Vβ panel of antibodies to observe TCR repertoires. B) CD4+ and CD8+ subpopulations of TIL032 were stained with the Vβ antibody panel and Vβ is plotted. C) CD4+ and CD8+ subpopulations of TIL041 were stained with the Vβ antibody panel and Vβ is plotted. All assays were carried out once (n=1).

3.2.5 Jurkat library 039 shows a non-specific reactivity to tumour

To address the issue of Vβ8 dominance, FACS sorting was used to selectively deplete the Jurkat libraries of Vβ8. While this carried the risk of excluding any tumour-reactive Vβ8-restricted TCRs from the library, it was theorised that decreasing this dominance of unexpected TCRs would give a more accurate representation of the TIL TCR repertoire. The following assays were first conducted in one Jurkat library, JL039, with a view to repeat with the other libraries if successful. JL039 was chosen as it had already been used for the E: T ratio assays, so was likely to be reactive to patient-matched tumour cells. After expanding the Vβ8-depleted Jurkat libraries, a 24-hr co-culture assay with patient-matched tumour line CTCM39.3 and CTCM41.1 (tumour from a non-HLA matched patient), the expression of markers CD69 and CD62L were

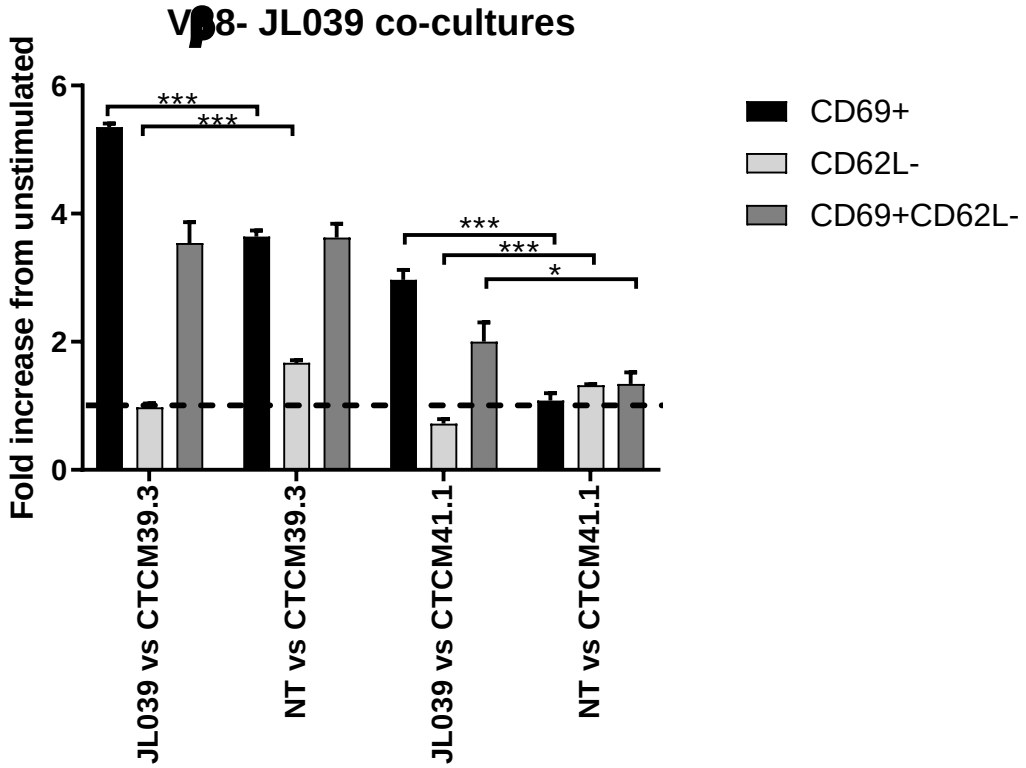

Figure 3.5. Vβ8-depleted Jurkat library 039 melanoma co-cultures. NT Jurkats and Vβ8-depleted Jurkat library 039 were co-cultured with patient-matched and patient-mismatched tumour cells for 24 hrs. Activation was measured by flow cytometry using CD69 and CD62L. Fold increase from unstimulated NT and JL039 cells when co-cultured with tumour lines CTCM39.3 and CTCM41.1 (patient matched and mismatched respectively). Three populations were measured based on their activation status. Statistical analysis was applied using GraphPad Prism software and used the recommended Holm-Sidak method for multiple T-tests. * = $P < 0.05$, *** = $p < 0.001$

measured, while CD3 staining was used to distinguish the Jurkat cells from the tumour cells. It was expected that a large increase in activation marker CD69 and a loss of CD62L would be observed upon co-culture with the matched tumour, but not the mis-matched tumour. As shown in figure 3.5, the Jurkat library cells significantly upregulated CD69 when co-cultured with the patient matched autologous tumour cells. However, the NT control cells also showed an increase in activation on co-culture with tumour, and JL039 also demonstrated reactivity towards a mismatched tumour line suggesting the activation could be non-specific. While it is possible that JL039 harbours an HLA-independent TCR, the overall low activation and activity seen with both the NT Jurkat cells and mismatched tumour show flaws in the model. This suggests that the activation seen against the CTCM41.1 cell line, and potentially the matched tumour line, is non-specific and not driven by pMHC-TCR interactions.

3.2.6 Depletion of Vβ8 was unsuccessful through two approaches

In the assay shown in figure 3.5, we assumed that using FACS sorting to eliminate the Vβ8-stained cells from the Jurkat library would sufficiently deplete this population. However, the overall low reactivity of the Jurkat library, coupled with activation seen in NT Jurkat cells, encouraged reconsideration of this assumption. Retrospectively, the Vβ panel was used to observe the degree of Vβ8 depletion in these cells. As shown in figure 3.6A, while the Vβ8 population was proportionally lower than before the depletion, allowing the proportion of other Vβ populations to increase, Vβ8 was still the most prevalent population in the two Jurkat libraries tested. Additionally, by observing the TIL041 Vβ repertoire in figure 3.4C, it does not appear that all the Vβ populations are expressed in JL041, such as the large proportion of Vβ13.2 cells seen in CD4+ TIL041 that are seemingly absent in the Jurkat library. Naturally, due to the continual culture of Jurkat cells, it is unlikely that the relative proportions of Vβ would resemble the true proportions of different TCRs in the TIL product.

After the first unsuccessful depletion sort, FACS sorting of tumour-reactive cells from the Jurkat libraries through activation markers was used in a separate attempt to deplete the Vβ8 population. The Jurkat libraries 032 and 039 were co-cultured with matched tumour cells in a 1: 1 ratio, and stained for CD3, CD69 and CD62L after 24 hrs.

After sorting the tumour-reactive population, the cells were expanded further in culture before a Vβ panel screen was used to observe the Vβ repertoire. Using a comparison with the original Jurkat library staining, seen in figure 3.6B., the Vβ repertoire expression did not change greatly between the original Jurkat library and the cells isolated based on expression of activation markers following co-culture with autologous tumour cells. The Vβ8 population was still highly dominant, showing around 30 % and 18 % for JL032 and JL039 respectively. Additionally, there was no large increase in any particular Vβ population after sorting of the tumour-reactive cells, indicating that no enrichment had occurred. It is likely that the results observed are a very non-biased effect of activation in response to the tumour, which suggests that the activation marker upregulation is non-specific. Any specific activation of Jurkat cells through the TCR is probably being masked by that effect, and could be investigated further with the use of co-receptor-transduction.

Out of the two different Vβ8 depletion approaches, the use of FACS sorting to separate out the Vβ8+ cells was more successful that isolating the CD69+CD62L- Jurkat cells. However, both approaches were disappointing regarding their Vβ8 depletion, and revealed several flaws of the Jurkat library model. Instead of investing further efforts into solving the problems of this model system, it was decided that a different model should be established that would be more reliable and more relevant for downstream applications.

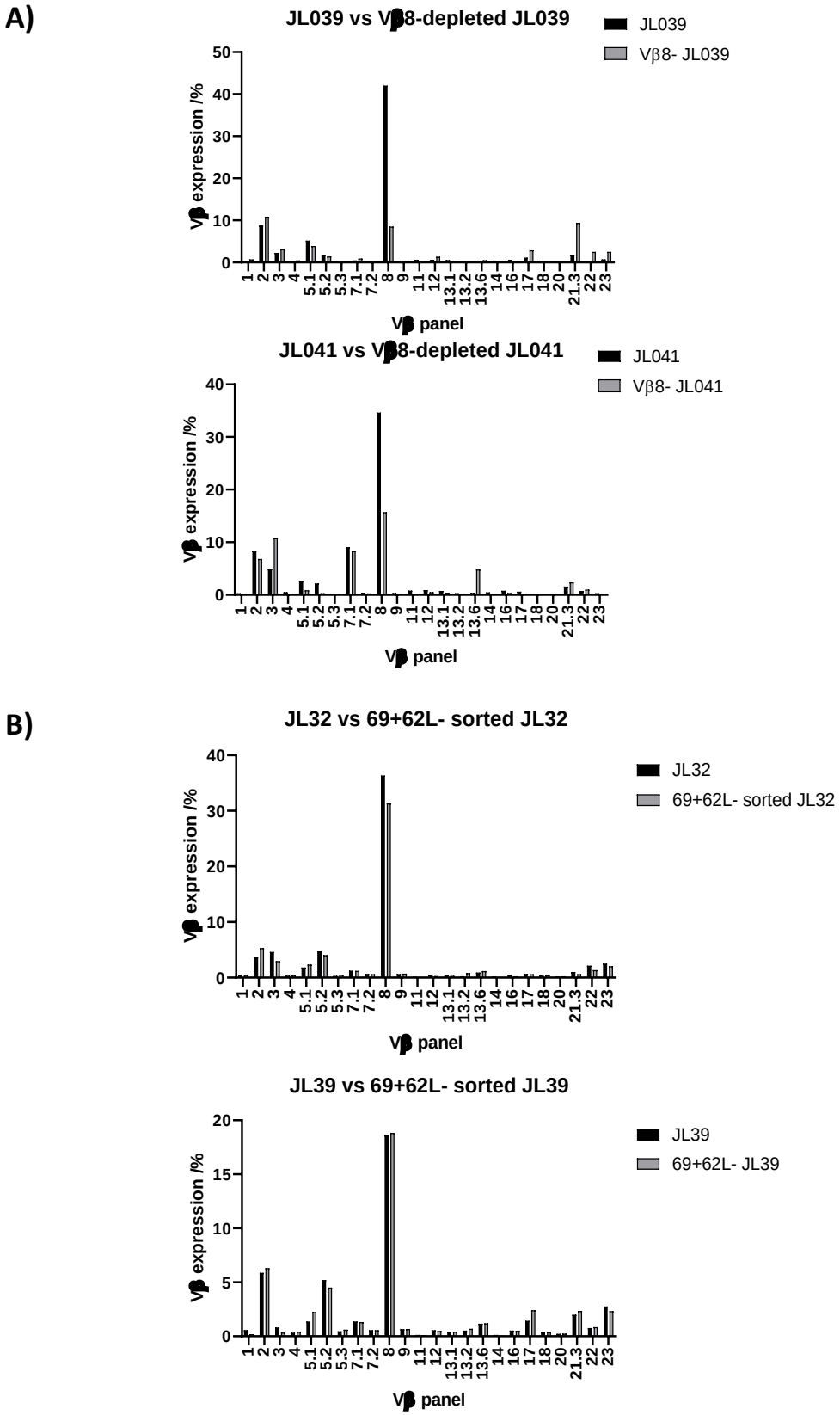

Figure 3.6. Two different approaches for depleting the Vβ8 population from the Jurkat libraries. A) The top two graphs compare the Vβ expression of two unaltered Jurkat libraries with matched, Vβ8-depleted Jurkat libraries when stained with the Vβ flow cytometry panel after flow sorting. B) The bottom two graphs compare the Vβ expression of two unaltered Jurkat libraries with matched, CD69+CD62L- flow-sorted Jurkat libraries. Staining was carried out on single populations (n=1).

3.3 Investigating tumour-reactivity by relative abundance of Vβ populations

3.3.1 Establishing background data from normal buffy coat donors.

As discussed in the introduction, a key paper by Pasetto et al. (2016) highlighted the potential of identifying tumour-reactive T-cell clones from TIL based on their relative abundance. This is based on the theory that tumour-reactive T-cells that traffic to the tumour and encounter their cognate antigen are stimulated to undergo oligoclonal expansion, increasing their frequency within the pre-REP TIL repertoire. Their results showed that it may be possible to identify tumour-reactive TCRs based on their relative abundance in pre-REP TIL. It was unknown if the same phenomenon might be observed in final TIL products that have undergone *in vitro* expansion, therefore it was chosen as the second model to investigate if this effect is conserved throughout the TIL expansion process, using final TIL products to identify potentially tumour-reactive TCRs based on relative Vβ expression.

To determine if a Vβ population is proportionally higher or lower than expected, a background level was required for comparison. Since the only sample collected for the TIL generation process was the tumour resection, and any TIL harboured within the tumour, a patient-specific background could not be established. As a means to validate the model without a patient-matched background, it was reasoned that using PBMCs isolated from NBC donors provided by the NHSBT service would suffice for establishing background Vβ data. The PBMCs were first isolated from the NBCs (see chapter 2.1.4), then T-cells were enriched using a negative T-cell isolation kit (see chapter 2.1.5). Vβ panel staining on the CD2+ population was then carried out for 8 NBC donor T-cell populations, and each Vβ expression averaged to create a background for future comparison to TIL; the NBC background is shown in figure 3.7A. The first observation was that overall, the error bars were fairly small considering only 8 donors had been used, but for some subpopulations, the range of Vβ expression was quite varied. Generally, when the overall subpopulation (e.g. CD4, CD8, double positive or double negative) was proportionally higher, like CD4 as indicated in figure 3.7B, the error bars were smaller, and if the subpopulation was proportionally lower, like the double positive subpopulation, the error bars were bigger. However, for the work in this project, the CD4 and CD8 subpopulations were focus, and the reliability of the data indicated by the error bars for these groups was considered satisfactory for using as a

background. The data showed that some Vβ populations, such as Vβ2 and Vβ5.1, were consistently proportionally high, whereas others, such as Vβ5.3 and Vβ18 were consistently low.

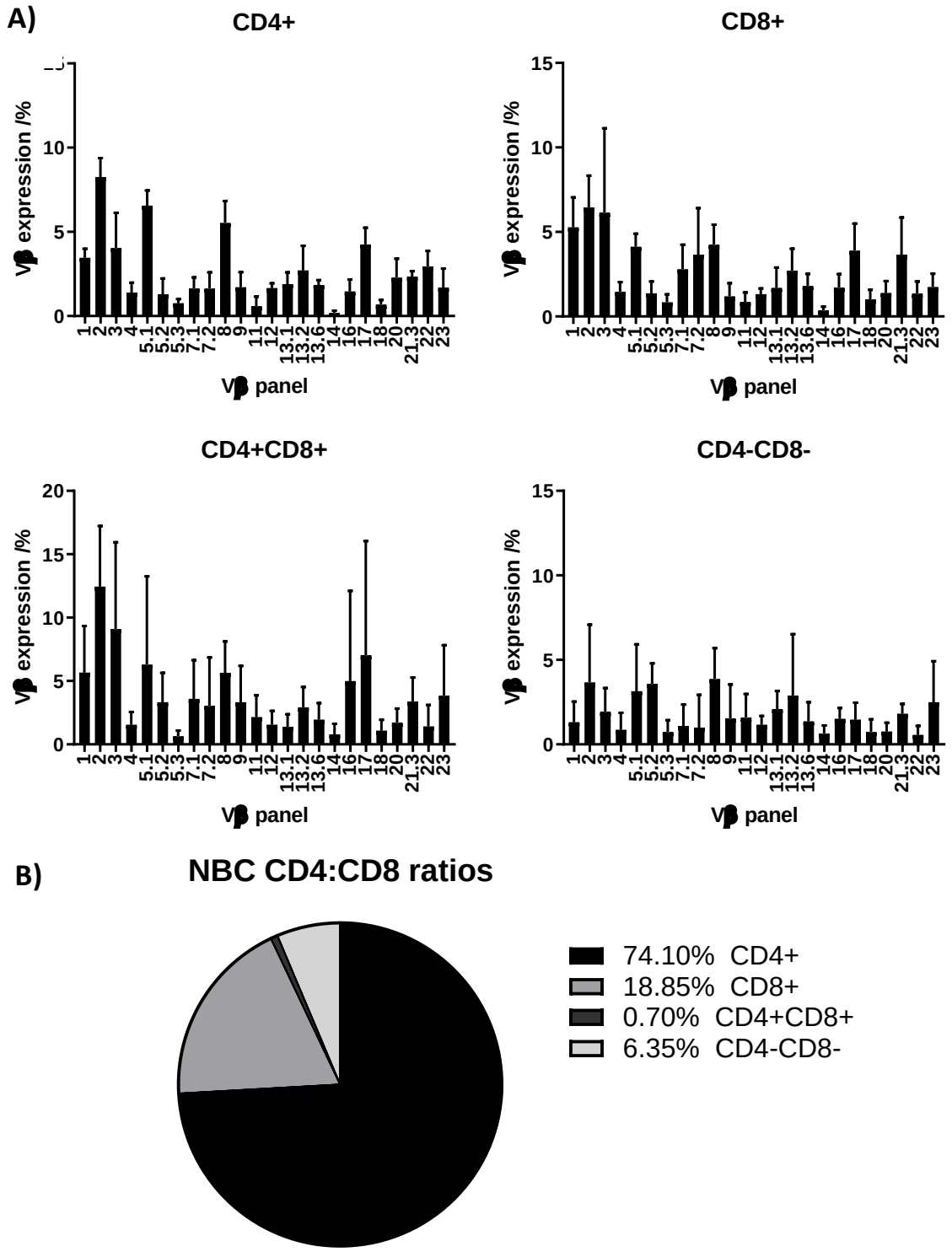

Figure 3.7. Graphs of Vβ expression from 8 NBC donor PBMC T-cells. A) The percentage Vβ expression is plotted for each subpopulation of T-cells, with the means and standard deviation shown for each Vβ made up of 8 NBC donors. B) The pie chart shows the mean percentage of each subpopulation, as accumulated from the 8 NBC donors.

3.3.2 Normal buffy coat background resembles background from literature.

The concept of constructing a pseudo-background from accumulating normal buffy coat donor T-cell Vβ data has been used by other researchers in the field. One such paper by van den Beemd et al. used a similar Vβ panel to the one used in this thesis, so the data were compared to assess the similarity between these normal donor datasets, illustrated in figure 3.8 (van den Beemd et al., 2000). The bar graphs show the accumulated mean values and standard deviations of all the individual data sets for each study, which was comprised of 8 donors in the current study, and 36 donors in the van den Beemd study. The data from the paper was provided as a series of mean Vβ expression by percentage, and standard deviations, separated by age groups of the 36 donors. For this data, the different age-related means were averaged together to give a single data set, and then compared to the mean and standard deviation from the 8 NBC donor Vβ expression analysed by flow cytometry. Statistical analysis was then carried out for each Vβ using multiple unpaired T-tests, with correction by Holm-Sidak method. The data were only compared for Vβ populations where Vβ antibodies used were of the same clone, to ensure the same population of cells would have been detected between the two protocols. The statistical analysis shows that for the majority of the detected Vβs, there is no significant difference between the two sets of data, which adds validity to the background established for this research. In the CD4 graph, statistical significance was observed for Vβ7.1, Vβ9.1 and Vβ14. For the CD8 datasets, statistically significant differences were observed for Vβ5.1, Vβ7.1 and Vβ14. Some trends can be observed between the two datasets, such as the highest proportion of cells staining for Vβ2 in both the CD4 and CD8 subpopulations, and other populations staining quite low for particular Vβs, such as Vβ11 and Vβ18.

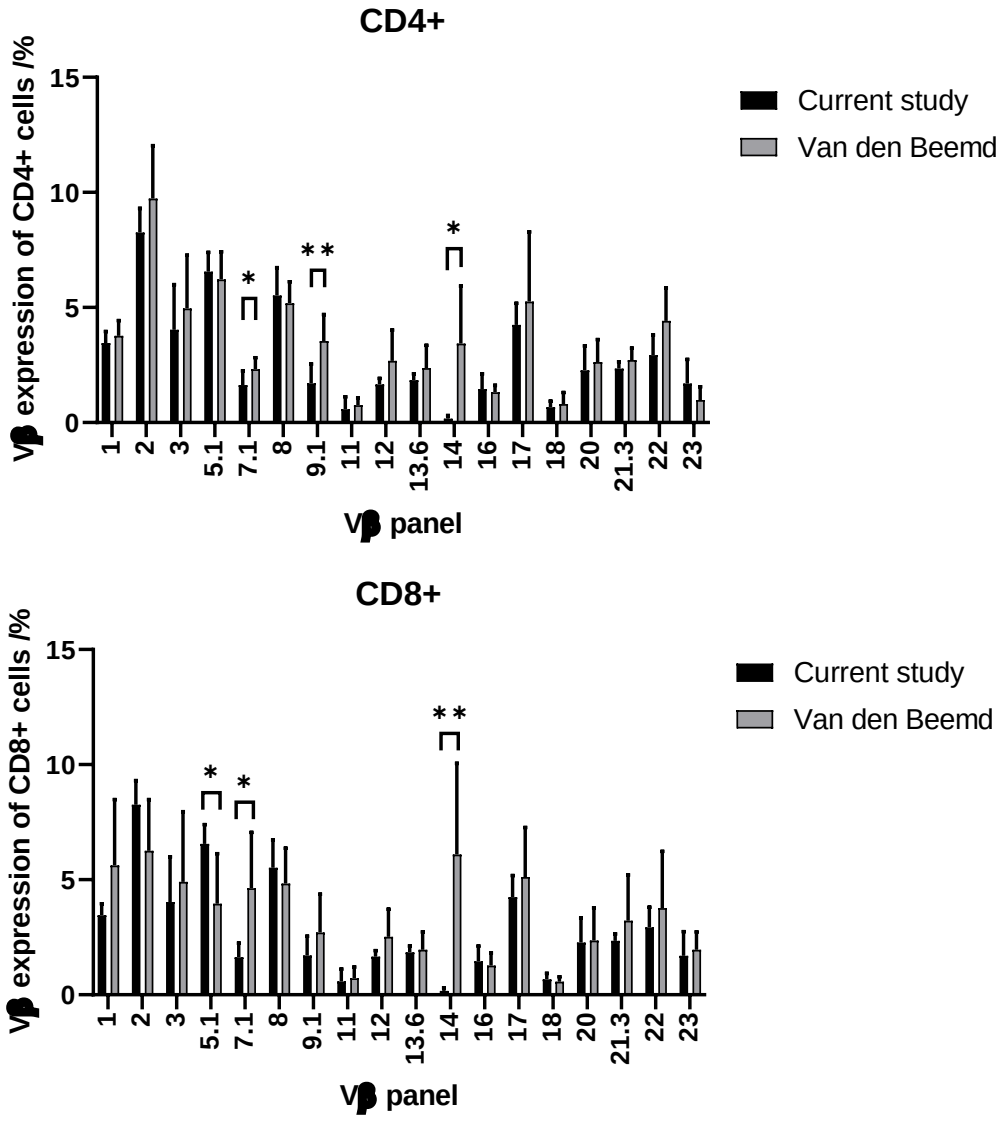

Figure 3.8. Comparison of NBC donor background Vβ expression with the van den Beemd et al. background. Vβ expression of CD4+ and CD8+ subpopulations from NBC background in figure 3.7A compared to background from the van den Beemd et al. (2000) paper. Statistical analysis was applied using GraphPad Prism software and used the recommended Holm-Sidak method for multiple T-tests. * = $P < 0.05$, ** = $p < 0.005$

3.3.3 Comparison of TIL Vβ distribution to the background data reveals potentially tumour-reactive clones.

For several banked TIL products from previously treated patients, the breadth of the TCR repertoire was assessed using the Vβ flow cytometry panel, co-stained with CD4 and CD8 antibodies to distinguish between different T-cell sub-populations. To analyse how the repertoires varied from the normal buffy coat background, the fold change

from the NBC background was recorded for each Vβ. In the heatmaps in figure 3.9, a fold change of greater than 1 is coloured red, increasing in gradient to a maximum of 25-fold change. If a Vβ expression had a fold change of greater than 25-fold, it is shown as a black square to easily identify populations of interest. If the fold change is less than 1, the square is coloured in a gradient towards blue. Along the *Y* axis are the different TIL, as well as the NBC donors to show the homogeneity of the background. Due to conservation of limited TIL samples, only single Vβ stains could be carried out. Unfortunately, data is missing for certain TIL stains, and these are represented by a black cross through the square. If stocks of the TIL products were more abundant, the stains would have been repeated to collect the full Vβ repertoire, and ideally these would be carried out in duplicate or triplicate for increased reliability of results. Next to the TIL numbers, coloured arrows represent the responses of the patients after TIL treatment. Patient response was assessed according to the response evaluation criteria in solid tumours (RECIST) criteria, defined by Eisenhower et al (2009) as:

> "Complete Response (CR): Disappearance of all target lesions. Any pathological lymph nodes (whether target or non-target) must have reduction in short axis to <10 mm.
>
> Partial Response (PR): At least a 30% decrease in the sum of diameters of target lesions, taking as reference the baseline sum diameters.
>
> Progressive Disease (PD): At least a 20% increase in the sum of diameters of target lesions, taking as reference the smallest sum on study (this includes the baseline sum if that is the smallest on study). In addition to the relative increase of 20%, the sum must also demonstrate an absolute increase of at least 5 mm. (Note: the appearance of one or more new lesions is also considered progression).
>
> Stable Disease (SD): Neither sufficient shrinkage to qualify for PR nor sufficient increase to qualify for PD, taking as reference the smallest sum diameters while on study"

In the CD4 heatmap, there are very few results that have a high fold change. This is to be expected, since the CD4 population is not generally involved in a cytotoxic anti-tumour response, and not associated with large clonal expansion. The most notable

fold change in Vβ is that of Vβ13.6 for TIL038. The green arrow indicates that the patient had a complete response to TIL therapy, and it would be interesting to investigate if this Vβ13.6 subpopulation contributed to the response. Other than a few other Vβ which have a fold change greater than one, the majority of Vβ fold changes are one or lower, shown by the abundance of white and blue squares.

The CD8 heatmap is where the highest number and extent of fold changes are observed. Firstly, there are a far greater number of red and black squares than the CD4 heatmap, and these can be observed for several different TIL samples. There are 5 black squares corresponding to Vβ13.6, showing over 25-fold increase from background for TIL001, TIL003, TIL038, TIL041 and TIL054. Interestingly, the black squares are restricted to TIL patients who have had a complete or partial response, as indicated by the coloured arrows. The TIL patients who achieved a good clinical response tend to have a higher proportion of red or black squares, across the Vβ panel, compared with patients who did not have a clinical response. The patients who had progressive disease, TIL037 and TIL040, show no Vβ in the panel is increased when compared to background levels, indicated by the white and blue squares for these TIL. Within the CD8 heatmap for TIL054, there are 5 different Vβ populations that are increased over 25-fold from the NBC background: Vβ8, Vβ13.6, Vβ17, Vβ18 and Vβ22. The abundance of highly elevated Vβ populations for this TIL, combined with the complete response the patient achieved, may be indicative of highly tumour-reactive TIL.

Using a Vβ screening model to identify potentially tumour-reactive TCRs has shown promise, with large expansions of particular Vβ populations when compared to NBC donor backgrounds. However, there is no way of directly identifying if these Vβ populations are tumour-reactive, for which another measure would be needed. This conclusion led to the third and final model of identifying tumour-reactive TCRs, which will be discussed below.

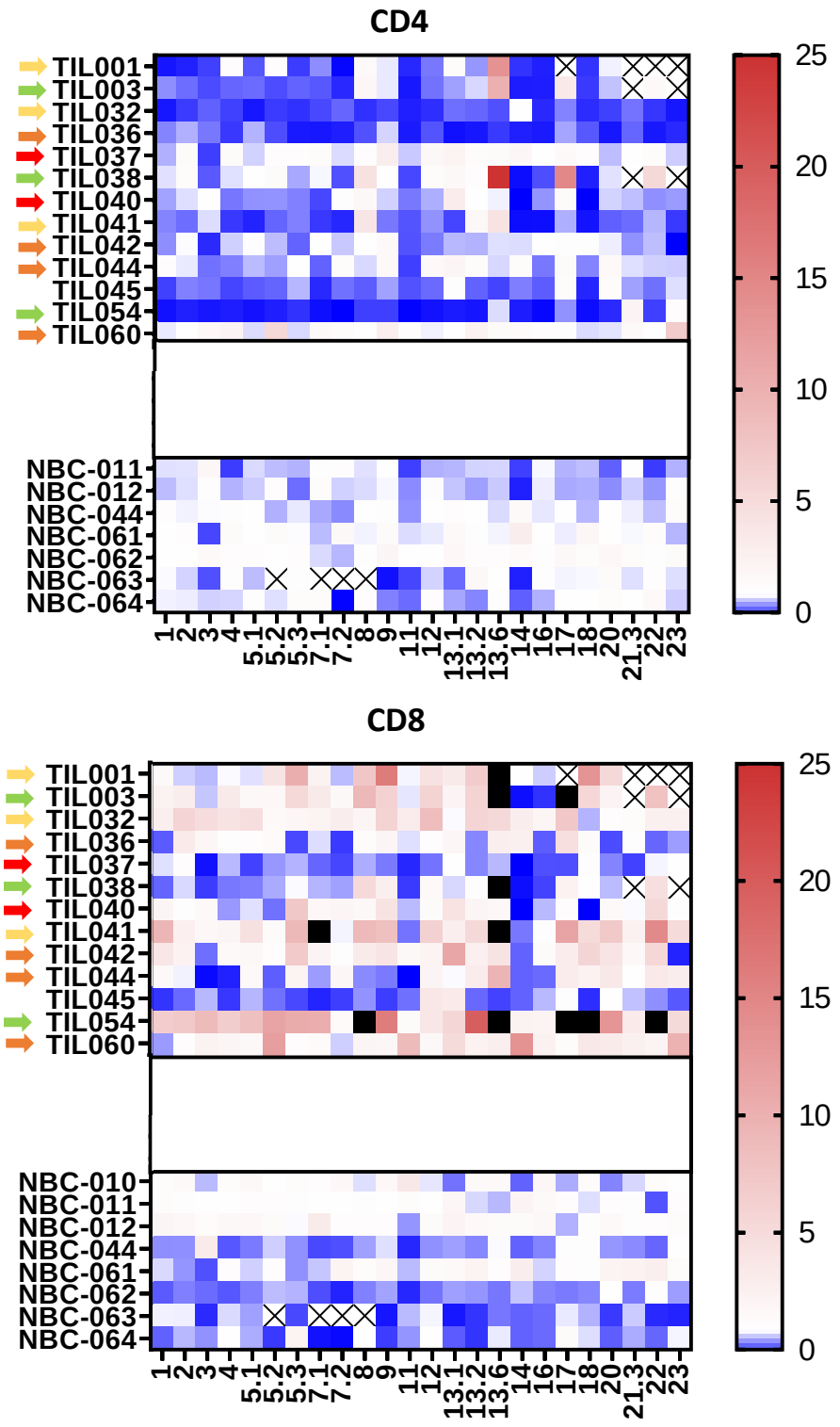

Figure 3.9. Heatmaps of fold change in Vβ expression for 13 TIL samples compared to the NBC donor background. Vβ expression was analysed by flow cytometry then fold change from NBC background measured. White squares = fold change = 1 (i.e. no change), white -> blue squares = fold change < 1, white -> red = fold change > 1, to an upper limit of 25. Black squares represent data with fold change > 25. White squares with a black cross indicate a lack of data. Arrows next to the TIL sample are colour coded based on patient response following TIL therapy: red = PD, orange = SD, yellow = PR, green = CR. All stains were carried out on single populations (n=1).

3.4 Validating an optimal marker of tumour-reactive TIL

3.4.1 CD137 is a sensitive, and specific activation marker.

With the Vβ screening model discussed above, predicting tumour-reactivity based on comparison with the NBC background was based on assuming clonal expansion of tumour-reactive cells, whereas a direct measurement of tumour-reactivity would be a more robust and reliable indicator. To this end, three different activation markers were selected from literature and investigated with respect to T-cell activation to HLA-matched tumour. CD107a, also known as Lysosomal-associated membrane protein 1 (LAMP-1), is a well-known degranulation marker that is produced intracellularly by activated cytotoxic T-cells, and its localisation at the cell surface during activation means it can be used to sort live cells, so was chosen as the first potential marker (Betts et al., 2003). The second marker was a fluorescent dye, Rhodamine 1,2,3 (from now referred to as Rhodamine). This dye has been found to accumulate in the mitochondria of live cells, and is particularly useful for distinguishing highly proliferative cells such as carcinoma cells (Bernal et al., 1983). It was theorised that this dye could be used to detect activated cells since they are stimulated to proliferate as a result of the activation process. A key advantage of this dye is that it is available for at 'good manufacturing protocol' (GMP) grade, meaning that it could be quickly adapted into a current TIL manufacturing process, and live cells can be stained and sorted with this reagent. Lastly, another well-validated activation marker, CD137, was chosen. This marker has been the topic of much research in the immunotherapy field in recent years, with papers even noting its ability to distinguish tumour-reactive cells (Ye et al., 2015). Its expression on the cell surface during activation is well known and can be used to directly isolate tumour-reactive cells by FACS sorting.

For this assay, T-cells from three different donors were isolated and transduced with a known TCR directed against a MART-1 epitope (Cole et al., 2009). The non-transduced and transduced cells were then co-cultured with HLA-matched and HLA-mis-matched tumour lines overnight to look for tumour-reactivity. The results in figure 3.10 revealed that both CD107a and Rhodamine showed no difference in the percentage of activated cells across all conditions, potentially due to high background activation after T-cell transduction, despite the T-cells being rested prior to co-culture. MFI was plotted as well as percentage expression, as another way of detecting differences between the

co-cultured populations (see figure S1). There was a slight increase in CD107a with the matched tumour, but this increase was not significant across the three donors. Looking at the MFI for the rhodamine-dyed T-cells, no increase could be observed when co-cultured with HLA-matched tumour. In contrast, the expression of CD137 in figure 3.10 was not only high but also very specific, and a significant increase was observed when the TCR-transduced cells were co-cultured with HLA-matched tumour. The MFI, while low overall, showed a similarly specific increase when in the HLA-matched tumour co-culture condition (figure S1). The appeal of this activation marker was clear from this data, and CD137 was taken forward as the optimal candidate marker for assessing tumour reactivity.

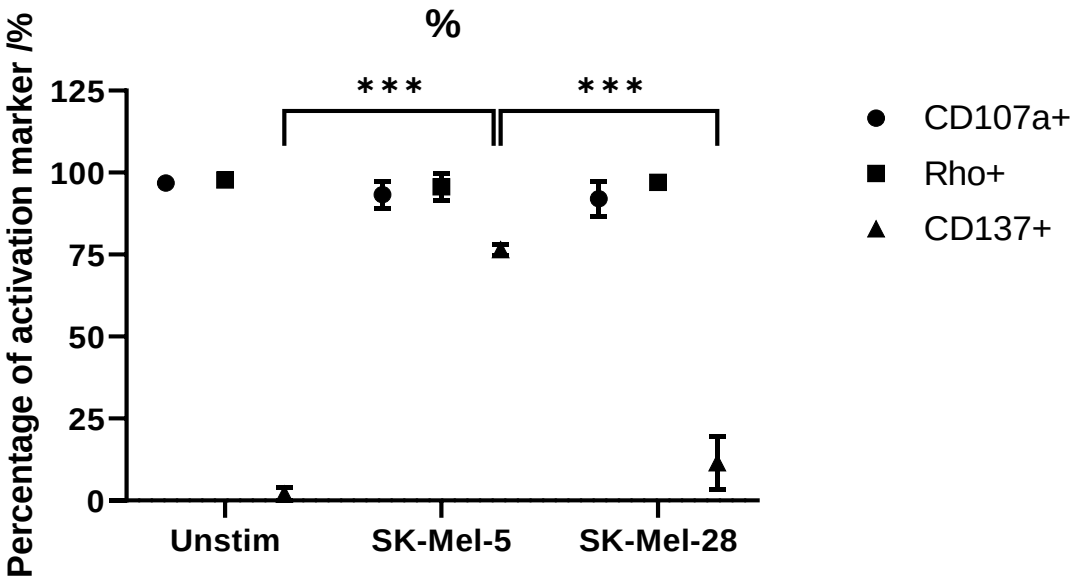

Figure 3.10. Percentage of MART-1 TCR+ cells expressing different activation markers. MART-1-reactive TCR-transduced CD8+ primary T-cells from three NBC donors (n=3) were co-cultured with SK-Mel-5 (HLA-matched) or SK-Mel-28 (HLA-mis-matched) commercially available cell lines. After 24 hrs, the percentages of cells expressing either CD107a, Rhodamine 1, 2,3 or CD137 were measured using flow cytometry. Statistical analysis was carried out using multiple T-tests for each activation marker, using Holm-Sidak method of correction for multiple comparisons. *** = $p < 0.001$.

3.4.2 CD137 can detect TCR-mediated activation from different affinity peptides.

One of the key advantages of using TIL therapy over TCR and CAR T-cell therapies is that the cell product is comprised of a heterogenous population of T-cells expressing TCRs against multiple unknown targets. It is widely accepted that some of the

interactions between TCRs and tumour-associated antigens are naturally low in affinity. For a model which can identify tumour-reactive TCRs from TIL-tumour co-culture, it would be important for the activation marker to detect the full range of these responses. To test the sensitivity of CD137 for this purpose, three different MART-1 peptides of ranging affinities were chosen. The index peptide, ELAGIGILTV (ELA), used in these assays is an optimised version of the natural Melan-A/MART-1 peptide Melan-$A_{26\text{-}35}$ (EAAGIGILTV) peptide, with the second alanine substituted by a leucine (Valmori et al., 1998). The TCR-pMHC affinity of this complex is 17 µM, which falls into the range of a typical tumour affinity (Aleksic et al., 2012; Krogsgaard et al., 2013). The peptide variant FATGIGILTV (FAT) was made as a result of three amino acid substitutions and has a TCR-pMHC complex affinity of 3 µM (Ekeruche-Makinde et al., 2012). This is higher affinity than most tumour antigens and represents more of a viral antigen affinity (Aleksic et al., 2012). The last peptide used was ELTGIGILTV (3T), which was identified in an attempt to lower the pMHC affinity of the cognate Melan-$A_{26\text{-}35}$ peptide antigen; it has an affinity of 82 µM (Clement et al., 2011). For the assay, antigen presenting T2 cells were pulsed with 10-fold decreasing levels of the different peptides and then co-cultured with MART-1 TCR-transduced primary T-cells. After 24 hrs, the T-cells were analysed for CD137 expression using flow cytometry. The graph in figure 3.11 displays the accumulated data from all three donors, and the results showed that all three peptides can induce specific and distinguishable CD137 expression by the T-cells, increasing in a concentration-dependent manner. At the lowest concentration, the peptide associated with low TCR-pMHC affinity (3T) induced CD137 expression in just under 20 % of T-cells, and this was a clearly distinguishable population compared with a very low unloaded-T2 background of just 1.41 % (data not plotted). For the affinity-enhanced peptide FAT, the lowest peptide concentration of 1 x 10^{-10} M caused 46.8 % of cells to be activated. However, this only increased to 68.7 % when the concentration of the peptide was increased to 1 x 10^{-4} M, potentially indicating the T-cells were reaching a maximal response. These data collectively show that CD137 as a marker of T-cell activation is capable of detecting different levels of activation induced by a range of affinity pMHC-TCR interactions.

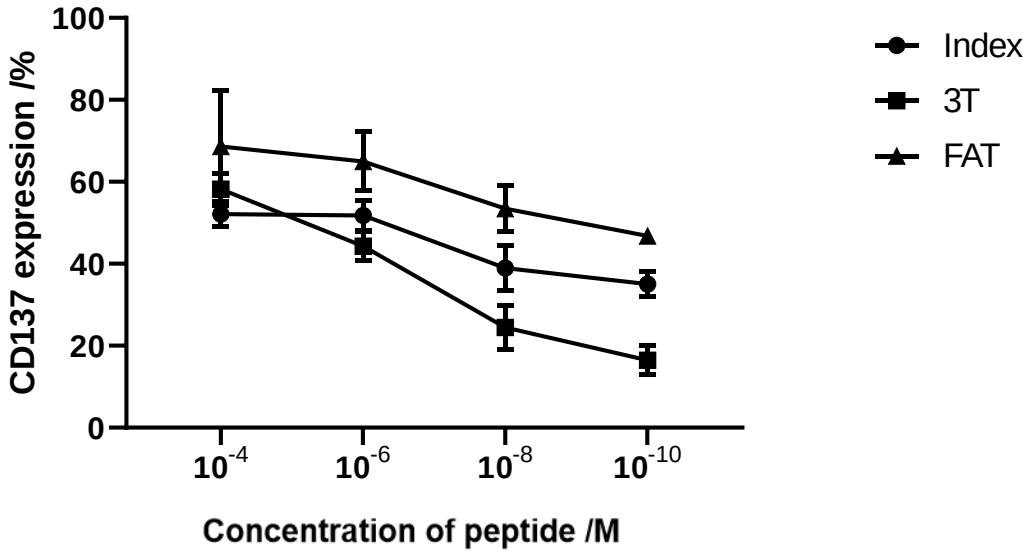

Figure 3.11. Peptide titration of different MART-1 peptides. MART-1 TCR-transduced CD8+ primary T-cells were co-cultured with T2 cells pulsed with decreasing concentrations of three MART-1 peptides representing different TCR-pMHC complex affinities. After 24 hrs the T-cells were stained for CD137 expression and analysed using flow cytometry. Index = ELAGIGILTV (17 µM), 3T = ELTGIGILTV (82 µM) and FAT = FATGIGILTV (3 µM). Assay was carried out in triplicate, with the mean values plotted.

3.4.3 Proportion of CD8 cells in the final TIL product does not correlate with patient response.

While it is generally accepted that having a high proportion of CD8 T-cells in a TIL infusion product is advantageous for a good clinical response, it has not been definitively correlated. To investigate the relationship between CD4: CD8 ratio and clinical response, a number of final TIL product samples were stained with CD4 and CD8 antibodies. As the graph in figure 3.12A shows, there is massive variation in the relative proportions of CD4 and CD8 cells in the TIL products, but when taken together, the 13 TIL have an average CD4 population of ~ 50 %, and an average CD8 population of ~ 40 %. This is best illustrated in the pie chart in figure 3.12B. Due to the broad spread of results across the different melanoma TIL samples, it is beneficial to look at the subpopulation ratios with respect to the patient response following TIL therapy. The colour coding of the points in figure 3.12A indicates the patient response of that corresponding patient. The data in the graph show that achieving a partial or complete response was not restricted to TIL with high proportion of CD8 T-cells, which is

particularly noticeable when observing the complete responders in green. Reversely, progressive disease is the worst patient response that can be observed, and some patients who experienced progressive disease had a CD8 subpopulation of up to 20 %. This data highlights the importance of elucidating the tumour-reactive portion of the TIL; it is likely that not all CD8 cells in the TIL product are able to exert an anti-tumour response, and that tumour-reactive cells could be harboured in the other subpopulations.

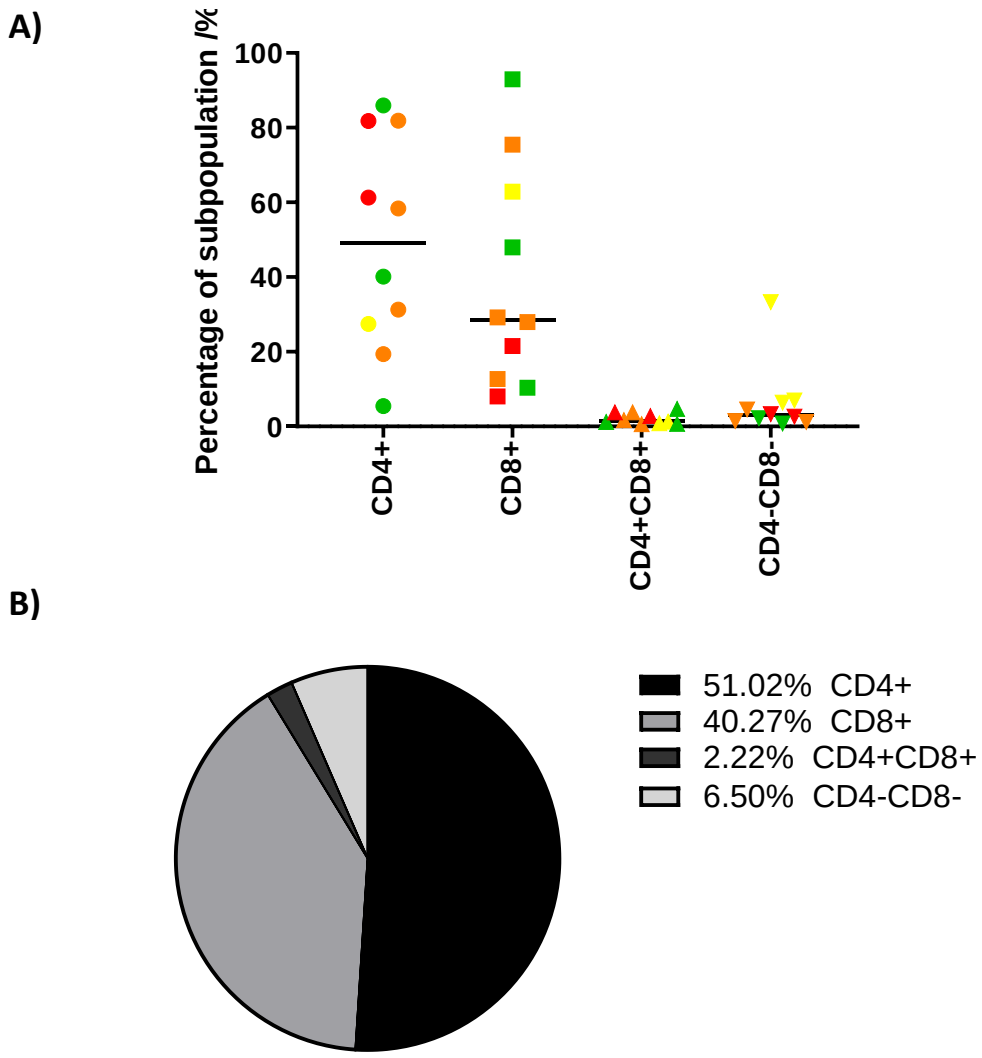

Figure 3.12. Subpopulations of T-cell distribution for 13 melanoma TIL samples. 13 different final product melanoma TIL were stained with CD4 and CD8 antibodies, and analysed by flow cytometry. A) The percentage of cells in each of four subpopulations of T-cells within TIL was plotted for 13 TIL. The bars represent the mean subpopulation when the different values from the 13 TIL were averaged, while individual values are plotted as different symbols for each subpopulation. The individual data points are plotted for each TIL, with the colour-coding based on the patient response to the TIL therapy: red = PD, orange = SD, yellow = PR, green = CR. B) The pie chart shows the same mean subpopulation percentages for all 13 melanoma TIL.

3.4.4 The proportion of tumour-reactive TIL varies greatly between patients.

To investigate the tumour-reactivity of different melanoma, co-cultures were set up using final TIL products and matched patient tumour cells, and CD137 expression was measured after 24 hrs. In such assays it is arguable whether using tumour digest or an immortalised cell line would be the best target cell to use. One advantage of tumour digest is that the cells are more representative of the heterogeneity of the tumour microenvironment, but disadvantages are that they are a much more precious resource and less available for scaling up assays. Immortalised tumour lines are much more readily available, but it is difficult to ascertain whether the heterogeneity of the original digest is maintained. The latter was chosen for these assays because of the precious nature of the digest which had to be maintained in case patients had to be retreated at any point. In addition to measuring expression of CD137, the co-receptors CD4 and CD8 were also measured so the reactivity of the different subpopulations could be assessed separately. TIL were selected based on the availability of patient-matched tumour cell lines, as well as availability or consent status of banked TIL products.

The first observation from the results in figure 3.13A is that overall, the tumour-reactivity is fairly low, with the highest CD137 reported from TIL041, showing a CD8 T-cell reactivity of around 35 %. The tumour-reactivity assessed by CD137 for TIL054 was 20.6 % in the CD8 population, with 10.6 % of the CD8- population expressing CD137. For the three TIL which are associated with stable disease responses on reinfusion to the patient (TIL042, TIL065 and TIL028), the CD137 expression for the CD8 populations was 2.8 %, 0.6 % and 18.6 % respectively. The CD137 expression for the patients who experienced stable disease is quite varied, however the definition of stable disease is very broad (less than 30 % reduction in sum of diameters, to less than 20 % increase in sum of diameters), so a variety of tumour reactivity is not unexpected (Eisenhower et al., 2009). For the patient corresponding to TIL051, who experienced disease progression on re-infusion of the TIL product, there was still CD137 expression in both the CD8+ and CD8- subpopulations following matched tumour co-culture, recording 4.9 % and 8.8 % respectively. To gain insight into the composition of the different TIL products, the percentage of CD8+ T-cells was plotted to see if this correlated with patient response. As shown in figure 3.13B, TIL054 was comprised of over 90 % CD8 T-

cells, which may have contributed to the patient's complete response. However, other TIL were also CD8 T-cell dominant, such as TIL065, and the clinical response achieved by that patient was only stable disease. This supports the data in figure 3.12A which does not show a trend between clinical response and CD4: CD8 TIL composition.

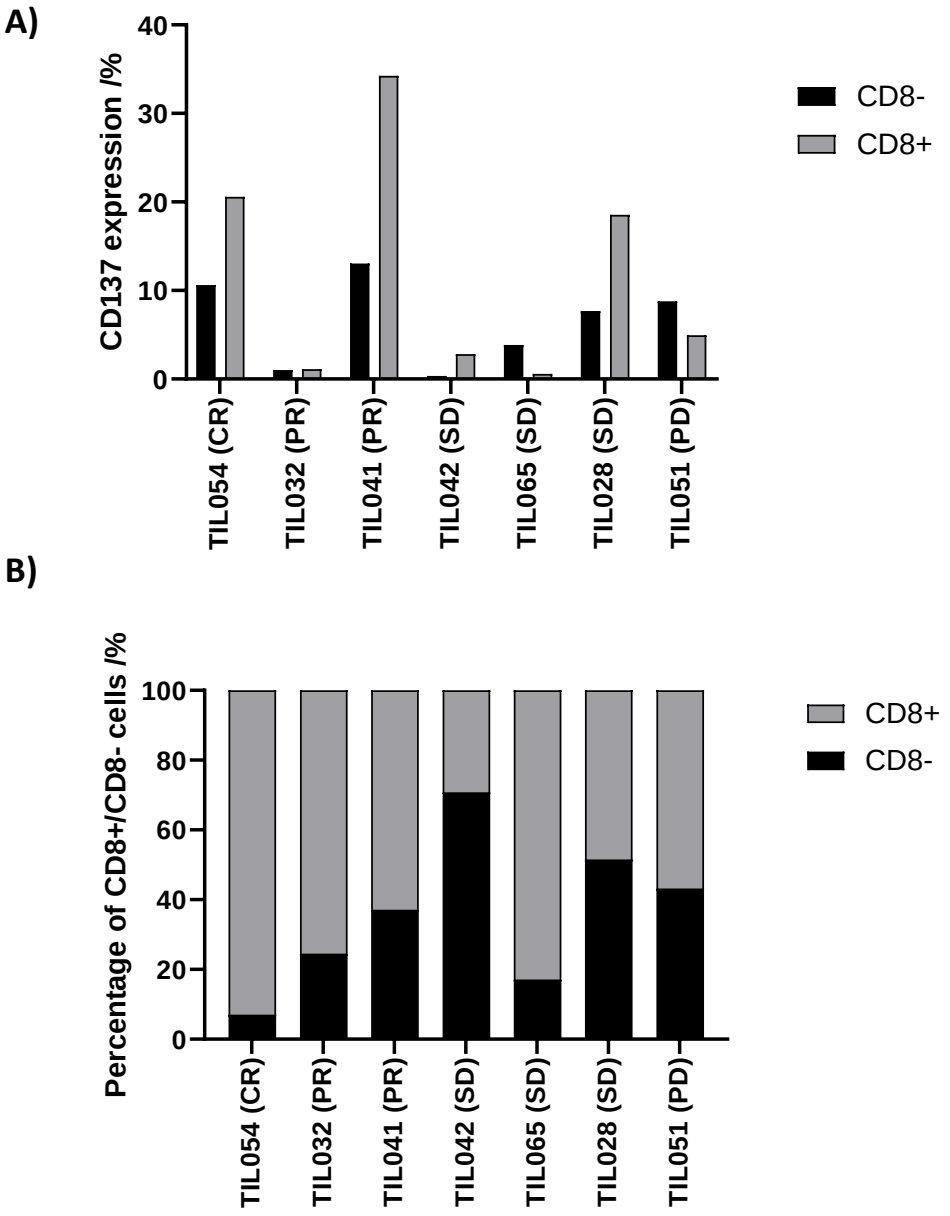

Figure 3.13. CD137 and CD8-: CD8+ ratios for 7 TIL product co-cultures. 7 different final product TIL were co-cultured with patient-matched tumour cell lines in a 1:1 ratio and measured for tumour-reactivity using CD137 staining by flow cytometry. A) Percentage of cells expressing CD137 when co-cultured with patient-matched tumour cells is plotted for the CD8+ and CD8- subpopulations, with the patient response after TIL therapy shown on the *X* axis. B) The mean ratio of CD8-:CD8+ cells for each of the 7 TIL is plotted as a composite bar graph.

To identify if CD137 expression is a statistically relevant output for this dataset, the data were averaged and the mean CD137 values compared for unstimulated TIL and stimulated (patient-matched co-cultured) TIL. Figure 3.14 shows these data in the form of a box and whisker plot, and the statistical analysis shows that the expression of CD137 is significantly higher ($p < 0.05$) for the stimulated TIL group compared to the unstimulated TIL group. It is likely that within this data, patient-matched samples contain a range of significant and non-significant results, however if the use of this marker was to be applied to a much larger data set, the averaged CD137 data would be a more relevant measure.

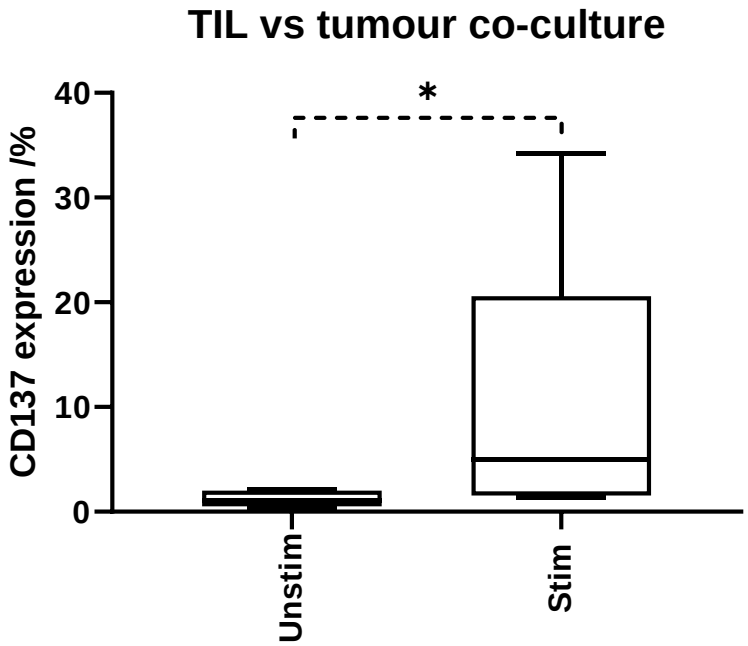

Figure 3.14. Mean CD137 expression for 7 TIL vs matched tumour co-cultures. The box and whisker plot data shows the averaged CD137 expression for unstimulated and stimulated TIL for 7 samples. The top and bottom of the box represents the upper and lower quartiles, with the line showing the median of the data, and the whiskers show the highest and lowest values. Statistical analysis was applied using GraphPad Prism software and used the unpaired T-tests. * = $P < 0.05$.

3.4.5 Increase in Vβ expression after autologous tumour co-culture can be observed in the tumour-reactive population.

To investigate how the breadth of the tumour-reactive population differs from the whole TIL population, co-cultures of matched patient TIL and tumour cells were established. Tumour lines had been established by Instil Bio UK prior to this project starting, as per the method in 2.1.1. Spare TIL final product was used that had been cryopreserved in liquid nitrogen after rapid expansion during the TIL generation process, which also occurred prior to this project. After 24 hrs, the cells were stained with a live-dead marker, as well as antibodies against CD2, CD137 and the TCR Vβ antibody panel. To analyse the data, live single cells were gated, followed by a CD2 gate encompassing the full T-cell population, and an overlapping gate for CD137+ cells within the CD2 gate. The cells from the CD2+ and CD2+CD137+ gates were then gated for Vβ expression with the co-staining Vβ panel. This gating strategy was used as it would be the most representative way of analysing the data for future flow sorting experiments later in this chapter, and can be visualised by the FACS plots in figure S2. It was hypothesised that upon co-culture, the relative Vβ proportions of the CD2+CD137+ subpopulation would change as only the tumour-reactive T-cells would make up that population of T-cells. However, upon analysis it was observed for most of the TIL analysed that the majority of the Vβs harboured cells that expressed CD137 to some degree, even if the percentage of some Vβs was low. The original theory was that these assays could be used to identify tumour-reactive subpopulations by selecting Vβ subpopulations of T-cells that were present in a higher proportion in the CD2+CD137+ group than the CD2+ group.

For some TIL, there were a few Vβ populations that were expressed at a greater proportion in the CD2+CD137+ subpopulation than the overall CD2+ population of cells. Looking at the graphs in figure 3.15, these can be identified by Vβs where the black bar is higher than the grey bar. For example, for TIL028 the Vβ5.2 and Vβ8 are expressed at a higher percentage in the CD2+CD137+ population, implying they are more likely to be contributing to an anti-tumour response. Interestingly, these Vβs were also increased in expression for other TIL including TIL032 and TIL065. These Vβs showed a difference in proportion in the CD2+ and CD2+CD137+ population of 7.9 % (Vβ8) and 9.2 % (Vβ5.2), which is clearly higher than the difference in percentage for

all other Vβs. For TIL032, the overall tumour-reactivity by CD137 expression was very low (figure 3.13A), and looking at the increase in percentage of Vβ expression for the CD2+CD137+ population, we can see this is notable for particular Vβs: Vβ5.1, Vβ5.2, Vβ8, Vβ18 and Vβ23. However, unlike the large change in proportion of Vβs for TIL028, the change in Vβ expression between CD2+ and CD137+ ranges from 1.5 % to 6.5 %. Other Vβs such as Vβ7.2 and Vβ13.2 remain consistent between the CD2+ and CD2+CD137+ population, suggesting they are not directly contributing to the tumour-reactive population. The same can be said of Vβs that decrease in proportion from the CD2+ to the CD2+CD137+ populations, such as Vβ2, Vβ3 and Vβ17.

As was observed in the heatmaps of figure 3.9, TIL041 harbours a largely dominant expression of Vβ7.1, and this Vβ makes up 28.8 % and 17.8 % of the CD2+ and CD2+CD137+ populations respectively. While the proportion of Vβ7.1 decreased from the CD2+ to CD2+CD137+ population, it was still the most abundant Vβ in the tumour-reactive population, followed by Vβ1, which expressed in 13.3 % of the cells. TIL042 is another TIL that had relatively low reactivity overall (shown in figure 3.13A as less than 5 % of CD8+ cells) and there are only a few Vβs where the proportion is at least 1 % higher in the CD2+CD137+ population than the CD2+ population in figure 3.15. This is observed for Vβ1 and Vβ2, however the increase in percentage between the populations is small, with Vβ1 and Vβ2 reading 1 % and 6.41 % respectively. Even though TIL051 had a low overall percentage of CD137 expression on matched tumour co-culture, the graph in figure 3.15 shows that the percentage of particular Vβs in the CD2+CD137+ subpopulation is high, particularly the proportion of Vβ5.2 and Vβ7.2 (25.2 % and 13.7 % respectively). TIL054 is one of the most interesting TIL samples to study because the patient had a complete response, and it has been shown that the TIL has a large majority of CD8 T-cells (over 90 %, shown in figure 3.13B). Looking at the breadth of the tumour-reactive CD2+CD137+ population, the repertoire is quite broad, with several Vβs expressing in over 4 % of cells, such as Vβ2, Vβ3, Vβ5.1, Vβ8, Vβ11, Vβ17 and Vβ21.3. There does not appear to dominance of particular Vβs, unlike the data shown for TIL028 or TIL051.

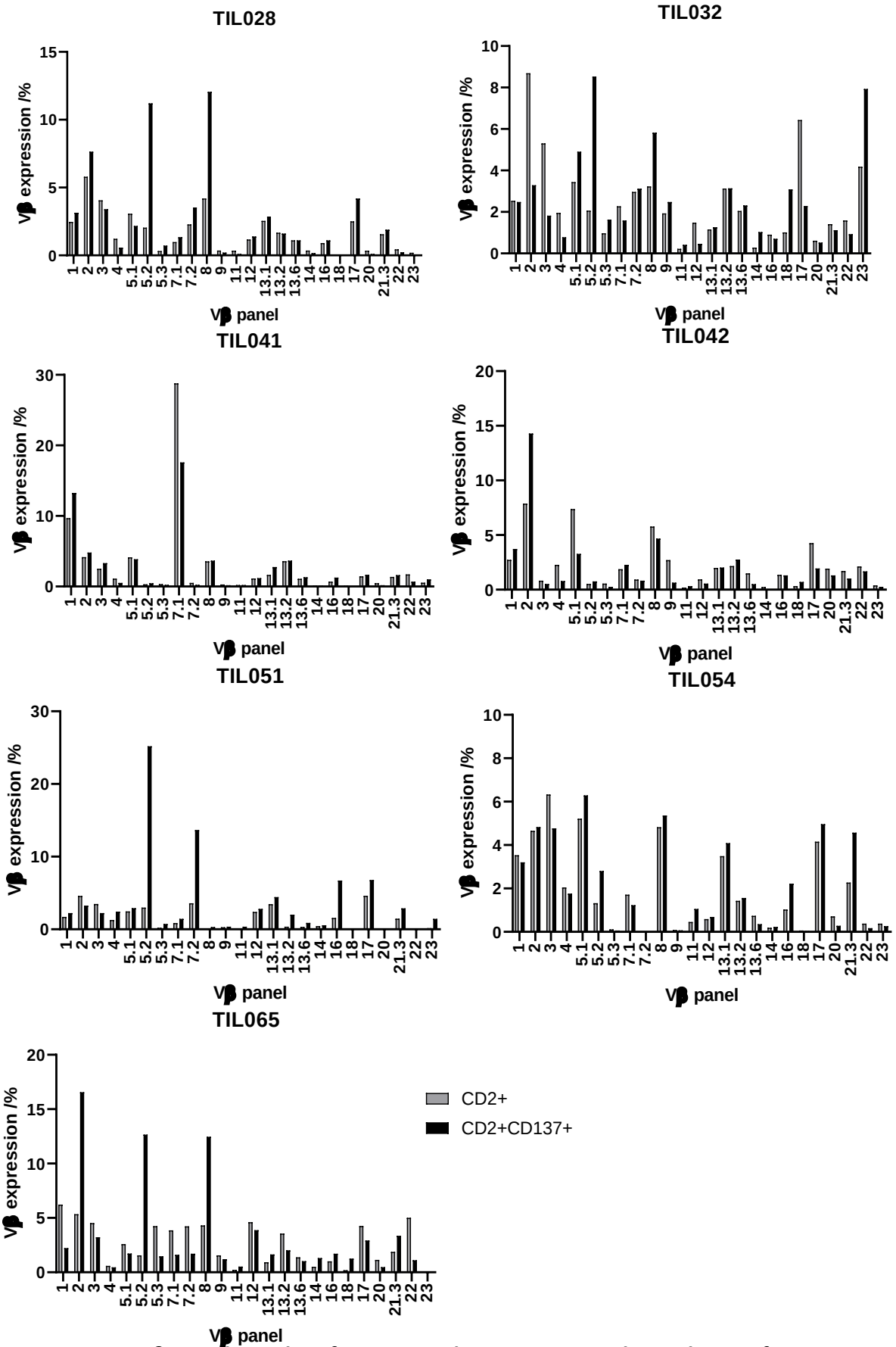

Figure 3.15. Vβ co-culture data for CD2+ and CD2+CD137+ subpopulations for 7 TIL. Single populations of TIL (n=1) were stained with the Vβ panel, CD2+ and CD137+ following co-culture with patient-matched tumour lines for 24 hrs. For each graph, grey bars represent the CD2+ data and the black bars represents the CD2+CD137+ data.

3.4.6 Expansion of tumour-reactive subpopulations occurs when TIL are co-cultured with matched tumour

In an attempt to model how the tumour-reactive population of TIL might expand *in vivo*, co-cultures were set up for TIL054 with patient-matched tumour line CTCM54.1. The TIL were analysed for Vβ repertoire and CD137 expression at three timepoints – day 1, day 5 and day 8. The theory was that if a tumour-reactive TCR came into contact with its cognate antigen on the tumour cells, it would selectively proliferate and the percentage of that Vβ would increase. If the percentage remained the same or decreased, it could be interpreted as that Vβ population not representing strongly tumour-reactive TCRs. When looking at figure 3.16, there are some very clear increases in Vβ expression over the three timepoints, most notably for Vβ5.1, Vβ5.2, Vβ8 and Vβ16. The most dramatic of these increases in proportion of Vβs in the CD137+ population were Vβ5.2, which was 2.7 % on day 1 and increased to 17.9 % by day 8, and Vβ8 which increased from 5.66 % to 19.6 % over the same time course. These were also Vβs that appeared in the CD2+CD137+ gate at a higher proportion than the CD2+ gate (figure 3.15), which adds validity to this data. These Vβ expansions could represent tumour-reactive TCRs that have clonally expanded in response to cognate antigen.

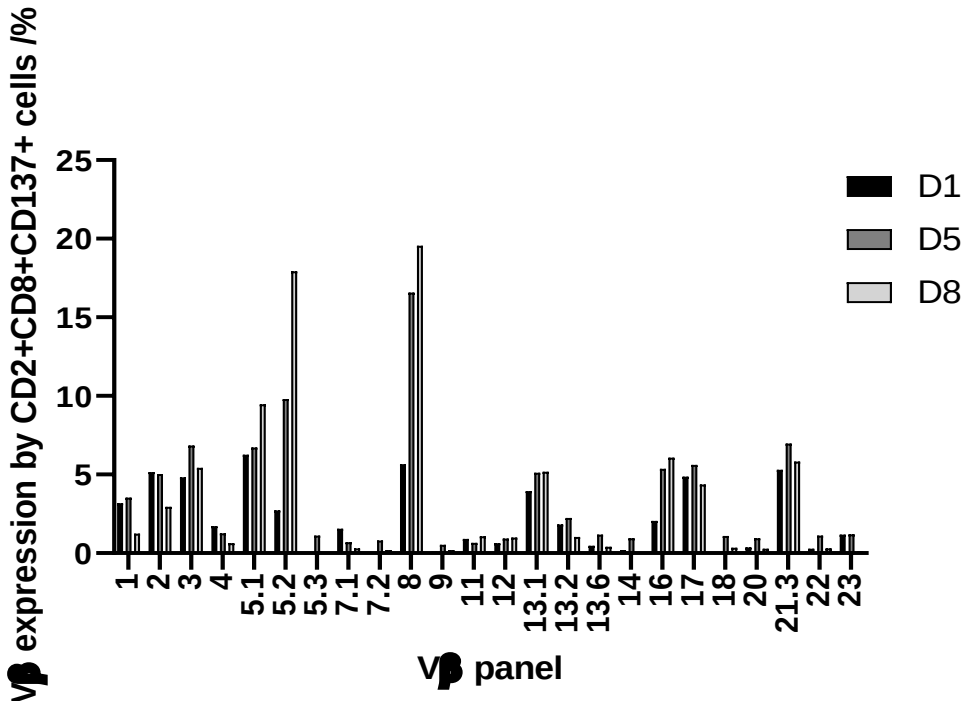

Figure 3.16. Comparison of Vβ subpopulations after an 8-day co-culture on patient-matched tumour. TIL054 cells were co-cultured with patient-matched CTCM54.1 cells in a 1:1 ratio for 8 days. Vβ expression of CD2+CD8+CD137+ TIL054 cells after co-culture with patient-matched tumour line CTCM54.1, tested at day 1 (D1), day 5 (D5) and day 8 (D8). The assay was carried out once (n=1).

While there were a lot of promising results in this TIL co-culture Vβ repertoire analysis, further validation was needed to evaluate if CD137 could be used as a marker of true tumour-reactivity. Using a more comprehensive method to definitively evaluate TCR repertoire would provide answers to some of the questions raised by this data as well as identify individual tumour-reactive TCR clonotypes. As shown by the flow diagram in figure 3.17, a model workflow was established which involved combining the patient matched TIL-tumour co-cultures with CD2+ or CD2+CD137+ FACS sorting and downstream 10x Genomics® TCR and gene expression analysis. The 10x Genomics® platform was chosen to enable the maximum information about the TIL TCR repertoire to be obtained, such as fully paired αβ TCR sequences and CDR3 region information. This would allow for downstream reconstruction of specific TCRs using the full sequence information, which would not be possible with a less informative method such as TCR-β sequencing. Additionally, the 10x Genomics® system allows gene expression analysis to be conducted concordantly on the same TIL populations, which

can be retrospectively linked through the use of barcoding technology. A description of how the 10x Genomics® protocol can be found in chapter 2.2.10.

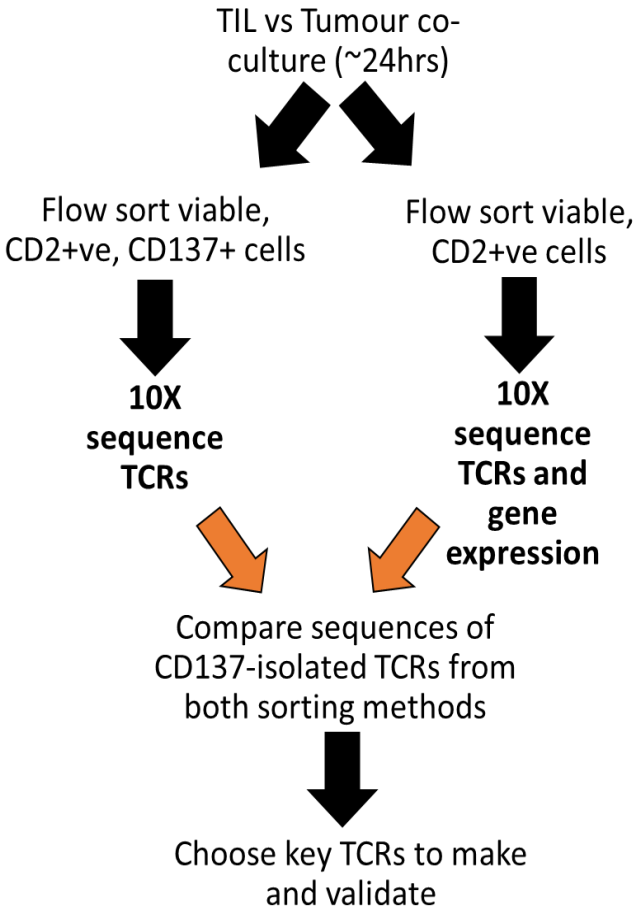

Figure 3.17. Diagram of work flow for CD137 model assays. Flow diagram shows the sequence of assays that made up the CD137 model of identifying and isolating potentially tumour-reactive T-cells from TIL.

3.4.7 Clonal expansion occurs in the patient as early as seven days after TIL infusion

The first use of the novel 10x Genomics® Chromium™ system single cell library construction technology by Instil Bio UK facilitated the next generation sequencing of three different TIL infusion products (IP) and matched post-infusion (PI) blood for those patients. Using the 10x Genomics® data TCR analysis software, Cell Ranger, which assesses the variable, diversity and joining regions (V(D)J), the relative percentages of individual TCR clones can assessed for each TIL sample. Firstly, the top ten TCR clonotypes from the infusion product and the post infusion blood were compared to see if there was any clonotype overlap, and if the clonotypes from the post-infusion blood could be detected at any level in the infusion product. As shown

for all three TIL in figure 3.18, there is specific expansion of a number of clones from the infusion product, which indicates that these TCRs have undergone further expansion *in vivo* upon antigen re-stimulation. It is unlikely that the expansion is random, as several other top 10 clonotypes in the infusion products decrease in percentage, implying they have not expanded in the patient. For TIL032, a very low overall CD137 expression, with restricted CD2+CD137+ Vβ expression, was observed upon co-culture with autologous tumour cells, which might be indicative of clonal response, and when the top 10 clonotypes were compared, there seemed to be a large expansion of one particular clone. For TIL038, there appeared to be expansion of more clones, with several of the top 10 clonotypes from the IP increasing in percentage in the PI blood as well. This patient also had a complete response, and the high proportion of tumour-reactive TIL clones in the IP also in the PI sample could represent an optimal profile for tumour-reactivity. For TIL054, there was only one TCR clonotype that was identified in the top 10 clonotypes for both the IP and the PI sample, with the others expanding from very low levels. This shows us that large scale expansion *in vivo* can occur, and indicates that even tumour-reactive TIL that make up a small percentage of the IP could be critically important for the anti-tumour immune response.

In an attempt to look at how similar the IP and PI repertoire were, the T-cell receptor beta variable region (TRBV) distribution was compared through a ranking method, where the highest ranked TCRs were the TCRs that were most abundant in the IP or PI repertoire, based on percentage of barcoded cells. The simple linear regression model was used to show the similarity between the distribution of clonotypes in the IP and the PI blood. The closer the line of regression is to 1, the more similar the two samples are. Clonotypes that are positioned below the line of best fit ranked higher in the PI sample than the IP sample, meaning they made up a higher proportion of the PI sample than the IP sample. This could mean that they are more likely to have encountered cognate antigen at the tumour and subsequently expanded in the body. These clonotypes are therefore likely to be the most tumour-reactive TCRs and should be investigated further. The GraphPad Prism software allows the user to hover over each point and identify which clonotype is plotted, providing easy identification of these TCRs.

It is worth noting that for TIL032 and TIL038, the PI sample was taken after 7 days, whereas in comparison TIL054 PI blood was a sample taken after 6 months. It is expected that there is more similarity between the IP and PI after 7 days, particularly since the patients received lymphodepleting treatment prior to TIL infusion; in contrast, any similarity between IP and PI after 6 months are likely to be clones that have persisted in the body due to antigen encounter at tumour sites. This also helps to explain why the top clone in the TIL054 PI blood was not one that originated from the IP, but the large clonal expansion of a clone from the IP is a strong indicator of a tumour-reactive TCR.

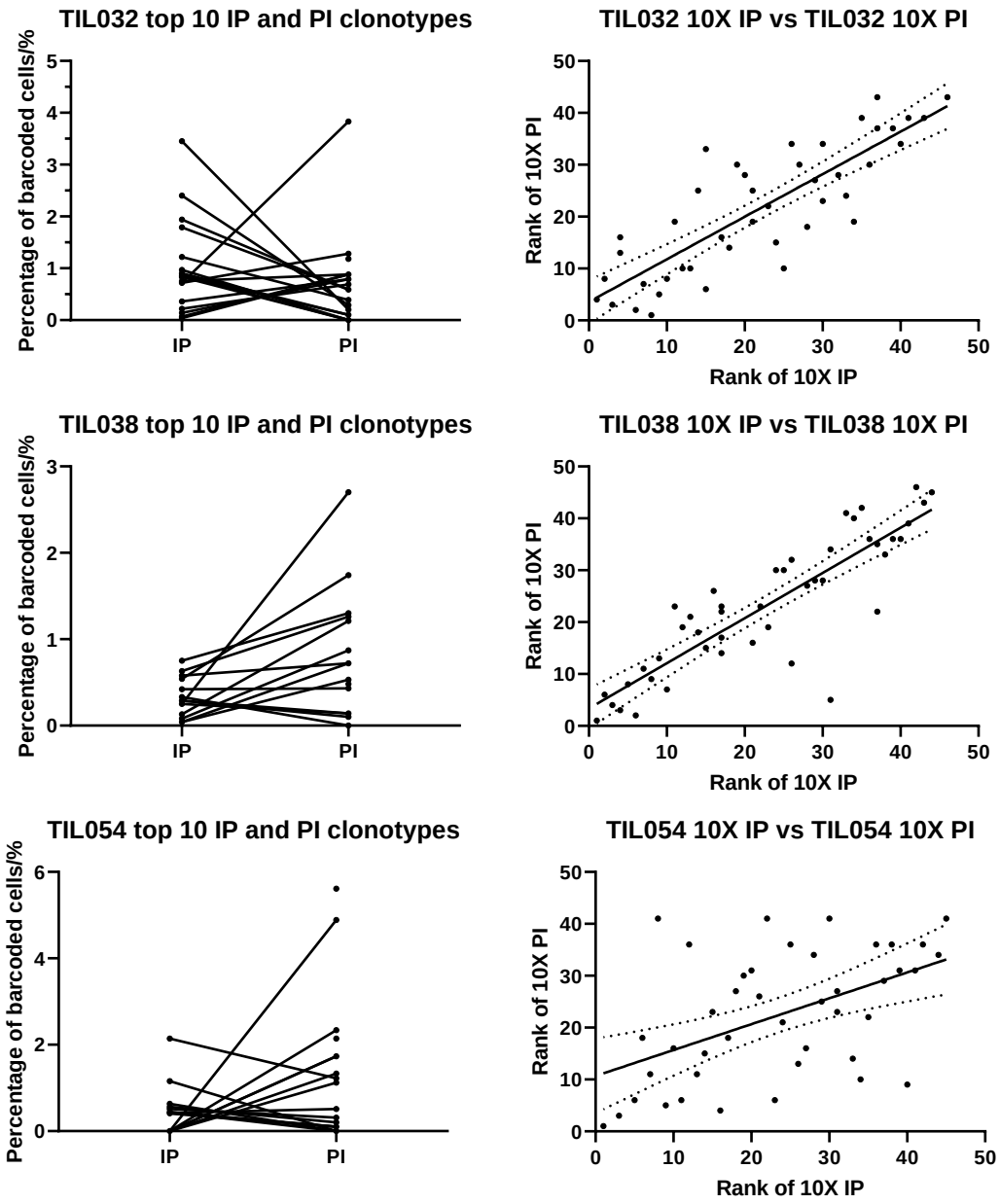

Figure 3.18. Top 10 TCR clonotype comparison between IP and PI datasets. Left graphs: Percentage of barcoded cells are plotted for the top 10 TCR clonotypes in both the infusion product (IP) and post-infusion blood (PI) for 3 different patient TIL product samples. Clonotypes present in both samples are connected by a line. Right graphs: TRBV expression was ranked according to percentage of barcoded cells for each clonotype and the ranks were compared between the IP and PI datasets. Simple linear regression analysis was carried out using GraphPad Prism software. PI for TIL032 and TIL038 was taken after 7 days, PI for TIL054 was taken at 6 months.

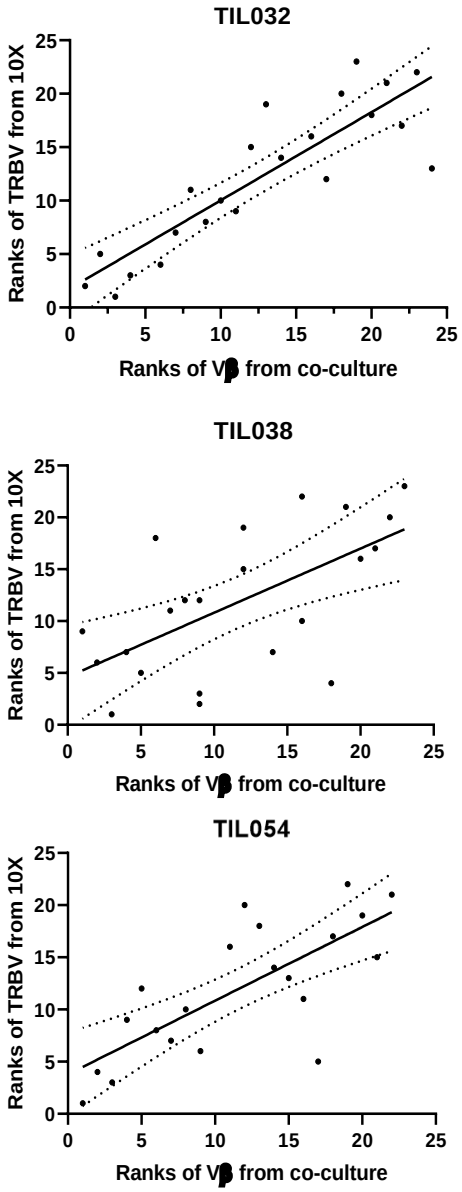

Figure 3.19. Rank of Vβ expression by flow cytometry compared to rank of TRBV of 10x Genomics® data. Three final TIL products were co-cultured with matched tumour cell lines before being isolated and TCR sequences identified using 10x Genomics®. The percentages of TVRB regions were ranked according to relative abundance in each TIL sample, and the ranks compared to the corresponding Vβ expression, also ranked by abundance. Simple linear regression analysis showing the similarity between detected Vβ and the corresponding TRBV region for three TIL samples. Dotted lines either side of the regression line indicate 95 % confidence limits.

The 10x Genomics® Chromium™ system single-cell sequencing method is very powerful, producing a large amount of data, however it is also costly and relatively time-consuming compared with other methods such as the Vβ flow cytometry panel. It is hard to directly correlate the results of the two techniques, but an attempt was made to compare the similarity in Vβ repertoire using a ranking method of analysis, shown in figure 3.19. Since the antibody panel used only captures 24 different Vβs, only the corresponding TRBVs can be compared. For some Vβ antibodies, multiple TRBV regions are detected, and this was taken into account during the analysis. In TIL032, there is a strong positive correlation between the ranks of Vβs from the flow cytometry and with the 10x Genomics® TRBV data. This positive correlation is present but not as strong for TIL038 and TIL054.

There are many reasons why the ranking method of evaluation is not optimal, and why differences may be observed. First of all, the sample sizes of TIL product tested are very small compared to the overall TIL product. For the Vβ panel stain, a sample of approximately 100,000 cells are used to stain just 2 Vβ antibodies at a time. For the 10x Genomics® library generation, the protocol selected aimed for capture of 5000 cells, although the actual number of cells with identifiable CDR3 regions analysed was lower, typically 1000-2000 cells. When we compare these numbers with the overall TIL product number, which is often greater than 1×10^9 the number of TIL analysed by both methods is very small. At this current moment in time, it is still difficult to confirm the exact breadth of the TCR repertoire in a given TIL product, and this is likely subject to inter-patient variation. Another way of assessing how broad the TCR repertoire could be to look at the degree of similarity between two vials of the same TIL product. It is unlikely that the Vβ distribution would be identical, but even with a currently unknown number of overall clonotypes in the TIL product, two vials of 1×10^7 cells are expected to show Vβ expression similarity. The ranking method was applied to Vβ panel data from repeats of the same assay and the correlation is very strong, as shown in figure 3.20. The correlation is particularly good for TIL032, where very few points fall outside the dotted lines representing 95 % confidence limits, and the regression line of best fit has a gradient close to 1 (where 1 would be perfectly matched samples). This method of analysing ranks is not a perfect model; however, the data here gives

confidence that two vials of the same TIL product have a good degree of similarity and are likely to show a very similar Vβ repertoire.

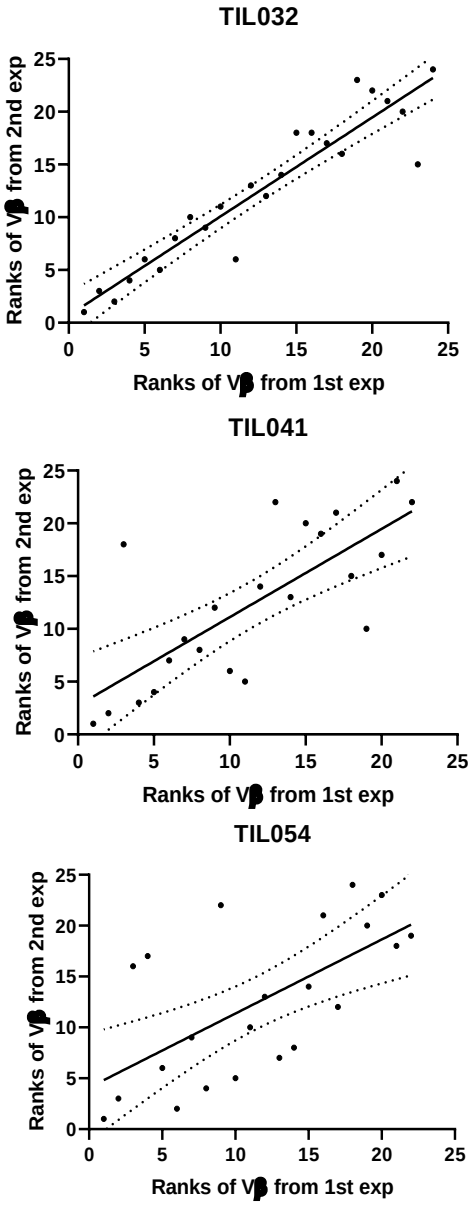

Figure 3.20. Rank of Vβ expression by flow cytometry for two samples of the same final TIL product. Two aliquots of the same final product TIL samples were stained with the Vβ panel at different timepoints. The Vβs for each sample were ranked according to their relative abundance. Simple linear regression analysis was performed in GraphPad Prism, showing the similarity between detected Vβ for each sample. Dotted lines either side of the regression line indicate 95 % confidence limits.

3.4.8 There is overlap between the most abundant TCRs in the TIL product, and the most abundant tumour-reactive TCRs.

To more conclusively elucidate the TCR repertoire of bulk and tumour-reactive TIL samples, following the workflow set out in figure 3.17, three TIL samples were co-cultured with autologous tumour cells overnight before staining and sorting the cells by flow cytometry. The cells were sorted into two groups: CD2+ cells and CD2+CD137+ cells. The cells were then counted and a sample of 8700 cells taken forward for clonotype library generation according to 10x Genomics® protocol described in chapter 2.2.10. For the CD2+ cells, V(D)J analysis and gene expression (GEX) analysis was carried out, and for the CD2+CD137+ samples, only V(D)J analysis was carried out at this stage. The theory behind this FACS sorting strategy was to use gene expression software analysis to retrospectively identify cells with high CD137 gene expression from the CD2+ population and compare this with the CD2+CD137+ sorted V(D)J library. This would serve two purposes; to validate the CD137 FACS sorting approach, or to allow for another way to identify tumour-reactive clones for samples where the overall CD137 population was too low to sort accurately, such as TIL042. As previously mentioned, the CD137+ TIL plots on the flow cytometer were not as distinct as first anticipated, therefore accurately identifying and sorting these cells was a greater challenge. The TIL samples chosen for 10x Genomics® V(D)J library construction were selected based on their availability, their initial CD137 tumour-response data (figure 3.13A) and the recorded response the patient had after TIL therapy; this data is summarised in table 3.1.

Table 3.1. TIL samples used for CD137 co-culture model.

TIL Sample	**TIL041**	**TIL042**	**TIL054**
Patient Response	PR	SD	CR
Melanoma type	Cutaneous	Uveal	Cutaneous
% CD137 after co-culture – CD4+	14.29	1.25	10.61
% CD137 after co-culture – CD8+	34.81	4.5	20.60
% CD8 in TIL product	62.88	29.21	93.0

Using the 10x Genomics® Cell Ranger software, the top 10 TCR clonotypes from the CD2+ and CD2+CD137+ V(D)J libraries identified were compared. By looking at the graphs in figure 3.21., for TIL041 and TIL054, the most abundant TCR clonotype is the same in both populations. This means that the most abundant clonotype in the TIL product is tumour-reactive, and that they make up a substantial portion of the overall tumour-reactive population, particularly for TIL054 where the top clonotype makes up nearly 25 % of tumour-reactive clonotypes. For TIL042, the results are a bit different. As the figure illustrates, the top TCR clonotypes from the CD2+ population only make up an extremely low proportion of the CD2+CD137+ population, or are not shared at all. The graph also shows CD2+CD137+ clonotypes are present in the CD2+ population at very low percentages. This patient experienced stable disease as a result of TIL therapy with this cell product. It could be hypothesised that although tumour-reactive cells are present in the TIL product, their low frequency in the product resulted in an attenuated patient response. For a tumour-reactive cell to exert an anti-tumour response in the patient, it has to encounter its cognate antigen presented by the tumour cells in the context of MHC. If the tumour-reactive cells are present at a very low frequency, they have a reduced chance of making their way into the tumour and encountering that antigen, especially if the antigen is not expressed by all tumour cells.

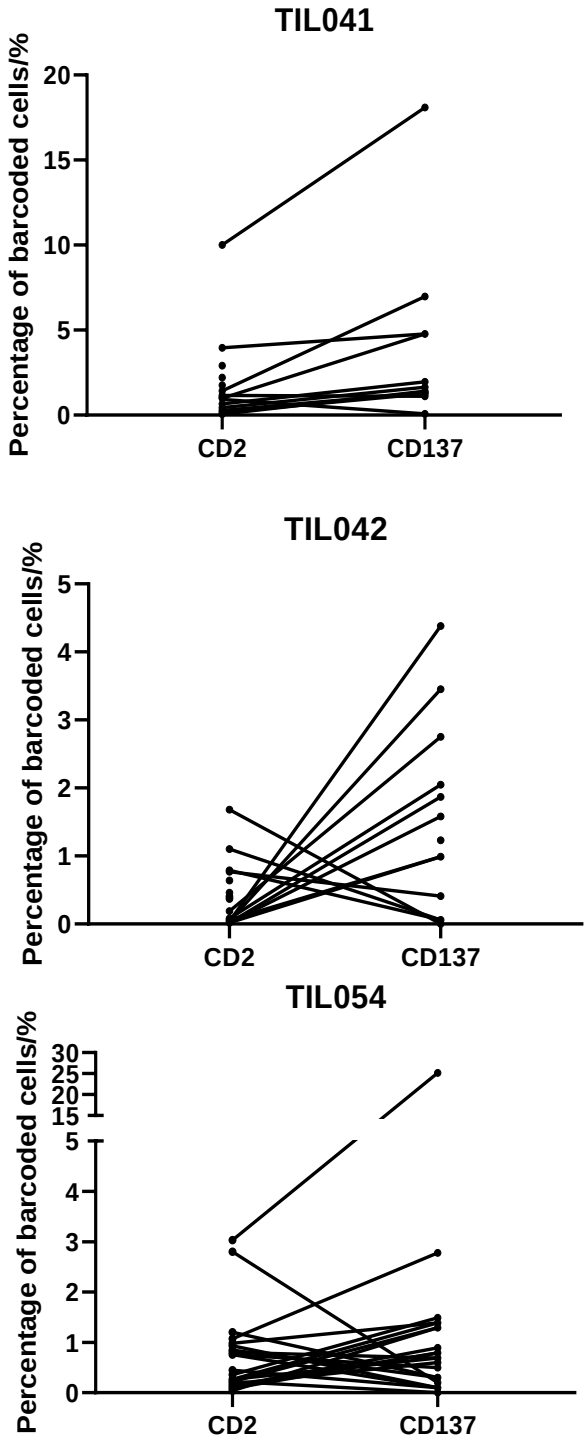

Figure 3.21. Top 10 TCR clonotype comparison between CD2 and CD137 datasets. Percentage of barcoded cells are plotted for the top 10 TCR clonotypes in both the CD2+ fraction and CD2+CD137+ fraction for 3 different TIL product samples, as identified through 10x Genomics® TCR sequencing. Clonotypes present in both samples are plotted and connected by a line.

The Venn diagrams in figure 3.22 show the top 10 TCR clonotype overlap between the CD2+ and CD2+CD137+ populations, as assessed by V(D)J analysis, and also the top 10 clonotypes of the CD2+ population identified by gene expression of CD2 and CD137 through the paired GEX data. Where the same TCR clonotype is detected through different methods, it is indicated by the number in the relevant overlapping circle segments. For TIL041, 5 of the top 10 TCR clonotypes are detected in both CD2+ and CD2+CD137+ populations, as well as being identified separately through GEX analysis. The remaining 5 TCRs that make up the top 10 CD2+ TCR clonotypes are identified through both V(D)J analysis and GEX analysis, showing a strong consensus of data evaluated through these different methods. The remaining 5 TCRs of the top 10 TCR clonotypes of the CD2+CD137+ population are not in the top 10 of the CD2+ population. For TIL042, there are no TCR clonotypes shared in the top 10 clonotypes between the CD2+ or CD2+CD137+ populations, through either method of analysis. However, 3 of the top 10 TCRs of the tumour-reactive CD2+CD137+ population could be detected in the CD2+ population through GEX analysis. However, 7 TCR clonotypes from the top 10 TCR clonotypes of both the CD2+ and CD2+CD137+ populations are not shared in this TIL sample. Much like TIL041, there are 5 of the top 10 TCR clonotypes shared between the CD2+ and CD2+CD137+ populations for TIL054, which were also identified through GEX analysis. A further 3 TCRs from the to 10 TCR clonotypes for CD2+ were identified through V(D)J analysis and GEX analysis, meaning that only 2 TCRs in the top 10 were not detected using both techniques.

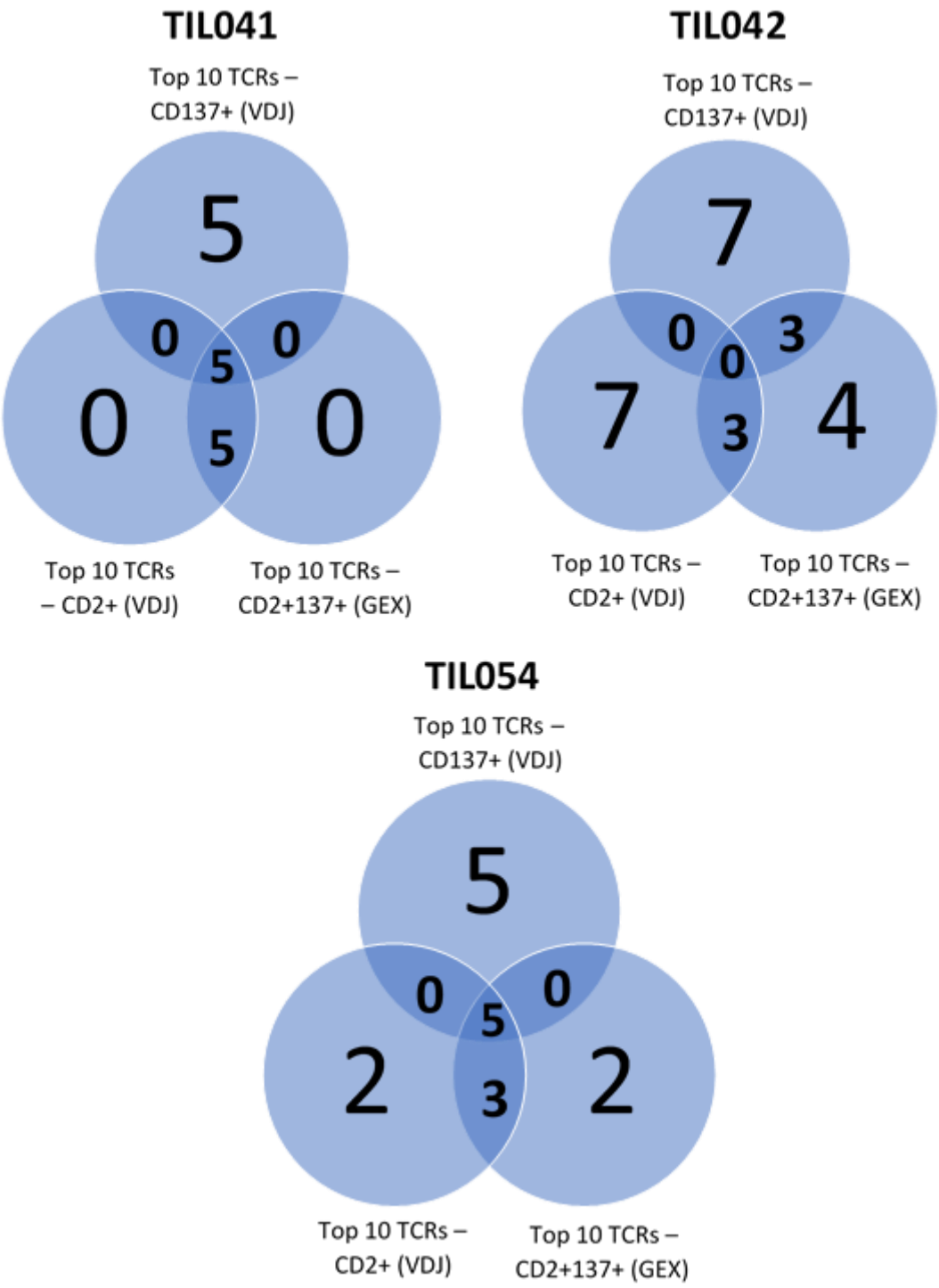

Figure 3.22. Venn diagrams showing top 10 TCR clonotype overlap when captured by different methods. Venn diagram for each TIL co-culture with matched tumour cell line, illustrating the number of the top 10 TCRs identified through CD2+ VDJ, CD137+ VDJ or CD2+ CD137 GEX using 10x Genomics®. The number of TCRs only detected by one method is in the non-overlapping sections, while the number of shared TCR clonotypes are detailed in the relevant overlapping segments.

3.4.9 Validating the tumour-reactive TCRs identified through 10x Genomics® single cell analysis

For the work in this thesis, CD137 expression has been used as the identifier for tumour-reactive TCRs, chosen through validation assays and literature review. To fully validate this marker of tumour-reactivity, three TCRs from the top 10 TCR clonotypes of the CD2+CD137+ sorted population of TIL054 were reconstructed into lentiviral vectors with a murine constant region to allow for transduction to be easily measured. The TCRs chosen are detailed in table 3.2 below.

Table 3.2. TIL054 TCRs reconstructed for TCR validation assays.

TCR	% of CD2+CD137+ population	% of CD2+ population	TRAV	TRBV	Corresponding Vβ
TCR1	22.06	3.03	TRAV14/DV4	TRBV7-3	Unknown
TCR2	2.8	0.98	TRAV38-2/DV8	TRBV13	23
TCR3	0.93	0.85	TRAV12-2	TRBV5-1	5.1

The most physiologically representative model for testing the TCRs was primary T-cells, so T-cells from two NBC donors were transduced with the three TIL054 TCRs. While initial transduction was good, unfortunately the transduction rates dropped dramatically after expansion through REP. Since the transduction of the different TCRs was similar, albeit low, an ELISA assay was set up by co-culturing the transduced primary T-cells with a variety of HLA-matched and mis-matched tumour cells, including the patient-matched tumour line. Details of the tumour lines selected can be found in table 2.3 in the methods and materials chapter. After 24 hrs, the production of IFNɣ was measured and normalised based on the tumour alone controls. The graphs in figure 3.23 show the IFNɣ production in pg/mL for the two different NBC donors. The first observation was that the NT controls produced relatively high levels of IFNɣ, although the amount was not increased from the unstimulated control when co-cultured with tumour cells, implying the IFNɣ production was not induced by the tumour cells. In contrast, the IFNɣ production for TCR1 and TCR3 in both donors

appeared to be induced by the HLA-matched melanoma cell lines which have been shown to stain strongly with an anti-Melanoma polyclonal antibody (data shown in Chapter 4). In both donors, TCR3 exhibited the highest IFNɣ production, when co-cultured with CTMM4.1, around 1500 pg/mL in both donors. On the other end of the scale, TCR2 showed very low IFNɣ production with all the tumour lines for both donors; the IFNɣ production was slightly higher in donor NBC-087, where the HLA-A*0201 tumour lines CTMM4.1 and patient-matched line CTCM54.1 induced a small response. It is worth taking into consideration that the TCRs only showed transduction rates of up to 2 % after REP, so repeating this assay with higher transduced T-cells or even TCR-sorted T-cells might result in much higher IFNɣ production.

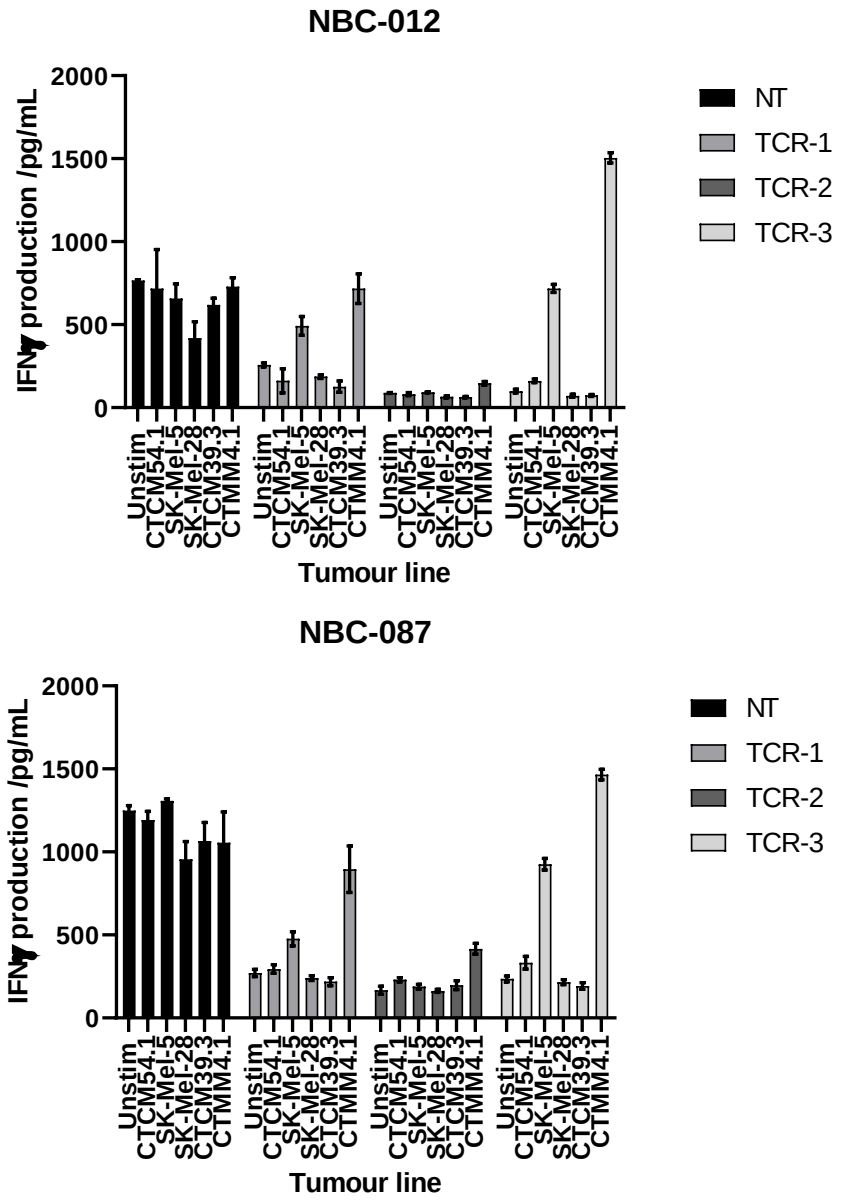

Figure 3.23. IFNɣ ELISA data for TIL054 TCRs co-cultured with different tumour lines. Primary T-cells from two NBC donors were transduced with three TIL054 TCRs, before being co-cultured with different HLA-matched and mis-matched tumour lines for 24 hrs. NT T-cells from the different NBC donors were used as controls. Supernatant was then removed for an IFNɣ ELISA assay, with the graphs showing the IFNγ production in pg/mL. Assays were carried out in triplicate to give three technical replicates, with the mean data plotted here.

Due to the unexpected drop in transduction in primary T-cells, another assay was planned using immortal T-cells to allow for large expansion of cells without affecting the transduction rate. The three TIL054 TCRs were transduced into two populations of TCR-negative J.RT3-T3.5 Jurkat cells (JRT3), one of which had been transduced with CD8+ co-receptor. This model was used to identify and facilitate better T-cell activation

for potentially co-receptor-dependent TCRs. The TCR-transduced Jurkat cells were then co-cultured with different tumour lines and activation markers CD69 and CD62L used to assess tumour-reactivity, including a control cell line, H508, which is a colorectal adenocarcinoma line. This line was included to see if the TCRs reacted to a non-melanoma tumour line. The graphs in figure 3.24 show the percentage of activated cells for each TIL054 TCR, as identified by the CD69+CD62L- population. The data for Jurkat cells is plotted next to the data for CD8+ Jurkat cells, to look for any differences in activation that are induced by the CD8+ co-receptor. The assays were conducted in triplicate, so any experimental variation is illustrated by the error bars.

For TCR1, the most activation was induced by cell lines SK-MEL-5 and CTMM4.1, which are both HLA-matched, high Melanoma marker expressing tumour lines. The percentage of cells in the CD69+CD62L- gate for the Jurkat population for these tumour lines was 23.0 % and 39.0 % respectively, and slightly lower for the CD8+ Jurkat cells, reading 19.7 % and 30.2 % respectively. This implies that the activation induced by this TCR is not co-receptor independent, and that the cognate antigen for the TCR is a shared Melanoma antigen. Some activation was induced by the patient-matched tumour line CTCM54.1, which was slightly higher for the CD8+ Jurkat population than the Jurkat population. The TCR1-transduced Jurkat cells did not respond to HLA-mismatched cell line SK-MEL-28, or HLA-matched, low Melanoma marker-expressing line CTCM39.3. The introduction of a CD8 co-receptor induces a small amount of induction (3.8 % and 4.4 % respectively) for these tumour lines, which could suggest non-specific activation. Neither the Jurkat or CD8+ Jurkat populations show any activation with H508 cells, which is a commercially available colorectal adenocarcinoma cell line, which are HLA-A2 restricted. The lack of activation by this tumour line indicates that the cognate antigen is Melanoma-restricted.

TIL054 TCR3 showed a very similar activation profile to TCR1, with the same tumour lines inducing a comparable degree of activation. The introduction of CD8 into the Jurkat cell line did not appear to affect the degree of activation induced by tumour cells, suggesting that neither TCR1 or TCR3 are particularly CD8 co-receptor dependent. In contrast to this data, the activation of Jurkat cells transduced with TIL054 TCR2 was clearly enhanced by the addition of CD8. Overall, the activation of TCR2-transduced cells was much lower than the other two TCRs, which corroborated

the results seen in the IFNɣ ELISA. The most activation was induced in the CD8+ Jurkat cells with CTMM4.1, where 11.2 % of cells were gated by CD69+CD92L-. After this, the most activation could be seen with the patient-matched tumour line CTCM54.1, although the 7.9 % of cells recorded for this result is similar to the activation induced by TCR1 (14.2 %) and TCR3 (7.8 %) in the CD8+ Jurkat population. This data, taken together with the results of the IFNɣ ELISA, showed that all three TIL054 TCRs can be activated by HLA-matched melanoma cell lines, likely responding to different shared Melanoma-restricted antigens. Out of the three TCRs, TCR2 shows the weakest activation, however activation was enhanced with the co-expression of CD8 coreceptor.

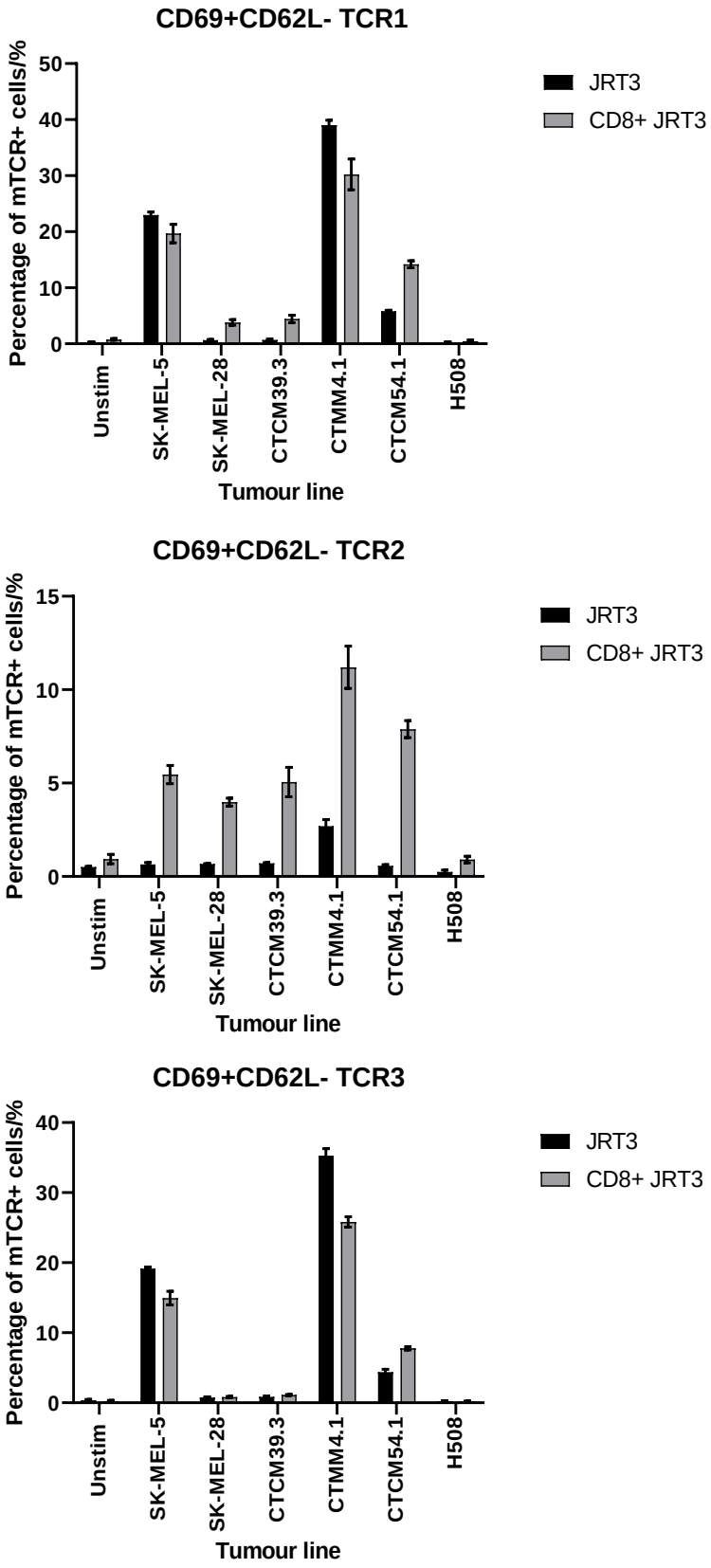

Figure 3.24. Activation of Jurkat and CD8+ Jurkat cells in response to different tumour cell lines. Jurkats (JRT3) and CD8+ Jurkats (CD8+ JRT3) cells were transduced with three TIL054 TCRs and co-cultured with different HLA-matched and mis-matched tumour lines for 24 hrs before activation was assessed through flow cytometry, using CD69 and CD62L antibodies. Assays were carried out in triplicate to give three technical repeats, with the means plotted here.

3.5 Conclusions and future work

In this chapter, three different models for assessing and identifying tumour-reactive populations of cells within TIL have been explored. The Jurkat library model, combining paired αβ-TCR single cell PCR technology with expression of TIL TCR libraries in Jurkat cells was the first model system tested. The main advantage of this system was that the breadth of the TCR repertoire could be investigated in detail through *in vitro* co-culture assays, without using up valuable banked final TIL product. However, there were unforeseen issues with accurately expressing the TIL TCR libraries in the Jurkat cell lines. These included a disproportional expression of Vβ8 in the Jurkat libraries and overall low expression of activation markers following autologous tumour co-culture.

One theory to suggest why Vβ8 dominance was observed in the Jurkat libraries relates to the endogenous Vβ8 TCR of the parental Jurkat line E6.1. The JRT3-T3.5 cell line was derived from the E6.1 Jurkat line through use of radiation to select a TCRβ-negative clone (Weiss and Stobo, 1984). However, it is likely that the TCRβ chain still remains in the cell line to some degree. The Vβ8 dominance in the Jurkat library transduced J.RT2-T3.5 cells suggests that through some process, potentially homologous recombination during the lentiviral library transfer, the Vβ8 transcript is being re-expressed as a full protein. Regarding the low expression of activation markers following autologous tumour co-culture, there have been a number of studies where TCR transduction into Jurkat cells has successfully induced activation through peptide-pulsed antigen presenting cells, but not induced reactivity to tumour cell lines (Cole et al., 1995; Calogero et al., 2000; Aarndouse et al., 2002). In these studies, it was suggested that co-transduction of CD8 co-receptor could recapitulate tumour-reactivity in these models, and that was demonstrated in the Aarndouse et al. paper. If this model were revisited, the use of CD8-transduced Jurkat cells might enhance the tumour-reactivity of TIL Jurkat libraries to the matched patient tumour cells. When validating the Jurkat activation assays, it was observed that loss of CD62L only occurred when CD69 expression was very high, such as when stimulated by PHA rather than tumour cells. From this observation, it was theorised that there is an activation threshold that must be reached for CD62L to be shed from the cells, and that this threshold is higher than that required for CD69 induction.

In concept, the Jurkat library model to represent the TCRs present within TIL was a smart one, utilising paired TCR sequencing method with the ease of culturing Jurkat cells for sustained *in vitro* cell culture. However, the unexpected dominance of Vβ8 in the Jurkat libraries was an unforeseen limitation of this model. Depletion of the Vβ8 population was attempted using flow sorting, but unfortunately this was to no avail. Additionally, to validate whether the results observed with the Jurkat libraries were representative of the TIL product, TIL Vβ and co-culture assays would be needed. Given that the benefit of this model system was to reduce the need to use precious TIL product samples, the amount of validation the Jurkat library system needed would outweigh this benefit. Additionally, due to the low tumour-reactivity, potentially due to the lack of co-receptor, the model was inadequate to address the aim of selecting tumour reactive cells. As one of the main aims of the PhD was to develop a model that could accurately identify the tumour-reactive population, it was decided that a TIL-tumour co-culture model system would better recapitulate an *in vivo* response.

For the second model of tumour-reactivity explored, a Vβ panel was used to gain insight into the breadth of the TCR repertoire, which included comparison to an NBC donor background. This model was experimentally simple and allowed a lot of data to be generated using a relatively small number of cells. Using the NBC donor background data proved to be comparable to similar experiments carried out in the literature, and when used to investigate relative abundance of Vβs, revealed some interesting results. These results were very encouraging for validating a background that could be used for future comparisons, however it is good to keep in mind a few unknown factors when considering the datasets used. While the exact ages of the donors corresponding to the normal buffy coats provided by the NHSBT, one can assume that they are from adult donors who are able to give blood, so likely older than 18. The background from the van den Beemd paper was comprised of a greater age range of donor, from neonates to over 80-year olds, and it is possible that age could affect the distribution of Vβs in a given donor. The question of how Vβ diversity changes with age has been investigated by many researchers, with the consensus being that there are more oligoclonal T-cell populations in elderly donors (van den Beemd et al., 2000; Britanova et al., 2014; Shao et al., 2014). There was also a total of 36 donors analysed in the van den Beemd paper dataset compared to the 8 donors analysed from NHSBT buffy coats,

although for many Vβ populations the standard deviation was greater for the van den Beemd dataset than the current study dataset. It is a generally accepted statistical principal that increasing the number of data analysed decreases the standard deviation if the samples are similar. Therefore, the larger error bars of the van den Beemd dataset could be a reflection on the wide age-range used. These factors could contribute to the few differences seen between the populations, although the similarity between the two data sets was reasonable. The background established in this PhD research could be improved by adding more donors, which could further decrease the error bars and giving it more statistical value. Of the Vβ populations where significant difference between the datasets is observed, the most striking of these is Vβ14. Throughout the work carried out for this thesis, Vβ14 consistently stained at very low levels, and this was considered accurate. Retrospectively, the data here indicated that this antibody might not stain the Vβ14 population as expected. In order to confirm whether the Vβ14 antibody in the panel is staining the Vβ14 population, a positive control such as a TCR expressing Vβ14 would have to be stained with the antibody to see if it is detected, like the experiment conducted in figure 3.3. This should be carried out in future work, and if the antibody is not staining correctly, it would show that the data involved Vβ14 is not reliable. It could be considered that more than one Vβ antibody is not staining accurately, however the Vβ panel has been well-validated in the literature, and the similarity between the expression of other Vβs in figure 3.8 is evident.

Comparisons of the TIL Vβ repertoire with the NBC donor Vβ background revealed several Vβ populations that show over 25-fold increase over the background levels. These highly-skewed Vβ populations, which were mostly observed in the CD8+ population, were restricted to TIL where the patients achieved at least a partial response during TIL treatment. In this way, the identification of highly skewed Vβ populations could act as a biomarker for predicting objective response to TIL therapy. This would need to be investigated further carrying out multiple Vβ panel stains on existing patient TIL to validate the results seen in figure 3.9, and see if this observation is consistent across all banked TIL samples. Another interesting next step in this research would be to use FACS sorting to isolate these particular Vβ populations and sequence them, to identify if high fold change is representative of oligoclonal

expansion. If single clones are being represented by high-fold change from background, then transducing these TCR clonotypes into primary cells and looking at tumour-reactivity would validate that Vβ panel screening and comparison to an NBC background could identify tumour-reactive cells. However, there are some caveats to this approach. While the logic for this approach is in line with the work carried out by Pasetto et al. showing relative abundance can correlate with tumour reactivity, there are other reasons why some Vβ populations might be more prevalent than others, such as the presence of unrelated bystander T-cells (Pasetto et al., 2006; Simoni et al., 2018). Another caveat to consider is that the T-cells used in this analysis were from final TIL product, as opposed to pre-REP TIL isolated immediately from tumour digest. Concerns about how the *ex vivo* expansion protocol affects TCR repertoire and tumour-reactivity have recently been addressed by Poschke et al. after the results in this thesis were generated (Poschke et al., 2020). They found that the TIL TCR repertoire changed massively during *in vitro* expansion, resulting in the loss of clonotypes that were dominant in the tumour, and facilitating the expansion of clones that were barely detectable in the tumour, which was driven by the capacity of the T-cells to expand in culture. Future work should investigate further the impact of the manufacturing process on TIL products.

The final model system that was investigated more directly identified the tumour-reactive population of TIL was the matched patient TIL-tumour co-culture model using CD137 expression as a marker of tumour-reactivity. In the literature, CD137 has been reported as being an accurate marker for identifying tumour-reactive T-cells within TIL, with some studies also using it as a selectable marker for sorting tumour-reactive TIL (Ye et al., 2013; Parkhurst et al., 2017; Seliktar-Ofir et al., 2017; Tan et al., 2019). This acknowledgement of CD137 as a marker of tumour-reactivity by the wider field of immunotherapy adds substantial validity to the results in this chapter, and shows that the same conclusion has been reached independently by different researchers globally. Collectively, the data in this chapter shows that the tumour-reactive population within TIL samples can be described using the activation marker CD137, and the breadth of the tumour-reactive TCR repertoire varies between patients. With a larger dataset, it might be possible to correlate the breadth of the tumour-reactive TCR repertoire with patient response, however that was not achievable for the data gathered in this

project. The overall tumour-reactivity of banked TIL product to patient-matched tumour lines was also very varied, but no higher than 35 % for any given TIL sample. An interesting result from the initial TIL-tumour co-culture assays was the reasonably low proportion of tumour-reactive cell in TIL054. The corresponding patient achieved a complete response upon TIL treatment, so it is possible that CD137 expression is not capturing the full tumour-reactive repertoire, or that the tumour-reactive cells were potent enough to induce a complete response. One theory why the overall TIL reactivity was not higher *in vitro* is that growing out an adherent tumour line from the tumour digest has changed the composition of the tumour and therefore, the antigens being expressed. In order to investigate this phenomenon, original tumour digest and tumour line cells could be sequenced and probed for different melanoma markers to compare how similar the two samples are.

Another reason why the tumour reactivity of the various TIL samples was not higher could be due to immunoediting by the tumour *in vivo* prior to resection. One way to improve on and add to the work set out in this chapter would be to use freshly-isolated pre-REP TIL and tumour, to best recapitulate the i*n vivo* environment, such as described by the work in the Ye et al. paper (2013). If identification and isolation of tumour-reactive T-cells occurred at this earlier stage, the overall proportion of these cells in the final TIL product could be improved, and this would hopefully lead to more potent TIL reactivity upon reinfusion. Additionally, other factors might cause a patient to have tumour-reactive TIL but only exhibit stable disease as a response, such as the length of follow up time. Patients were not treated as part of a clinical trial and as such, there was not a defined follow up protocol, particularly when patients were not local and received further aftercare back in their country of residence. As a result, patients who achieved a partial response over a longer period of time than they were being monitored would not be accurately reflected in the database. On the other hand, patients may have expired through other unrelated illnesses or old age. These other factors should be kept in consideration when evaluating this data, or any other data where patient response rate is recorded.

When CD137 was used as a selection marker and tumour-reactive TIL isolated using flow sorting, the resulting analysis of TCR repertoire using the Vβ panel revealed some interesting results for different TIL. For example, there was a dominance of Vβ7.1 in

TIL041, however this population was proportionally higher in the CD2+ population than in the CD2+CD137+ population. One possibility for why this was observed is that the tumour-reactive population is made up of different Vβ7.1 TCR clones and only a few are tumour-reactive. Another possibility to explain the presence of a large non-tumour-reactive clone in the final TIL product could be the result of a bacterial or viral infection, resulting in a large bystander population. However, the proportion of Vβ7.1 in the CD2+CD137+ population, while a lower proportion than the CD2+ population, is still substantial. Further work should be carried out on this Vβ population beyond this project to elucidate why there is a dominant TCR clone present in the TIL product that does not match the reactivity of the CD2+CD137+ population.

For TIL054, the Vβ distribution for CD2+CD137+ population was shown to be quite broad, which is interesting when taking into consideration the patient's complete response to TIL therapy. While it could be interesting to suggest that the breadth of the tumour-reactive population was a contributing factor to the patient's complete response, too few TIL samples have been assessed to make that statement. During cell culture, it also became clear that the cells in the TIL054 product had retained a high proliferative capacity compared to other some TIL samples, and after expanding the cells further through another standard REP, the cells were still highly proliferative. This could mean that the patient's complete response was partially attributable to T-cells ability to persist and expand better *in vivo*.

One of the challenges in interpreting the TIL Vβ panel data after co-culture with matched tumour was gating the CD2+CD137+ population. In the optimisation assays carried out previously, a defined model of MART-1 TCR-transduced primary T-cells was used as these are known to react to both tumour lines and peptide-pulsed T2 cells. In those assays, there was a very distinct population of tumour-reactive cells shown by CD137 expression that appeared very separate from either the mismatched co-culture or non-transduced controls. In the case of analysing the matched TIL-tumour co-cultures, the FACS plots were often less well defined, and the increase in CD137 population was sometimes seen as a smear rather than two distinct populations of CD137+ and CD137- cells (data not shown). To minimise inaccurate gating, rather than attempting to assign cells to a CD137- gate, the full CD2+ repertoire of T-cells was gated, then the CD137+ gate was created based on the unstimulated TIL control. An

example of this gating that was used for flow sorting of TIL054 can be seen in figure S2. One factor that might have attributed to less distinct CD2+CD137+ populations could be the background CD137 expression of the TIL. It was assumed that like the primary T-cells used previously, this would be very low. However, analysis recently carried out by another member of the group has seen that this isn't always the case, with one unstimulated TIL sample exhibiting CD137 expression of over 20 % (Instil Bio UK, unpublished data). There are many factors that could influence resting CD137 expression levels, including how well rested the cells are in culture prior to testing with the CD137 antibody. The amount of IL-2 used to culture the cells, as well as the density of the cells in culture and the freshness of the culture medium, can all contribute to the activation status of T-cells, and in retrospect, these measures could have been more tightly regulated when these assays were conducted. It would be interesting to observe how CD137 expression is affected by these factors when no other stimuli or cells are present to influence the result.

With regards to the techniques and methods used in the CD137 model system, the workflow set out in figure 3.17 is both logical and efficient. While the initial CD137 validation assays gave clear and convincing results, in retrospect it would have been more useful to conduct these using TIL rather than TCR-transduced primary cells. Using the MART-1 TCR-transduced primary T-cells resulted in a much cleaner system, and holds the benefit of being able to investigate CD137 expression while titrating peptides of known affinity, problems were encountered when the model was applied to TIL and the CD137+ populations were not as well defined.

Combining the CD137 marker of activation with the immense V(D)J and gene expression sequencing analysis of the 10x Genomics® system proved successful. The results for this section of work were collected in the final year of the project, as a culmination of the previous assays. As a result, the data presented here barely scratches the surface of the data that can be uncovered using the 10x Genomics® V(D)J and GEX analysis software. The many other lines of investigation for these TIL TCR datasets which could not be investigated in the scope of this project should be taken forward for future work. For example, other genes of interest that might be worth investigating regarding characterising the tumour-reactive population of TIL include PD-1, IFNɣ, CD107a, CD25 and any other marker of activation. The differentiation

status of different TIL subsets could also be investigated using gene expression data. Lastly, the gene expression datasets from the three TIL analysed could be searched collectively to look for potential new targets or markers of tumour-reactive cells. Additionally, the gene expression data for the CD137-sorted TIL samples could be obtained to provide even more insight into this population of cells.

Another question that should be addressed in future work if stronger conclusions are to be made about overlap of tumour-reactive populations are how the results are subject to under-sampling. Without sequencing the entirety of a TIL product, the breadth of the TCR repertoire cannot be definitively ascertained, and has already been discussed that this is an unrealistic effort. Furthermore, even though elucidating the entire TCR repertoire might be interesting, there are more important questions that could be answered, such as whether a higher proportion of tumour-reactive cells in the cell product leads to a better response in the patient. To assess how tumour-reactive TIL might contribute to patient response, a better model would be needed, potentially utilising a 3D tumour spheroid co-culture system, or establishing an in vivo model system.

Comparing TCR diversity and the degree of TCR sample overlap for any two or more given T-cell populations is not a straightforward task. Some of the issues facing researchers are highlighted in a very thorough paper of potential statistical models by Rempala and Seweryn (2013); these include under-sampling, low cell counts and unique, rare populations. To avoid making incorrect judgements about the overall TCR diversity of the whole TIL population based on very small sample size, the top 10 clonotypes were chosen for comparison from each population. While this is a very small number of clonotypes overall, in some cases they make up a substantial amount of the cell product, such as the 25 % of CD137+ cells from TIL054 belonging to a single TCR clone. By this method, the analysis is assessing TCR clonotypes based on their prevalence in TIL samples as opposed to the extent of their tumour reactivity. To improve this methodology, power calculations could be utilised to determine the number of T-cells that would need to be assessed to ensure a reliable TCR clonotype estimate to be made.

In the pursuit of a model which better represents the *in vivo* tumour-response, the TIL-tumour co-culture model could be improved further by developing a 3D tumour

culture model, encouraging the tumours to grow into spheroids as opposed to on plastic. The main advantage this could carry is reducing the change to the tumour phenotype over time, and give a more representative model. When designing *in vitro* experiments, the aim is always to create a model that answers the *in vivo* question in the most representative way possible. While considerable work would be required to develop a new spheroidal tumour culture system, the benefits of using a more physiologically relevant model would be worth the initial efforts.

4.0 Pre-clinical validation of melanoma-reactive T-cell receptors from TIL

4.1 Background

4.1.1 TCR T-cell therapy trials

In the introduction of this thesis, TCR T-cell therapy was discussed as one of the adoptive cell therapies for cancer immunotherapy, particularly in the melanoma setting. TCR T-cell therapy involves the transduction of T-cells with TCRs reactive to known antigens before reinfusion back to the patient. While TCR T-cell therapy seems to have been overshadowed in recent years by successes in the CAR T-cell field, given that CAR T-cell therapy has yet to show much promise for solid tumours, TCR T-cell therapy still holds therapeutic benefit.

Earlier this year, a review was published covering some of the key clinical successes and failings in TCR T-cell therapy (Oppermans et al., 2020). Overall, there were found to be 104 clinical trials in the clinical trials database (correct as of May 2020) that involved the treatment of cancer with TCR-transduced lymphocytes. These were predominantly for the treatment of melanoma, which is expected given that it is a highly immunogenic cancer type with many well-defined antigens for targeting. However, from the few completed trials that provided results, the objective response rates observed were underwhelming. This was not helped by the early termination of several trials, some of which had good initial data, due to low accrual. With regards to adoptive cell therapies for cancer it is worth bearing in mind that patients recruited onto such trials have often progressed on first-line therapeutic interventions including surgery, chemotherapy and in some cases, checkpoint inhibitors. This means that many patients who would likely respond very well to an adoptive cell therapy such as TCR T-cell therapy have already had good responses through other interventions and do not need to enrol on a clinical trial. That being said, the efficacy of TCR T-cell therapy still needs to improve to show better response rates if it is going to be considered as an effective therapy for solid cancers.

4.1.2 High-affinity TCRs

Of the successes seen in the field of TCR T-cell therapy, several have arisen with the advent of identifying or developing high-affinity TCRs. The term 'high-affinity' refers to the strength of the interaction between a TCR and the pMHC complex present on antigen presenting cells. In naturally occurring tumour-reactive TCRs, such as those isolated from patient TIL, the TCR-pMHC interaction is typically weak, as the process of thymic selection deletes clones that exhibit strong reaction to self-antigens (Aleksic et al., 2012). This lends to the theory that TCRs that show a strong interaction with pMHC could result in better cytotoxic T-cell responses. The interaction between pMHC and TCRs has been studied extensively, with the structure of the complex investigated to elucidate why some TCRs induce stronger responses than others (Bridgeman et al., 2011; Irving et al, 2012). There is evidence that making small genetic alterations, or selecting TCRs that exhibit higher pMHC binding properties than normally observed can greatly impact the efficacy of the TCR-pMHC interaction and result in an optimal effector T-cell response (Tan et al., 2015). An example of this has been well-documented for a MART-1-reactive TCR used to treat patients with melanoma. The original TCR identified for the initial clinical trial, known as DMF4, was isolated from a TIL sample and identified as being MART-1 reactive (Morgan et al., 2006). When this TCR was validated, it showed good response to MART-1-expressing tumour and was taken forward for use in clinical trials. In an attempt to identify more variants with superior anti-tumour properties of this TCR, MART-1 reactive TIL clones were isolated from the same patient and the group discovered a higher affinity TCR variant, termed DMF5 (Johnson et al., 2006). When this TCR was used to treat melanoma patients, it showed an improved patient response rate of 30%, compared to DMF4 which had a patient response rate of approximately 13% (Johnson et al., 2009). However, severe on-target off-tumour toxicity of the eye and ear was observed with the DMF5 variant that was not seen with the original DMF4 TCR. This was attributed to the increased sensitivity and persistence of the DMF5 TCR that led to the transduced T-cells attacking healthy melanocytes upon reinfusion to the patient. This is a key example that evidences the unexpected toxicity that can arise when specifically selecting high-affinity TCRs. Examples such as this have caused a big debate around the level of off-

tumour or off-target side effects that are acceptable when associated with a good patient response.

4.1.3 The importance of antigen targeting

For an optimal TCR T-cell therapy, the choice of targeted antigen is critically important. It remains a challenge in this area of adoptive cell therapy to identify antigen targets for TCRs that can induce superior patient responses without causing severe off-tumour side effects. As discussed in the introduction, antigens that are not expressed in healthy tissues make the safest antigen targets, however they are often not expressed widely in tumours or between patients. Some types of antigen are expressed at a higher rate in tumours so are easier and more effective to target, but they also tend to be expressed in healthy tissues, such as the group of over-expressed antigens in melanocytes and melanomas. While the search for highly expressed, tumour-specific shared antigens continues, researchers are utilising known antigens to the best of their ability. Often the therapeutic benefit of treating the cancer outweighs the negative side effects that can arise from on-target off-tumour toxicity. This is at least the case when the side effects are transient and regress either with or without further intervention. For melanoma TCR T-cell therapy treatment, over-expressed antigens such as MART-1 and gp100 are commonly targeted, and toxicity arising from the targeting of healthy melanocytes often includes skin abnormalities such as vitiligo, such as in the DMF5 MART-1 TCR example discussed above. As a symptom, vitiligo has even been noted as an indicator of good patient response and a more favourable prognosis in melanoma patients following immunotherapy (Teulings et al., 2015; Hua et al., 2016). From the list of clinical trials in the Oppermans et al. review, it is shown that a number of clinical trials currently recruiting are using NY-ESO-1 reactive TCRs; NY-ESO-1 is a CT antigen that should not induce on-target off-tumour responses in the way that the MART-1 reactive TCR has, such as targeting of healthy melanocytes in other tissues. Furthermore, NY-ESO-1 being more broadly expressed across a range of different tumours has advantages over targets such as MART-1 or gp100 which are more melanoma specific in their expression profile. A clinical trial was conducted by the Rosenberg group using NY-ESO-1 TCR T-cell therapy to treat patients with either synovial sarcoma or melanoma, and reported response rates of 45 % and 18 %

respectively (Robbins et al., 2011). This is reflective of the higher NY-ESO-1 expression for synovial sarcoma (around 80 %) compared to melanoma (around 25 %). Importantly, the only toxicities that were observed during this trial were neutropenia and thrombocytopenia, both of which were transient and were known to be attributed to the high IL-2 supportive therapy regime. This is an exciting development in the field of TCR T-cell therapy, and it will be interesting to see how effective NY-ESO-1 TCR T-cell therapy proves to be.

One of the most important lessons to be learnt surrounding high-affinity TCR T-cell therapy and choice of target antigen came from a phase I trial for an affinity-enhanced MAGE-A3-reactive TCR to target melanoma and myeloma, which unfortunately resulted in patient death due to unexpected off-target reactivity (Linette et al., 2013). When the first patient died after treatment with the MAGE-A3 TCR transduced T-cells, it was not considered abnormal since the patient had a history of cardiac arrest. However, when the second patient also died of heart-related complications, further autopsy investigations for both patients were conducted where a large influx of the MAGE-A3 T-cells in the cardiac tissue was observed. Through further *in vitro* investigation, they discovered that the MAGE-A3 T-cells were cross-reacting with a protein known as titin, which has a very similar structure to MAGE-A3. These results alerted the scientific community to the dangers of non-thymically selected TCRs that are not thoroughly profiled with regards to their cross-reactivity to other cognate peptides. This has led some researchers to establish a much more extensive pre-clinical validation process as part of therapeutic TCR selection. These processes include peptide scans and TCR-pMHC affinity studies; a full workflow of suggested assay can be found in a 2017 paper by Kunert et al. (Kunert et al., 2017).

4.1.4 Murinisation of T-cell receptors

Some of the challenges facing TCR T-cell therapy researchers involve efficient TCR transduction into peripheral blood lymphocytes (PBL), mispairing of the introduced TCR with the endogenous TCR and tracking of the transduced T-cells in the patient after infusion. There are several different approaches taken by researchers to overcome the limitations of TCR transfer, such as extra disulphide bonds and clustered

regularly interspaced short palindromic repeats (CRISPR) knockout of endogenous αβ TCRs (Cohen et al., 2007; Legut et al., 2018). However, the technique that has been utilised in this project was TCR murinisation, due to the ability of using the murine region as a built-in marker of TCR transduction (Sommermeyer et al., 2006). Murinisation of TCRs involves replacing the α and β chain constant regions with corresponding murine constant regions, whilst keeping the rest of the human TCR the same. It was previously shown that murinised TCRs are preferentially expressed by T-cells, replacing the expression of endogenous TCR likely due to more stable associations with the CD3 complex (Sommermeyer et al., 2006). Additionally, murinised TCR-transduced T-cells have shown enhanced cytokine production in response to peptide-pulsed APCs, and are even capable of conferring increased tumour recognition of MHC class I restricted tumour cells by CD4+ T-cells (Cohen et al., 2006; Goff et al., 2010b). The use of murine-constant TCRs (mTCRs) has been adopted by several research groups with successful use of them in both *in vitro* and *in vivo* studies (Johnson et al., 2006; Hart et al., 2008). While there has been evidence that antibodies are raised to the introduced murine constant region, further investigation determined this was unlikely to affect clinical outcome (Davies et al., 2010). One of the main benefits of this mTCR system is that no antibiotic resistance gene is needed to purify the cell population; isolation of mTCR+ cells can be achieved through cell sorting the transduced population. One concern surrounding the transduction of mTCRs into PBMC T-cells could be the mispairing of the mTCR with the endogenously expressed TCRs. However, this was addressed by Sommermeyer and Uckert who showed that both murinised TCRs and minimally murinised TCRs (where just key murine constant region residues were substituted) preferentially pair with each other and result in more stable complexes (Sommermeyer and Uckert, 2010). This is an appealing solution, as knocking out endogenous TCRs from T-cells are not required in this model, which saves considerable time and money. The identification of mTCR-transduced T-cells can be achieved with the use of commercially available antibodies against the murine region of the TCR, which is a desirable property for *in vitro* and *in vivo* assays. Such antibodies can be bought already conjugated to a wide variety of fluorophores, for easy incorporation into a flow cytometry panel.

4.1.5 gp100 as a target antigen

One of the top antigens that has been utilised for TCR T-cell therapy clinical trials for melanoma is the shared overexpressed melanoma antigen gp100. Gp100, also known as Pmel17, is a membrane-bound glycoprotein expressed by melanocytes that has a role in melanosome generation and the polymerisation of melanin (Pitcovski et al., 2017). Several gp100-restricted TCRs have been identified and isolated from melanoma TIL samples, which have also been proven to show cytotoxic T-cell responses to gp100-expressing tumour and peptides (Seiter et al., 2002). In conjunction with these data, there are several different known MHC-class-I-restricted, gp100 antigenic peptides, which are known to induce immune responses (Kawakami et al., 1994a; Salgaller et al., 1995). The most common gp100 epitopes that have been identified to date are $gp100_{154}$ (KTWGQYWQV), $gp100_{209}$ (ITDQVPFSV) and $gp100_{280}$ (YLEPGPVTA), the positions of which can be identified in the *PMEL* structure in figure 4.1 below (Denkberg et al., 2002). These different gp100 peptides were shown to induce effector functions when gp100-specific cytotoxic T-cells from HLA-A*02+ve melanoma patients were stimulated by patient-matched, peptide-pulsed PBMCs (Salgaller et al., 1995).

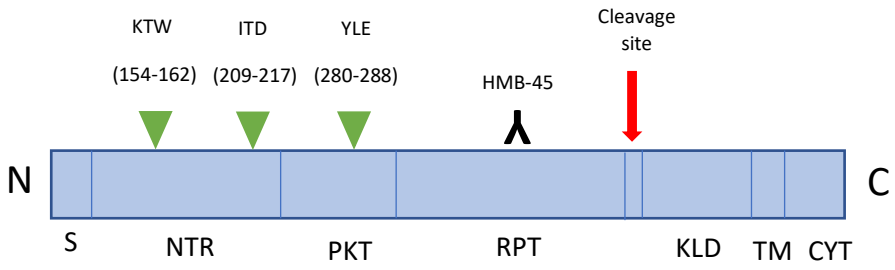

Figure 4.1 Simplified structure of gp100. Three common gp100 epitopes and their amino acid positions are indicated by green arrows. The region in which HMB-45 monoclonal antibody binds is indicated. N = N terminal; C= C terminal; S = signal region; NTR = N-terminal region; PKD = polycystic kidney disease homology domain; RPT = proline, serine, threonine-rich repeat domain; KLD = Kringle-like domain; TM = transmembrane domain; CYT = cytoplasmic domain.

From this preliminary work, there have been a few gp100-TCR T-cell clinical trials in the clinic, with varying degrees of success; these can be found listed in table 4.1. These data give some insight into the past and current state of clinical trials and where they are located (Clinical trial database, 2020). Searches of the clinical trial database show

that there have not been many clinical trials using gp100-TCR transduced PBL conducted or currently recruiting, with the majority of gp100-related clinical trials found in the search instead utilising gp100 peptide vaccines. There are a few clinical trials in the table below which use both gp100-transduced PBL and gp100 vaccines, showing that combinatorial immunotherapies are also being explored in gp100 research. Due to the collaborative nature of clinical trials, the clinical trials tend to only take place where there is a relevant research group, either academic or industrial, as well as the necessary partners to carry out the work; a GMP-grade cell manufacturer, an experienced surgeon or physician who is willing to support the trial and a hospital that can facilitate the treatment of the patients to name a few. This can be seen reflected in the list of clinical trials and their locations, and though the principal investigator data is not shown, these trials tend to be led by a select few people with the appropriate expertise in those locations.

Table 4.1. Clinical trials utilising gp100-TCR transduced T-cells. Information gathered from the clinical trials database and correct as of August 2020.

Trial number	Status	Phase	Condition	Treatment	Country	Response rate
NCT00923195	Completed	2	Melanoma	anti-gp100$_{154-162}$ TCR PBL, gp100$_{154-162}$ peptide, Radiation, IL-2, Montanide ISA 51 VG	USA	0 of 2
NCT00203879	Completed	2	Melanoma	MAGE-3/Melan-A/gp100/NA PBMC, IL-12	USA	No results posted
NCT00665470	Completed	2	Melanoma	Gp100-reactive PBL, IL-2	USA	0 of 10
NCT00085462	Completed	1	Melanoma	gp100-TCR transduced TIL or PBL, IL-2, filgrastim, gp100 fowlpox vaccine	USA	No results posted
NCT01211262	Completed	1	Melanoma	IMCgp100*	USA, UK	6 of 69

NCT02535078	Recruiting	1 / 2	Melanoma	IMCgp100*, durvalumab, tremelimumab	USA, Canada, Denmark, Germany, Italy, UK	N/A
NCT03070392	Recruiting	2	Uveal Melanoma	IMCgp100*	USA, Australia, Belgium, Canada, France, Germany, Italy, Netherlands, Poland, Russia, Spain, Switzerland, Ukraine, UK	N/A
NCT02570308	Active, not recruiting	1	Uveal Melanoma	IMCgp100*	USA, Canada, Germany, Spain, UK,	N/A
NCT00610311	Terminated (low accrual)	2	Melanoma	anti-gp100$_{154-162}$ TCR PBL, IL-2, ALVAC gp100 vaccine**	USA	1 of 3
NCT00509496	Terminated (low accrual)	2	Melanoma	anti-gp100$_{154-162}$ TCR PBL, IL-2	USA	3 of 19 PBL arm, 1 of 2 TIL arm
NCT02889861	Terminated (sponsor decision)	2	Melanoma	IMCgp100*	USA, UK	Results submitted

* IMCgp100 = Bispecific soluble HLA-A2 restricted gp100-specific TCR fused to anti-CD3

** ALVAC gp100 vaccine = plaque purified canarypox vector gp100

Another factor compounding the low number of trials in this area is the overall low success rate, despite the Rosenberg group noting good responses in their 2009 paper (Johnson et al., 2009). If pre-clinical and clinical data do not look promising, principal investigators either in academia or industry often decrease their research efforts into that intervention, or change focus entirely, which can be seen in the clinical trial database where trials are terminated due to the principal investigator changing research interests. The abundance of NY-ESO-1 TCR T-cell therapy clinical trials, with more promising early data, could be an indication of a shift in focus to a more widely

expressed, tumour-restricted antigen (Oppermans et al., 2020). However, given that several notable papers researching the composition of TIL report that potent melanoma-reactive TCRs can be found within TIL that show strong cytotoxic capabilities, it is surprising that clinical data using gp100-TCRs has not been more successful. One reason for this could be the choice of TCR used in the TCR T-cell therapy studies. The originally promising gp100-TCR results from the Rosenberg group utilised a transgenic mouse model, as a gp100-TCR could not be isolated from the TIL samples they used (Johnson et al., 2009). It is possible that a lack of thymically-selected and efficacious gp100 TCRs has been a limiting factor in melanoma-reactive TCR T-cell therapy trials.

4.1.6 Aims

In this chapter, the main aim is to pre-clinically validate melanoma-specific TCRs, identified from patient TIL through dextramer panning with known melanoma antigens. As part of the collaboration with GigaGen Ltd., the American company sought to identify melanoma-reactive TCRs from the TIL Jurkat libraries they had constructed (see chapter 3). There were some key reasons that this approach was taken. Firstly, there has been a lot of work in the area of shared melanoma antigens for TCR T-cell therapy, which means there are a lot of useful methods and resources available. Also, by first establishing a set of reliable validation assays in a known antigen TCR system, the assays could be utilised downstream of the CD137 TCR identification and isolation model described in chapter 3. To identify melanoma-reactive TCRs, GigaGen Ltd. used dextramers made from common melanoma/tumour antigens such as MART-1, gp100, NY-ESO-1 and MAGE-A3 to pan the libraries for reactivity against these particular peptides (Spindler et al., 2020). From the three libraries they panned, only the Jurkat library for TIL039 showed specific reactivity, and this was restricted to one peptide used in the panning process, $gp100_{154\text{-}162}$ (KTWGQYWQV). Within this library, they identified five HLA-A*0201 TCRs that could recognise this antigen. The frequencies of these TCRs in the Jurkat library were very low, so they used successive rounds of dextramer panning and sorting to expand these populations, shown in figure 4.2. Once the populations were sufficiently enriched for these TCRs, the individual TCR sequences were identified and recapitulated into

lentiviral vectors with a puromycin resistance gene for transduced cell selection. The details of these TCRs and their corresponding Vβ can be found in table 4.2. GigaGen Ltd. began to characterise the TCRs, by showing they had specific reactivity to gp100 when transduced into Jurkat cells. Mis-matched TCRs were also created by co-expressing the Jurkat α chain with the gp100 TCR β chains to demonstrate the specificity of the gp100 TCRs, and these mis-matched TCRs lacked reactivity to the index gp100 peptide (Spindler et al., 2020).

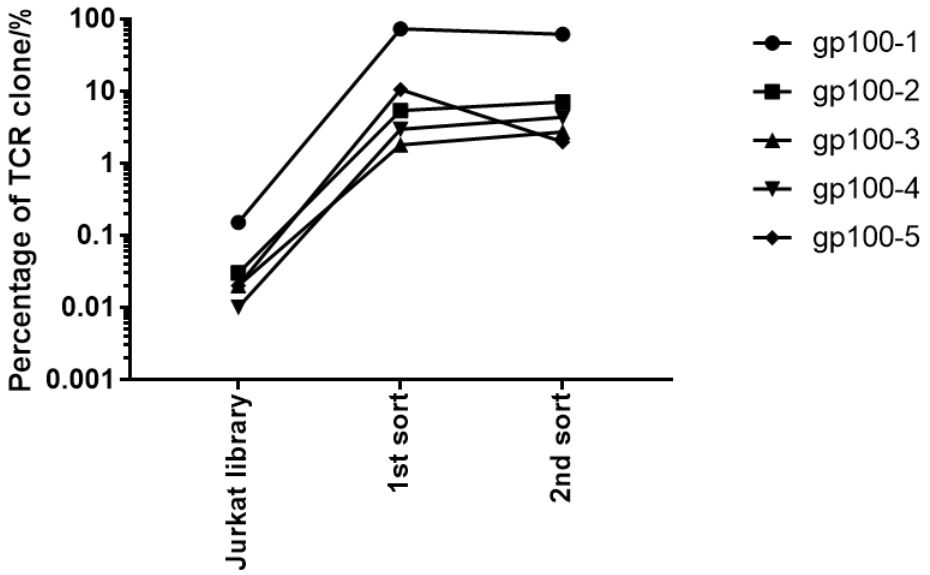

Figure 4.2. gp100 clone frequency through successive rounds of dextramer panning. Five HLA-A*0201 gp100-reactive TCRs were identified from Jurkat library 039 through dextramer panning with pMHC dextramers loaded with $gp100_{154\text{-}162}$. The frequency in the starting Jurkat library is plotted, and the enrichment after successive rounds of flow sorting and further dextramer enrichment. These data were provided by GigaGen Ltd., with more details in the Spindler et al. (2020) paper.

Table 4.2. Information of five HLA-A*0201-restricted gp100-reactive TCRs isolated from JL039.

TCR	TRAV	TRAJ	CDR3-α	TRBV	TRBJ	CDR3-β	Corresponding Vβ
Gp100-1	TRAV30*01	TRAJ48	CGIGNEKLTF	TRBV7-6*01	TRBJ2-3	CASSVAGGTDTQYF	Not allocated
Gp100-2	TRAV12-2*02	TRAJ24	CAVSTDSWGKLQF	TRBV7-6*01	TRBJ2-7	CASSLADSEQYF	Not allocated

Gp100-3	TRAV35*02	TRAJ30	CAPGGDDKIIF	TRBV7-6*01	TRBJ2-1 F	CASSLGGGADEQF	Not allocated
Gp100-4	TRAV5*01	TRAJ30	CAEIANRDDKIIF	TRBV4-1*01	TRBJ2-2	CASSQAVNTGELFF	7.1
Gp100-5	TRAV5*01	TRAJ34	CAEDTDKLIF	TRBV11-2*01	TRBJ2-2	CASSLGGGELFF	21.3

When selecting a TCR for therapeutic use, two of the most important aspects are the sensitivity of the TCR to cognate antigen and the specificity or cross-reactivity of the TCR. A TCR affinity should be high enough that if the antigen is presented at low levels in the tumour, it is still able to induce an anti-tumour response, but not so high that there is severe on-target off-tumour reactivity; the higher the TCR affinity for pMHC class I, the more cross-reactive the TCR is (Stone, Harris and Kranz, 2015). With these criteria in mind, the aim for the work conducted in this chapter was to begin the process of pre-clinically validating the five HLA-A*0201-restricted gp100 TCRs.

4.2 Validation of gp100-mTCRs in a Jurkat cell system

4.2.1 Transduction of gp100-mTCRs into Jurkat cells

On receiving the gp100 plasmids from GigaGen Ltd., attempts were made to transduce J.RT3.T3.5 Jurkat cells with the gp100 lentiviruses. The Jurkat transduction rates can be seen in figure 4.3. The transduction, as measured by percentage of CD3+ live cells, was low for all five TCRs, however as NT Jurkat cells can also express low levels of CD3, a better marker of TCR transduction was needed. Selection by Vβ antibodies would be effective, however some of the TCR β-chains did not have corresponding antibodies to the TRBV regions, so transduction by this method could only be defined for two TCRs – gp100-4 and gp100-5. Figure 4.3B shows the flow plots of the percentage of CD3+ cells that stained with the corresponding Vβ antibody for the gp100-4 or -5 TCR.

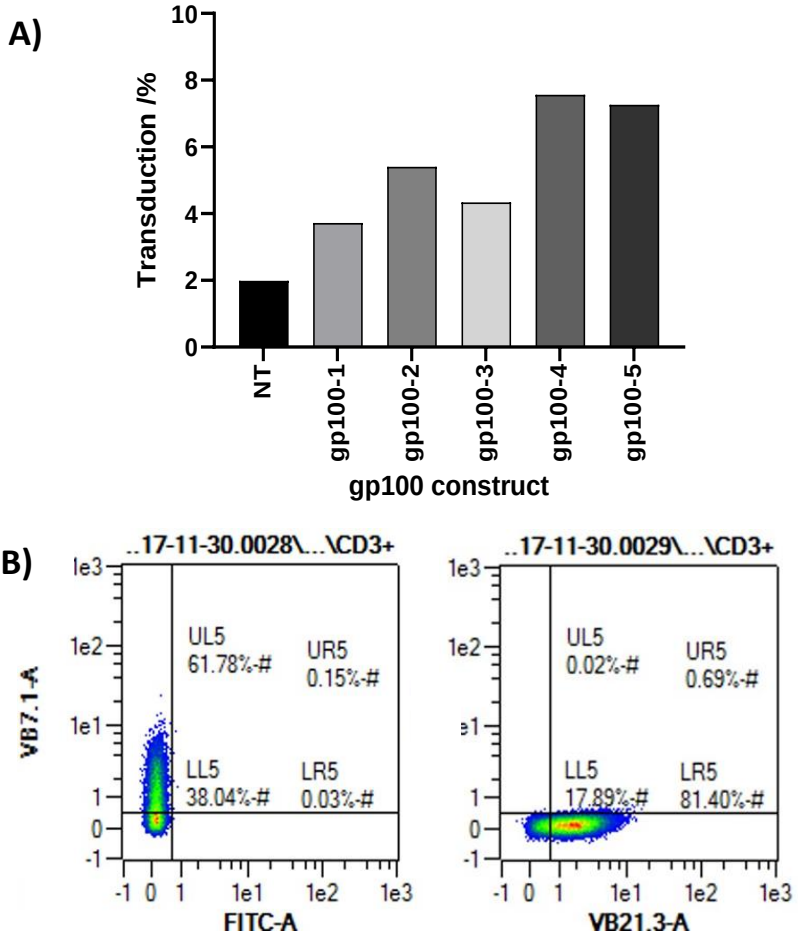

Figure 4.3. gp100 TCR transduction in JRT3.T3.5 cells. A) Transduction rates for the five HLA-A*0201 gp100 TCRs when transduced into JRT3.T3.5 Jurkat cells, as measured by CD3 flow cytometry. B) Flow cytometry plots showing staining of gp100-4 (left plot) TCRs and gp100-5 (right plot) TCRs with their respective Vβ antibodies. Gating was established using NT JRT3 controls (not shown).

To select the gp100 TCR transduced Jurkat cells, puromycin was added to the cultures as the gp100 TCR plasmids contained a puromycin resistance gene. Using the concentration of puromycin recommended by GigaGen Ltd. to successfully select the transduced cells resulted in low cell counts that struggled to expand in culture, potentially due to the low transduction rate. To circumvent this issue, TCRs were designed that used a murine constant region that could be identified using an anti-mouse TCR-β antibody, providing an 'in-built' marker for cell sorting the resultant population. These gp100-mTCRs were used for the remainder of the assays in this chapter, and for the rest of this chapter, the transduced J.RT3-T3.5 cells will be referred to as Jurkats.

4.2.2 The five gp100-mTCRs exhibit different sensitivities to index peptide

To compare the sensitivity of the five gp100-mTCRs, a peptide titration assay was carried out using a 1: 1 ratio of Jurkat cells to peptide-pulsed T2 cells. T2 cells are antigen-presenting cells express MHC class I molecules that can be pulsed with exogenous peptides examining cytotoxic lymphocyte responses to tumour antigens (Bossi et al., 2013). In this assay, the T2 cells were pulsed with titrating levels of the index $gp100_{154-162}$ peptide using serial dilutions, from 1×10^{-6} to 1×10^{-9} M. When gating the CD69+ or CD62L- cells on the MACS Quant flow cytometer, it became apparent that the two markers showed different activation profiles. For all concentrations of peptide, the Jurkat cells expressed moderate levels of CD69 as a distinct population. In contrast, only at the highest concentrations of peptide did the cells lose CD62L expression. This is illustrated by the flow plots in figure 4.4A. When the two markers were assessed simultaneously, it was found that the CD69+ population of cells were the same population that lost CD62L when the stimulation was high. Therefore, the two markers were assessed in conjunction to best investigate the degree of activation of the Jurkat cells.

The graphs showing activation of the gp100-mTCR Jurkat cells when co-cultured with the T2 cells pulsed with decreasing concentration of peptide can be found in figure 4.4B. Fold change in CD69+CD62L- cells, as measured from a background of unloaded T2 cells was used as the readout, to allow normalisation of the data so the different

gp100-mTCRs could be compared. The assay was conducted twice, each time with three technical replicates, with the mean fold change plotted on the graph. At the highest concentration of peptide, gp100-4 and gp100-5 had the highest level of activation, showing 13.7-fold and 12.2-fold change respectively. The other TCRs, gp100-1, -2, and -3, displayed a fold change in activated cells of less than 5-fold even at the highest concentration of peptide. As the concentration of peptide decreased, the fold change of gp100-4 mTCR Jurkat cells decreased by approximately half in the first serial dilution, and continued in this manner to give a 1.6-fold change at the lowest peptide concentration. In contrast, the fold change of gp100-5 decreased at a lower rate until the lowest concentration of peptide, when the activation of gp100-5 still remained 4.6-fold higher than unloaded T2s.

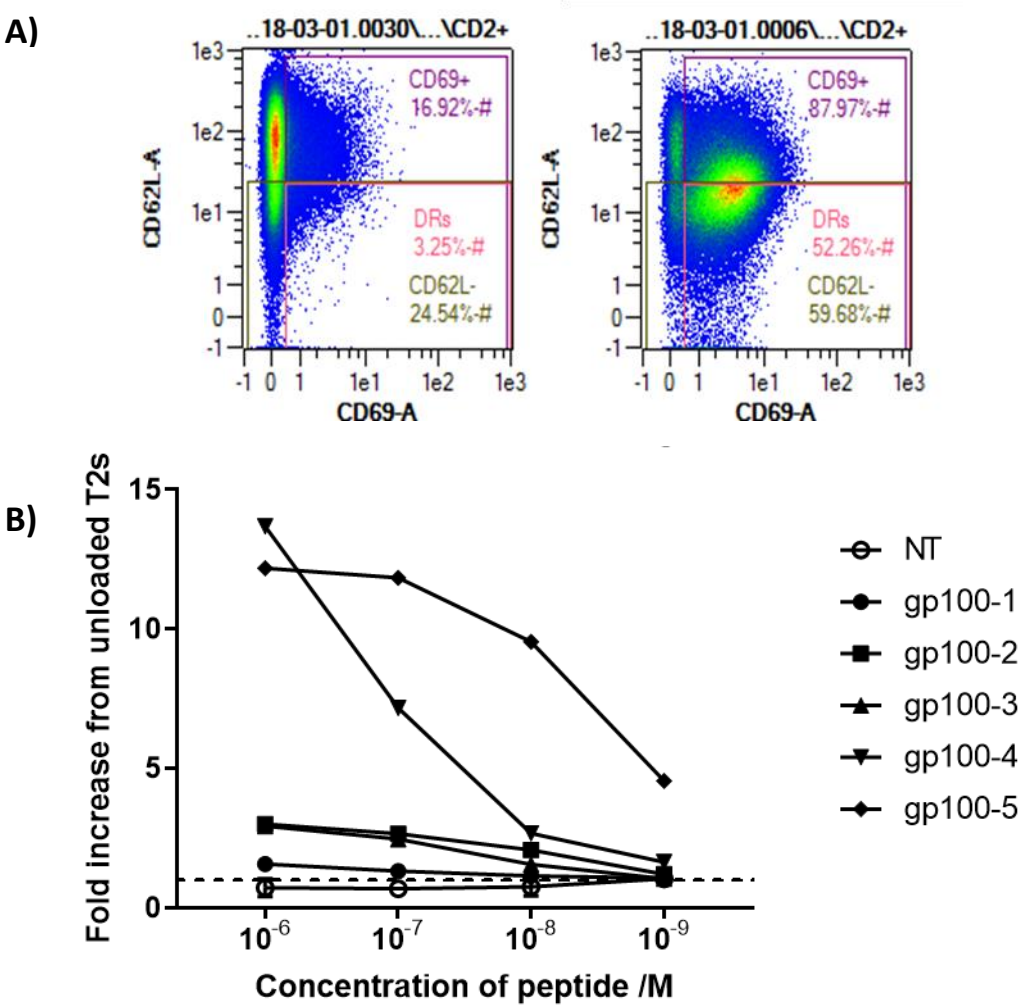

Figure 4.4. Peptide sensitivity assessed through Jurkat peptide titration assay. A) Flow cytometry plots illustrating the difference between CD69 and CD62L expression for a weak and a strong TCR-pMHC interaction (left and right plots respectively). Gating was established using NT JRT3 cells, with unstimulated controls included for each TCR as well. CD69+CD62L- cells are gated as double responders (DR), which was chosen as the optimal gating strategy for Jurkat activation. B) The graph shows the fold change in activated gp100-mTCR transduced T-cells upon co-culture with T2 antigen presenting cells that were pulsed with titrating concentrations of index $gp100_{154\text{-}162}$ peptide. Activated cells were measured as CD69+CD62L- live cells when assessed by flow cytometry, using unloaded T2 cells as the background. Mean values from three technical repeats are plotted.

4.2.3 The five gp100-mTCRs show differences in cross-reactivity profiles

To begin to investigate cross-reactivity of the TIL-derived gp100-mTCRs, an alanine peptide scan was conducted using gp100-mTCR-transduced Jurkat cells and peptide-pulsed T2 cells. The assay was carried out in triplicate to give three technical replicates. A full description of this assay can be found in chapter 2.2.7. The index $gp100_{154\text{-}162}$ peptide and peptide variants were used at 1×10^{-4} M for optimal activation, which was higher than the maximum concentration used in the previous peptide sensitivity assay to ensure strong activation with index peptide would be observed for all TCRs. For MHC class I peptides, the anchor residues are typically found at positions 2 and 9 of the 9-mer, and this is illustrated in the diagram in figure 4.5A (Falk et al., 1991). The graph in figure 4.5B shows the fold change from the index $gp100_{154\text{-}162}$ peptide of CD69+CD62L- gp100-mTCR Jurkat cells when co-cultured with the different alanine-substituted peptides. For most alanine substitutions, the fold change of activated cells was lower than 1, meaning the gp100-mTCR-pMHC interaction caused less activation than with the index peptide. This is a favourable result with regards to the cross-reactivity of the gp100-mTCRs, as a substitution that induces a lot of activation for a TCR would be undesirable. For many alanine substitutions positions (denoted Px) such as P1, P3, P5 and P7, gp100-1 had the highest activation, followed by gp100-2 and gp100-3, and the lowest activation came from gp100-4 and gp100-5. For other positions, this pattern was not preserved, for example P2, P4, P8 an P9. Most notably, at P4 and P8 the fold change for gp100-3 and gp100-4 respectively exceeded 1-fold, indicating a higher level of activation than the cognate antigen peptide.

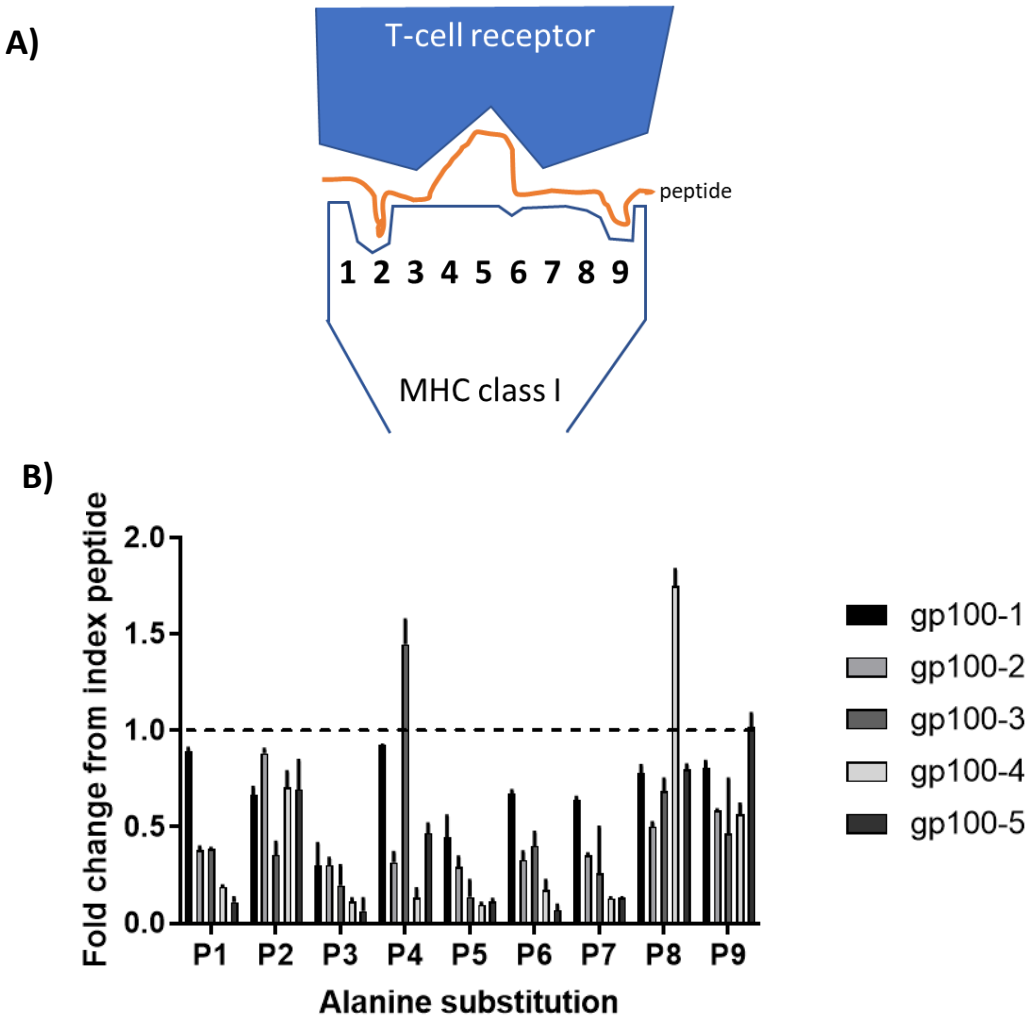

Figure 4.5. Alanine scan of five HLA-A*0201 gp100-mTCR Jurkat cells. A) Diagram to illustrate the TCR-pMHC interaction, including the anchor residues for a 9-mer peptide binding to MHC class I. B) Antigen-presenting T2 cells were pulsed with index $gp100_{154\text{-}162}$ peptide or an alanine-substituted variant of the gp100 peptide prior to co-culture with the gp100 TCR-transduced T-cells. Response was measured by the percentage of CD69+CD62L- cells and the fold change from the index peptide is plotted. The dashed line represents 1-fold which is no change from index peptide. The mean values from three technical repeats are plotted.

4.2.4. Tumour line validation for tumour marker expression

The next Jurkat assay that was conducted for the gp100-mTCRs was a co-culture with different tumour cells of varying gp100 expression, in an effort to determine the gp100-mediated tumour reactivity. The activation profile was assessed by analysis of CD69 and CD62L as in previous assays. Tumour lines were chosen based on two factors: HLA-type and gp100 expression. To first establish which tumour lines might be suitable, a selection of commercially-available and patient-derived melanoma cell lines

were stained with a panel of different tumour markers and assessed by flow cytometry. Since the gp100-mTCRs were restricted to HLA-A*0201, the tumour lines selected also needed to present peptide in the context of HLA-A*0201. The heatmap in figure 4.6A shows the tumour panel validation, with the expression of the different markers along the *x* axis, and the different melanoma lines on the *y* axis. It is evident from the heatmap that the expression of various melanoma cell markers is varied and heterogenous across the different cell lines. Generally, the expression of certain markers was high across the board, such as MHC class I, CD54 and CD58, while other markers expressed at much lower levels, such as Gal9 and MCSP. The expression of HLA-A2 is very varied, and useful for identifying which patient tumour lines could be used to look for reactivity of any HLA-A2-restricted TCRs, such as the gp100-mTCRs. Another useful marker which shows varying expression across the different tumour cell lines is the anti-Melanoma marker.

The anti-Melanoma marker used was a commercially-available, polyclonal antibody of three different melanoma markers: gp100, MART-1 and tyrosinase; this antibody mix was previously being used to help distinguish between melanoma cells and fibroblasts in tumour digest, but was included in this assay to assess melanoma marker expression. The results of tumour cell staining with this marker is highlighted in 4.6B, which shows that the highest staining comes from SK-MEL-5, SK-MEL-28, CTMM4.1, CTAM28.1 and CTAM36.1, whereas low staining is observed with CTCM39.3 and middling expression is apparent with CTCM54.1. The drawback of using this antibody was that it was not possible to identify the presence and proportion of the three markers individually. At this point in the project, commercial antibodies to individually stain the melanoma markers for flow cytometry were not widely available, and the anti-Melanoma antibody mix was discontinued. In an effort to dissect the melanoma marker composition of different tumour lines, individual antibodies were conjugated to different fluorophores for individual flow cytometry marker staining. Rather than conjugating each marker to the same fluorophore, like the original antibody mix, the different markers were conjugated with different fluorophores. This was to allow a mix to be created where the proportion of each marker could be analysed in a single stain. MART-1 was available commercially as a PE-conjugated antibody, while tyrosinase was available conjugated to Alexa Fluor™ 488 or Alexa Fluor™ 647. Gp100 was available as

an unconjugated antibody for the use in immunoprecipitation assays, but not as a fluorochrome-conjugated antibody validated for flow cytometry staining. Taking into account the fluorochromes that were already being used, Alexa Fluor™ 488 was chosen as the conjugate for gp100, and it was also conjugated to Alexa Fluor™ 647 to allow the optimal conjugate to be selected.

Tumour cells from a variety of different melanoma cell lines were stained individually with the different melanoma marker antibodies, shown in figure 4.6C. In theory, the different conjugated antibodies for gp100 and tyrosinase should have stained the same percentage of tumour cells expressing those markers. However, the results of this staining were inconclusive. The percentage of cells stained with the Alexa Fluor™ 488-conjugated antibodies did not consistently reflect the staining seen with the Alexa Fluor™ 647-conjugated antibodies. Not shown, a non-melanoma cell line was also stained with the melanoma antibodies and a high background staining was observed, bringing up questions of how accurately and reliably these antibodies stain tumour cells for flow cytometry.

To more conclusively identify which markers were being expressed by the tumour cells, qPCR was used to compare gene expression of the different markers. The graph in figure 4.6B shows the relative *PMEL* expression, the gene coding for gp100, for four tumour cell lines. The highest *PMEL* gene expression was observed for CTCM39.3, the patient-matched cell line that the TIL-derived gp100-TCRs were isolated from. It is logical that the gp100 expression would be high given that TCRs reactive to gp100 could be identified from the tumour-infiltrating cell population. However, staining with the anti-Melanoma antibody showed the lowest melanoma marker expression for this tumour line, shown by figure 4.6A.

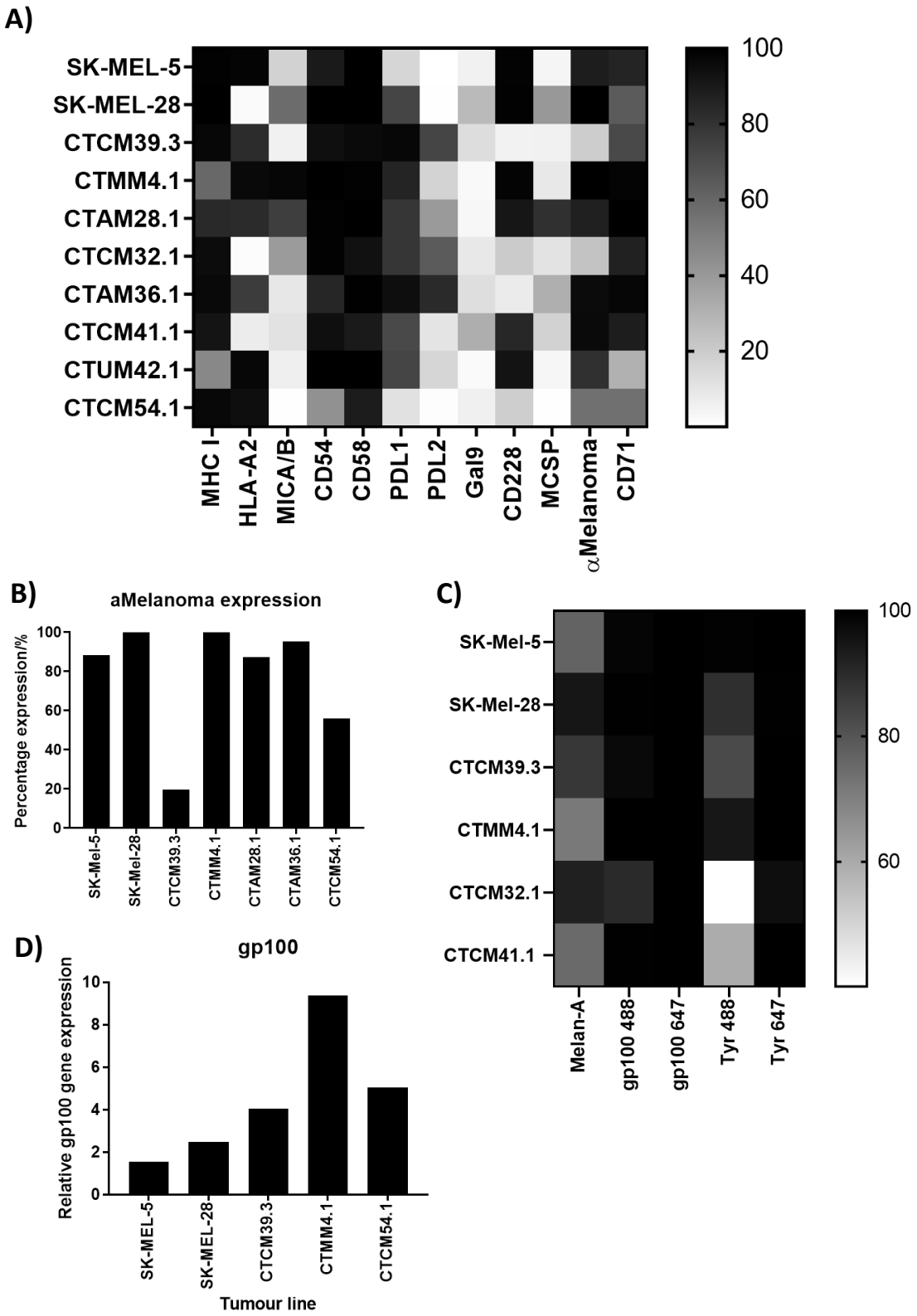

Figure 4.6. Tumour Immunophenotyping and gp100 expression validation. A) Heatmap showing the percentage of different tumour cell markers, as assessed by flow cytometry. Gating was established based on unstimulated tumour cells and isotype controls. B) Percentage of cells that stained with the anti-Melanoma polyclonal antibody (measuring MART-1, gp100 and tyrosinase), for key tumour lines used in this project. C) Heatmap showing the percentage of cells stained with individual melanoma markers, including antibodies conjugated in house. D) Relative gp100 gene expression of four main tumour lines as assessed by TaqMan® qRT-PCR, calculated using GAPDH as the housekeeping gene. No template controls were also used for TaqMan® qRT-PCR.

4.2.5 The five gp100-mTCRs show reactivity to HLA-matched melanoma cell lines

Based on the HLA-expression and predicted gp100 expression, four main tumour lines were chosen for gp100-mTCR tumour-reactivity assay: SK-MEL-5, SK-MEL-28, CTCM39.3, CTMM4.1. SK-MEL-5 and SK-MEL-28 are two commercially-available melanoma cell lines, the main difference between them being that SK-MEL-5 expresses HLA-A*0201, and SK-MEL-28 does not (Adams et al., 2005). The latter was chosen as a negative control cell line for the gp100-mTCRs, as any cross-reactivity with this non-HLA-matched cell line would be undesirable. CTCM39.3, as previously mentioned, is the cell line established from tumour digest for the same patient the gp100 TCRs were derived from. Lastly, CTMM4.1 is a different patient-derived tumour line that has HLA-A*0201 and high anti-Melanoma marker expression. An additional three tumour lines were added to show reactivity to a wider range of anti-Melanoma expressing cells, for example CTCM54.1 which showed 55 % anti-Melanoma marker expression compared to 98 % for CTMM4.1 (figure 4.6B). To assess the reactivity of the gp100-mTCR Jurkat cells to these different tumour cells, co-cultures were set up at a 1: 1 ratio and activation markers were measured by flow cytometry after overnight culture. The assay was carried out in triplicate to give three technical replicates. The graph in figure 4.7 shows the fold change in CD69+CD62L- expression compared to unstimulated gp100 Jurkat cells when co-cultured with the seven selected cell lines. It was clearly evident that gp100-5 had the strongest activation when co-cultured with HLA-matched, gp100-high tumour cell lines. Out of the other TCRs, gp100-4 had the next highest fold change in activation profile, which is still at least 5-fold lower than gp100-5. Gp100-2 and gp100-3 appeared very comparable, with gp100-1 having the lowest fold change in activation markers, only slightly above the background seen with NT Jurkat cells. Interestingly, none of the TCRs showed strong reactivity to the matched patient-derived cell line, the most being a 2-fold change, although this is comparable with the NT data indicating that this was likely due to non-specific activation. From the additional three tumour lines tested, CTAM28.1, CTAM36.1 and CTCM54.1, the strongest activation shown in gp100-5 was induced by CTAM28.1, which had the highest anti-Melanoma marker staining in the initial tumour characterisation assay.

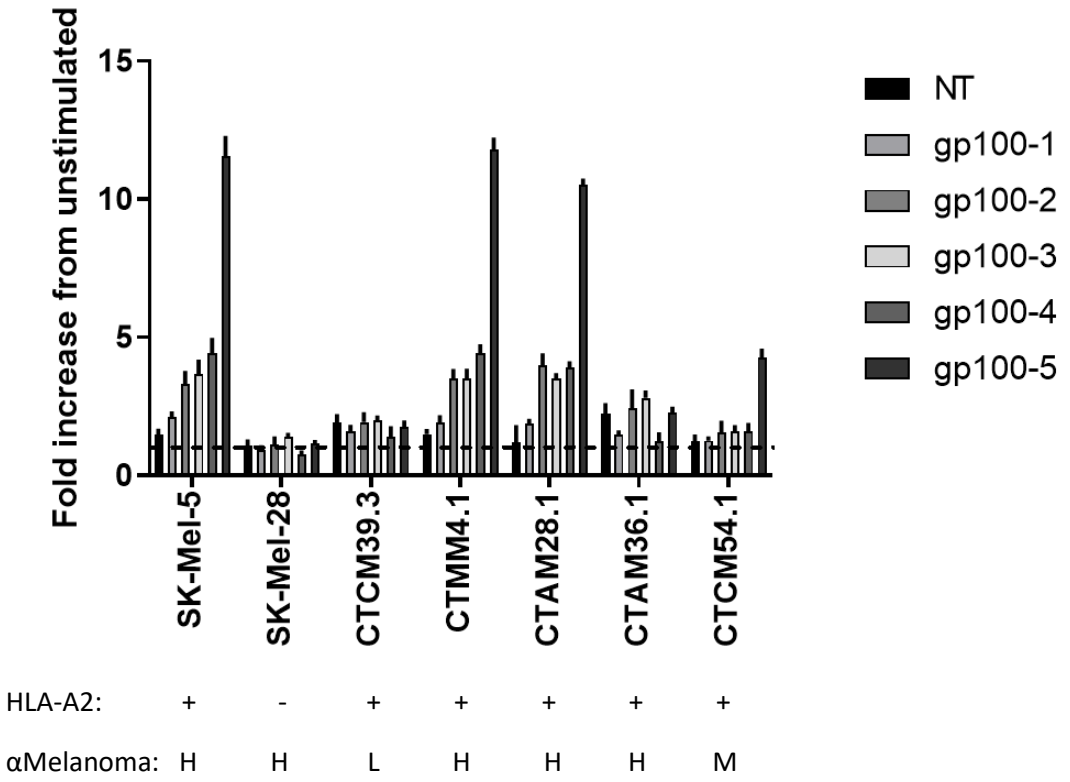

Figure 4.7 Reactivity to various tumour lines for the five HLA-A*0201 gp100-mTCR Jurkats. Co-cultures were set up for the five different TCRs and NT Jurkat cells at a 1:1 ratio with a variety of tumour lines. Characteristics of the tumour lines are shown below the graph, with HLA-A2 expression shown by + or – symbols and anti-Melanoma polyclonal antibody staining denoted as L (low – 0-33 %), M (medium - 33-66 %) or H (high – 66-100 %). Tumour reactivity was measured as the fold increase in CD69+CD62L- Jurkat cells from an unstimulated control. The mean values of three technical repeats are plotted.

4.2.6. Conclusions on the gp100-mTCR Jurkat system

Through these *in vitro* Jurkat-based assays, it has been shown that gp100-5 was the optimal candidate TCR as it was the most sensitive to low concentrations of peptide, had the lowest cross-reactivity profile by alanine scan, and had the highest level of activation when co-cultured with HLA-matched melanoma cell lines. However, one must consider both the positive and negative implications of the Jurkat system when regarding these results. A key advantage of the Jurkat system is that the cells are easy to culture and expand, meaning that if initial transduction is low, very few cells can be isolated and still re-established in culture without difficulty. The benefit of this feature is that generating high cell numbers for multiple assays is not a concern, and this allows high-throughput assays that require a large number of cells to be conducted in a

shorter time-scale, such as the T2-based peptide titration or cross-reactivity assays. Another advantage of the Jurkat system is that the lack of co-receptor allows TCRs to be assessed and compared regardless of the subpopulation they originated from. However, this advantage is also a disadvantage; many TCRs require the presence of a co-receptor for optimal activation, meaning while gp100-5 looks like the most promising TCR out of the five gp100 TCRs, these results might not be mirrored if co-receptors were present. This is a hypothesis that was tested in the remainder of this chapter through the use of a primary T-cell system.

4.3 Validation of the gp100-mTCRs in a primary T-cell system

4.3.1 The five gp100-mTCRs express differently in primary CD8 T-cells

To pre-clinically validate the gp100-mTCRs in a system more analogous with TCR T-cell therapy, the receptors were transduced into primary T-cells isolated from PBMCs from normal buffy coats. The T-cells used for these assays were CD8+ T-cells that were isolated using a CD8 negative selection kit. The graph in figure 4.8A shows the percentage of transduced CD8+ T-cells for the five gp100-mTCRs. Both TCRs gp100-1 and gp100-2 consistently transduced very poorly, with a mean transduction of less than 5 %, making confident gating above NT cells difficult. In contrast, gp100-3, -4 and -5 had mean transduction rates of nearer 20 %, with some donors transducing as high as 50 % of cells. There was a much larger spread of transduction rates across the donors for gp100-3, -4 and -5 however, and the lowest transduction rates were comparable with those observed for gp100-1 and -2. After multiple attempts to expand gp100-1 and gp100-2 CD8+ T-cells to sufficient numbers, taking into account the initial data from the gp100 Jurkat data, the decision was made to focus efforts on gp100-3, -4 and -5 TCRs. With better transduction rates as well as superior Jurkat T-cell data, comparing these three TCRs would provide sufficient validation data to identify an optimal gp100 TCR.

Even with continuing the work with the three best gp100 TCRs, the transduction rates still varied greatly between donors. To investigate if this effect was due to the efficacy of the gp100 viruses, the viral titre for each of the top three gp100-mTCRs was calculated, as per the protocol in chapter 2.2.5. Figures 4.8B and 4.8C show the viral titration and viral titre for these three TCRs. While the viral titration is fairly consistent for each TCR, the calculated viral titre for gp100-4 is slightly lower than the other two TCRs, an effect which was often reflected in the transduction for this TCR. From assay to assay, as referred to in the following text, normalisation for transduction was achieved by gating on the transduced cells using anti-mTCR-β antibodies, sorting of mTCR-β expressing cells, or by spiking in NT cells to equilibrate expression.

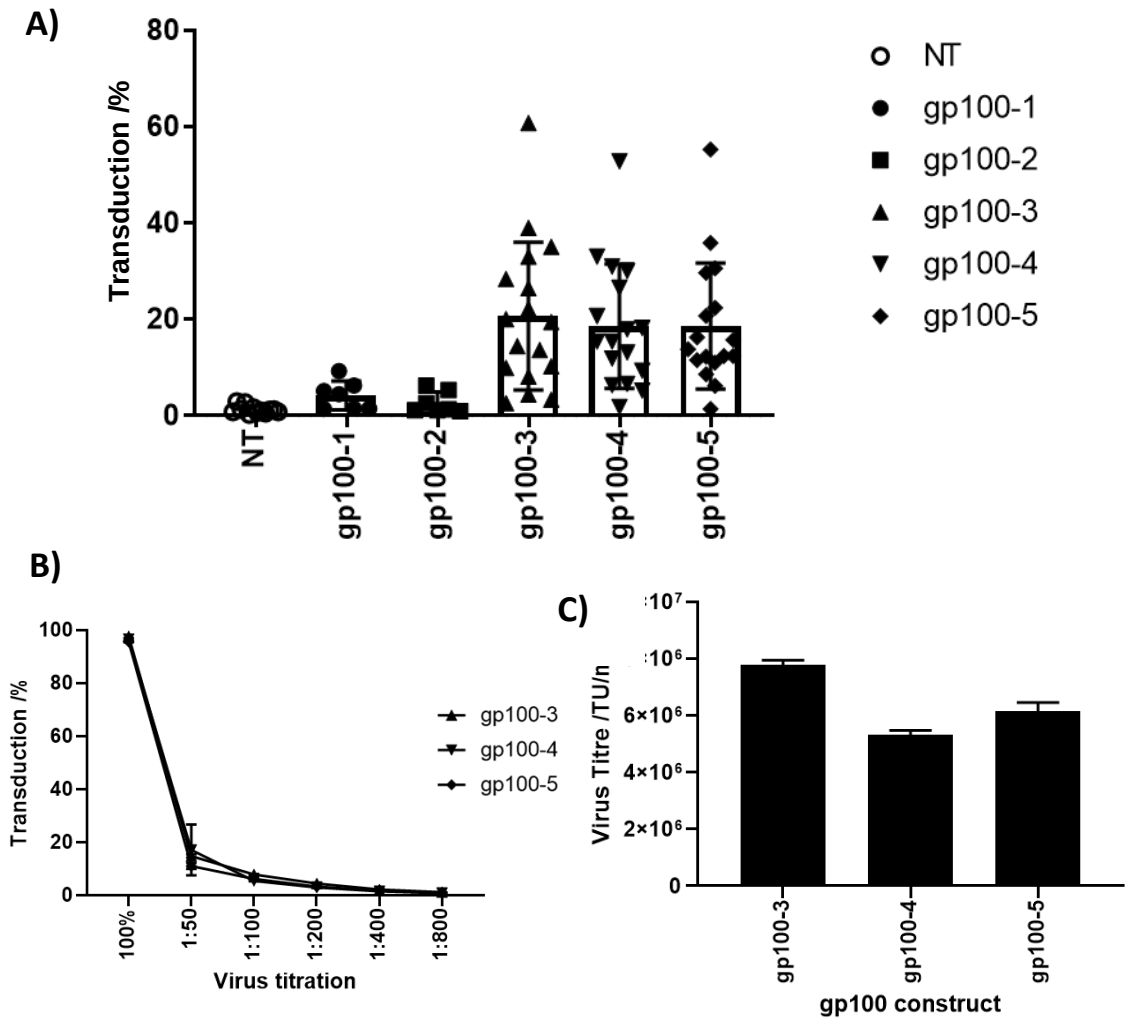

Figure 4.8. Primary T-cell transduction and viral titration of gp100-mTCR viruses using Jurkats. A) Transduction rates of different NBC donor CD8+ T-cells with the five HLA-A*0201 gp100-mTCRs. The bars show the mean of the data with the error bars showing the standard deviation. B) Jurkat cells were transduced with neat virus or titrations of virus down to a minimum of 1:800 with T-cell media. The transduction rate is plotted at each titration. C) The viral titre was calculated using the data in B) using the equation in chapter 2.2.5.

4.3.2 Peptide sensitivity varies between the three optimal gp100-mTCRs

To investigate the sensitivity of the gp100-mTCRs in the context of primary CD8+ T-cells, the peptide titration assay was used, as described in the Jurkat model however the maximal peptide concentration was increased to 1 x 10^{-4} M to assess the effect of peptides across a broader peptide range. For analysis, each TCR was normalised against the unstimulated control to correct for background marker expression. As shown on the graphs in figure 4.9., there was a concentration-dependent reactivity of

the gp100-mTCR T-cells to the peptide-pulsed T2 cells when measuring expression of intracellular CD137, TNFα, IFNɣ and IL-2. For the markers CD137, TNFα and IL-2, the most sensitive TCR was gp100-5, which consistently had the highest activation marker or cytokine expression at all peptide concentrations. This mirrored the result seen in the Jurkat system, where gp100-5 had the highest fold change of CD69+CD62L- cells. With regards to IFNγ, gp100-4 had the highest level of cytokine expression compared to the other two TCRs, gp1003 and -5. In each graph, gp100-3 appeared to produce the least amount of cytokine or activation marker at most concentrations of peptide. The greatest difference between activation marker expression for the three TCRs was the high level of IL-2 production by gp100-5 TCR cells.

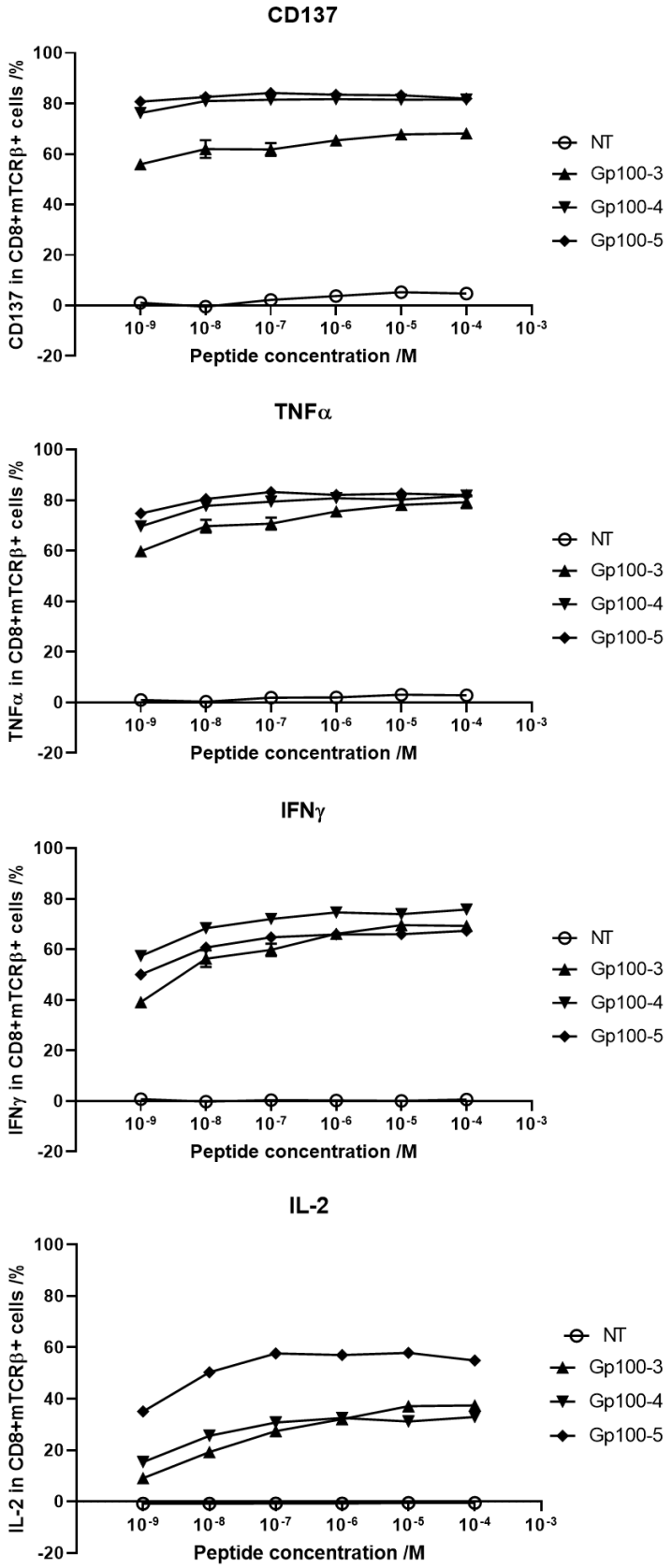

Figure 4.9. Peptide sensitivity assay for gp100-3, -4 and -5 mTCR CD8+ primary T-cells. NT or gp100-mTCR transduced CD8+ T-cells were co-cultured at a 1:1 ratio with T2 cells that had been pulsed with decreasing peptide concentrations of the index $gp100_{154\text{-}162}$ peptide. CD137, TNFα, IFNɣ and IL-2 were measured intracellularly using flow cytometry. The mean values from three technical repeats are plotted (n=1).

4.3.3 Cross-reactivity profiles differ between the three optimal gp100-mTCRs

To investigate the cross-reactivity of the gp100-mTCRs in the more physiologically relevant primary T-cell system, CD8+ T-cells from three healthy donors were transduced with the indicated TCRs and co-cultured with alanine-substituted peptide-pulsed T2 cells in triplicate, as described earlier for the Jurkat T-cells. Figure 4.10 shows the average fold change from index peptide of the three gp100-mTCRs, with respect to the indicated effector function (CD137, TNFα, IFNγ and IL-2). The dashed line represents 1-fold which is no change from the index peptide. The cross-reactivity profiles were very similar to those seen in Jurkat T-cells. Key differences were observed between the different effector functions, with CD137, IFNγ and TNFα displaying more apparent variation between the TCRs compared to IL-2. There were a few alanine substitutions where the TCRs exhibited similar levels of activation across the four markers. At positions P2 and P9, which are the known critical anchor residues, as described previously in the Jurkat system, alanine substitution did not affect activation. Activation for all TCRs was comparable with the index peptide at P4 and P8, whereas at P7 all TCRs were affected by alanine substitution, suggesting this is a key residue for all the TCRs contact with gp100 peptide. CD137, TNFα and IFNγ analysis highlighted the differences in peptide reactivity between the three TCRs at P1 and P3 where alanine substitution had a significant impact on gp100-5 and gp100-4/5 alone respectively. For a few positions, there was one TCR that was considerably more activated or less activated than the others, such as gp100-5 at P1, or P6. Looking at all nine positions cumulatively, gp100-5 showed higher activation at the fewest number of positions compared to the other two TCRs. The results also accurately mirrored the cross-reactivity profile observed in the Jurkat model system.

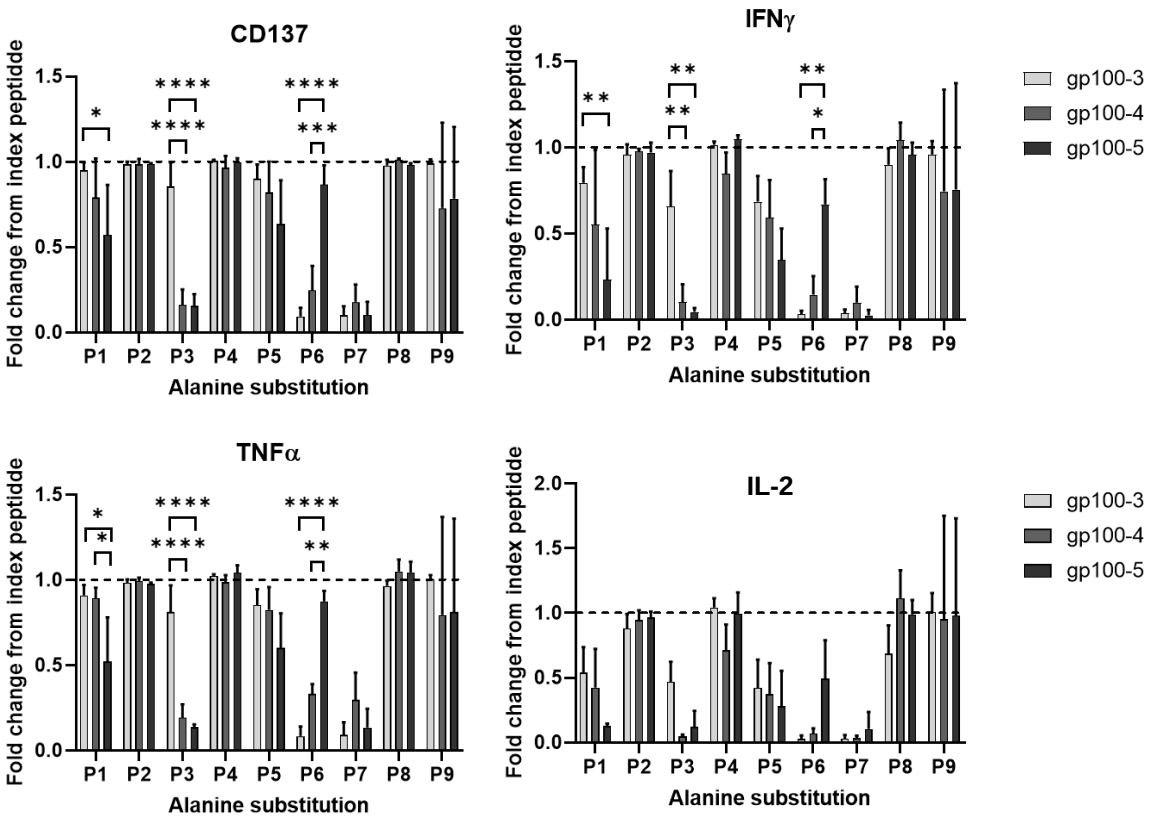

Figure 4.10. Alanine scan of the three optimal gp100-mTCR CD8+ T-cells. Antigen-presenting T2 cells were pulsed with index $gp100_{154-162}$ peptide or an alanine-substituted variant of the gp100 peptide prior to co-culture with the gp100 TCR-transduced CD8+ T-cells. Response was measured by the percentage of intracellular CD137, TNFα, IFNɣ and IL-2 using flow cytometry and the fold change from the index peptide is plotted. The dashed line represents 1-fold which is no change from index peptide. Assay was carried out using three biological replicates (n=3). Statistics were applied using a two-way analysis of variance (ANOVA) using Tukey's multiple comparisons test. * - P < 0.05, ** - P <0.005, *** - P<0.0005, **** - P < 0.00001

4.3.4 All three optimal gp100-mTCRs are activated by HLA-matched melanoma marker expressing tumour cell lines

Next, tumour reactivity was assessed for the three optimal gp100-mTCRs. The assay was carried out as described previously for the Jurkat assay, with the same tumour lines as before, with the measurement of activation being assessed through flow cytometry detection of CD137, TNFα, IFNɣ and IL-2 effector activity. The assay was carried using three different NBC donor T-cells to give biological triplicates, each time with three technical replicates. The graphs in figure 4.11 show the percentage of

intracellular marker or cytokine for each co-culture condition. Analysis of CD137 and TNFα demonstrated a significant increase in effector function in all three TCR engineered T-cells compared to NT T-cells for SK-MEL-5 and CTMM4.1 co-culture, but not for CTCM39.3 or SK-Mel-28. Additionally, in all co-cultures no difference was seen between the three TCRs. With respect to IFNγ, a non-significant increase was observed in effector activity for gp100-3 and 5 but not 4, and for IL-2 only gp100-5 above NT cells. For the activation marker CD137, the mean expression with SK-MEL-5 and CTMM4.1 was between 70 % and 90 %, with gp100-5 having the highest mean expression of 86 %. For the intracellular cytokines, TNFα had the highest expression for all three TCRs, with the mean expression of TNFα typically between 60 and 80 % for SK-MEL-5 and CTMM4.1. The percentage of cells expressing IFNɣ was lower, with mean expression falling between 30 and 50 for the three TCRs for the high melanoma marker cell lines. Lastly, IL-2 expression was the lowest, with a mean percentage expression of 20 % to 40 %. For this cytokine, gp100-5 was the only TCR to show statistically significant expression when compared to NT control cells.

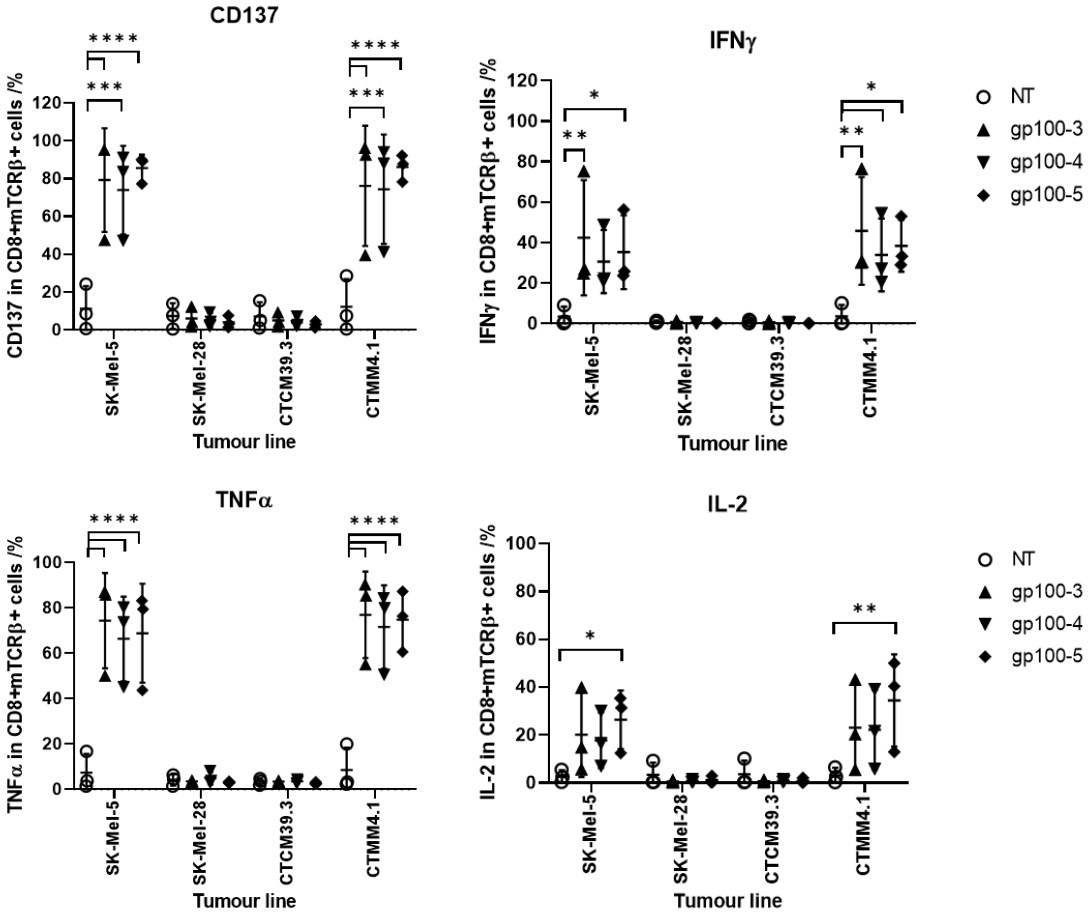

Figure 4.11. Tumour reactivity profiles for the three optimal gp100-mTCRs in primary CD8+ T-cells. Overnight co-cultures were set up at a 1:1 ratio for NT or gp100-mTCR transduced CD8+ T-cells with four tumour lines. Intracellular CD137, TNFα, IFNɣ and IL-2 was measured by flow cytometry. The mean values are plotted from three biological repeats (n = 3). Statistics were applied using a two-way ANOVA using Tukey's multiple comparisons test. * - P < 0.05, ** - P <0.005, *** - P<0.0005, **** - P < 0.00001

4.3.5 Co-culture with HLA-matched melanoma marker expressing tumour cell lines causes degranulation in all three optimal gp100-mTCR transduced T-cells

In addition to measuring CD137 and various intracellular cytokines, the expression of CD107a was also assessed, as a more direct measurement of cytotoxic T-cell activity. Co-culture assays were set up in the same manner as the overnight intracellular cytokine assays, however the anti-CD107a antibody was added during the co-culture and cells were incubated for 4 hrs, which was previously shown to be the optimal timepoint to measure degranulation by CD107a (data not included). The assay was also carried out using pan-isolated T-cells (CD4+ and CD8+ T-cells), from three healthy

donors, to allow the measurement in both CD8+ and CD4+ T-cells. The percentage of CD107a expression in gp100-mTCR transduced T-cells was measured by flow cytometry, as shown in figure 4.12. Degranulation was observed in all three gp100-mTCR transduced T-cell populations, and was significantly increased compared to NT cells for all three TCR-transduced T-cell populations against HLA-A*02 matched SK-Mel-5 and CTMM4.1, but not against the patient-matched CTCM39.3 nor the HLA-A*02-negative SK-Mel-28 line. This effect was observed in both CD4+ and CD8+ T-cells, albeit to a lesser degree in CD4+ compared to CD8+ cells.

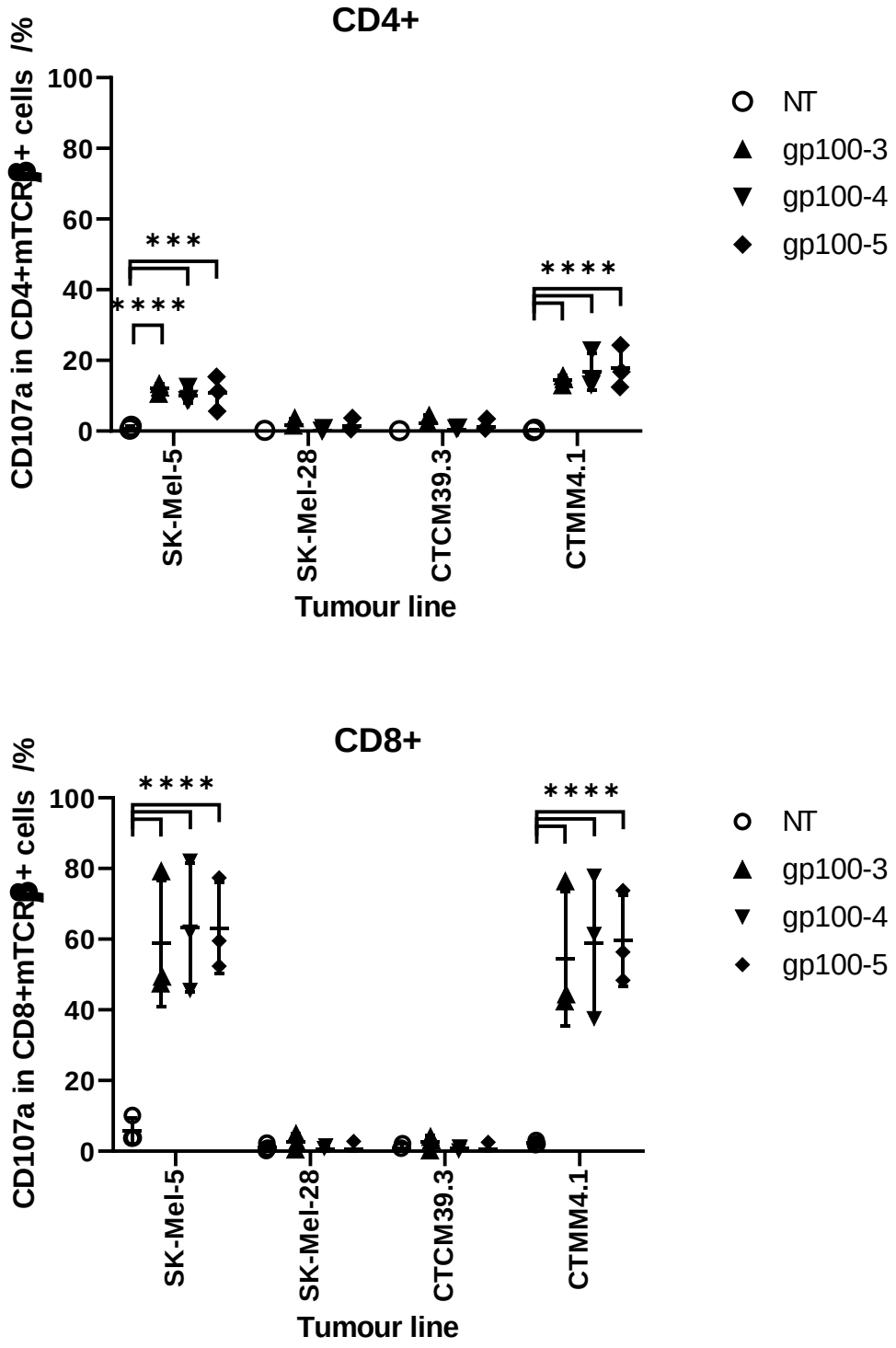

Figure 4.12. Expression of CD107a in CD4 and CD8 gp100-mTCR transduced T-cells upon co-culture with tumour cells. Co-cultures of NT or gp100-mTCR transduced pan T-cells were set up at a 1:1 ratio and incubated for 4 hours. CD107a expression was measured by flow cytometry. The mean values are plotted from three biological repeats (n=3). Statistics were applied using a two-way ANOVA using Tukey's multiple comparisons test. * - $P < 0.05$, ** - $P < 0.005$, *** - $P < 0.0005$, **** - $P < 0.00001$

4.3.6 *Co-culture of all three optimal gp100-mTCR transduced T-cells with HLA-matched melanoma marker expressing tumour cell lines results in tumour-cell death*

Whilst the use of activation markers such as CD137 and intracellular cytokine production are reliable measures of tumour-reactivity, they are not direct measures of tumour-killing. In order for the pre-clinical development of TIL-derived TCRs to progress, a more direct measurement of tumour-killing was needed to better validate the interaction between the gp100-mTCR transduced T-cells and the tumour cells. In this case, the colorimetric WST-1 assay was chosen to measure the proportion of tumour-killing by the different TCRs. gp100-mTCR transduced CD8+ T-cells were co-cultured with SK-MEL-5, SK-MEL-28, CTCM39.3 or CTMM4.1 tumour cells at a 1: 1 ratio. WST-1 was measured as per the protocol in chapter 2.2.9, and the readout converted to percentage cytotoxicity to best illustrate the cytotoxic activity of the TCR-transduced T-cells. The graph in figure 4.13 shows the tumour killing for NT, gp100-3, -4 and -5 for each tumour line. Cytotoxicity mediated against the HLA-A*02-matched cell lines SK-Mel-5 and CTMM4.1 was observed, with a particularly potent response to the latter. Responses to SK-Mel-5 were more varied, with gp100-5 demonstrating the strongest cytotoxic effect at 90 % killing over 24 hrs, whereas gp100-4 mediated a lower level of around 70 % cytotoxicity over the same time period. A robust response of between 30 % and 60 % killing was seen against the HLA-mismatched line SK-Mel-28 suggesting a degree of alloreactivity; the degree of cytotoxicity was greater than that seen against the patient-matched line CTCM39.3.

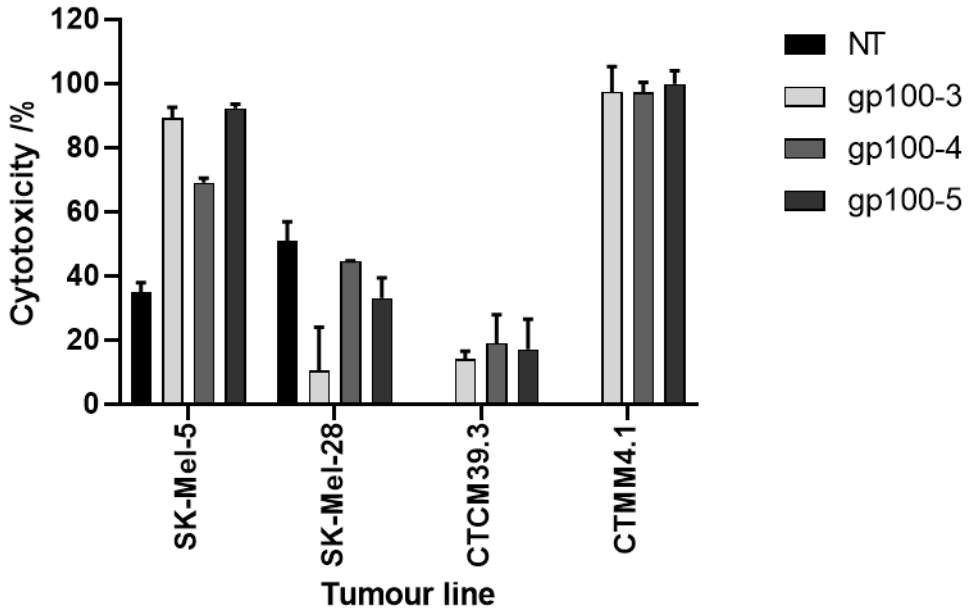

Figure 4.13. Cytotoxicity as measured by WST-1 assay for the three optimal gp100-mTCRs in CD8+ T-cells. Overnight co-cultures were set up Co-cultures of NT or gp100-mTCR transduced CD8+ T-cells were set up at a 1:1 ratio with tumour cells. The next day WST-1 reagent was added to the cells and incubated for 30 minutes. Supernatant was assessed using a plate reader and readings were converted into percentage cytotoxicity. Assay was carried out once with three technical repeats. Cytotoxicity was calculated from tumour-only and T-cell only controls.

4.3.7 Conclusions on the gp100-mTCR primary T-cell system

In this section, it has been shown that the three optimal gp100-mTCRs expressed well in primary T-cells, and had comparable sensitivity and specificity. They were all tumour-reactive and capable of killing HLA-matched melanoma cells in an antigen-dependent manner, as shown through activation marker flow cytometry assays and tumour-killing assays. When the results were viewed collectively, gp100-5 had the most favourable results, particularly regarding cross-reactivity and peptide sensitivity. The IL-2 production of T-cells transduced with this receptor was significantly higher when exposed to index peptide-pulsed T2 cells, and showed superior activation at the lowest peptide concentration. All of these attributes made the gp100-5 TCR a better candidate TCR for potential use in TCR T-cell therapy. In a clinical setting, the expression of gp100 is likely to vary between different patients and tumours, so selecting a TCR that showed good T-cell activation at low peptide concentrations confers a better chance to generate an anti-tumour response.

The next theory that was addressed for this chapter of work was that TIL-derived TCRs are as therapeutically beneficial as genetically-altered TCRs derived by other means, but carry safety benefits due to having been exposed to thymic selection. The next stage of the research conducted for this chapter was to compare the gp100-5 TCR to a previously-validated gp100 TCR that had already been used in the clinic. One such TCR was identified from the Rosenberg research group at the National Institute for Health in Maryland, USA, that had been raised in a transgenic mouse model and had shown good initial results in clinical trials, summarised in the table below (Johnson et al., 2009). The sequence was identified for this TCR and it was reconstructed in a lentiviral vector with a murine constant region, as per the other gp100 TCRs. This TCR will be referred to as the control TCR, or gp100-c.

4.4 Comparison of gp100-5 with a clinically-relevant gp100 TCR

4.4.1 gp100-c consistently expresses better than gp100-5

The sequence of the gp100-c TCR was extracted from the literature and synthesis of the TCR performed by GENEWIZ®. The graph in figure 4.14A. shows the transduction rates of gp100-5 compared with transduction data for gp100-c. The first observation that could be made regarding the control gp100-mTCR was that the plasmid encoding this TCR, which was identical to gp100-5 plasmid apart from the TCR itself, generated high titre virus, and as a result a much higher transduction rate than gp100-5 was observed, with the mean transduction from multiple NBC donors reading just under 40

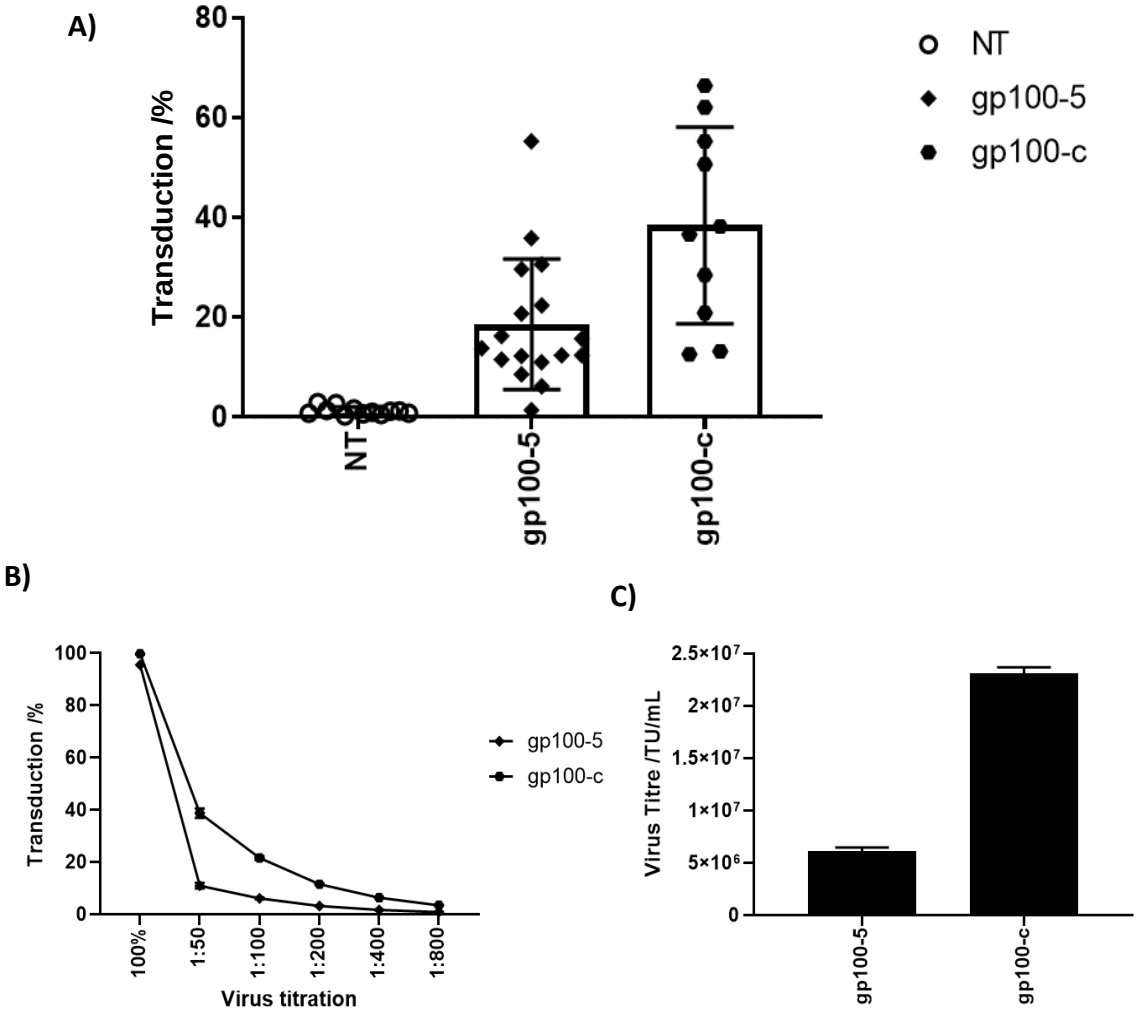

Figure 4.14. Primary T-cell transduction and viral titration of gp100-5 and gp100-c mTCR viruses using Jurkats. A) Transduction rates of different NBC donor CD8+ T-cells with the gp100-5 and gp100-c mTCRs. The bars show the mean of the data with the error bars showing the standard deviation. B) Jurkat cells were transduced with neat virus or titrations of virus down to a minimum of 1:800 with T-cell media. The transduction rate is plotted at each titration. C) The viral titre was calculated using the data in B) using the equation in chapter 2.2.5.

%, compared to approximately 20 % for gp100-5. In figure 4.14C, it can be seen that gp100-5 generated viral titres of approximately 5 x 10^6 TU/mL, whereas gp100-c generated titres over 4-fold greater at around 2.25 x 10^7 TU/mL.

4.4.2 gp100-5 and gp100-c TCRs have comparable peptide sensitivity

The initial experiment performed was to evaluate the effect of peptide concentration on activation of cells harbouring the two TCRs. To this end, gp100-mTCR-transduced primary human T-cells from two healthy donors were co-incubated with T2 cells pulsed with the gp100 index peptide. The graphs in figure 4.15 show the percentage of intracellular CD137, TNFα, IFNɣ and IL-2 for gp100-5 and gp100-c CD8+ T-cells. The assay was carried out in two NBC donors, one of which is shown in the graphs below; each time, the assay was carried out in triplicate to give three technical replicates. The strongest response was observed for CD137 expression with the highest peptide concentration inducing around 80 % expression in gp100-5 and -c transduced cells. This decreased to around 75 % at the lowest peptide concentration used. For CD137 and IL-2, the two TCRs showed very comparable peptide sensitivity data, even at the lowest concentration of index peptide. For TNFα and IFNɣ, gp100-c tended to have slightly higher cytokine production, however this was a very minor difference. For both TCRs at all concentrations of peptide, there was a noticeable difference between the transduced and NT cells, however for statistical analysis to be carried out to confirm this is a true difference, more biological replicates would be required. Overall, both TCRs were sensitive to gp100, demonstrating high expression of CD137 at even 1 x 10^{-10} M peptide. For a proper peptide titration, this assay would need to be repeated with even lower peptide concentrations, for the chance to see a true difference between the two TCRs. For both TCRs, cytokine expression was fairly low, however still higher than the NT background.

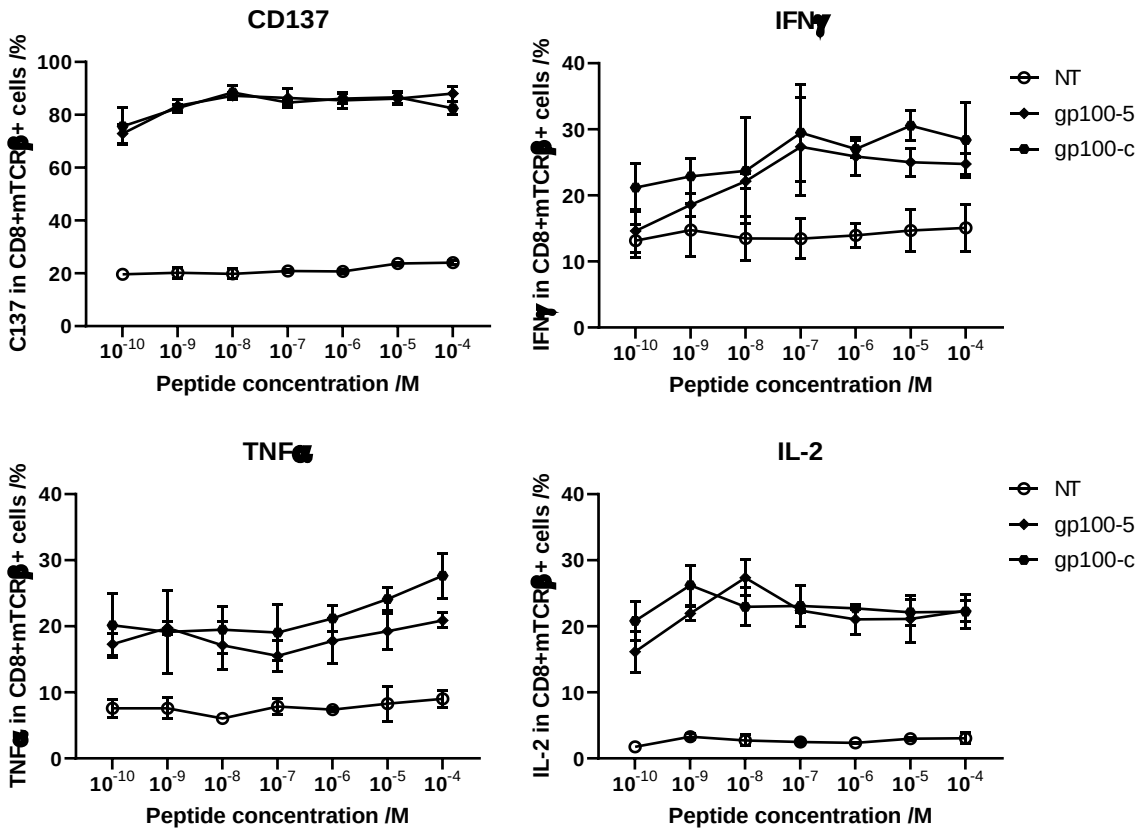

Figure 4.15. Peptide sensitivity assay for gp100-5 and gp100-c in CD8+ T-cells. NT or gp100-mTCR transduced CD8+ T-cells were co-cultured at a 1:1 ratio with T2 cells that had been pulsed with decreasing peptide concentrations of the index $gp100_{154\text{-}162}$ peptide. CD137, TNFα, IFNɣ and IL-2 were measured intracellularly using flow cytometry. Assay was carried out using two biological repeats, with the mean values plotted here.

4.4.3 The gp100-c mTCR displays a broader cross-reactivity profile than the gp100-5 mTCR

Peptide sensitivity assays had revealed a similar degree of responsiveness between the two TCRs, however differences between the cross-reactivity profiles were yet to be determined. To this end, an alanine scanning assay was performed. It was hypothesised that gp100-c would show more cross-reactivity than gp100-5, since it was isolated from a transgenic mouse model, as opposed to TIL which had been thymically selected. The graphs in figure 4.16 show the fold change in activation marker or cytokine expression for each alanine position, compared to the index $gp100_{154\text{-}162}$ peptide. As before, the dashed line represents 1-fold or no change when compared to the index peptide. This assay was carried out in triplicate and for three

NBC donor CD8+ T-cells transduced with the gp100-mTCRs to give 3 biological replicates, with the bars indicating the mean fold change and the error bars representing the standard deviation of the three donor datasets. Statistically significant differences between the two gp100-mTCRs are indicated by asterisks.

As demonstrated with the analysis of the three optimal gp100 TCRs previously, CD137 expression was least affected by alanine positional scanning, possibly because of its increased sensitivity following T-cell activation. Alanine substitutions at P1 and P3 showed significant differences between gp100-c and gp100-5 using this readout, whereas both TCRs were affected comparably by alanine substitutions at P5 and P7. Analysis of TNFα and IL-2 also demonstrated that gp100-5 was significantly more affected by alanine substitutions at P6 and P8, and additionally P4 when IFNγ production was analysed. Even at other alanine substitution positions that were not statistically significant, such as P5 and P7, there was a trend for gp100-c to have a higher fold change than gp100-5. For all three cytokines, there were several positions where the fold change for gp100-c exceeded 1, showing that the transduced cells produced more cytokine when activated by these altered peptides than with the index peptide. When taken together, the graphs indicated that gp100-5 is less cross-reactive than gp100-c.

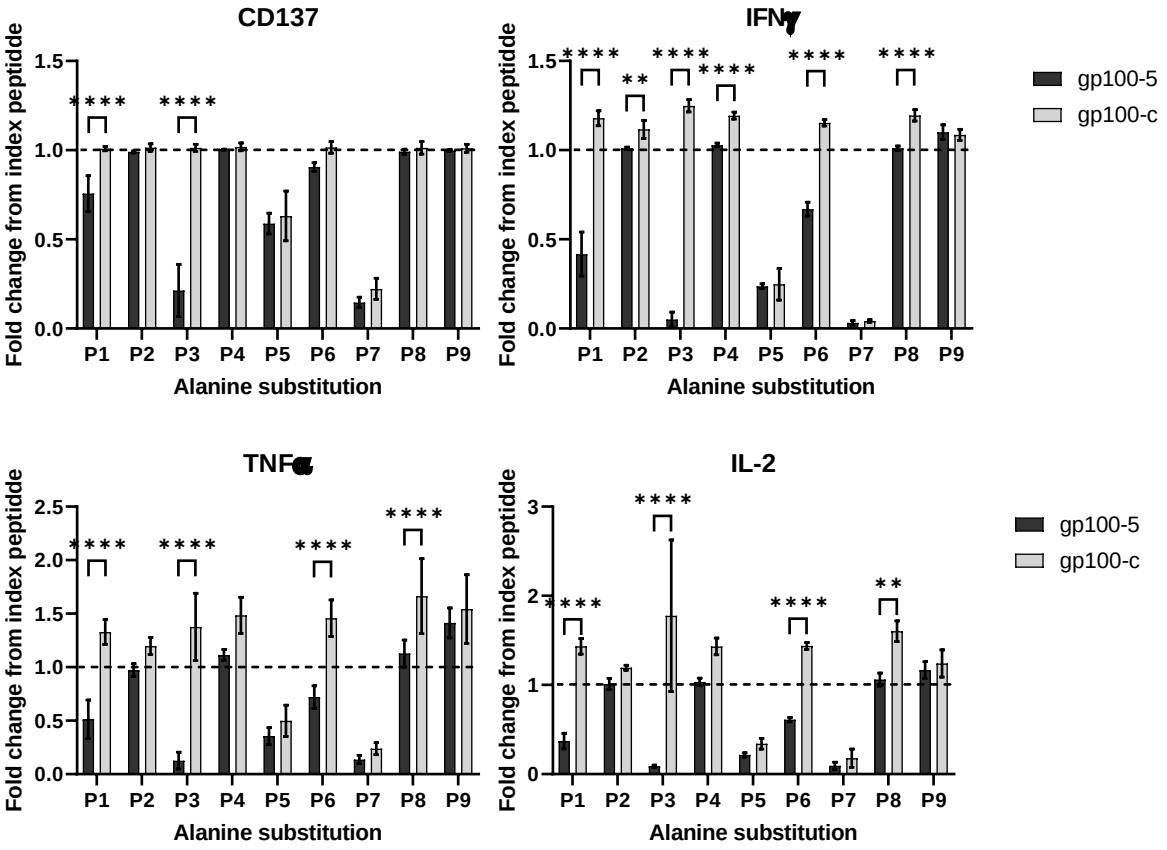

Figure 4.16. Alanine scan of gp100-5 and gp100-c mTCR CD8+ T-cells. Antigen-presenting T2 cells were pulsed with index $gp100_{154-162}$ peptide or an alanine-substituted variant of the gp100 peptide prior to co-culture with the gp100 mTCR-transduced T-cells. Response was measured by the percentage of intracellular CD137, TNFα, IFNɣ and IL-2 using flow cytometry and the fold change from the index peptide is plotted. The dashed line represents 1-fold which is no change from index peptide. Assay was carried out using three biological repeats (n=3). Statistics were applied using multiple T-tests, using Sidak's multiple comparisons test. * - P < 0.05, ** - P <0.005, *** - P<0.0005, **** - P < 0.00001

4.4.4 Tumour-reactivity is comparable between gp100-5 and gp100-c

While it is beneficial to compare TCRs in terms of peptide sensitivity and specificity against peptide-pulsed antigen presenting cells, it is important to understand the response against tumour-presented peptide. By observing what happens when the TCR-transduced T-cells come into contact with tumour cells, one can gain insight into how those cells might behave *in vivo*. The graphs in figure 4.17 show the T-cell expression of CD137, as well as intracellular cytokines TNFα, IFNɣ and IL-2, when co-cultured with the previously validated panel of tumour cells: SK-MEL-5, SK-MEL-28, CTCM39.3 and CTMM4.1. The assay was carried out using three NBC donors to give

three biological replicates, as well as each time in triplicate for three technical replicates. For CD137, the expression was around 90 % and comparable between the two TCRs for the HLA-matched, high melanoma marker expressing tumour lines. There was also a small but significant difference in CD137 expression from NT cells when co-cultured with patient-matched CTCM39.3 for both TCRs. For cytokines TNFα and IFNɣ, expression was very similar, averaging over 60 %, for SK-MEL-5 and CTMM4.1 for both TCRs. There was a trend for the IL-2 expression to be higher for gp100-5 than gp100-c, however this was not statistically significant. For all four markers of activation, there were no statistically significant differences between the gp100-5 TCR and the gp100-c TCR, but both were statistically significant compared to the NT control T-cells. For CD137, TNFα and IFNɣ, there appeared to be a slight trend that gp100-c had higher activation marker and cytokine expression than gp100-5, however the difference was very small. This trend could also be seen in the non-HLA-matched tumour line, so might be indicative of higher non-specific activation levels. For IL-2, gp100-5 showed higher expression than gp100-c, which was in line with previous results showing IL-2 expression for this TCR, although again the difference was very small. Ultimately, the main conclusion that could be drawn from this data was that both gp100 TCRs showed comparable tumour-reactivity to HLA-matched, high melanoma marker expressing tumours.

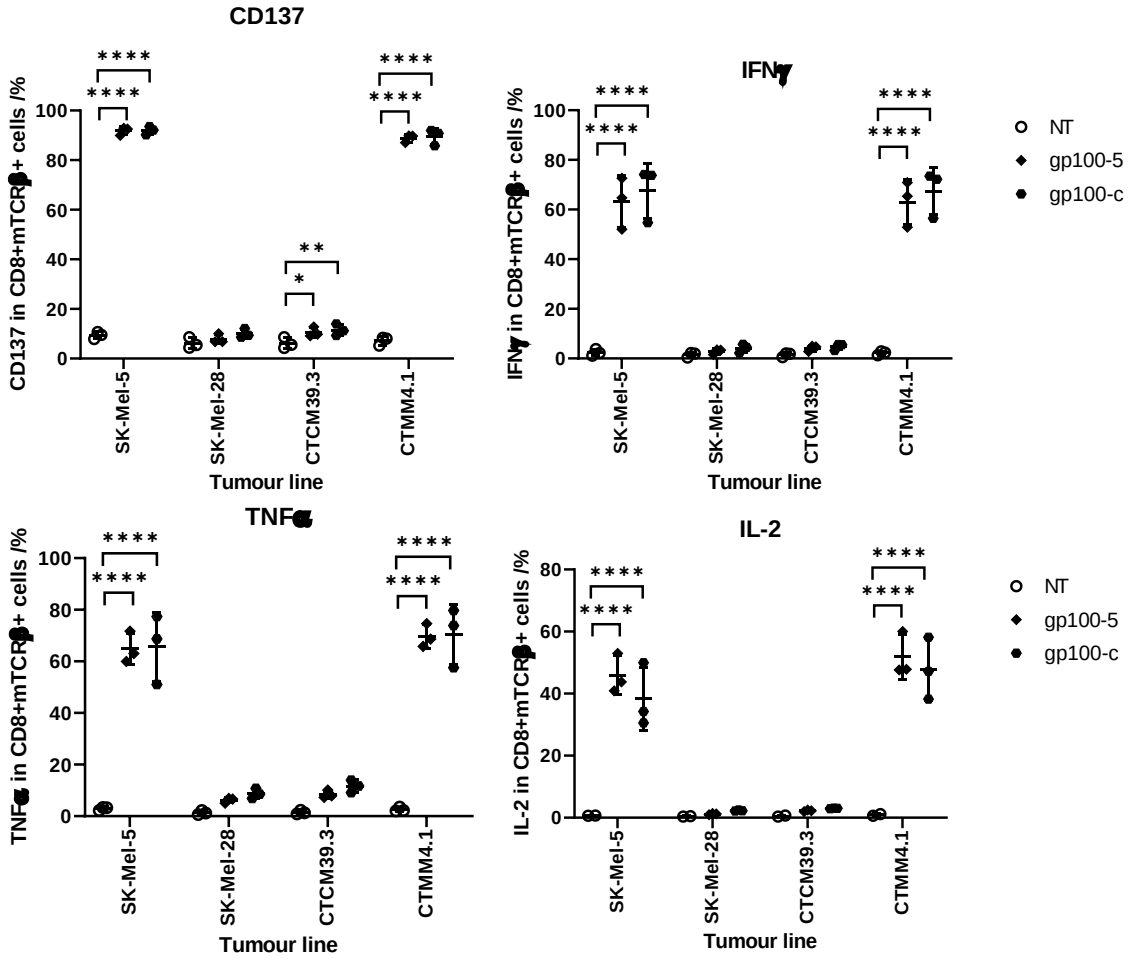

Figure 4.17. Tumour reactivity profiles for gp100-5 and gp100-c mTCRs in primary CD8+ T-cells. Overnight co-cultures were set up at a 1:1 ratio for NT or gp100-mTCR transduced CD8+ T-cells with four tumour lines. Intracellular CD137, TNFα, IFNɣ and IL-2 was measured by flow cytometry. The value for each donor is shown by individual points in the graph, and collectively the mean and standard deviation are shown as bar and whiskers that can be seen under the points. Assay was carried out using three biological repeats (n=3). Statistics were applied using a two-way ANOVA using Tukey's multiple comparisons test. * - P < 0.05, ** - P <0.005, *** - P<0.0005, **** - P < 0.00001

4.4.5 Degranulation occurs in gp100-5 and gp100-c mTCR-transduced CD4+ and CD8+ T-cells

To better understand how the gp100-5 and gp100-c mTCRs compared with regards to cytotoxic capacity, co-cultures with tumour cells were established to measure CD107a presentation. This assay was conducted in pan-isolated T-cells so that the CD107a presentation could be measured for both the CD4 and CD8 subpopulations. The graphs in figure 4.18 show the percentage of cells expressing CD107a for the NT, gp100-5 and

gp100-c mTCR-transduced T-cell population. The assay was carried out in triplicate and in three NBC donors, so statistical analysis was used to compare the biological replicates. As expected, both gp100-5 and gp100-c induced degranulation responses to the HLA-matched, high melanoma marker cell lines, compared to NT control cells. In the CD4+ subpopulation, the CD107a presentation was significantly higher in the gp100-c cells than gp100-5, suggesting that the gp100-5 TCR is more co-receptor dependent than gp100-c. In the CD8+ subpopulation, there was no statistical difference between the gp100-5 and gp100-c mTCRs, however there was a trend that the gp100-5 TCRs express more CD107a.

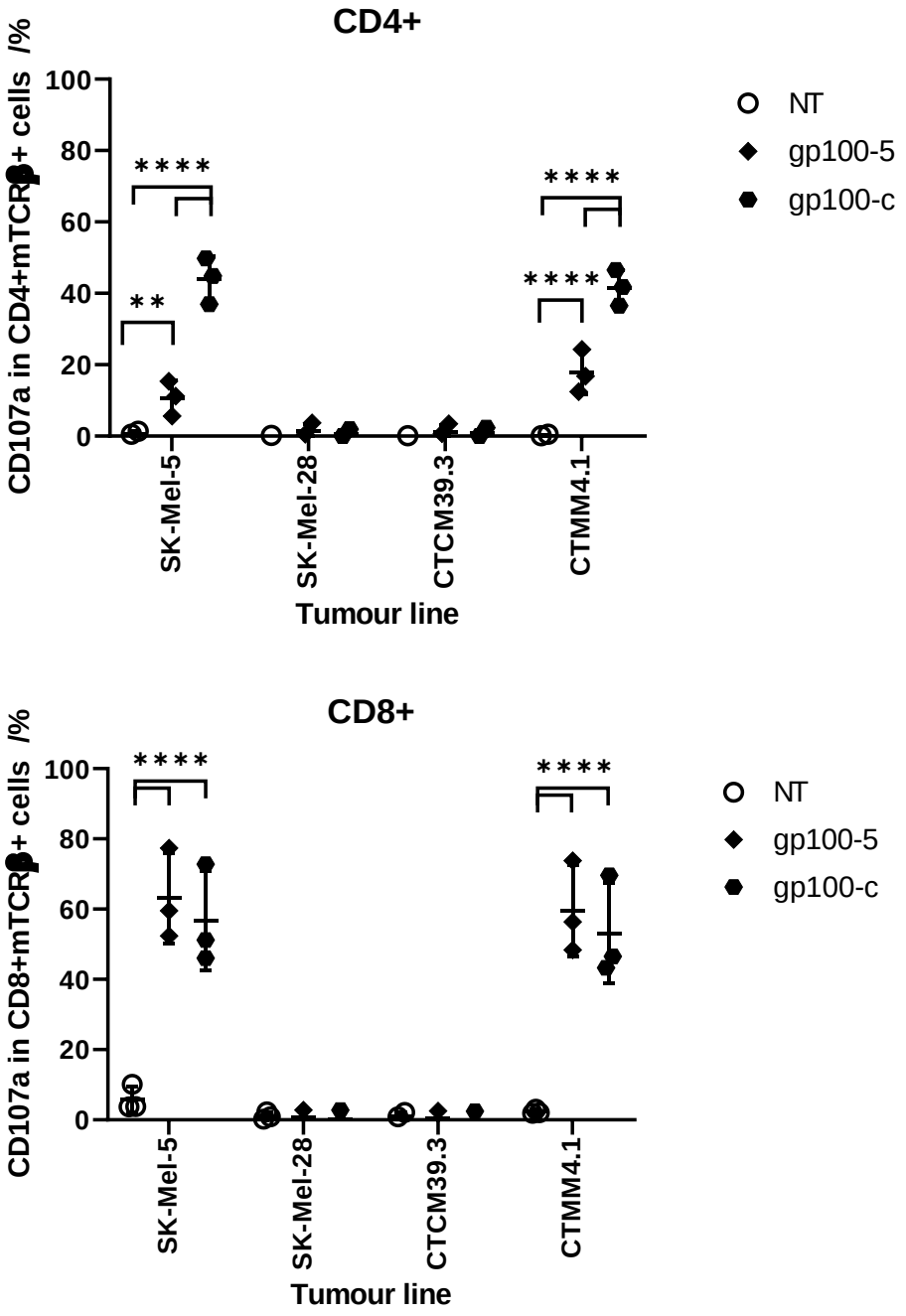

Figure 4.18. Expression of CD107a in CD4 and CD8 gp100-5 and gp100-c mTCR transduced T-cells upon co-culture with tumour cells. Co-cultures of NT or gp100-mTCR transduced pan T-cells were set up at a 1:1 ratio and incubated for 4 hours. CD107a expression was measured by flow cytometry. Assay was carried out using three biological repeats (n=3). Statistics were applied using a two-way ANOVA using Tukey's multiple comparisons test. * - $P < 0.05$, ** - $P < 0.005$, *** - $P < 0.0005$, **** - $P < 0.00001$

4.5 - Conclusions and future work

In this chapter of work, five different HLA-A*0201-restricted, $gp100_{154-162}$-reactive TCRs were identified from the Jurkat library of one TIL patient, and isolated for characterisation. Using first a Jurkat cell system, the five TCRs were investigated regarding their sensitivity to index gp100 peptide, their cross-reactivity to alanine-substituted index peptide variations and their reactivity to HLA-matched and mis-matched melanoma cell lines. Three of the five gp100-mTCRs were then validated in a more physiologically-representative system, using CD8+ primary T-cells from normal buffy coat donors, where one TCR was then identified as the most optimal candidate gp100-mTCR. Finally, the optimal TCR, gp100-5, was investigated comparatively with a previously-validated gp100 TCR from a transgenic mouse model; these data showed that the TCRs were comparably tumour-reactive, however gp100-5 appeared less cross-reactive, suggesting a safety benefit may be conferred from using TIL-derived TCRs.

Several researchers have demonstrated the high proportion of shared melanoma antigens expressed by tumour samples, and responses to these antigens by melanoma TIL. Barrow et al. used immunohistochemistry of over 400 tumour samples to show that the differentiation antigens such as gp100, MART-1 and tyrosinase were expressed in around 93 % of tumours, compared to CT antigens such as MAGE-A1 and NY-ESO-1, which were expressed in 20 % and 45 % respectively (Barrow et al., 2006). Andersen et al. analysed the responses of over 60 TIL cultures from 19 melanoma patients to a panel of 175 melanoma-associated antigens, detecting 90 T-cell responses from 15 patients (Andersen et al., 2012). Out of these responses 55/90 were considered low frequency (<0.1 % of CD8 T-cells), and only 20/90 were considered high frequency (>1 % of CD8 T-cells); these were restricted to $MART\text{-}1_{ELA}$, $gp100_{YLE}$, $gp100_{KTW}$, $AIM\text{-}2_{RSD}$, and $MAGE\text{-}A1_{RVR}$.

With this in mind, it was interesting that during GigaGen's dextramer panning assays, only one patient TIL out of the five TIL samples provided by Instil Bio UK harboured TCRs to the known antigens tested, which included MART-1, NY-ESO-1 and gp100. There are a few theories that could explain why this was the case. Firstly, it could be down to chance that the few TIL samples that were panned with dextramers did not contain TCRs to known antigens, with the exception of the five gp100 TCRs identified.

A second possibility is that the frequency of TCRs reactive to known antigens in the other TIL samples were below the limit of detection through the dextramer panning method. This could be investigated through the use of single-cell TCR sequencing and subsequent sequence analysis to try to identify known TCR sequence motifs that could indicate target TCRs within other TIL populations. It would be interesting to conduct the dextramer panning protocol described above on the TIL samples as opposed to the Jurkat libraries, to see if other melanoma-reactive TCRs could be identified. The advantage of using the Jurkat libraries generated by GigaGen Ltd. was that Jurkat cells grow rapidly and easily, without becoming exhausted or needing exogenous cytokine support in the form of IL-2. This also meant when selection of the Jurkat cells took place, the cells could recover from a low cell number, which was a challenge seen in primary T-cell culture. Another reason that more melanoma-reactive TCRs were not identified could be that the proportion of melanoma-reactive TCRs in the TIL product did not reflect those seen in the Jurkat libraries, due to changing frequencies of TCRs through extended Jurkat cell culture.

Pre-clinical validation for the five gp100-reactive TCRs was conducted with a multifaceted approach, investigating peptide sensitivity, cross-reactivity and tumour-reactivity, first in a Jurkat system and later in a primary T-cell system. From the initial Jurkat system validation assays, gp100-4 and gp100-5 gave the most promising peptide sensitivity data, with gp100-5 showing a much higher degree of activation at the lowest peptide concentration compared to all other TCRs. This result indicated that only low concentrations of cognate antigen were required to induce strong activation in the gp100-5 mTCR, a property that would be beneficial when transferred to an *in vivo* system where antigen expression might be low. Although all showed good initial validation regarding cross-reactivity profiles, gp100-1 and gp100-2 gave consistently poor transduction in primary T-cells and it was decided the primary T-cell validation would continue for gp100-3, -4 and -5 only.

One of the challenges in carrying out the gp100 primary T-cell assays was maintaining a consistent transduction level. Even though the same protocol was followed, some donors achieved a better transduction efficiency than others, as illustrated by the graph in figure 4.8A. For the majority of the experiments carried out in this chapter, primary CD8+ T-cells were used as the effector function of this subpopulation was the

population of interest. However, it was soon apparent that the selection of this subpopulation led to difficulties culturing the T-cells, and without the CD4+ T-cells to support the CD8+ T-cells, they struggled to survive in culture. This meant that when the transduction rate was very low, after sorting the transduced cells, the numbers were very low and the cells would often have to undergo two REPs to provide the cell numbers needed to carry out the assays. By putting the cells through two REP cycles, the resulting cells at the end of the protocol lost proliferative and reactive capabilities reactivity, with activation-induced cell death often noticeable in the cell assays. To circumvent this issue in future assays, donor T-cells could be characterised prior to transduction to assess and compare their proliferative potential and CD8 ratio. Another step that could be taken would be to sort pan T-cells for transduction, and use a CD8-enrichment kit after the REP stage to give the T-cells a better chance of growing and surviving the REP stage. The caveat with that approach however, is that you cannot exclusively transduce the CD8 subpopulation, and if the donor T-cells are more CD4 rich, the resulting transduction for the CD8 subpopulation could be too low. It could be that the optimal protocol would be to transduce CD8+ T-cells and then spike the transduced cells into a REP with matched-donor or irradiated CD4 cells, with a final CD8+ cell isolation or CD8+mTCR+ FACS sort.

In the primary T-cell cross-reactivity assays, there were a few instances where the fold change exceeded 1 at certain positions for some gp100 TCRs, as can be seen in figures 4.10 and 4.16. The reason for an alanine substitution at certain positions causing an increase in T-cell reactivity could be related to the structure of the pMHC complex and the interaction with the TCR, illustrated in figure 4.4A. As previously mentioned, positions 2 and 9 in a 9-mer pMHC class I complex have been described as key anchor residues where the peptide binds to the MHC proteins (Falk et al., 1991). The substitution of an alanine at these positions could potentially stabilise the peptide within the binding groove, which in turn would result in a more stable TCR-pMHC interaction, and ultimately a higher level of activation. This has previously been demonstrated for several different gp100 epitopes, where the use of anchor-modified heteroclitic gp100 peptides induced more responses from melanoma patient PBL (Parkhurst et al., 1996). The increased activation of some TCRs at P4 and P8 on the other hand might be related to the interactions between the TCR and the pMHC

complex, indicating these residues might be crucial for this interaction to result in activation. With regards to cross-reactivity, changing one of these amino acids might carry more risk of cross-reacting with an endogenous human peptide for these TCRs than a substitution at a different position. Without knowing the exact amino acids that are critical for TCR-pMHC interactions, it is unclear if showing reactivity at certain positions is likely to result in a cross-reactive TCR. Further investigation should be carried out for these TCRs with a more comprehensive peptide scan, where every possible amino acid is substituted at each position to fully validate the cross-reactivity profile of the different TCRs.

Tumour line characterisation with the original panel of antibodies for tumour-associated markers (see figure 4.6A) was deemed successful. However, challenges arose when trying to identify the proportions of individual melanoma-associated antigens MART-1, gp100 and tyrosinase. The antibodies used for flow cytometry had not been previously validated for flow cytometry uses, and there was a lack of consistent staining between differently conjugated antibodies. With these data, it was decided that the anti-Melanoma polyclonal antibody staining was more reliable than the self-conjugated antibody staining to use as a reference point, but in future work the accurate proportions of these different melanoma markers should be addressed. The use of a different technique, such as Western blot, should help with this question.

Combined with the inconclusive results from the tumour line characterisation, the lack of T-cell reactivity against matched patient cell line CTCM39.3 bring up questions regarding the true gp100 expression by these tumour cells. It has been previously demonstrated that a threshold of gp100 mRNA expression is required for T-cell activation and downstream effector functions, however the RT-PCR carried out in this work showed that CTCM39.3 had high gp100 RNA expression when compared to GAPDH (Riker et al., 2000). One theory is that the original tumour had high gp100 expression, that subsequently underwent immune evasion by down-regulating expression of gp100, and these were the cells that a tumour-cell line was established from. This theory would explain how at least five different gp100-reactive TCRs were able to traffic to and infiltrate the tumour originally; this event would be highly unlikely if the tumour had very low gp100 expression. This hypothesis could be tested in theory, by staining original tumour digest cells for gp100, through Western blot or flow

cytometry. It is also possible that downregulation of gp100 occurred as a result of adherent cell culture over an extended period of time. While being an extremely useful tool for *in vitro* assays, it highlights one of the drawbacks of using tumour cell lines and should be taken into consideration when designing future assays or interpreting data. Another possible theory to explain why the *PMEL* gene expression was high but reactivity to tumour was low is that the gp100 protein is not being fully expressed. A paper by Yasumoto et al. show that there are two truncation steps that occur between translation of the full-length protein to the truncated, refolded mature protein that gets expressed (Yasumoto et al., 2004). Using Western blot analysis, they demonstrated that the HMB-45 monoclonal gp100 antibody, which was also used in this project, only detected a low molecular weight (34 – 38 kDa) protein fragment. It could be the case in the CTCM39.3 tumour cells that the HMB-45 antibody binds to a portion of the gp100 protein that gets cleaved during one of the truncation steps. Another potential reason why the TCRs did not react to CTCM39.3 could be related to the sensitivity of the TCRs. While the peptide sensitivity assay showed that all the TCRs produced cytokine in response to 1×10^{-9} M peptide, previous work from other groups showed that the $gp100_{154}$ peptide induced fewer or weaker responses compared to other gp100 peptides (Salgaller et al., 1995; Salgaller et al., 1996).

Given that in the Jurkat model, gp100-5 had the best activation profile with regards to tumour-reactivity, it might have been expected to show a higher activation compared with the other two TCRs. However, all three TCRs are comparable and show a relatively high activation marker expression when co-cultured with the two HLA-matched gp100-high tumours. The highest percentages of expression for gp100-5, seen for CD137 and IL-2, correlates with the peptide titration expression profile for gp100-5, which also showed a comparatively higher IL-2 production. The last stage of validation was to compare the gp100-5 mTCR to a TCR that had previously been used in a clinical trial for gp100-TCR T-cell therapy, which was termed gp100-c. The validation assays carried out to compare these two TCRs showed that the TCRs showed comparable sensitivity and tumour-reactivity, however gp100-5 showed a more favourable cross-reactivity profile. In addition, when an *in vivo* mouse study was carried out, the group treated with gp100-5-mTCR T-cells appeared to show the greatest reduction in tumour volume. For further validation, a larger mouse study should be conducted to investigate if

treatment with gp100-5 T-cells does give a favourable prognosis than treatment with gp100-c T-cells. If this experiment is conducted, a better control group should be used of mice treated with NT T-cells; this was not included in the preliminary mouse experiment due to a lack of NT T-cells for this donor.

For the work carried out in this project, existing patient final TIL samples were utilised in order to retrospectively analyse the TIL. This approach also allowed matched patient tumour lines to be used, and gave valuable insight in the form of patient response data. Using patient-matched tumour cell lines grown out from tumour digest carries advantages and disadvantages. An obvious advantage is that autologous co-cultures can be established which creates a patient-specific *in vitro* model. Additionally, the tumour lines generated from patient tumour digest are likely to be more representative of the majority of melanoma tumours compared to commercially available cell lines which are typically chosen based on favourable characteristics such as immunogenicity, marker expression such as PD-1 and rate of cell proliferation. Through culturing and characterising a variety of patient melanoma tumour lines, it was apparent that the different tumour lines were very heterogeneous, showing a wide variety of marker expression and proliferation rates. When translating this into the TCR T-cell therapy model, an ideal TCR would be reactive to a variety of different melanoma lines with varying antigen levels as opposed to only the most highly expressing tumour cell lines.

To compare and contrast the approach taken here, it would also be interesting to carry out the Jurkat library construction or dextramer-panning on TIL that was freshly isolated from resected tumours, particularly for the same patient TIL and tumour tested in this chapter. The composition of the TIL and proportion of tumour-reactive cells could be different than in the final TIL product, which would provide valuable information about how the outgrowth and REP stages influence the TIL product. Given the interesting result regarding the lack of reactivity of the gp100 TCRs to the patient-matched cell line CTCM39.3, it is possible that the frequency of gp100 TCRs might be higher in the tumour digest. It would also be interesting to carry out Western blot analysis and qPCR to assess gp100 expression in the tumour digest, to see if the antigen is more highly expressed than in the established tumour cell line. If gp100 expression is higher in the tumour digest than the cell line, this would give valuable

insight into how adherent cell culture of tumour cells could trigger a phenotypic change to downregulate gp100.

5.0 Summary and General Discussions

5.1 Summary of work

Tumour-infiltrating lymphocytes are a valuable research tool in the field of cancer immunotherapy, providing an insight into how the immune system in the human body responds to cancer. As well as a source of material for the increasingly popular ACT known as TIL therapy, the individual cells within this tumour-infiltrating population can be investigated to find and validate thymically-selected, potent tumour-killing cells. For this body of work, melanoma patient final TIL products were utilised to explore the identification and pre-clinical development of tumour-reactive TCRs. In chapter 3, several model systems were trialled to best identify the tumour-reactive population within TIL. The Jurkat library system was an excellent concept that circumvented issues such as T-cell exhaustion from prolonged cell culture and limited TIL resources. However, in reality, the Jurkat library Vβ expression was disproportionate to that seen in the TIL and the lack of co-receptor in the Jurkat model may have negatively impacted the TCR library's capacity for activation. Taking a different approach, CD137 was selected as an optimal candidate marker for tumour-reactivity in TIL. Using CD137, it was shown that tumour-reactivity of final melanoma patient TIL products to matched tumour cell lines varied but overall, was fairly low. To identify tumour-reactive TCRs from selected TIL products, a workflow was developed using FACS sorting to isolate CD2+ and CD2+CD137+ TIL after matched tumour co-culture, with downstream V(D)J and GEX library creation through the 10x Genomics® Chromium™ controller and single-cell, next-generation sequencing approach. Through this method, it was shown that there is overlap between the most abundant TIL in the final product and the most abundant tumour-reactive TIL, as identified by CD137. From one patient V(D)J library, three CD137-isolated TCRs were re-expressed for validation in primary T-cells and Jurkats, showing reactivity to matched tumour, as well as other melanoma cell lines, indicating the likelihood of having identified shared melanoma antigen-reactive TCRs, which will be explored in further research.

To continue the aim of validating thymically-selected, tumour-reactive TCRs from TIL, in chapter 4, five HLA-A*0201-restricted gp100-reactive TCRs were identified from Jurkat library 039 and pre-clinical validation was carried out to compare the different TCRs. This was first carried out in a TCR-negative Jurkat system, where it was shown

that the five TCRs show different sensitivities and specificities to the index $gp100_{154-162}$ peptide. When these TCRs were transferred to a CD8+ primary T-cell system, three out of the five TCRs expressed well, so these taken forward for further validation. The three optimal gp100 TCRs showed slightly different cross-reactivity profiles through alanine scanning, and demonstrated comparable tumour-reactivity, however gp100-5 was found to be the most sensitive to decreasing concentrations of the cognate peptide. Considering all the data, gp100-5 was chosen as the best candidate TCR to take forward into the final step of pre-clinical validation, which involved comparison with a control gp100 TCR which had been used successfully in clinical trials for melanoma treatment, with a 19 % ORR (3 out of 16 patients) (Johnson et al., 2009). The two TCRs showed comparable tumour-reactivity in CD8+ T-cells to certain HLA-matched melanoma cell lines, however gp100-c exhibited co-receptor independent activation of CD4+ T-cells, which may have been a factor in generating a patient response in the clinical trial mentioned above. The two TCRs also generated highly comparable survival data when treating mice with SK-MEL-5 tumours. However, gp100-5 was considerably less cross-reactive than gp100-c, supporting the hypothesis that TIL-derived TCRs are safer than those generated in transgenic mouse model systems.

5.2 General conclusions from this PhD project

The first conclusion that can be drawn from this thesis is that CD137 is a good marker of tumour-reactive T-cells in melanoma TIL, as demonstrated by the melanoma TIL product and autologous tumour line co-culture system that was utilised in this project. This agrees with the work carried out by other researchers who used a different system of pre-REP TIL and tumour digest (Ye el al., 2014). As discussed in chapter 1, there is evidence that the diversity and prevalence of tumour-reactive clones can be negatively affected by large scale TIL product manufacture through TIL outgrowth and REP (Poschke et al., 2020). In this way, it was encouraging to see that some tumour-reactivity is still maintained in the final TIL products used in this thesis, although the low and varied tumour-reactivity observed in figure 3.13A raises questions surrounding the reactivity of these TIL before they were subjected to large-scale expansion. In future work, resource permitting, it would be insightful to carry out the CD137 T-cell

isolation using pre-REP TIL and tumour digest to compare the overall reactivity of these TIL products. In addition, if carried out for TIL054, it would be interesting to investigate the pre-REP frequency of the CD137-isolated TCRs to see how the manufacturing process impacted the proportion of these tumour-reactive T-cells. It was promising that the all three of the TCRs identified from the CD137+ TIL054 V(D)J library showed reactivity to the matched tumour, however stronger reactivity was observed to other HLA-A*0201-restricted melanoma lines SK-MEL-5 and CTMM4.1. These tumour lines both exhibited high levels of staining with the polyclonal anti-Melanoma antibody (reactive to MART-1, gp100 and tyrosinase) compared to CTCM54.1. This indicates the likelihood of the TCRs being reactive to a shared antigen such as gp100 or MART-1. Further validation of these TCRs should be carried out in future work, particularly for TIL054-derived TCR-3 which showed the highest anti-tumour activity as measured by IFNɣ ELISA in response to HLA-matched melanoma cell lines. It is important to identify the cognate antigens for these TCRs, as this could potentially reveal new, antigen targets shared between melanoma patients. This approach could also be used to identify antigens from other cancer indications, such as ovarian cancer or colorectal cancer, where there are fewer known shared antigens. The HLA-matched tumour cell lines from different patients described in this work can be leveraged to search for and identify shared antigen reactive clones by selectively cloning T-cells which show reactivity to a variety of melanoma cell lines. The inclusion of HLA-mismatched tumour lines in this work could possibly lead to identification of alloreactive TCRs that are non-HLA restricted, although these would present in the same way as cross-reactive TCRs in this assay, so caution should be taken when identifying such TCRs. The use of known invariant TCR sequences and mathematical modelling could be used to help discriminate between cross-reactive and HLA-independent TCRs, such as the recently identified Major histocompatibility complex class I-related gene protein (MR1)-reactive TCR (Crowther et al., 2020). Once identified, novel tumour-reactive TCRs could then undergo pre-clinical validation using the flow cytometry-based assays described in chapter 4.

The second conclusion to be taken from this body of work is that TIL-derived TCRs can carry significant safety benefits over transgenic mouse-derived TCRs, whilst exhibiting comparable anti-tumour effects. To support this statement, a more comprehensive

screening of HLA-A*0201 peptides should be carried out, by means of a full peptide scan. This would provide more conclusive data regarding the cross-reactivity profile of gp100-5 and gp100-c. As previously discussed, progress in the field of TCR T-cell therapy has been hindered in previous years after clinical trials using affinity-matured TCRs resulted in severe off-target toxicities led to patient death in multiple clinical trials, as a result of insufficient pre-screening for cross-reacting epitopes (Morgan et al., 2013; Linette et al., 2013). Providing an optimal TIL-derived candidate TCR that shows superior safety data whilst maintaining cytotoxicity would be an exciting step forward in melanoma TCR T-cell therapy. By fully elucidating the cross-reactivity profile of these gp100 TCRs, more data would be gathered to support the hypothesis that TIL-derived TCRs are safer than transgenic mouse derived TCRs. However, in order to fully prove or disprove that hypothesis, the experiments should be expanded to include several other TCRs isolated from TIL as well as transgenic mouse TCRs. In addition to further validation of the cross-reactivity profile, *in vivo* studies could be carried out using gp100-5 and gp100-c, to utilise a more physiologically-representative model than *in vitro* co-culture. Once fully validated, a gp100-TCR *in vivo* model should serve as a platform to investigate different combinations of immunotherapeutic interventions, such as radiotherapy or checkpoint inhibitors.

By combining the TCR identification and pre-clinical validation steps described in this thesis, a novel TIL-derived TCR discovery platform is presented that can be adapted to different cancer settings such as ovarian or colorectal cancer. These two tumour types are suggested as they are reasonably immunogenic, and it has been shown that TIL and tumour lines can be established for these cancers (Aoki et al., 1991; Koch et al., 2006). There could also be an advantage of using this approach in tumour settings with few neoantigens, such as the uveal melanoma TIL042 used in this project, to potentially identify TCRs against new shared antigens for this cancer indication. The combination of TIL therapy and TCR identification could also prove particularly valuable in cases where the overall tumour-reactivity of the TIL is low and the patient does not show a favourable clinical response. In future work, it could be possible to trial this TIL-derived TCR discovery and pre-clinical validation model in a different disease setting to discover more therapeutic TCRs to either new or known antigens and optimise the process further.

5.3 Unsolved questions and future work

There are some unsolved questions that arose during this PhD project that were not fully addressed, due to time and resource constraints. These include:

1. Why the transduction of gp100-1 and gp100-2 were much lower than the other three gp100 TCRs.
2. Why the gp100 TCRs did not recognise the matched patient tumour cell line.
3. What the TIL054 TCRs recognise.

To address the first question, the sequences of gp100-1 and gp100-2 TCRs could be interrogated to look for key differences between these TCRs and the others that might contribute to the low expression. However, considering that from the Jurkat system onwards, the best gp100 TCR was shown to be gp100-5, there is very little benefit that could be gained from going back and trying to increase the expression of these two TCRs.

From the initial validation in Jurkat cells, it was surprising that the gp100 TCRs did not recognise the patient-matched tumour cell line. Considering that five different gp100-reactive TCRs were isolated from TIL039, it would be unusual for the tumour cells not to induce a response from the T-cells. A few theories have been proposed which should be pursued in future work to elucidate this result. The first theory is that gp100 is produced by the CTCM39.3 tumour cells, but it isn't being processed or presented by the tumour cells. This would explain why the relative *PMEL* expression was high but the protein expression, as assessed by flow cytometry, was low. This theory is supported by a 2004 paper which discusses the various truncation steps of gp100 processing, and highlights that the anti-gp100 antibody used in the FACS analysis, HMB-45, binds a specific portion of the peptide which is only present in the most mature form of the protein in stage II melanosomes (Yasumoto et al., 2004). The maturation of gp100 is observed during the development of melanosomes, which are organelles specific to melanocytes and are responsible for melanin production. Given than CTCM39.3 appears to be an amelanotic (unpigmented) tumour cell line, it is possible that gp100 is not expressed in the form that can be recognised by the HMB-45 antibody. An earlier paper has described how this could occur through a deficiency in a small GTPase called Rab7 preventing the maturation of gp100 in stage II melanosomes

(Kawakami et al., 2008). This theory could be tested for the CTCM39.3 line by using antibodies detect gp100 which recognise and bind a different portion of the protein, such as HMB-50, as well as investigating the amount of Rab7 produced by the cells. The second theory is that by growing out the tumour cells on plastic cell culture flasks, the phenotype of the tumour cells has changed, in turn downregulating gp100, or that a non-gp100 expressing tumour clone outgrew other cells to create the CTCM39.3 cell line. In accordance with the in-house tumour line numbering system, CTCM39.3 is the third and most successful tumour line that was grown out from the patient tumour, so this is a realistic possibility. A third theory is that the patient's tumour originally expressed gp100, but that the presence of the gp100-reactive TIL, from which the TCRs were identified, is indicative of an early response to this antigen and subsequent immune editing process leading to a tumour escape mechanism based on the loss of gp100-expressing cells. This theory could be tested using frozen banked tumour digest from this patient if available, through qPCR and western blot. Ultimately however, it would be almost impossible to prove or disprove this theory as early tumour biopsies from the patient do not exist.

The process of validating the TCRs identified from CD137-isolated TIL054 was started within the scope of this project, with initial ELISA and tumour-reactivity in the Jurkat system investigated. The results of these assays suggest that the TIL054-TCRs are HLA-A*0201-restricted and recognise a shared melanoma antigen, due to reactivity to HLA-matched melanoma cell lines from different patients. In order to conclusively elucidate what the TCRs recognise, the first assay that should be carried out is a sizing scan, which uses antigen-presenting cells pulsed with random peptides of differing amino acid lengths (typically 8-13 amino acids in length), to decipher the index peptide length. Once the index peptide length has been ascertained, there are a few different approaches which could be taken to identify the cross-reactivity of the TCRs.

One approach is to use a combinatorial peptide scan of relevant length to determine the most likely amino acids at each position of the peptide as well as highlighting the cross-reactivity profile for the TCRs, a classic approach which has been utilised widely in TCR T-cell research (Wooldridge et al., 2012; Bijen et al., 2018). One caveat of this method is that it would not necessarily reveal if the target gene is mutated, in which case the peptide scan could be combined with whole exome sequencing to acquire this

information. The use of *in silico* mathematical modelling approaches are also becoming more popular for predicting TCR reactivity, although these techniques should still be combined with 'wet lab' assays to prove the results found from the *in-silico* analysis (Antunes et al., 2011; Cai et al., 2020). Another technique which was recently described by Crowther et al. uses CRISPR Cas9 screening to knock out target genes from tumour cells, before mixing with T-cells; the T-cells are not able to kill the tumour cells where the target antigen has been knocked out, so these surviving tumour cells can be sequenced to identify which gene has been knocked out. However, one caveat with this method is that if the target antigen is encoded by a gene that is essential for tumour cell survival, the tumour cells would die after the CRISPR-mediated knock out. Other more novel approaches that have been developed by different research groups include 'T-scan', which involves lentiviral vector delivery of antigen libraries to antigen-presenting cells for presentation on MHC molecules, and ligand discovery through using trogocytosis, a process by which T-cell membrane proteins are transferred to target cells presenting cognate peptide through MHC molecules (Kula et al., 2019, Li et al., 2019).

In the time frame of the PhD, only TCRs from TIL054 10x Genomics® V(D)J library could be reconstructed for validation, however candidate TCRs from TIL041 and TIL042 have also been identified. Further experiments should be carried out to investigate the tumour reactivity of these T-cells to give confidence that CD137-selected cells from final TIL are truly tumour reactive. In future, the TCR-matched gene expression analysis could be utilised further to try to predict the degree of tumour-reactivity of certain clonotypes. It could be that the most abundant clonotypes present in the CD137-sorted population are only mildly tumour-reactive, whereas TCRs that are less abundant might have greater tumour killing potential. To investigate this, CD137+ TCR clonotypes that also have increased gene expression of genes such as TNFα, IFNɣ and IL-2 for example could be identified using the gene expression clustering analysis software. In this way, new tumour-reactive markers might also be found by comparing the gene expression datasets of predicted tumour-reactive clonotypes. Analysing the gene expression data in more detail would also allow for further investigation of the phenotype of TIL products, such as CD8+ expression or the proportion of effector

memory cells, both of which have been key areas of interest for other TIL therapy researchers.

5.4 Future directions for TIL therapy

As discussed in chapter 1, there are 57 ongoing clinical trials identified from searching the clinical trials database that involve treatment with TIL therapy. From looking at the specific TIL therapy interventions, there is a trend towards using some form of enhanced TIL therapy, as opposed to standard TIL therapy. Other TIL trials seem to be adopting previously investigated alterations to the TIL generation protocol, such as using 'young' TIL or an attenuated IL-2 supportive regime. It is also clear that there is a tangible effort to conduct TIL clinical trials in cancers other than melanoma, even though the majority are still in this disease setting. With the prospect of licensing trials for standard TIL therapy for melanoma on the horizon, it is likely that continuing research efforts will be put towards improving upon standard TIL therapy, and also on validating TIL therapy in different cancer settings; the two will likely be investigated in conjunction with one another, as less immunogenic cancers may require enhanced TIL to see a clinical response. Another popular direction of clinical trials currently in the clinic is combination trials, where standard TIL therapy is compared to TIL therapy accompanied by another immunotherapy. These other immunotherapies include irradiation, peptide vaccines and checkpoint inhibitors. This is a logical next step in TIL therapy trials, since the two different therapies being combined usually have already been validated independently, so there is little risk involved with the combined treatment, and potentially great reward.

TIL selection strategies including isolating PD-1+ TIL, CD8+ TIL and even neoantigen-specific TIL are also being investigated in active clinical trials. These tend to involve methods such as magnetic bead capture or FACS to isolate specific populations of T-cells from TIL, based on the expression of specific markers. This is much like the workflow that has been investigated for CD137 in this project. The advantage of selecting specific TIL populations is that it increases the proportion of cells likely to be actively involved in the immune response against the tumour cells. However, more research should be conducted concerning the role of different populations within TIL and the interaction between the subpopulations. For example, the importance of the

CD4+ subpopulation is still widely debated, with researchers still attempting to elucidate whether CD4+ cells play a critical role in anti-tumour responses or are simply required to support the cytotoxic CD8+ population (Friedman et al., 2012). Whilst a more tumour-reactive population might be selectable, this action could come at a cost of losing cells more integral to long-term persistence *in vivo*, or those with greater proliferative potential. This is another reason many researchers are also putting considerable effort into identifying the optimal culture conditions to expand TIL, including removal of endogenous cells such as NK cells that may act as homeostatic cytokine 'sinks', and the use of artificial antigen presenting cells to enhance the resulting TIL product (Gattinoni et al., 2005b; Ye et al., 2011).

There are a number of reasons why TIL therapy has not reached its full potential as an immunotherapeutic treatment for cancer. In order to be prescribed as a licensed medicine, a large-scale licensing trial is required. While this may be just on the horizon for standard TIL therapy, several factors may hinder the progress of this therapy in the clinic. One of the issues facing TIL therapy is the cost of the treatment. TIL therapy is a personalised medicine, where one patient's immune cells are used autologously to target their tumour, which means that a higher cost is associated with manufacturing the therapy, compared to traditional drugs which can be manufactured in bulk for treating multiple patients. The TIL manufacturing process, despite considerable optimisation, is still quite lengthy and requires a high-level of co-ordination and appropriate infrastructure. Additionally, the high-dose IL-2 that is routinely administered after the reinfusion of TIL to support the T-cells is quite toxic, and the side-effects associated with this treatment often mean the patients are kept in hospital for longer, contributing to the overall cost of the therapy. The attenuation of IL-2, and low-dose IL-2 regimes being investigated in clinical trials should help to lower costs, particularly if it allows TIL to be administered as an outpatient treatment.

Regarding the future of TIL therapy, in the short term, combination therapy is most likely to show good success in clinical trials. In order for more significant breakthroughs in the field of TIL therapy, a more in-depth investigation into why some patients respond and others do not is essential. This is not only to further our understanding of TIL therapy, but also to introduce pre-treatment stratification of patients who are likely to respond. While it might be best to treat all melanoma patients with TIL

therapy given our current knowledge, this is also a very costly approach and there is always a chance that the patients will not respond. By putting further efforts into elucidating why a patient has achieved a clinical response, new factors can be identified which could help predict if TIL therapy is a viable treatment option for metastatic melanoma patients. This includes investigating and elucidating the breadth and repertoire of tumour-reactive cells within different patient TIL, which can also help to identify new targets and TCRs for other ACTs.

5.5 Future directions for TCR T-cell therapy

There are currently around 50 actively-recruiting clinical trials using TCR T-cell therapy for treating a variety of cancers (Oppermans et al., 2020). Due to the limited number of well-validated antigens to date, these are mostly for the treatment of metastatic melanoma, however the abundance of trials using TCRs reactive to CT antigen, NY-ESO-1 trials is encouraging. This is particularly important for cancer types that have a poorer prognosis, or haven't seen clinical success with CAR or TIL therapies. The advantage of TCR therapy compared to TIL therapy is that, providing the patient tumour expresses the target antigen, there can be more confidence that TCR therapy may succeed compared with TIL therapy, where neither the antigen or TCRs present are known entities. The converse to this is that TIL demonstrate a broad spectrum of reactivities to different antigens, which can be advantageous if the target antigen for TCR therapy is not expressed by tumour or only expressed at low levels. A multiple target approach inspired by TIL therapy could even be utilised by TCR T-cell therapy, by transducing TCRs of different reactivities into PBMCs for administration, increasing the chance of tumour cell killing by the transduced population. The majority of TCR T-cell clinical trials are supported by early clinical data that demonstrates the safety of the chosen TCR, or utilise a TCR that has previously been safe and efficacious in the clinic. With researchers keen to achieve better clinical response rates in this therapy space, there are a few clinical trials that are using affinity-enhanced TCRs, however these should be heeded carefully to look out for off-target toxicity problems seen in previous trials. Fortunately, the pre-clinical testing of TCRs is more stringent in recent years, and the need of extensive pre-clinical validation prior to TCR selection is widely accepted.

One interesting direction that has been observed is the introduction of personalised TCR T-cell therapy, which utilises TCRs to neoantigens to overcome some of the side effects of shared antigen cross-reactivities (Wang and Cao, 2020). There are a number of trials that are recruiting patients for treatment with patient-specific TCRs, where the TCRs are be identified from patient TIL or PBL, that are reactive to patient-specific neoantigen (NCT03778814, NCT03891706, as discussed by Chen et al., 2019). This highly personalised approach is interesting and likely to produce good clinical responses due to the specificity of neoantigens, however as mentioned previously, personalised healthcare often comes at a much higher cost. It would be interesting to see if personalised TCR T-cell therapy is more efficacious than TIL therapy, since TIL therapy is likely to be the cheaper to manufacture and less complex of the two immunotherapies; unfortunately, it is unlikely these two approaches will be directly compared by clinical trial.

Some factors that are currently holding back the advancement of TCR T-cell therapy in the clinic have been discussed in previous chapters, and include disappointing clinical data, lack of faith in the therapy following clinical trial patient deaths and deficit of tumour-specific targets. These factors may also be attributing to a low rate of patient accrual, which has led to the termination of several TCR T-cell clinical trials. This unfortunately hinders the progress of promising TCR therapy interventions. However, low patient accrual is unsurprising given the stringent inclusion criteria often set out by these clinical trials. For a patient to be treated with TCR T-cell therapy, they generally need to match the HLA haplotype of the TCR used, show target antigen expression in the tumour and often have failed on previous therapy options; these are just some of the inclusion criteria for TCR T-cell therapy trials. The combination of these different criteria, combined with other clinical trials recruiting the same cohort of potential patients such as TIL trials for melanoma, lead to an overall low and slow accrual onto the clinical trials. Hopefully with significant research efforts in optimising TIL and TCR T-cell therapies for other cancer indications, there will be less overlap between patient cohorts for clinical trials in the future.

As previously mentioned, a promising development in TCR T-cell therapy going forward is the abundance of clinical trials using CT antigen-reactive TCRs such as NY-ESO-1. One of the first evidences of NY-ESO-1 TCRs being used in the clinic resulted in objective,

durable clinical responses in both melanoma and synovial sarcoma (Robbins et al., 2011). An expansion of this early trial, with a long-term follow-up showing the predicted 3- and 5- year survival rates to be 38 % and 14 % respectively for synovial sarcoma, and 33 % for both survival rates in melanoma (Robbins et al., 2015). In this same year, highly encouraging clinical response rate of 80% was achieved in myeloma using affinity-enhanced NY-ESO-1 and LAGE-1-restriced TCR (Rapoport et al., 2015). More recently, early phase I data has shown that NY-ESO-1 TCR T-cell therapy can also produce good responses in patients with late-stage NSCLC, demonstrating the variety of tumour types that can be treated with this TCR (Xia et al., 2018). This multi-tumour targeting occurs because the CT antigens are not restricted to a particular cell type, unlike the overexpressed antigens present on melanocytes that have been favoured previously in TCR T-cell therapy. This encouraging data is a prime example of how important antigen selection and identifying a safe TCR for clinical use can be, and when achieved, have highly promising results.

The main drawback with NY-ESO-1 TCR T-cell therapy is that the number and variety of patients treated is still limited by the need for a matched HLA haplotype of the patients. One development that circumvents the problem of HLA restriction is the discovery of HLA-independent TCRs, expressed by some T-cell populations such as mucosal-associated invariant T-cells (MAIT cells), and γδ TCRs expressed by a subpopulation of T-cells. These are TCRs that are capable of recognising non-peptide antigens without the need of MHC peptide presentation. The utilisation of HLA-independent TCRs for cancer immunotherapy is an exciting idea which is being explored increasingly by different research groups (Wolf, Choi and Exley, 2018; Zhu et al., 2019; Kabelitz et al., 2020). The use of invariant TCRs in TCR T-cell therapy is an exciting idea, as it would allow patients with a variety of HLA haplotypes to be included in the same clinical trial, expanding the number of patients eligible for recruitment greatly. This would also be of particular interest to patients with a rarer HLA type that might not be able to treated with any known therapeutic TCRs. It is yet to be seen how many patient tumours express these non-peptide antigens, but recent studies have demonstrated that MR1-specific invariant TCR-transduced T-cells are capable of recognising both autologous and non-autologous tumour in an *in vivo* setting (Crowther et al., 2020). The cytotoxic potential of these TCRs is also something that

requires more investigation, as well as the cross-reactivity profile, but this appears to be a promising new direction for TCR T-cell therapy. These invariant TCR populations can be identified and investigated by utilising TIL selection and sequencing strategies such as the one presented in this thesis.

In conclusion, adoptive cell therapies such as TIL and TCR T-cell therapy have shown great success so far for various cancer types, but have been especially successful for the highly immunogenic metastatic melanoma. Despite this, there is still much to be learnt about how these therapies work and why they are effective for some patients than others. Unfortunately, there are many factors which can affect why a patient achieves a good clinical response, and dissecting which factors are attributable to a clinical response is complex. Recent advances in single cell sequencing techniques, mathematical modelling and gene expression analysis can be utilised to identify new tumour-reactive TCRs from TIL populations. By establishing a thorough set of pre-clinical validation assays, these tumour-reactive TCRs can be screened effectively for TCRs that are both safe and efficacious. Combining new gene editing techniques with more stringent pre-clinical validation methods should drive forward the next generation of TIL and TCR T-cell therapies to bring more effective therapies to the clinic and expand the number of eligible patients that can be enrolled on clinical trials.

6.0 Supplementary data

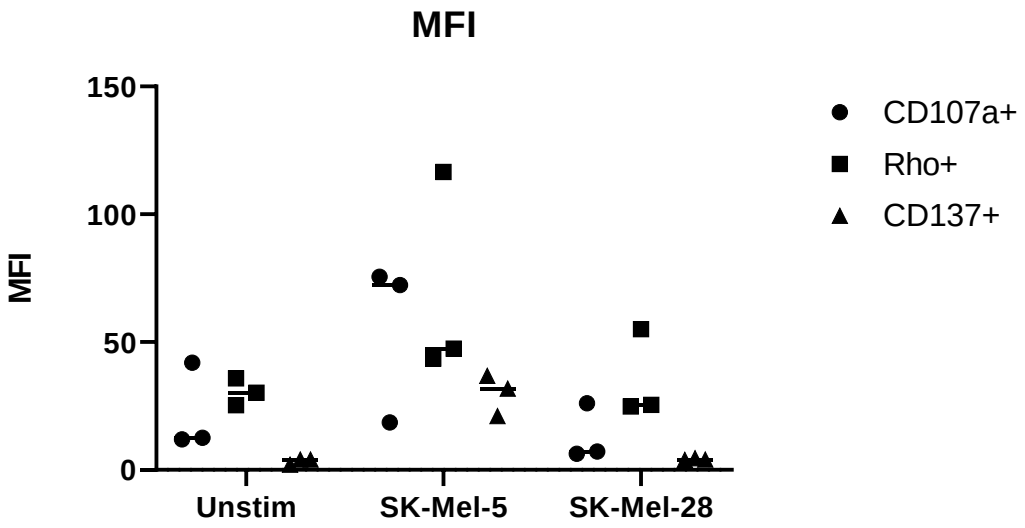

Figure S1. MFI of MART-1 TCR+ve cells expressing different activation markers. MFI of cells expressing either CD107a, Rhodamine 1, 2,3 or CD137 was plotted for unstimulated MART-1-reactive TCR+ve cells alongside co-cultures with SK-Mel-5 (HLA-matched) or SK-Mel-28 (HLA-mis-matched) commercially available cell lines.

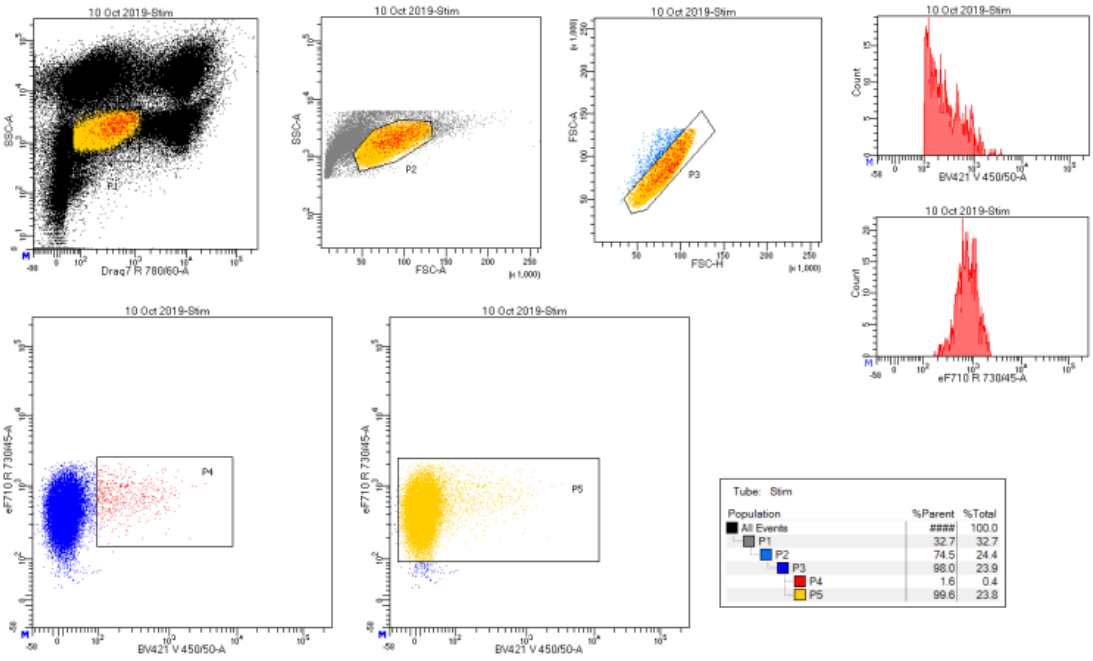

Figure S2. FACS sorting gating strategy for isolating CD2+ or CD2+CD137+ cells from TIL. A screen shot of the gating strategy used for the isolation of CD2+CD137+ (P4) and CD2+ (P5) populations of TIL, which are first gated by live, single cells.

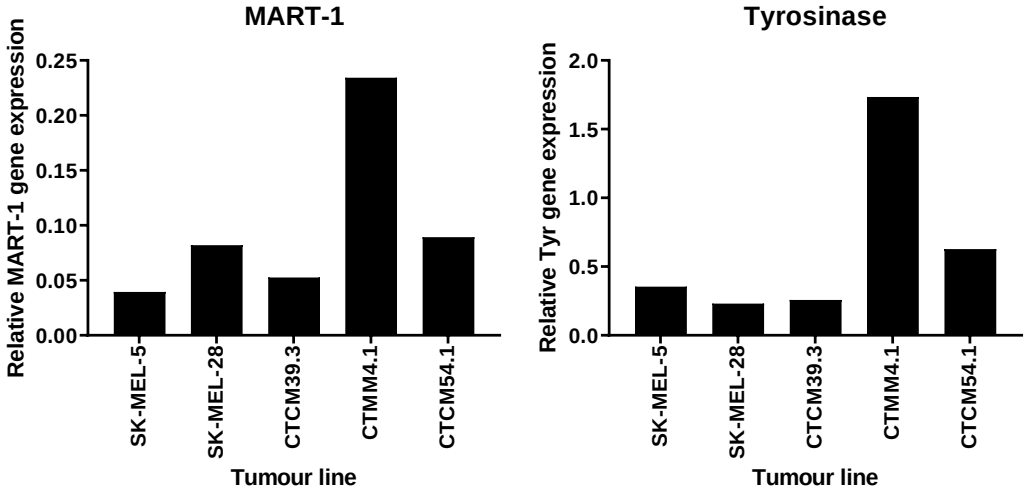

Figure S3. Relative expression of MART-1 and Tyrosinase genes. Using RT-qPCR, the relative gene expression of MART-1 and Tyrosinase genes in a number of different melanoma cell lines was assessed, in comparison to the house-keeping gene, GAPDH.

Table S1. Ongoing clinical trials involving TIL treatment. Information is correct as of May 2020.

Trial number	Status	Phase	Condition	Treatment	Country
NCT03296137	Active, not recruiting	1, 2	Cancer	TIL, IL-2, Ipilumumab, Nivolumab,	Denmark
NCT03287674	Active, not recruiting	1, 2	Metastatic Ovarian Cancer	TIL, IL-2, Ipilimumab	Denmark
NCT03215810	Active, not recruiting	1	NSCLC, Squamous Cell Carcinoma, Adenocarcinoma	TIL, IL-2, Nivolumab	USA

NCT03158935	Active, not recruiting	1	Ovarian Cancer, Malignant Melanoma	TIL, IL-2, Pembrolizumab	Canada
NCT02652455	Active, not recruiting	1	Melanoma	TIL, IL-2, Nivolumab, CD137	USA
NCT02500576	Active, not recruiting	2	Metastatic Melanoma	TIL, IL-2 (low/high), Pembrolizumab	USA
NCT02360579	Active, not recruiting	2	Metastatic Melanoma	TIL, IL-2	USA, France, Germany, Hungary, Italy, Spain, Switzerland, United Kingdom
NCT01993719	Active, not recruiting	2	Metastatic Melanoma	young TIL, IL-2, Pembrolizumab	USA
NCT01883297	Active, not recruiting	1	Ovarian, Fallopian Tube or Peritoneal Cancer	"Re-stimulated" TIL, IL-2,	Canada
NCT01807182	Active, not recruiting	2	Melanoma	TIL, IL-2,	USA
NCT01740557	Active, not recruiting	1, 2	Metastatic Melanoma	CXCR2- or NGFR-transduced TIL, IL-2	USA
NCT01701674	Active, not	N/A	Metastatic Melanoma	TIL, IL-2, Ipilimumab	USA

	recruiting				
NCT01659151	Active, not recruiting	2	Metastatic Melanoma	TIL, IL-2, Vemurafenib	USA
NCT01319565	Active, not recruiting	2	Metastatic Melanoma	young TIL, IL-2, TBI	USA
NCT01005745	Active, not recruiting	N/A	Metastatic Melanoma	TIL, IL-2	USA
NCT04383067	Not yet recruiting	2	Metastatic Urothelial Carcinoma	TIL, IL-2	Israel
NCT04357509	Not yet recruiting	1	Melanoma	PD-1+ve circulating TIL, transduced with 'enhanced receptor' and 'superamplification factor'	China
NCT04165967	Not yet recruiting	1	Advanced Melanoma	TIL, IL-2 (low), Nivolumab	Switzerland
NCT03991741	Not yet recruiting	1	Metastatic Melanoma, Metastatic Head and Neck Cancer	TIL, IL-2	USA
NCT03658785	Not yet recruiting	1, 2	Solid, Metastatic cancer	TIL, IL-2	China

NCT02621021	Not yet recruiting	1, 2	Metastatic Ovarian Cancer	unmodified and modified TIL, IL-2	United Kingdom
NCT04443296	Recruiting	2	Cervical Cancer	CCRT + TIL	China
NCT04426669	Recruiting	1, 2	Gastrointestinal Cancers, Colorectal Cancer, Pancreatic Cancer, Gall Bladder Cancer, Colon Cancer, Oesophageal Cancer, Stomach Cancer	neoantigen-specific TIL (CRISPR modified for CISH-inhibition), IL-2	USA
NCT04268108	Recruiting	Unknown	Advanced Solid Tumours (failed on anti-PD-1 therapy)	PD1+ TIL,	China
NCT04217473	Recruiting	1	Metastatic Melanoma	TILT-123 (TNFalpha and IL-2 coding oncolytic adenovirus TILT-123) + TIL	Denmark, France (not yet recruiting)
NCT04072263	Recruiting	1, 2	Recurrent Ovarian Cancer	TIL, IFNa 2A, carboplatin, Paclitaxel	Netherlands
NCT04052334	Recruiting	1	Sarcoma	TIL, IL-2	USA
NCT03992326	Recruiting	1	Solid Tumour, Adult	TIL, IL-2, low, low dose irradiation	Switzerland
NCT03935893	Recruiting	2	Gastric Cancer, Colorectal Cancer, Pancreatic Cancer, Sarcoma,	TIL (potent), IL-2	USA

			Mesothelioma, Neuroendocrine Tumours, Squamous Cell Cancer, Merkel Cell Carcinoma, Mismatch Repair Deficiency and Microsatellite Instability Cancers		
NCT03904537	Recruiting	1, 2	Colorectal Cancer	anti-PD-1 antibody-activated TILs	China
NCT03903887	Recruiting	1, 2	NSCLC	anti-PD-1 antibody-activated TILs	China
NCT03801083	Recruiting	2	Biliary Tract Cancer, Cholangiocarcinoma	TIL, IL-2 (a)	USA
NCT03725605	Recruiting	2	Soft Tissue Sarcoma	LTX-315 (oncolytic peptide), TILs	Denmark
NCT03645928	Recruiting	2	Metastatic Melanoma, Squamous Cell Carcinoma of the Head and Neck, NSCLC	TIL, IL-2, Pembrolizumab,	USA, Canada, France, Spain, Switzerland, United Kingdom
NCT03638375	Recruiting	1, 2	Melanoma	TIL, Nivolumab, IFNa	Netherlands
NCT03610490	Recruiting	2	Colorectal Cancer, Ovarian Cancer, Pancreatic Ductal Adenocarcnoma	TIL, IL-2	USA

NCT03526185	Recruiting	1	Metastatic Melanoma	TIL, Nivolumab, Ipilumumab	USA
NCT03475134	Recruiting	1	Metastatic Melanoma	TIL, IL-2, Nivolumab	Switzerland
NCT03467516	Recruiting	2	Uveal Melanoma	TIL, IL-2 (a)	USA
NCT03449108	Recruiting	2	Bone Sarcoma, Dedifferentiated Chondrosarcoma, Giant Cell Tumor of the Bone, Ovarian Carcinosarcoma, Ovarian Carcinoma, Soft Tissue Sarcoma	TIL, IL-2,	USA
NCT03412526	Recruiting	2	Metastatic Ovarian Cancer	TIL, IL-2, Radiation	Israel
NCT03374839	Recruiting	1, 2	Melanoma	TIL, IL-2, Nivolumab	France
NCT03347097	Recruiting	1	Glioblastoma Multiforme	TIL, transgenic PD-1 TIL	China
NCT03166397	Recruiting	2	Melanoma	TIL, IL-2	Israel
NCT03083873	Recruiting	2	Squamous Cell Carcinoma of the Head and Neck	TIL, IL-2	USA
NCT02926053	Recruiting	1	Metastatic Renal Cell Carcinoma	TIL, IL-2	Denmark
NCT02650986	Recruiting	1, 2	Advanced/Metastatic Fallopian Tube Carcinoma, Melanoma, Ovarian Carcinoma, Peritoneal	TGFbDNRII-transduced Autologous Tumor Infiltrating Lymphocytes	USA

			Carcinoma, Synovial Sarcoma		
NCT02621021	Recruiting	2	Melanoma	young TIL, IL-2, Pembrolizumab	USA
NCT02414945	Recruiting	1, 2	Pleural Mesothelioma	TIL, IL-2 (low)	Canada
NCT02278887	Recruiting	3	Metastatic Melanoma	TIL, IL-2, Ipilumumab	Denmark, Netherlands
NCT02133196	Recruiting	2	NSCLC, Squamous Cell Carcinoma, Adenocarcinoma, Adenosquamous Carcinoma	young TIL, IL-2	USA
NCT01955460	Recruiting	1	Metastatic Melanoma	TGFbDNRII- or NGFR-transduced TIL, IL-2	USA
NCT01174121	Recruiting	2	Metastatic Colorectal Cancer, Glioblastoma, Metastatic Pancreatic Cancer, Metastatic Ovarian Cancer, Metastatic Breast Carcinoma	young TIL, IL-2, Pembrolizumab	USA
NCT00604136	Recruiting	2	Metastatic Melanoma	TIL, IL-2	Israel
NCT04111510	Recruiting	2	Triple negative Breast Cancer	TIL, IL-2	USA
NCT03108495	Recruiting	2	Cervical Cancer	TIL, IL-2, Pembrolizumab (Cohort 3, US only)	USA, France, Germany, Italy, Netherlands, Spain, Switzerland, United Kingdom

NCT00338377	Recruiting	2	Melanoma	TIL, IL-2, dendritic cell immunisation, Mesna	USA

7.0 References

Aarnoudse, C. A., Krüse, M., Konopitzky, R., Brouwenstijn, N., & Schrier, P. I. (2002). TCR reconstitution in Jurkat reporter cells facilitates the identification of novel tumor antigens by cDNA expression cloning. International Journal of Cancer, 99(1), 7–13.

Adams, S., Robbins, F. M., Chen, D., Wagage, D., Holbeck, S. L., Morse, H. C., Stroncek, D., & Marincola, F. M. (2005). HLA class I and II genotype of the NCI-60 cell lines. Journal of Translational Medicine, 3, 11.

Aktas, E., Kucuksezer, U. C., Bilgic, S., Erten, G., & Deniz, G. (2009). Relationship between CD107a expression and cytotoxic activity. Cellular Immunology, 254(2), 149–154.

Aleksic, M., Liddy, N., Molloy, P. E., Pumphrey, N., Vuidepot, A., Chang, K.-M., & Jakobsen, B. K. (2012). Different affinity windows for virus and cancer-specific T-cell receptors: Implications for therapeutic strategies. European Journal of Immunology, 42(12), 3174–3179.

Algazi, A. P., Tsai, K. K., Shoushtari, A. N., Munhoz, R. R., Eroglu, Z., Piulats, J. M., Ott, P. A., Johnson, D. B., Hwang, J., Daud, A. I., Sosman, J. A., Carvajal, R. D., Chmielowski, B., Postow, M. A., Weber, J. S., & Sullivan, R. J. (2016). Clinical outcomes in metastatic uveal melanoma treated with PD-1 and PD-L1 antibodies. Cancer, 122(21), 3344–3353.

Andersen, R. S., Thrue, C. A., Junker, N., Lyngaa, R., Donia, M., Ellebæk, E., Svane, I. M., Schumacher, T. N., Straten, P. T., & Hadrup, S. R. (2012). Dissection of T-cell antigen specificity in human melanoma. Cancer Research, 72(7), 1642–1650.

Andersen, R., Donia, M., Ellebaek, E., Borch, T. H., Kongsted, P., Iversen, T. Z., Hölmich, L. R., Hendel, H. W., Met, Ö., Andersen, M. H., Straten, P. T., & Svane, I. M. (2016). Long-Lasting complete responses in patients with metastatic melanoma after adoptive cell therapy with tumor-infiltrating lymphocytes and an attenuated IL-2 regimen. Clinical Cancer Research, 22(15), 3734–3745.

Antony, P. A., Piccirillo, C. A., Akpinarli, A., Finkelstein, S. E., Speiss, P. J., Surman, D. R., Palmer, D. C., Chan, C-C., Klebanoff, C. A., Overwijk, W. W., Rosenberg, S. A., & Restifo, N. P. (2005). CD8 + T Cell Immunity Against a Tumor/Self-Antigen Is Augmented by CD4

+ T Helper Cells and Hindered by Naturally Occurring T Regulatory Cells. The Journal of Immunology, 174(5), 2591–2601.

Antunes, D. A., Rigo, M. M., Silva, J. P., Cibulski, S. P., Sinigaglia, M., Chies, J. A. B., & Vieira, G. F. (2011). Structural in silico analysis of cross-genotype-reactivity among naturally occurring HCV NS3-1073-variants in the context of HLA-A*02:01 allele. Molecular Immunology, 48, 1461–1467.

Aoki, Y., Takakuwa, K., Kodama, S., Tanaka, K., Takahashi, M., Tokunaga, A., & Takahashi, T. (1991). Use of Adoptive Transfer of Tumor-infiltrating Lymphocytes Alone or in Combination with Cisplatin-containing Chemotherapy in Patients with Epithelial Ovarian Cancer. Cancer Research, 51(7).

Arce Vargas, F., Furness, A. J. S., Solomon, I., Joshi, K., Mekkaoui, L., Lesko, M. H., … Quezada, S. A. (2017). Fc-Optimized Anti-CD25 Depletes Tumor-Infiltrating Regulatory T Cells and Synergizes with PD-1 Blockade to Eradicate Established Tumors. Immunity, 46(4), 577–586.

Armocida, D., Pesce, A., Di Giammarco, F., Frati, A., Santoro, A., & Salvati, M. (2019). Long Term Survival in Patients Suffering from Glio-blastoma Multiforme: A Single-Center Observational Cohort Study. Diagnostics, 9(4), 209.

Atkins, M. B., Lotze, M. T., Dutcher, J. P., Fisher, R. I., Weiss, G., Margolin, K., Abrams, J., Sznol, M., Parkinson, D., & Rosenberg, S. A. (1999). High-dose recombinant interleukin 2 therapy for patients with metastatic melanoma: Analysis of 270 patients treated between 1985 and 1993. Journal of Clinical Oncology, 17(7), 2105–2116.

Baldan, V., Griffiths, R., Hawkins, R. E., & Gilham, D. E. (2015). Efficient and reproducible generation of tumour-infiltrating lymphocytes for renal cell carcinoma. British Journal of Cancer, 112(9), 1510–1518.

Barrow, C., Browning, J., MacGregor, D., Davis, I. D., Sturrock, S., Jungbluth, A. A., & Cebon, J. (2006). Tumor Antigen Expression in Melanoma Varies According to Antigen and Stage. Clinical Cancer Research, 12(3), 764–771.

Beane, J. D., Lee, G., Zheng, Z., Mendel, M., Abate-Daga, D., Bharathan, M., Black, M., Gandhi, N., Yu, Z., Chandran, S., Giedlin, M., Ando, D., Miller, J., Paschon, D., Guschin, D., Rebar, E. J., Reik, A., Holmes, M. C., Gregory, P. D., Restifo, N. P., Rosenberg, S. A.,

Morgan, R. A., & Feldman, S. A. (2015). Clinical Scale Zinc Finger Nuclease-mediated Gene Editing of PD-1 in Tumor Infiltrating Lymphocytes for the Treatment of Metastatic Melanoma. Molecular Therapy, 23(8), 1380–1390.

Beatty, G. L., & Gladney, W. L. (2015). Immune Escape Mechanisms as a Guide for Cancer Immunotherapy. Clin Cancer Res, 21(4).

Bergman, Y. (1999). Allelic exclusion in B and T lymphopoiesis. Seminars in Immunology, 11(5), 319–328.

Bernal, S. D., Lampidis, T. J., Mcisaac, R. M., & Chen, L. B. (1983). Anticarcinoma activity in vivo of rhodamine 123, a mitochondrial-specific dye. Science, 222(4620), 169–172.

Besser, M. J., Shapira-Frommer, R., Treves, A. J., Zippel, D., Itzhaki, O., Schallmach, E., Kubi, A., Shalmon, B., Hardan, I., Catane, R., Segal, E., Markel, G., Apter, S., Nun, A. B., Kuchuk, I., Shimoni, A., Nagler, A., & Schachter, J. (2009). Minimally cultured or selected autologous tumor-infiltrating lymphocytes after a lympho-depleting chemotherapy regimen in metastatic melanoma patients. Journal of Immunotherapy, 32(4), 415–423.

Besser, M. J., Shoham, T., Harari-Steinberg, O., Zabari, N., Ortenberg, R., Yakirevitch, A., Nagler, A., Loewenthal, R., Schachter, J., & Markel, G. (2013). Development of Allogeneic NK Cell Adoptive Transfer Therapy in Metastatic Melanoma Patients: In Vitro Preclinical Optimization Studies. PLoS ONE, 8(3).

Betts, M. R., Brenchley, J. M., Price, D. A., De Rosa, S. C., Douek, D. C., Roederer, M., & Koup, R. A. (2003). Sensitive and viable identification of antigen-specific CD8+ T cells by a flow cytometric assay for degranulation. Journal of Immunological Methods, 281(1–2), 65–78.

Bijen, H. M., van der Steen, D. M., Hagedoorn, R. S., Wouters, A. K., Wooldridge, L., Falkenburg, J. H. F., & Heemskerk, M. H. M. (2018). Preclinical Strategies to Identify Off-Target Toxicity of High-Affinity TCRs. Molecular Therapy, 26(5), 1206–1214.

Blanchard, T., Srivastava, P. K., & Duan, F. (2013). Vaccines against advanced melanoma. Clinics in Dermatology, 31(2), 179–190.

Bos, R., Marquardt, K. L., Cheung, J., & Sherman, L. A. (2012). Functional differences between low- and high-affinity CD8+ T cells in the tumor environment. OncoImmunology, 1(8), 1239–1247.

Bossi, G., Gerry, A. B., Paston, S. J., Sutton, D. H., Hassan, N. J., & Jakobsen, B. K. (2013). Examining the presentation of tumor-associated antigens on peptide-pulsed T2 cells. OncoImmunology, 2(11), e26840.

Bouneaud, C., Kourilsky, P., & Bousso, P. (2000). Impact of negative selection on the T cell repertoire reactive to a self-peptide: A large fraction of T cell clones escapes clonal deletion. Immunity, 13(6), 829–840.

Brentjens, R. J., Davila, M. L., Riviere, I., Park, J., Wang, X., Cowell, L. G., Bartido, S., Stefanski, J., Taylor, C., Olszewska, M., Borquez-Ojeda, O., Qu, J., Wasielewska, T., He, Q., Bernal, Y., Rijo, I. V., Hedvat, C., Kobos, R., Curran, K., Steinherz, P., Jurcic, J., Rosenblat, T., Maslak, P., Frattini, M., & Sadelain, M. (2013). CD19-targeted T cells rapidly induce molecular remissions in adults with chemotherapy-refractory acute lymphoblastic leukemia. Science Translational Medicine, 5(177), 177ra38.

Brentjens, R., Yeh, R., Bernal, Y., Riviere, I., & Sadelain, M. (2010). Treatment of chronic lymphocytic leukemia with genetically targeted autologous t cells: Case report of an unforeseen adverse event in a phase I clinical trial. Molecular Therapy, 18(4), 666-668.

Brichard, V., Van Pel, A., Wölfel, T., Wölfel, C., De Plaen, E., Lethé, B., Coulie, P., & Boon, T. (1993). The tyrosinase gene codes for an antigen recognized by autologous cytolytic T lymphocytes on HLA-A2 melanomas. Journal of Experimental Medicine, 178(2), 489–495.

Bridgeman, J. S., Hawkins, R. E., Bagley, S., Blaylock, M., Holland, M., & Gilham, D. E. (2010). The Optimal Antigen Response of Chimeric Antigen Receptors Harboring the CD3ζ Transmembrane Domain Is Dependent upon Incorporation of the Receptor into the Endogenous TCR/CD3 Complex. The Journal of Immunology, 184(12), 6938–6949.

Bridgeman, J. S., Sewell, A. K., Miles, J. J., Price, D. A., & Cole, D. K. (2011). Structural and biophysical determinants of αβ T-cell antigen recognition. Immunology, 135(1), 9–18.

Britanova, O. V., Putintseva, E. V., Shugay, M., Merzlyak, E. M., Turchaninova, M. A., Staroverov, D. B., Bolotin, D. A., Lukyanov, S., Bogdanova, E. A., Mamedov, I. Z., Lebedev, Y. B., & Chudakov, D. M. (2014). Age-Related Decrease in TCR Repertoire Diversity Measured with Deep and Normalized Sequence Profiling. The Journal of Immunology, 192(6), 2689–2698.

Brown, S. D., & Holt, R. A. (2019). Neoantigen characteristics in the context of the complete predicted MHC class I self-immunopeptidome. OncoImmunology, 8(3), 1556080.

Brown, S. D., Warren, R. L., Gibb, E. A., Martin, S. D., Spinelli, J. J., Nelson, B. H., & Holt, R. A. (2014). Neo-antigens predicted by tumor genome meta-analysis correlate with increased patient survival. Genome Research, 24(5), 743–750.

Buchbinder, E. I., & Desai, A. (2016). CTLA-4 and PD-1 pathways similarities, differences, and implications of their inhibition. American Journal of Clinical Oncology: Cancer Clinical Trials, 39(1), 98-106.

Buckley, A. F., Kuo, C. T., & Leiden, J. M. (2001). Transcription factor LKLF is sufficient to program T cell quiescence via a c-Myc-dependent pathway. Nature Immunology, 2(8), 698–704.

Cai, L., Caraballo Galva, L. D., Peng, Y., Luo, X., Zhu, W., Yao, Y., Ji, Y., & He, Y. (2020). Preclinical Studies of the Off-Target Reactivity of AFP158-Specific TCR Engineered T Cells. Frontiers in Immunology, 11, 607, 1-12.

Calogero, A., Hospers, G. A. P., Krüse, K. M., Schrier, P. I., Mulder, N. H., Hooijberg, E., & De Leij, L. F. M. H. (2000). Retargeting of a T cell line by anti-MAGE-3/HLA-A2 αβ TCR gene transfer. Anti-cancer Research, 20(3A), 1793–1799.

Campoli, M., & Ferrone, S. (2008). HLA antigen changes in malignant cells: Epigenetic mechanisms and biologic significance. Oncogene, 27(45), 5869-5885.

Caruso, A., Licenziati, S., Corulli, M., Canaris, A. D., Francesco, M. A. De, Fiorentini, S., Peroni, L., Fallacara, F., Dima, F., Balsari, A., & Turano, A. (1997). Flow cytometric analysis of activation markers on stimulated T cells and their correlation with cell proliferation. Cytometry, 27(1), 71–76.

Carvajal, R. D., Sosman, J. A., Quevedo, J. F., Milhem, M. M., Joshua, A. M., Kudchadkar, R. R., Linette, G. P., Gajewski, T. F., Lutzky, J., Lawson, D. H., Lao, C. D., Flynn, P. J., Albertini, M. R., Sato, T., Lewis, K., Doyle, A., Ancell, K., Panageas, K. S., Bluth, M., Hedvat, C., Erinjeri, J., Ambrosini, G., Marr, B., Abramson, D. H., Dickson, M. A., Wolchok, J. D., Chapman, P. B., & Schwartz, G. K. (2014). Effect of selumetinib vs chemotherapy on progression-free survival in uveal melanoma: A randomized clinical trial. JAMA - Journal of the American Medical Association, 311(23), 2397–2405.

Chacon, J. A., Wu, R. C., Sukhumalchandra, P., Molldrem, J. J., Sarnaik, A., Pilon-Thomas, S., Weber, J., Hwu, P., Radvanyi, L. (2013). Co-Stimulation through 4-1BB/CD137 Improves the Expansion and Function of CD8+ Melanoma Tumor-Infiltrating Lymphocytes for Adoptive T-Cell Therapy. PLoS ONE, 8(4), e60031.

Chandran, S. S., Somerville, R. P. T., Yang, J. C., Sherry, R. M., Klebanoff, C. A., Goff, S. L., Wunderlich, J. R., Danforth, D. N., Zlott, D., Paria, B. C., Sabesan, A. C., Srivastava, A. K., Xi, L., Pham, T. H., Raffeld, M., White, D. E., Toomey, M. A., Rosenberg, S. A., & Kammula, U. S. (2017). Treatment of metastatic uveal melanoma with adoptive transfer of tumour-infiltrating lymphocytes: a single-centre, two-stage, single-arm, phase 2 study. The Lancet Oncology, 18(6), 792–802.

Chang, A., Karnell, L., & Menck, H. (1998). The National Cancer Data Base Report on Cutaneous and Noncutaneous Melanoma: A Summary of 84,836 Cases from the Past Decade. The American College of Surgeons Commission on Cancer and the American Cancer Society. Cancer, 83(8), 1664-1678

Chattopadhyay, C., Kim, D. W., Gombos, D. S., Oba, J., Qin, Y., Williams, M. D., Esmaeli, B., Grimm, E. A., Wargo, J. A., Woodman, S. E., & Patel, S. P. (2016). Uveal melanoma: From diagnosis to treatment and the science in between. Cancer, 122(15), 2299-2312.

Chen, D. S., & Mellman, I. (2013). Oncology meets immunology: The cancer-immunity cycle. Immunity, 39(1), 1-10.

Chen, L., Qiao, D., Wang, J., Tian, G., & Wang, M. (2019). Cancer immunotherapy with lymphocytes genetically engineered with T cell receptors for solid cancers. Immunology Letters, 216, 51-62.

Chen, Z., Zhang, C., Pan, Y., Xu, R., Xu, C., Chen, Z., Lu, Z., & Ke, Y. (2016). T cell receptor β-chain repertoire analysis reveals intratumour heterogeneity of tumour-infiltrating lymphocytes in oesophageal squamous cell carcinoma. Journal of Pathology, 239(4), 450–458.

Chesney, J. A., Lutzky, J., Thomas, S. S., Nieva, J. J., Munoz Couselo, E., Martin-Liberal, J., Rodriguez-Moreno, J. F., Cacovean, A., Li, H., Fardis, M., & Gettinger, S. N. (2019). A phase II study of autologous tumor infiltrating lymphocytes (TIL, LN-144/LN-145) in patients with solid tumors. Journal of Clinical Oncology, 37(15_suppl), TPS2648–TPS2648.

Clement, M., Ladell, K., Ekeruche-Makinde, J., Miles, J. J., Edwards, E. S. J., Dolton, G., Williams, T., Schauenburg, A. J. A., Cole, D. K., Lauder, S. N., Gallimore, A. M., Godkin, A. J., Burrows, S. R., Price, D. A., Sewell, A. K., & Wooldridge, L. (2011). Anti-CD8 Antibodies Can Trigger CD8 + T Cell Effector Function in the Absence of TCR Engagement and Improve Peptide–MHCI Tetramer Staining. The Journal of Immunology, 187(2), 654–663.

Cohen, C. J., Li, Y. F., El-Gamil, M., Robbins, P. F., Rosenberg, S. A., & Morgan, R. A. (2007). Enhanced antitumor activity of T cells engineered to express T-cell receptors with a second disulfide bond. Cancer Research, 67(8), 3898–3903.

Cohen, C. J., Zhao, Y., Zheng, Z., Rosenberg, S. A., & Morgan, R. A. (2006). Enhanced antitumor activity of murine-human hybrid T-cell receptor (TCR) in human lymphocytes is associated with improved pairing and TCR/CD3 stability. Cancer Research, 66(17), 8878–8886.

Cole, D. J., Weil, D. P., Shilyansky, J., Custer, M., Kawakami, Y., Rosenberg, S. A., & Nishimura, M. I. (1995). Characterization of the Functional Specificity of a Cloned T-Cell Receptor Heterodimer Recognizing the MART-1 Melanoma Antigen. Cancer Research, 55(4), 748-752.

Cole, D. K., Yuan, F., Rizkallah, P. J., Miles, J. J., Gostick, E., Price, D. A., Gao, G. F., Jakobsen, B. K. and Sewell, A. K. (2009). Germ line-governed recognition of a cancer epitope by an immunodominant human T-cell receptor. Journal of Biological Chemistry, 284(40), 27281–27289.

Corse, E., Gottschalk, R. A., & Allison, J. P. (2011). Strength of TCR–Peptide/MHC Interactions and In Vivo T Cell Responses. The Journal of Immunology, 186(9), 5039–5045.

Crowther, M. D., Dolton, G., Legut, M., Caillaud, M. E., Lloyd, A., Attaf, M., Galloway, S. A.E., Rius, C., Farrell, C. P., Szomolay, B., Ager, A., Parker, A. L., Fuller, A., Donia, M., McCluskey, J., Rossjohn, J., Svane, I. M., Phillips, J. D., & Sewell, A. K. (2020). Genome-wide CRISPR–Cas9 screening reveals ubiquitous T cell cancer targeting via the monomorphic MHC class I-related protein MR1. Nature Immunology, 21(2), 178–185.

Curiel, T. J. (2008). Regulatory T cells and treatment of cancer. Current Opinion in Immunology, 20(2), 241-246.

Davis, M. M., & Bjorkman, P. J. (1988). T-cell antigen receptor genes and T-cell recognition. Nature, 334(6181), 395-402.

De Sanjose, S., Quint, W. G. V., Alemany, L., Geraets, D. T., Klaustermeier, J. E., Lloveras, B., Tous, S., Felix, A., Bravo, L. E., Shin, H. R., Vallejos, C. S., de Ruiz, P. A., Lima, M. A., Guimera, N., Clavero, O., Alejo, M., Llombart-Bosch, A., Cheng-Yang, C., Tatti, S. A., Kasamatsu, E., Iljazovic, E., Odida, M., Prado, R., Seoud, M., Grce, M., Usubutun, A., Jain, A., Suarez, G. A. H., Lombardi, L. E., Banjo, A., Menéndez, C., Domingo, E. J., Velasco, J., Nessa, A., Chichareon, S. C. B., Qiao, Y. L., Lerma, E., Garland, S. M., Sasagawa, T., Ferrera, A., Hammouda, D., Mariani, L., Pelayo, A., Steiner, I., Oliva, E., Meijer, C. J. L. M., Al-Jassar, W. F., Cruz, E., Wright, T. C., Puras, A., Llave, C. L., Tzardi, M., Agorastos, T., Garcia-Barriola, V., Clavel, C., Ordi, J., Andújar, M., Castellsagué, X., Sánchez, G. I., Nowakowski, A. M., Bornstein, J., Muñoz, N. & Bosch, F. X. (2010). Human papillomavirus genotype attribution in invasive cervical cancer: a retrospective cross-sectional worldwide study. The Lancet Oncology, 11(11), 1048–1056.

De Simone, M., Rossetti, G., & Pagani, M. (2018). Single Cell T Cell Receptor Sequencing: Techniques and Future Challenges. Frontiers in Immunology, 9(JUL), 1638.

De Vries, T. J., Trančíkova, D., Ruiter, D. J., & Van Muijen, G. N. P. (1998). High expression of immunotherapy candidate proteins gp100, MART-1, tyrosinase and TRP-1 in uveal melanoma. British Journal of Cancer, 78(9), 1156–1161.

Denkberg, G., Cohen, C. J., Lev, A., Chames, P., Hoogenboom, H. R., & Reiter, Y. (2002). Direct visualization of distinct T cell epitopes derived from a melanoma tumor-associated antigen by using human recombinant antibodies with MHC-restricted T cell receptor-like specificity. Proceedings of the National Academy of Sciences of the United States of America, 99(14), 9421–9426.

Dorval, T., Fridman, W. H., Mathiot, C., & Pouillart, P. (1992). Interleukin-2 therapy for metastatic uveal melanoma. European Journal of Cancer, 23(19), 5779-5788.

Driessens, G., Kline, J., & Gajewski, T. F. (2009, May). Costimulatory and coinhibitory receptors in anti-tumor immunity. Immunological Reviews, 229(1), 126-144.

Dudley, M. E., Gross, C. A., Langhan, M. M., Garcia, M. R., Sherry, R. M., Yang, J. C., Phan, G. Q., Kammula, U. S., Hughes, M. S., Citrin, D. E., Restifo, N. P., Wunderlich, J. R., Prieto, P. A., Hong, J. J., Langan, R. C., Zlott, D. A., Morton, K. E., White, D. E., Laurencot, C. M. & Rosenberg, S. A. (2010). CD8+ enriched “Young” tumor infiltrating lymphocytes can mediate regression of metastatic melanoma. Clinical Cancer Research, 16(24), 6122–6131.

Dudley, M. E., Gross, C. A., Somerville, R. P. T., Hong, Y., Schaub, N. P., Rosati, S. F., White, D. E., Nathan, D., Restifo, N. P., Steinberg, S. M., Wunderlich, J. R., Kammula, U. S., Sherry, R. M., Yang, J. C., Phan, G. Q., Hughes, M. S., Laurencot, C. M., & Rosenberg, S. A. (2013). Randomized selection design trial evaluating CD8+-enriched versus unselected tumor-infiltrating lymphocytes for adoptive cell therapy for patients with melanoma. Journal of Clinical Oncology, 31(17), 2152–2159.

Dudley, M. E., Wunderlich, J. R., Shelton, T. E., Even, J., & Rosenberg, S. A. (2003). Generation of Tumor-Infiltrating Lymphocyte Cultures for Use in Adoptive Transfer Therapy for Melanoma Patients. Journal of Immunotherapy, 26(4), 332–342.

Dudley, M. E., Yang, J. C., Sherry, R., Hughes, M. S., Royal, R., Kammula, U., Robbins, P. F., Huang, J. P., Citrin, D. E., Leitman, S. F., Wunderlich, J., Restifo, N. P., Thomasian, A., Downey, S. G., Smith, F. O., Klapper, J., Morton, K., Laurencot, C., White, D. E., & Rosenberg, S. A. (2008). Adoptive cell therapy for patients with metastatic melanoma: Evaluation of intensive myeloablative chemoradiation preparative regimens. Journal of Clinical Oncology, 26(32), 5233–5239.

Eisenhauer, E. A., Therasse, P., Bogaerts, J., Schwartz, L. H., Sargent, D., Ford, R., Dancey, J., Arbuck, S., Gwyther, S., Mooney, M., Rubinstein, L., Shankar, L., Dodd, L., Kaplan, R., Lacombe, D., & Verweij, J. (2009). New response evaluation criteria in solid tumours: Revised RECIST guideline (version 1.1). European Journal of Cancer, 45, 228–247.

Ekeruche-Makinde, J., Clement, M., Cole, D. K., Edwards, E. S. J., Ladell, K., Miles, J. J., Matthews, K. K., Fuller, A., Lloyd, K. A., Madura, F., Dolton, G. M., Pentier, J., Lissina, A., Gostick, E., Baxter, T. K., Baker, B. M., Rizkallah, P. J., Price, D. A., Wooldridge, L., & Sewell, A. K. (2012). T-cell receptor-optimized peptide skewing of the T-cell repertoire can enhance antigen targeting. Journal of Biological Chemistry, 287(44), 37269–37281.

Ellebaek, E., Iversen, T. Z., Junker, N., Donia, M., Engell-Noerregaard, L., Met, Ö., Hölmich, L. R., Andersen, R. S., Hadrup, S. R., Andersen, M. H., Straten, P. T., & Svane, I. M. (2012). Adoptive cell therapy with autologous tumor infiltrating lymphocytes and low-dose Interleukin-2 in metastatic melanoma patients. Journal of Translational Medicine, 10(1).

Emerson, R. O., Sherwood, A. M., Rieder, M. J., Guenthoer, J., Williamson, D. W., Carlson, C. S., Drescher, C. W., Tewari, M., Bielas, J. H., & Robins, H. S. (2013). High-throughput sequencing of T cell receptors reveals a homogeneous repertoire of tumor-infiltrating lymphocytes in ovarian cancer. The Journal of Pathology, 231(4), 433.

Engels, B., Engelhard, V. H., Sidney, J., Sette, A., Binder, D. C., Liu, R. B., Kranz, D. M., Meredith, S. C., Rowley, D. A., & Schreiber, H. (2013). Relapse or eradication of cancer is predicted by peptide-major histocompatibility complex affinity. Cancer Cell, 23(4), 516–526.

Erdag, G., Schaefer, J. T., Smolkin, M. E., Deacon, D. H., Shea, S. M., Dengel, L. T., Patterson, J. D., & Slingluff, C. L. (2012). Microenvironment and Immunology Immunotype and Immunohistologic Characteristics of Tumor-Infiltrating Immune Cells Are Associated with Clinical Outcome in Metastatic Melanoma. Cancer Research, 72(5), 1070-1080.

Falk, K., Rötzschke, O., Stevanović, S., Jung, G., & Rammensee, H. G. (1991). Allele-specific motifs revealed by sequencing of self-peptides eluted from MHC molecules. Nature, 351(6324), 290–296.

Fang, H., Yamaguchi, R., Liu, X., Daigo, Y., Yin Yew, P., Tanikawa, C., Matsuda, K., Imoto, S., Miyano, S., & Nakamura, Y. (2014). Quantitative T cell repertoire analysis by deep cDNA sequencing of T cell receptor a and b chains using next-generation sequencing (NGS). OncoImmunology, 3(12), e968467.

Ferradini, L., Mackensen, A., Genevée, C., Bosq, J., Duvillard, P., Avril, M. F., & Hercend, T. (1993). Analysis of T cell receptor variability in tumor-infiltrating lymphocytes from a human regressive melanoma: Evidence for in situ T cell clonal expansion. Journal of Clinical Investigation, 91(3), 1183–1190.

Freeman, J. D., Warren, R. L., Webb, J. R., Nelson, B. H., & Holt, R. A. (2009). Profiling the T-cell receptor beta-chain repertoire by massively parallel sequencing. Genome Research, 19(10), 1817–1824.

Friedman, K. M., Prieto, P. A., Devillier, L. E., Gross, C. A., Yang, J. C., Wunderlich, J. R., Rosenberg, S. A., & Dudley, M. E. (2012). Tumor-specific CD4+ melanoma tumor-infiltrating lymphocytes. Journal of Immunotherapy, 35(5), 400–408.

Fyfe, G., Fisher, R. I., Rosenberg, S. A., Sznol, M., Parkinson, D. R., & Louie, A. C. (1995). Results of treatment of 255 patients with metastatic renal cell carcinoma who received high-dose recombinant interleukin-2 therapy. Journal of Clinical Oncology, 13(3), 688–696.

Gajewski, T. F., Schreiber, H., & Fu, Y. X. (2013). Innate and adaptive immune cells in the tumor microenvironment. Nature Immunology, 14(10), 1014-1022.

Galón, J., Costes, A., Sanchez-Cabo, F., Kirilovsky, A., Mlecnik, B., Lagorce-Pagès, C., Tosolini, M., Camus, M., Berger, A., Wind, P., Zinzindohoué, F., Bruneval, P., Cugnenc, P. H., Trajanoski, Z., Fridman, W. H., & Pagès, F. (2006). Type, density, and location of immune cells within human colorectal tumors predict clinical outcome. Science, 313(5795), 1960–1964.

Galón, J., Mlecnik, B., Bindea, G., Angell, H. K., Berger, A., Lagorce, C., Lugli, A., Zlobec, I., Hartmann, A., Bifulco, C., Nagtegaal, I. D., Palmqvist, R., Masucci, G. V., Botti, G., Tatangelo, F., Delrio, P., Maio, M., Laghi, L., Grizzi, F., Asslaber, M., D'Arrigo, C., Vidal-Vanaclocha, F., Zavadova, E., Chouchane, L., Ohashi, P. S., Hafezi-Bakhtiari, S., Wouters, B. G., Roehrl, M., Nguyen, L., Kawakami, Y., Hazama, S., Okuno, K., Ogino, S., Gibbs, P.,

Waring, P., Sato, N., Torigoe, T., Itoh, K., Patel, P. S., Shukla, S. N., Wang, Y., Kopetz, S., Sinicrope, F. A., Scripcariu, V., Ascierto, P. A., Marincola, F. M., Fox, B. A. & Pagès, F. (2014). Towards the introduction of the 'Immunoscore' in the classification of malignant tumours. The Journal of Pathology, 232(2), 199–209.

Gao, G. F., Rao, Z., & Bell, J. I. (2002). Molecular coordination of αβ T-cell receptors and coreceptors CD8 and CD4 in their recognition of peptide-MHC ligands. Trends in Immunology, 23(8), 408-413.

Garcia, K. C., Degano, M., Stanfield, R. L., Brunmark, A., Jackson, M. R., Peterson, P. A., Teyton, L., & Wilson, I. A. (2010). An αβ T cell receptor structure at 2.5 Å and its orientation in the TCR-MHC complex. Journal of Immunology, 185(11), 209–219.

Gattinoni, L., Klebanoff, C. A., Palmer, D. C., Wrzesinski, C., Kerstann, K., Yu, Z., Finkelstein, S. E., Theoret, M. R., Rosenberg, S. A., & Restifo, N. P. (2005a). Acquisition of full effector function in vitro paradoxically impairs the in vivo antitumor efficacy of adoptively transferred CD8+ T cells. Journal of Clinical Investigation, 115(6), 1616–1626.

Gattinoni, L., Finkelstein, S. E., Klebanoff, C. A., Antony, P. A., Palmer, D. C., Spiess, P. J., Hwang, L. N., Yu, Z., Wrzesinski, C., Heimann, D. M., Surh, C. D., Rosenberg, S. A., & Restifo, N. P. (2005b). Removal of homeostatic cytokine sinks by lymphodepletion enhances the efficacy of adoptively transferred tumor-specific CD8+ T cells. Journal of Experimental Medicine, 202(7), 907–912.

Geller, M. A., Cooley, S., Judson, P. L., Ghebre, R., Carson, L. F., Argenta, P. A., Jonson, A. L., Panoskaltsis-Mortari, A., Curtsinger, J., McKenna, D., Dusenbery, K., Bliss, R., Downs, L. S., & Miller, J. S. (2011). A phase II study of allogeneic natural killer cell therapy to treat patients with recurrent ovarian and breast cancer. Cytotherapy, 13(1), 98–107.

Gerlinger, M., Quezada, S. A., Peggs, K. S., Furness, A. J., Fisher, R., Marafioti, T., Shende, V. H., McGranahan, N., Rowan, A. J., Hazell, S., Hamm, D., Robins, H. S., Pickering, L., Gore, M., Nicol, D. L., Larkin, J., & Swanton, C. (2013). Ultra-deep T cell receptor sequencing reveals the complexity and intratumour heterogeneity of T cell clones in renal cell carcinomas. The Journal of Pathology, 231(4), 424–432.

Goff, S. L., Dudley, M. E., Citrin, D. E., Somerville, R. P., Wunderlich, J. R., Danforth, D. N., Zlott, D. A., Yang, J. C., Sherry, R. M., Kammula, U. S., Klebanoff, C. A., Hughes, M. S., Restifo, N. P., Langhan, M. M., Shelton, T. E., Lu, L., Kwong, M. L. M., Ilyas, S., Klemen, N. D., Payabyab, E. C., Morton, K. E., Toomey, M. A., Steinberg, S. M., White, D. E., & Rosenberg, S. A. (2016). Randomized, prospective evaluation comparing intensity of lymphodepletion before adoptive transfer of tumor-infiltrating lymphocytes for patients with metastatic melanoma. Journal of Clinical Oncology, 34(20), 2389–2397.

Goff, S. L., Smith, F. O., Klapper, J. A., Sherry, R., Wunderlich, J. R., Steinberg, S. M., White, D., Rosenberg, S. A., Dudley, M. E. & Yang, J. C. (2010a). Tumor infiltrating lymphocyte therapy for metastatic melanoma: Analysis of tumors resected for TIL. Journal of Immunotherapy, 33(8), 840–847.

Goff, S. L., Johnson, L. A., Black, M. A., Xu, H., Zheng, Z., Cohen, C. J., Morgan, R. A., Rosenberg, S. A., & Feldman, S. A. (2010b). Enhanced receptor expression and in vitro effector function of a murine-human hybrid MART-1-reactive T cell receptor following a rapid expansion. Cancer Immunology, Immunotherapy, 59(10), 1551–1560.

Golubovskaya, V., & Wu, L. (2016). Different subsets of T cells, memory, effector functions, and CAR-T immunotherapy. Cancers, 8(36).

Grosso, J. F., Kelleher, C. C., Harris, T. J., Maris, C. H., Hipkiss, E. L., De Marzo, A., Anders, R., Netto, G., Getnet, D., Bruno, T. C., Goldberg, M. V., Pardoll, D. M., & Drake, C. G. (2007). LAG-3 regulates CD8+ T cell accumulation and effector function in murine self- and tumor-tolerance systems. Journal of Clinical Investigation, 117(11), 3383–3392.

Guo, F., Cofie, L. E., & Berenson, A. B. (2018). Cervical Cancer Incidence in Young U.S. Females After Human Papillomavirus Vaccine Introduction. American Journal of Preventive Medicine, 55(2), 197–204.

Haass, N. K., Smalley, K. S. M., Li, L., & Herlyn, M. (2005). Adhesion, migration and communication in melanocytes and melanoma. Pigment Cell Research, 18(3), 150–159.

Hall, M. L., Liu, H., Malafa, M., Centeno, B., Hodul, P. J., Pimiento, J., Pilon-Thomas, S., & Sarnaik, A. A. (2016). Expansion of tumor-infiltrating lymphocytes (TIL) from human pancreatic tumors. Journal for ImmunoTherapy of Cancer, 4(1), 1–12.

Han, A., Glanville, J., Hansmann, L., & Davis, M. M. (2014). Linking T-cell receptor sequence to functional phenotype at the single-cell level. Nature Biotechnology, 32(7), 684–692.

Hanahan, D., & Weinberg, R. A. (2011, March 4). Hallmarks of cancer: The next generation. Cell, 144(5), 646-674.

Hart, D. P., Xue, S. A., Thomas, S., Cesco-Gaspere, M., Tranter, A., Willcox, B., Lee, S. P., Steven, N., Morris, E. C., & Stauss, H. J. (2008). Retroviral transfer of a dominant TCR prevents surface expression of a large proportion of the endogenous TCR repertoire in human T cells. Gene Therapy, 15(8), 625–631.

Heemskerk, B., Liu, K., Dudley, M. E., Johnson, L. A., Kaiser, A., Downey, S., Zheng, Z., Shelton, T. E., Matsuda, K., Robbins, P. F., Morgan, R. A., & Rosenberg, S. A. (2008). Adoptive cell therapy for patients with melanoma, using tumor-infiltrating lymphocytes genetically engineered to secrete interleukin-2. Human Gene Therapy, 19(5), 496–510.

Hodi, F. S., Chesney, J., Pavlick, A. C., Robert, C., Grossmann, K. F., McDermott, D. F., Linette, G. P., Meyer, N., Giguere, J. K., Agarwala, S. S., Shaheen, M., Ernstoff, M. S., Minor, D. R., Salama, A. K., Taylor, M. H., Ott, P. A., Horak, C., Gagnier, P., Jiang, J., Wolchok, J. D., & Postow, M. A. (2016). Combined nivolumab and ipilimumab versus ipilimumab alone in patients with advanced melanoma: 2-year overall survival outcomes in a multicentre, randomised, controlled, phase 2 trial. The Lancet Oncology, 17(11), 1558–1568.

Hodi, F. S., O'Day, S. J., McDermott, D. F., Weber, R. W., Sosman, J. A., Haanen, J. B., Gonzalez, R., Robert, C., Schadendorf, D., Hassel, J. C., Akerley, W., Van Den Eertwegh, A. J. M., Lutzky, J., Lorigan, P., Vaubel, J. M., Linette, G. P., Hogg, D., Ottensmeier, C. H., Lebbé, C., Peschel, C., Quirt, I., Clark, J. I., Wolchok, J. D., Weber, J. S., Tian, J., Yellin, M. J., Nichol, G. M., Hoos, A., & Urba, W. J. (2010). Improved survival with ipilimumab in patients with metastatic melanoma. New England Journal of Medicine, 363(8), 711–723.

Hou, X., Wang, M., Lu, C., Xie, Q., Cui, G., Chen, J., Du, Y., Dai, Y., & Diao, H. (2016). Analysis of the Repertoire Features of TCR Beta Chain CDR3 in Human by High-Throughput Sequencing. Cellular Physiology and Biochemistry, 39(2), 651–667.

Howie, B., Sherwood, A. M., Berkebile, A. D., Berka, J., Emerson, R. O., Williamson, D. W., Kirsch, I., Vignali, M., Rieder, M. J., Carlson, C. S., & Robins, H. S. (2015). High-throughput pairing of T cell receptor α and β sequences. Science Translational Medicine, 7(301), 301ra131-301ra131.

Hua, C., Boussemart, L., Mateus, C., Routier, E., Boutros, C., Cazenave, H., Viollet, R., Thomas, M., Roy, S., Benannoune, N., Tomasic, G., Soria, J. C., Champiat, S., Texier, M., Lanoy, E., & Robert, C. (2016). Association of vitiligo with tumor response in patients with metastatic melanoma treated with pembrolizumab. JAMA Dermatology, 152(1), 45–51.

Huang, J., Khong, H. T., Dudley, M. E., El-Gamil, M., Li, Y. F., Rosenberg, S. A., & Robbins, P. F. (2005). Survival, persistence, and progressive differentiation of adoptively transferred tumor-reactive T cells associated with tumor regression. Journal of Immunotherapy, 28(3), 258–267.

Hwang, M. L., Lukens, J. R., & Bullock, T. N. J. (2007). Cognate Memory CD4 + T Cells Generated with Dendritic Cell Priming Influence the Expansion, Trafficking, and Differentiation of Secondary CD8 + T Cells and Enhance Tumor Control. The Journal of Immunology, 179(9), 5829–5838.

Ino, Y., Yamazaki-Itoh, R., Shimada, K., Iwasaki, M., Kosuge, T., Kanai, Y., & Hiraoka, N. (2013). Immune cell infiltration as an indicator of the immune microenvironment of pancreatic cancer. British Journal of Cancer, 108(4), 914–923.

Inoue, K., Ogawa, H., Sonoda, Y., Kimura, T., Sakabe, H., Oka, Y., Miyake, S., Tamaki, H., Oji, Y., Yamagami, T., Tatekawa, T., Soma, T., Kishimoto, T., & Sugiyama, H. (1997). Aberrant overexpression of the Wilms tumor gene (WT1) in human leukemia. Blood, 89(4), 1405–1412.

Inozume, T., Hanada, K. I., Wang, Q. J., Ahmadzadeh, M., Wunderlich, J. R., Rosenberg, S. A., & Yang, J. C. (2010). Selection of CD8++PD-1+ lymphocytes in fresh human

melanomas enriches for tumor-reactive T cells. Journal of Immunotherapy, 33(9), 956–964.

Irving, M., Zoete, V., Hebeisen, M., Schmid, D., Baumgartner, P., Guillaume, P., Romero, P., Speiser, D., Luescher, I., Rufer, N., & Michielin, O. (2012). Interplay between T cell receptor binding kinetics and the level of cognate peptide presented by major histocompatibility complexes governs CD8+ T cell responsiveness. Journal of Biological Chemistry, 287(27), 23068–23078.

Itzhaki, O., Hovav, E., Ziporen, Y., Levy, D., Kubi, A., Zikich, D., Hershkovitz, L., Treves, A. J., Shalmon, B., Zippel, D., Markel, G., Shapira-Frommer, R., Schachter, J., & Besser, M. J. (2011). Establishment and Large-scale Expansion of Minimally cultured "Young" Tumor Infiltrating Lymphocytes for Adoptive Transfer Therapy. Journal of Immunotherapy, 34(2), 212–220.

Johnson, L. A., Heemskerk, B., Powell, D. J., Cohen, C. J., Morgan, R. A., Dudley, M. E., Robbins, P. F., & Rosenberg, S. A. (2006). Gene Transfer of Tumor-Reactive TCR Confers Both High Avidity and Tumor Reactivity to Nonreactive Peripheral Blood Mononuclear Cells and Tumor-Infiltrating Lymphocytes. The Journal of Immunology, 177(9), 6548–6559.

Johnson, L. A., Morgan, R. A., Dudley, M. E., Cassard, L., Yang, J. C., Hughes, M. S., Kammula, U. S., Royal, R. E., Sherry, R. M., Wunderlich, J. R., Lee, C. C R., Restifo, N. P., Schwarz, S. L., Cogdill, A. P., Bishop, R. J., Kim, H., Brewer, C. C., Rudy, S. F., VanWaes, C., Davis, J. L., Mathur, A., Ripley, R. T., Nathan, D. A., Laurencot, C. M., & Rosenberg, S. A. (2009). Gene therapy with human and mouse T-cell receptors mediates cancer regression and targets normal tissues expressing cognate antigen. Blood, 114(3), 535–546.

Joseph, R. W., Peddareddigari, V. R., Liu, P., Miller, P. W., Overwijk, W. W., Bekele, N. B., Ross, M. I., Lee, J. E., Gershenwald, J. E., Lucci, A., Prieto, V. G., McMannis, J. D., Papadopoulos, N., Kim, K., Homsi, J., Bedikian, A., Hwu, W. J., Hwu, P., & Radvanyi, L. G. (2011). Impact of clinical and pathologic features on tumor-infiltrating lymphocyte expansion from surgically excised melanoma metastases for adoptive T-cell therapy. Clinical Cancer Research, 17(14), 4882–4891.

Kabelitz, D., Serrano, R., Kouakanou, L., Peters, C., & Kalyan, S. (2020). Cancer immunotherapy with γδ T cells: many paths ahead of us. Cellular and Molecular Immunology, 17(9), 925-939.

Kalergis, A. H., Boucheron, N., Doucey, M. A., Palmieri, E., Goyarts, E. C., Vegh, Z., Luescher, I. F., & Nathenson, S. G. (2001). Efficient T cell activation requires an optimal dwell-time of interaction between the TCR and the pMHC complex. Nature Immunology, 2(3), 229–234.

Kammula, U. S., White, D. E., & Rosenberg, S. A. (1998). Trends in the safety of high dose bolus interleukin-2 administration in patients with metastatic cancer. Cancer, 83(4), 797–805.

Kaunitz, G. J., Cottrell, T. R., Lilo, M., Muthappan, V., Esandrio, J., Berry, S., Xu, H., Ogurtsova, A., Anders, R. A., Fischer, A. H., Kraft, S., Gerstenblith, M. R., Thompson, C. L., Honda, K., Cuda, J. D., Eberhart, C. G., Handa, J. T., Lipson, E. J., & Taube, J. M. (2017). Melanoma subtypes demonstrate distinct PD-L1 expression profiles. Laboratory Investigation, 97(9), 1063–1071.

Kawakami, A., Sakane, F., Imai, S. I., Yasuda, S., Kai, M., Kanoh, H., Jin, H. Y., Hirosaki, K., Yamashita, T., Fisher, D. E. & Jimbow, K. (2008). Rab7 regulates maturation of melanosomal matrix protein gp100/Pmel17/Silv. Journal of Investigative Dermatology, 128(1), 143–150.

Kawakami, Y., Eliyahu, S., Delgado, C. H., Robbins, P. F., Sakaguchi, K., Appella, E., Yannelli, J. R., Adema, G. J., Miki, T., & Rosenberg, S. A. (1994a). Identification of a human melanoma antigen recognized by tumor- infiltrating lymphocytes associated with in vivo tumor rejection. Proceedings of the National Academy of Sciences of the United States of America, 91(14), 6458–6462.

Kawakami, Y., Eliyahu, S., Delgado, C. H., Robbins, P. F., Rivoltini, L., Topalian, S. L., Miki, T., & Rosenberg, S. A. (1994b). Cloning of the gene coding for a shared human melanoma antigen recognized by autologous T cells infiltrating into tumor. Proceedings of the National Academy of Sciences of the United States of America, 91(9), 3515–3519.

Kelderman, S., Heemskerk, B., Fanchi, L., Philips, D., Toebes, M., Kvistborg, P., van Buuren, M. M., van Rooij, N., Michels, S., Germeroth, L., Haanen, J. B. A. G., & Schumacher, N. M. (2016). Antigen-specific TIL therapy for melanoma: A flexible platform for personalized cancer immunotherapy. European Journal of Immunology, 46(6), 1351–1360.

Kershaw, M. H., Wang, G., Westwood, J. A., Pachynski, R. K., Tiffany, H. L., Marincola, F. M., Wang, E., Young, H. A., Murphy, P. M., & Hwu, P. (2002). Redirecting migration of T cells to chemokine secreted from tumors by genetic modification with CXCR2. Human Gene Therapy, 13(16), 1971–1980.

Kim, J. W., Nam, K. H., Ahn, S. H., Park, D. J., Kim, H. H., Kim, S. H., Chang, H., Lee, J. O., Kim, Y. J., Lee, H. S., Kim, J. H., Bang, S. M., Lee, J. S., & Lee, K. W. (2016). Prognostic implications of immunosuppressive protein expression in tumors as well as immune cell infiltration within the tumor microenvironment in gastric cancer. Gastric Cancer, 19(1), 42–52.

Kim, S.-M., Bhonsle, L., Besgen, P., Nickel, J., Backes, A., Held, K., Vollmer, S., Dornmair, K., & Prinz, J. C. (2012). Analysis of the Paired TCR α- and β-chains of Single Human T Cells. PLoS ONE, 7(5), e37338.

Koch, M., Beckhove, P., Op Den Winkel, J., Autenrieth, D., Wagner, P., Nummer, D., Specht, S., Antolovic, D., Galindo, L., Schmitz-Winnenthal, F. H., Schirrmacher, V., Büchler, M. W., & Weitz, J. (2006). Tumor infiltrating T lymphocytes in colorectal cancer: Tumor-selective activation and cytotoxic activity in situ. Annals of Surgery, 244(6), 986–992.

Kono, K., Kawaida, H., Takahashi, A., Sugai, H., Mimura, K., Miyagawa, N., Omata, H, & Fujii, H. (2006). CD4(+)CD25high regulatory T cells increase with tumor stage in patients with gastric and esophageal cancers. Cancer Immunology, Immunotherapy, 55(9), 1064–1071.

Kowolik, C. M., Topp, M. S., Gonzalez, S., Pfeiffer, T., Olivares, S., Gonzalez, N., Smith, D. D., Forman, S. J., & Cooper, L. J. N. (2006). CD28 costimulation provided through a CD19-specific chimeric antigen receptor enhances in vivo persistence and antitumor efficacy of adoptively transferred T cells. Cancer Research, 66(22), 10995–11004.

Krogsgaard, M., Zhong, S., Malecek, K., Johnson, L. A., Yu, Z., Vega-Saenz de Miera, E., Darvishian, F., McGary-Shipper, K., Huang, K., Boyer, J., Corse, E., Shao, Y., Rosenberg, S. A., & Osman, I. (2013). T cell receptor affinity and avidity defines antitumor response and autoimmunity in T cell immunotherapy. Journal for ImmunoTherapy of Cancer, 1, P242.

Krouse, R. S., Royal, R. E., Heywood, G., Weintraub, B. D., White, D. E., Steinberg, S. M., Rosenberg, S. A., & Schwartzentruber, D. J. (1995). Thyroid dysfunction in 281 patients with metastatic melanoma or renal carcinoma treated with interleukin-2 alone. Journal of Immunotherapy with Emphasis on Tumor Immunology, 272–278.

Kula, T., Dezfulian, M. H., Wang, C. I., Abdelfattah, N. S., Hartman, Z. C., Wucherpfennig, K. W., Lyerly, H. K., & Elledge, S. J. (2019). T-Scan: A Genome-wide Method for the Systematic Discovery of T Cell Epitopes. Cell, 178(4), 1016-1028.e13.

Kunert, A., Obenaus, M., Lamers, C. H. J., Blankenstein, T., & Debets, R. (2017). T-cell receptors for clinical therapy: In vitro assessment of toxicity risk. Clinical Cancer Research, 23(20), 6012-6020.

Kupcova Skalnikova, H., Cizkova, J., Cervenka, J., & Vodicka, P. (2017). Advances in Proteomic Techniques for Cytokine Analysis: Focus on Melanoma Research. International Journal of Molecular Sciences, 18(12), 2697.

Kverneland, A. H., Pedersen, M., Westergaard, M. C. W., Nielsen, M., Borch, T. H., Olsen, L. R., Aasbjerg, G., Santegoets, S. J., van der Burg, S. H., Milne, K., Nelson, B. H., Met, Ö., Donia, M., & Svane, I. M. (2020). Adoptive cell therapy in combination with checkpoint inhibitors in ovarian cancer. Oncotarget, 11(22), 2092–2105.

Kvistborg, P., Shu, C. J., Heemskerk, B., Fankhauser, M., Thrue, C. A., Toebes, M., Van Rooij, N., Linnemann, C., Van Buuren, M. M., Urbanus, J. H. M., Beltman, J. B., Straten, P., Li, Y. F., Robbins, P. F., Besser, M. J., Schachter, J., Kenter, G. G., Dudley, M. E., Rosenberg, S. A., Haanen, J. B. A. G., Hadrup, S. R., & Schumacher, T. N. M. (2012). TIL therapy broadens the tumor-reactive CD8+ T cell compartment in melanoma patients. OncoImmunology, 1(4), 409–418.

Laugel, B., Van Den Berg, H. A., Gostick, E., Cole, D. K., Wooldridge, L., Boulter, J., Milicic, A., Price, D. A., & Sewell, A. K. (2007). Different T Cell Receptor Affinity

Thresholds and CD8 Coreceptor Dependence Govern Cytotoxic T Lymphocyte Activation and Tetramer Binding Properties. Journal of Biological Chemistry, 282(33), 23799–23810.

Lawrence, M. S., Stojanov, P., Polak, P., Kryukov, G. V., Cibulskis, K., Sivachenko, A., Carter, S. L., Stewart, C., Mermel, C. H., Roberts, S. A., Kiezun, A., Hammerman, P. S., McKenna, A., Drier, Y., Zou, L., Ramos, A. H., Pugh, T. J., Stransky, N., Helman, E., Kim, J., Sougnez, C., Ambrogio, L., Nickerson, E., Shefler, E., Cortés, M. L., Auclair, D., Saksena, G., Voet, D., Noble, M., Dicara, D., Lin, P., Lichtenstein, L., Heiman, D. I., Fennell, T., Imielinski, M., Hernandez, B., Hodis, E., Baca, S., Dulak, A. M., Lohr, J., Landau, D. A., Wu, C. J., Melendez-Zajgla, J., Hidalgo-Miranda, A., Koren, A., McCarroll, S. A., Mora, J., Lee, R. S., Crompton, B., Onofrio, R., Parkin, M., Winckler, W., Ardlie, K., Gabriel, S. B., Roberts, C. W.M., Biegel, J. A., Stegmaier, K., Bass, A. J., Garraway, L. A., Meyerson, M., Golub, T. R., Gordenin, D. A., Sunyaev, S., Lander, E., & S. Getz, G. (2013). Mutational heterogeneity in cancer and the search for new cancer-associated genes. Nature, 499(7457), 214–218.

Lee, S. J., Lim, H. J., Choi, Y. H., Chang, Y. H., Lee, W. J., Kim, D. W., & Yoon, G. S. (2013). The clinical significance of tumor-infiltrating lymphocytes and microscopic satellites in acral Melanoma in a Korean population. Annals of Dermatology, 25(1), 61–66.

Legut, M., Dolton, G., Mian, A. A., Ottmann, O. G., & Sewell, A. K. (2018). CRISPR-mediated TCR replacement generates superior anticancer transgenic t cells. Blood, 131(3), 311–322.

Li, G., Bethune, M. T., Wong, S., Joglekar, A. V., Leonard, M. T., Wang, J. K., Kim, J. T., Cheng, D., Peng, S., Zaretsky, J. M., Su, Y., Luo, Y., Heath, J. R., Ribas, A., Witte, O. N., & Baltimore, D. (2019). T cell antigen discovery via trogocytosis. Nature Methods, 16(2),

Li, J., Chen, Q. Y., He, J., Li, Z. L., Tang, X. F., Chen, S. P., Xie, C. M., Li, Y. Q., Huang, L. X., Ye, S. B., Ke, M. L., Tang, L. Q., Liu, H., Zhang, L., Guo, S. S., Xia, J. C., Zhang, X. S., Zheng, L. M., Guo, X., Qian, C. N., Mai, H. Q. & Zeng, Y. X. (2015). Phase I trial of adoptively transferred tumor-infiltrating lymphocyte immunotherapy following concurrent chemoradiotherapy in patients with locoregionally advanced nasopharyngeal carcinoma. OncoImmunology, 4(2), 1–10.

Li, X., Ye, F., Chen, H., Lu, W., Wan, X., & Xie, X. (2007). Human ovarian carcinoma cells generate CD4+CD25+ regulatory T cells from peripheral CD4+CD25- T cells through secreting TGF-β. Cancer Letters, 253(1), 144–153.

Linette, G. P., Stadtmauer, E. A., Maus, M. V, Rapoport, A. P., Levine, B. L., Emery, L., … June, C. H. (2013). Cardiovascular toxicity and titin cross-reactivity of affinity-enhanced T cells in myeloma and melanoma. Blood, 122(6), 863-871.

Liu, Y., & Cao, X. (2016). Immunosuppressive cells in tumor immune escape and metastasis. Journal of Molecular Medicine, 94(5), 509–522.

Lowe, S. W., & Lin, A. W. (2000). Apoptosis in cancer. Carcinogenesis, 21(3), 485-495.

Lu, Y. C., & Robbins, P. F. (2016). Cancer immunotherapy targeting neoantigens. Seminars in Immunology, 28(1), 22-27.

Malaponte, G., Libra, M., Gangemi, P., Bevelacqua, V., Mangano, K., D'Amico, F., Mazzarino, M. C., Stivala, F., McCubrey, J. A., & Travali, S. (2006). Detection of BRAF gene mutation in primary choroidal melanoma tissue. Cancer Biology and Therapy, 5(2), 225–227.

Mammoto, T., & Ingber, D. E. (2010). Mechanical control of tissue and organ development. Development, 137(9), 1407-1420.

Marchesi, J. R., Dutilh, B. E., Hall, N., Peters, W. H. M., Roelofs, R., Boleij, A., & Tjalsma, H. (2011). Towards the human colorectal cancer microbiome. PLoS ONE, 6(5), e20447.

Marrack, P., Lo, D., Brinster, R., Palmiter, R., Burkly, L., Flavell, R. H., & Kappler, J. (1988). The effect of thymus environment on T cell development and tolerance. Cell, 53(4), 627–634.

Meier, F., Will, S., Ellwanger, U., Schlagenhauff, B., Schittek, B., Rassner, G., & Garbe, C. (2002). Metastatic pathways and time courses in the orderly progression of cutaneous melanoma. British Journal of Dermatology, 147(1), 62–70.

Mlecnik, B., Bindea, G., Angell, H. K., Maby, P., Angelova, M., Tougeron, D., Church, S. E., Lafontaine, L., Fischer, M., Fredriksen, T., Sasso, M., Bilocq, A. M., Kirilovsky, A., Obi, A. C., Hamieh, M., Berger, A., Bruneval, P., Tuech, J. J., Sabourin, J. C., Le Pessot, F., Mauillon, J., Rafii, A., Laurent-Puig, P., Speicher, M. R., Trajanoski, Z., Michel, P.,

Sesboüe, R., Frebourg, T., Pagès, F., Valge-Archer, V., Latouche, J. B., & Galon, J. (2016). Integrative Analyses of Colorectal Cancer Show Immunoscore Is a Stronger Predictor of Patient Survival Than Microsatellite Instability. Immunity, 44(3), 698–711.

Morgan, R. A., Chinnasamy, N., Abate-Daga, D., Gros, A., Robbins, P. F., Zheng, Z., Dudley, M. E., Feldman, S. A., Yang, J. C., Sherry, R. M., Phan, G. Q., Hughes, M. S., Kammula, U. S., Miller, A. D., Hessman, C. J., Stewart, A. A., Restifo, N. P., Quezado, M. M., Alimchandani, M., Rosenberg, A. Z., Nath, A., Wang, T., Bielekova, B., Wuest, S. C., Akula, N., McMahon, F. J., Wilde, S., Mosetter, B., Schendel, D. J., Laurencot, C. M., & Rosenberg, S. A. (2013). Cancer regression and neurological toxicity following anti-MAGE-A3 TCR gene therapy. Journal of Immunotherapy, 36(2), 133–151.

Morgan, R. A., Dudley, M. E., Wunderlich, J. R., Hughes, M. S., Yang, J. C., Sherry, R. M., Royal, R. E., Topalían, S. L., Kammula, U. S., Restifo, N. P., Zheng, Z., Nahvi, A., De Vries, C. R., Rogers-Freezer, L. J., Mavroukakis, S. A., & Rosenberg, S. A. (2006). Cancer regression in patients after transfer of genetically engineered lymphocytes. Science, 314(5796), 126–129.

Morgan, R. A., Yang, J. C., Kitano, M., Dudley, M. E., Laurencot, C. M., & Rosenberg, S. A. (2010). Case Report of a Serious Adverse Event Following the Administration of T Cells Transduced with a Chimeric Antigen Receptor Recognizing ERBB2. Molecular Therapy, 18(4), 843–851.

Mullinax, J. E., Hall, M., Prabhakaran, S., Weber, J., Khushalani, N., Eroglu, Z., Brohl, A. S., Markowitz, J., Royster, E., Richards, A., Stark, V., Zager, J. S., Kelley, L., Cox, C., Sondak, V. K., Mulé, J. J., Pilon-Thomas, S., & Sarnaik, A. A. (2018). Combination of Ipilimumab and Adoptive Cell Therapy with Tumor-Infiltrating Lymphocytes for Patients with Metastatic Melanoma. Frontiers in Oncology, 8, 44.

Murata, K., Nakatsugawa, M., Rahman, M. A., Nguyen, L. T., Millar, D. G., Mulder, D. T., Sugata, K., Saijo, H., Matsunaga, Y., Kagoya, Y., Guo, T., Anczurowski, M., Wang, C. H., Burt, B. D., Ly, D., Saso, K., Easson, A., Goldstein, D. P., Reedijk, M., Ghazarian, D. A., Pugh, T. J., Butler, M. O., Mak, T. W., Ohashi, P. S., & Hirano, N. (2020). Landscape mapping of shared antigenic epitopes and their cognate TCRs of tumor-infiltrating T lymphocytes in Melanoma. eLife, 9(4).

Murphy, K. (2012). Janeway's Immunobiology. Garland Science. Retrieved from https://blackwells.co.uk/bookshop/product/Janeways-Immunobiology-by-Kenneth-Murphy-author-Casey-Weaver-author/9780815345053

Nakakubo, Y., Miyamoto, M., Cho, Y., Hida, Y., Oshikiri, T., Suzuoki, M., Hiraoka, K., Itoh, T., Kondo, S., & Katoh, H. (2003). Clinical significance of immune cell infiltration within gallbladder cancer. British Journal of Cancer, 89(9), 1736–1742.

Newick, K., O'Brien, S., Moon, E., & Albelda, S. M. (2017). CAR T Cell Therapy for Solid Tumors. Annual Review of Medicine, 68(1), 139–152.

Nielsen, M., Lundegaard, C., Blicher, T., Lamberth, K., Harndahl, M., Justesen, S., Røder, G., Peters, B., Sette, A., Lund, O., & Buus, S. (2007). NetMHCpan, a method for quantitative predictions of peptide binding to any HLA-A and -B locus protein of known sequence. PLoS ONE, 2(8).

Nishimura, M. I., Kawakami, Y., Charmley, P., O'Neil, B., Shilyansky, J., Yannelli, J. R., Rosenberg, S. A., & Hood, L. (1994). T-Cell Receptor Repertoire in Tumor-Infiltrating Lymphocytes. Analysis of Melanoma-Specific Long-Term Lines. Journal of Immunotherapy, 16(2), 85–94.

Nonomura, C., Otsuka, M., Kondou, R., Iizuka, A., Miyata, H., Ashizawa, T., Sakura, N., Yoshikawa, S., Kiyohara, Y., Ohshima, K., Urakami, K., Nagashima, T., Ohnami, S., Kusuhara, M., Mitsuya, K., Hayashi, N., Nakasu, Y., Mochizuki, T., Yamaguchi, K., & Akiyama, Y. (2019). Identification of a neoantigen epitope in a melanoma patient with good response to anti-PD-1 antibody therapy. Immunology Letters, 208, 52–59.

Nordlund, J. J., Kirkwood, J. M., Forget, B. M., Milton, G., Albert, D. M., & Lerner, A. B. (1983). Vitiligo in patients with metastatic melanoma: A good prognostic sign. Journal of the American Academy of Dermatology, 9(5), 689–696.

Ohashi, P. S., Mak, T. W., Van Den Elsen, P., Yanagi, Y., Yoshikai, Y., Calman, A. F., Terhorst, C., Stobo, J. D., & Weiss, A. (1985). Reconstitution of an active surface T3/T-cell antigen receptor by DNA transfer. Nature, 316(6029), 606–609.

Oji, Y., Miyoshi, S., Maeda, H., Hayashi, S., Tamaki, H., Nakatsuka, S. I., Yao, M., Takahashi, E., Nakano, Y., Hirabayashi, H., Shintani, Y., Oka, Y., Tsuboi, A., Hosen, N., Asada, M., Fujioka, T., Murakami, M., Kanato, K., Motomura, M., Kim, E. H., Kawakami,

M., Ikegame, K., Ogawa, H., Aozasa, K., Kawase, I., & Sugiyama, H. (2002). Overexpression of the Wilms' tumor gene WT1 in de novo lung cancers. International Journal of Cancer, 100(3), 297–303.

Ophir, E., Bobisse, S., Coukos, G., Harari, A., & Kandalaft, L. E. (2016). Personalized approaches to active immunotherapy in cancer. Biochimica et Biophysica Acta - Reviews on Cancer, 1865(1), 72–82.

Oppermans, N., Kueberuwa, G., Hawkins, R. E., & Bridgeman, J. S. (2020). Transgenic T-cell receptor immunotherapy for cancer: building on clinical success. Therapeutic Advances in Vaccines and Immunotherapy, 8, 251513552093350.

Pagès, F., Galon, J., Dieu-Nosjean, M. C., Tartour, E., Sautès-Fridman, C., & Fridman, W. H. (2010, February). Immune infiltration in human tumors: A prognostic factor that should not be ignored. Oncogene. Nature Publishing Group.

Papiernik, M., de Moraes, M. L., Pontoux, C., Vasseur, F., & Pénit, C. (1998). Regulatory CD4 T cells: expression of IL-2R alpha chain, resistance to clonal deletion and IL-2 dependency. | International Immunology | Oxford Academic. International Immunology, 10(4), 371–378.

Pardoll, D. M. (2012, April). The blockade of immune checkpoints in cancer immunotherapy. Nature Reviews Cancer, 12(4), 252-264.

Parkhurst, M. R., Salgaller, M. L., Southwood, S., Robbins, P. F., Sette, A., Rosenberg, S. A., & Kawakami, Y. (1996). Improved induction of melanoma-reactive CTL with peptides from the melanoma antigen gp100 modified at HLA-A*0201-binding residues. The Journal of Immunology, 157(6), 2539-2548.

Parkhurst, M., Gros, A., Pasetto, A., Prickett, T., Crystal, J. S., Robbins, P., & Rosenberg, S. A. (2017). Isolation of T-cell receptors specifically reactive with mutated tumor-associated antigens from tumor-infiltrating lymphocytes based on CD137 expression. Clinical Cancer Research, 23(10), 2491–2505.

Pasetto, A., Gros, A., Robbins, P. F., Deniger, D. C., Prickett, T. D., Matus-Nicodemos, R., Douek, D. C., Howie, B., Robins, H., Parkhurst, M. R., Gartner, J., Trebska-McGowan, K., Crystal, J. S., & Rosenberg, S. A. (2016). Tumor- and neoantigen-reactive T-cell

receptors can be identified based on their frequency in fresh tumor. Cancer Immunology Research, 4(9), 734–743.

Peng, Y., Laouar, Y., Li, M. O., Green, E. A., & Flavell, R. A. (2004). TGF-β regulates in vivo expansion of Foxp3-expressing CD4 +CD25+ regulatory T cells responsible for protection against diabetes. Proceedings of the National Academy of Sciences of the United States of America, 101(13), 4572–4577.

Peskin, A. V., & Winterbourn, C. C. (2000). A microtiter plate assay for superoxide dismutase using a water-soluble tetrazolium salt (WST-1). Clinica Chimica Acta, 293(1–2), 157–166.

Pickup, M. W., Mouw, J. K., & Weaver, V. M. (2014). The extracellular matrix modulates the hallmarks of cancer. EMBO Reports, 15(12), 1243–1253.

Pilch, H., Höhn, H., Freitag, K., Neukirch, C., Necker, A., Haddad, P., Tanner, B., Knapstein, P. G., & Maeurer, M. J. (2002). Improved assessment of T-cell receptor (TCR) VB repertoire in clinical specimens: Combination of TCR-CDR3 spectratyping with flow cytometry-based TCR VB frequency analysis. Clinical and Diagnostic Laboratory Immunology, 9(2), 257–266.

Pitcovski, J., Shahar, E., Aizenshtein, E., & Gorodetsky, R. (2017). Melanoma antigens and related immunological markers. Critical Reviews in Oncology/Hematology, 115, 36-49.

Poschke, I. C., Hassel, J. C., Rodriguez Ehrenfried, A., Lindner, K. A. M., Heras-Murillo, I., Appel, L. M., Lehmann, J., Lövgren, T., Wickström, S. L., Lauenstein, C., Roth, J., König, A-K., Haanen, J. B. A. G., van den Berg, J., Kiessling, R., Bergmann, F., Flossdorf, M., Strobel, O., & Offringa, R. (2020). The outcome of ex vivo TIL expansion is highly influenced by spatial heterogeneity of the tumor T-cell repertoire and differences in intrinsic in vitro growth capacity between T-cell clones. Clinical Cancer Research, 26(16), 4289–4301.

Postow, M. A., Chesney, J., Pavlick, A. C., Robert, C., Grossmann, K., McDermott, D., Linette, G. P., Meyer, N., Giguere, J. K., Agarwala, S. S., Shaheen, M., Ernstoff, M. S., Minor, D., Salama, A. K., Taylor, M., Ott, P. A., Rollin, L. M., Horak, C., & Hodi, F. S.

(2015). Nivolumab and Ipilimumab versus Ipilimumab in Untreated Melanoma. New England Journal of Medicine, 372(21), 2006–2017.

Powell, D. J., Dudley, M. E., Robbins, P. F., & Rosenberg, S. A. (2005). Transition of late-stage effector T cells to CD27+ CD28 + tumor-reactive effector memory T cells in humans after adoptive cell transfer therapy. Blood, 105(1), 241–250.

Prieto, P. A., Durflinger, K. H., Wunderlich, J. R., Rosenberg, S. A., & Dudley, M. E. (2010). Enrichment of CD8+ Cells from Melanoma Tumor-infiltrating Lymphocyte Cultures Reveals Tumor Reactivity for Use in Adoptive Cell Therapy. Journal of Immunotherapy, 33(5), 547–556.

Qin, Y., Petaccia de Macedo, M., Reuben, A., Forget, M. A., Haymaker, C., Bernatchez, C., Spencer, C. N., Gopalakrishnan, V., Reddy, S., Cooper, Z. A., Fulbright, O. J., Ramachandran, R., Wahl, A., Flores, E., Thorsen, S. T., Tavera, R. J., Conrad, C., Williams, M. D., Tetzlaff, M. T., Wang, W. L., Gombos, D. S., Esmaeli, B., Amaria, R. N., Hwu, P., Wargo, J. A., Lazar, A. J. & Patel, S. P. (2017). Parallel profiling of immune infiltrate subsets in uveal melanoma versus cutaneous melanoma unveils similarities and differences: A pilot study. OncoImmunology, 6(6).

Radvanyi, L. G. (2015). Tumor-Infiltrating Lymphocyte Therapy. The Cancer Journal, 21(6), 450–464.

Radvanyi, L. G., Bernatchez, C., Zhang, M., Fox, P. S., Miller, P., Chacon, J., Wu, R., Lizee, G., Mahoney, S., Alvarado, G., Glass, M., Johnson, V. E., McMannis, J. D., Shpall, E., Prieto, V., Papadopoulos, N., Kim, K., Homsi, J., Bedikian, A., Hwu, W. J., Patel, S., Ross, M. I., Lee, J. E., Gershenwald, J. E., Lucci, A., Royal, R., Cormier, J. N., Davies, M. A., Mansaray, R., Fulbright, O. J., Toth, C., Ramachandran, R., Wardell, S., Gonzalez, A., & Hwu, P. (2012). Specific lymphocyte subsets predict response to adoptive cell therapy using expanded autologous tumor-infiltrating lymphocytes in metastatic melanoma patients. Clinical Cancer Research, 18(24), 6758–6770.

Rapoport, A. P., Stadtmauer, E. A., Binder-Scholl, G. K., Goloubeva, O., Vogl, D. T., Lacey, S. F., Badros, A. Z., Garfall, A., Weiss, B., Finklestein, J., Kulikovskaya, I., Sinha, S. K., Kronsberg, S., Gupta, M., Bond, S., Melchiori, L., Brewer, J. E., Bennett, A. D., Gerry, A. B., Pumphrey, N. J., Williams, D., Tayton-Martin, H. K., Ribeiro, L., Holdich, T., Yanovich, S., Hardy, N., Yared, J., Kerr, N., Philip, S., Westphal, S., Siegel, D. L., Levine,

B. L., Jakobsen, B. K., Kalos, M., & June, C. H. (2015). NY-ESO-1-specific TCR-engineered T cells mediate sustained antigen-specific antitumor effects in myeloma. Nature Medicine, 21(8), 914–921.

Ratto, G. B., Zino, P., Mirabelli, S., Minuti, P., Aquilina, R., Fantino, G., Spessa, E., Ponte, M., Bruzzi, P., & Melioli, G. (1996). A randomized trial of adoptive immunotherapy with tumor-infiltrating lymphocytes and interleukin-2 versus standard therapy in the postoperative treatment of resected nonsmall cell lung cancer. Cancer, 78(2), 244–251.

Rempala, G. A., & Seweryn, M. (2013). Methods for diversity and overlap analysis in T-cell receptor populations. Journal of Mathematical Biology, 67(6–7), 1339–1368.

Ribas, A., Wolchok, J. D., Robert, C., Kefford, R., Hamid, O., Daud, A., Hwu, W-J., Weber, J. S., Joshua, A. M., Gangadhar, T. C., Patnaik, A., Hersey, P., Dronca, R., Zarour, H., Gergich, K., Lindia, J. A., Giannotti, M., Li, X. N., Ebbinghaus, S., Kang, S. P. & Hodi, F. S. (2015). P0116 Updated clinical efficacy of the anti-PD-1 monoclonal antibody pembrolizumab (MK-3475) in 411 patients with melanoma. European Journal of Cancer, 51, e24.

Riker, A. I., Kammula, U. S., Panelli, M. C., Wang, E., Ohnmacht, G. A., Steinberg, S. M., Rosenberg, S. A., & Marincola, F. M. (2000). Threshold levels of gene expression of the melanoma antigen gp100 correlate with tumor cell recognition by cytotoxic T lymphocytes. International Journal of Cancer, 86(6), 818–826.

Robbins, P. F., Kassim, S. H., Tran, T. L. N., Crystal, J. S., Morgan, R. A., Feldman, S. A., Yang, J. C., Dudley, M. E., Wunderlich, J. R., Sherry, R. M., Kammula, U. S., Hughes, M. S., Restifo, N. P., Raffeld, M., Lee, C. C. R., Li, Y. F., El-Gamil, M., & Rosenberg, S. A. (2015). A pilot trial using lymphocytes genetically engineered with an NY-ESO-1-reactive T-cell receptor: Long-term follow-up and correlates with response. Clinical Cancer Research, 21(5), 1019–1027.

Robbins, P. F., Lu, Y. C., El-Gamil, M., Li, Y. F., Gross, C., Gartner, J., Lin, J. C., Teer, J. K., Cliften, P., Tycksen, E., Samuels, Y., & Rosenberg, S. A. (2013). Mining exomic sequencing data to identify mutated antigens recognized by adoptively transferred tumor-reactive T cells. Nature Medicine, 19(6), 747–752.

Robbins, P. F., Morgan, R. A., Feldman, S. A., Yang, J. C., Sherry, R. M., Dudley, M. E., Wunderlich, J. R., Nahvi, A. V., Helman, L. J., Mackall, C. L., Kammula, U. S., Hughes, M. S., Restifo, N. P., Raffeld, M., Lee, C. C. R., Levy, C. L., Li, Y. F., El-Gamil, M., Schwarz, S. L., Laurencot, C., & Rosenberg, S. A. (2011). Tumor regression in patients with metastatic synovial cell sarcoma and melanoma using genetically engineered lymphocytes reactive with NY-ESO-1. Journal of Clinical Oncology, 29(7), 917–924.

Robert, C., Long, G. V., Brady, B., Dutriaux, C., Maio, M., Mortier, L., Hassel, J. C., Rutkowski, P., McNeil, C., Kalinka-Warzocha, E., Savage, K. J., Hernberg, M. M., Lebbé, C., Charles, J., Mihalcioiu, C., Chiarion-Sileni, V., Mauch, C., Cognetti, F., Arance, A., Schmidt, H., Schadendorf, D., Gogas, H., Lundgren-Eriksson, L., Horak, C., Sharkey, B., Waxman, I. M., Atkinson, V., & Ascierto, P. A. (2015a). Nivolumab in Previously Untreated Melanoma without BRAF Mutation. New England Journal of Medicine, 372(4), 320–330.

Robert, C., Schachter, J., Long, G. V., Arance, A., Grob, J. J., Mortier, L., Daud, A., Carlino, M. S., McNeil, C., Lotem, M., Larkin, J., Lorigan, P., Neyns, B., Blank, C. U., Hamid, O., Mateus, C., Shapira-Frommer, R., Kosh, M., Zhou, H., Ibrahim, N., Ebbinghaus, S., & Ribas, A. (2015b). Pembrolizumab versus Ipilimumab in Advanced Melanoma. New England Journal of Medicine, 372(26), 2521–2532.

Rosenberg, S. A., Packard, B. S., Aebersold, P. M., Solomon, D., Topalian, S. L., Toy, S. T., Simon, P., Lotze, M. T., Yang, J. C., Seipp, C. A., Simpson, C., Carter, C., Bock, S., Schwartzentruber, D., Wei, J. P., & White, D. E. (1988). Use of Tumor-Infiltrating Lymphocytes and Interleukin-2 in the Immunotherapy of Patients with Metastatic Melanoma. New England Journal of Medicine, 319(25), 1676–1680.

Rosenberg, S. A., Spiess, P., & Lafreniere, R. (1986). A new approach to the adoptive immunotherapy of cancer with tumor-infiltrating lymphocytes. Science, 233(4770), 1318–1321.

Rosenberg, S. A., Yang, J. C., Sherry, R. M., Kammula, U. S., Hughes, M. S., Phan, G. Q., Citrin, D. E., Restifo, N. P., Robbins, P. F., Wunderlich, J. R., Morton, K. E., Laurencot, C. M., Steinberg, S. M., White, D. E. & Dudley, M. E. (2011). Durable complete responses in heavily pretreated patients with metastatic melanoma using T-cell transfer immunotherapy. Clinical Cancer Research, 17(13), 4550–4557.

Rosenberg, S. A., Yannelli, J. R., Yang, J. C., Topalian, S. L., Schwartzentruber, D. J., Weber, J. S., Parkinson, D. R., Seipp, C. A., Einhorn, J. H., & White, D. E. (1994). Treatment of Patients with Metastatic Melanoma with Autologous Tumor-Infiltrating Lymphocytes and Interleukin 2 | JNCI: Journal of the National Cancer Institute | Oxford Academic. JNCI: Journal of the National Cancer Institute, 86(15), 1159–1166.

Rudolph, M. G., Stanfield, R. L., & Wilson, I. A. (2006). How TCRs Bind MHCs, Peptides and Co-Receptors. Annual Review of Immunology, 24(1), 419–466.

Rudqvist, N. P., Pilones, K. A., Lhuillier, C., Wennerberg, E., Sidhom, J. W., Emerson, R. O., Robins, H. S., Schneck, J., & Demaria, S. (2018). Radiotherapy and CTLA-4 blockade shape the TCR repertoire of tumor-infiltrating t cells. Cancer Immunology Research, 6(2), 139–150.

Ruggiero, E., Nicolay, J. P., Fronza, R., Arens, A., Paruzynski, A., Nowrouzi, A., Ürenden, G., Lulay, C., Schneider, S., Goerdt, S., Glimm, H., Krammer, P. H., Schmidt, M., & Von Kalle, C. (2015). High-resolution analysis of the human T-cell receptor repertoire. Nature Communications, 6(1), 1–7.

Sadeghi, A., Pauler, L., Annerén, C., Friberg, A., Brandhorst, D., Korsgren, O., & Tötterman, T. H. (2011). Large-scale bioreactor expansion of tumor-infiltrating lymphocytes. Journal of Immunological Methods, 364(1–2), 94–100.

Salgaller, M., Afshar, A., Marincola, F., Rivoltini, L., Kawakami, Y., & Rosenberg, S. (1995). Recognition of multiple epitopes in the human melanoma antigen gp100 by peripheral blood lymphocytes stimulated in vitro with synthetic peptides - PubMed. Cancer Research, 55(21), 4972–4979.

Salgaller, M. L., Marincola, F. M., Cormier, J. N., & Rosenberg, S. A. (1996). Immunization against Epitopes in the Human Melanoma Antigen gp100 following Patient Immunization with Synthetic Peptides. Cancer Research, 56(20, 4749-4757.

Sanchez-Paulete, A. R., Labiano, S., Rodriguez-Ruiz, M. E., Azpilikueta, A., Etxeberria, I., Bolaños, E., Lang, V., Rodriguez, M., Aznar, M. A., Jure-Kunkel, M., & Melero, I. (2016). Deciphering CD137 (4-1BB) signaling in T-cell costimulation for translation into successful cancer immunotherapy. European Journal of Immunology, 46(3), 513–522.

Schwartzentruber, D. J., Lawson, D., Richards, J., Conry, R. M., Miller, D., Triesman, J., Gailani, F., Riley, L. B., Vena, D., & Hwu, P. (2009). A phase III multi-institutional randomized study of immunization with the gp100: 209–217(210M) peptide followed by high-dose IL-2 compared with high-dose IL-2 alone in patients with metastatic melanoma. Journal of Clinical Oncology, 27(18_suppl), CRA9011–CRA9011.

Sebastian, M., Schröder, A., Scheel, B., Hong, H. S., Muth, A., Von Boehmer, L., Zippelius, A., Mayer, F., Reck, M., Atanackovic, D., Thomas, M., Schneller, F., Stöhlmacher, J., Bernhard, H., Gröschel, A., Lander, T., Probst, J., Strack, T., Wiegand, V., Gnad-Vogt, U., Kallen, K-J., Hoerr, I., Von Der Muelbe, F., Fotin-Mleczek, M., Knuth, A. and Koch, S. D. (2019). A phase I/IIa study of the mRNA-based cancer immunotherapy CV9201 in patients with stage IIIB/IV non-small cell lung cancer, 68, 799–812.

Seiter, S., Monsurro, V., Nielsen, M.-B., Wang, E., Provenzano, M., Wunderlich, J. R., Rosenberg, S. A., & Marincola, F. M. (2002). Frequency of MART-1/MelanA and gp100/PMel17-Specific T Cells in Tumor Metastases and Cultured Tumor-Infiltrating Lymphocytes. Journal of Immunotherapy, 25(3), 252.

Seliktar-Ofir, S., Merhavi-Shoham, E., Itzhaki, O., Yunger, S., Markel, G., Schachter, J., & Besser, M. J. (2017). Selection of Shared and Neoantigen-Reactive T Cells for Adoptive Cell Therapy Based on CD137 Separation. Frontiers in Immunology, 8(OCT), 1211.

Seyfried, T. N., & Huysentruyt, L. C. (2013). On the origin of cancer metastasis. Critical Reviews in Oncogenesis, 18(1–2), 43–73.

Shang, B., Liu, Y., Jiang, S. J., & Liu, Y. (2015). Prognostic value of tumor-infiltrating FoxP3+ regulatory T cells in cancers: A systematic review and meta-analysis. Scientific Reports, 5(1), 1–9.

Shao, H., Ou, Y., Wang, T., Shen, H., Wu, F., Zhang, W., Tao, C., Yuan, Y., Bo, H., Wang, H., & Huang, S. (2014). Differences in TCR-Vβ repertoire and effector phenotype between tumor infiltrating lymphocytes and peripheral blood lymphocytes increase with age. PLoS ONE, 9(7).

Shen, X., Zhou, J., Hathcock, K. S., Robbins, P., Powell, D. J., Rosenberg, S. A., & Hodes, R. J. (2007). Persistence of tumor infiltrating lymphocytes in adoptive immunotherapy correlates with telomere length. Journal of Immunotherapy, 30(1), 123–129.

Sherwood, A. M., Emerson, R. O., Scherer, D., Habermann, N., Buck, K., Staffa, J., Desmarais, C., Halama, N., Jaeger, D., Schirmacher, P., Herpel, E., Kloor, M., Ulrich, A., Schneider, M., Ulrich, C. M., & Robins, H. (2013). Tumor-infiltrating lymphocytes in colorectal tumors display a diversity of T cell receptor sequences that differ from the T cells in adjacent mucosal tissue. Cancer Immunology, Immunotherapy, 62(9), 1453–1461.

Simoni, Y., Becht, E., Fehlings, M., Loh, C. Y., Koo, S. L., Teng, K. W. W., Yeong, J. P. S., Nahar, R., Zhang, T., Kared, H., Duan, K., Ang, N., Poidinger, M., Lee, Y. Y., Larbi, A., Khng, A. J., Tan, E., Fu, C., Mathew, R., Teo, M., Lim, W. T., Toh, C. K., Ong, B. H., Koh, T., Hillmer, A. M., Takano, A., Lim, T. K. H., Tan, E. H., Zhai, W., Tan, D. S. W., Tan, I. B., & Newell, E. W. (2018). Bystander CD8+ T cells are abundant and phenotypically distinct in human tumour infiltrates. Nature, 557(7706), 575–579.

Smith, F. O., Downey, S. G., Klapper, J. A., C.Yang, J., Sherry, R. M., Royal, R. E., Kammula, U. S., Hughes, M. S., Restifo, N. P., Levy, C. L., White, D. E., Steinberg, S. M., & Rosenberg, S. A. (2008). Treatment of metastatic melanoma using Interleukin-2 alone or in conjunction with vaccines. Clinical Cancer Research, 14(17), 5610–5618.

Smith, P. J., Marquez, N., Wiltshire, M., Chappell, S., Njoh, K., Campbell, L., Khan, I. A., Silvestre, O., & Errington, R. J. (2007). Mitotic bypass via an occult cell cycle phase following DNA topoisomerase II inhibition in p53 functional human tumor cells. Cell Cycle, 6(16), 2071–2081.

Sobin, L. H., Gospodarowicz, M. K., & Wittekind, C. (2017). TNM Classification of Malignant Tumours. (J. D. Brierley, M. K. Gospodarowicz, B. O'Sullivan, & C. Wittekind, Eds.) (8th ed.). Retrieved from https://books.google.co.uk/books?hl=en&lr=&id=642GDQAAQBAJ&oi=fnd&pg=PP12&dq=TNM+classification&ots=dzRYVLLIli&sig=kRImiAtskccVN8s4MfOJ3IcnbDs#v=onepage&q=TNM classification&f=false

Sommermeyer, D., Neudorfer, J., Weinhold, M., Leisegang, M., Engels, B., Noessner, E., Heemskerk, M. H. M., Charo, J., Schendel, D. J., Blankenstein, T., Bernhard, H., &

Uckert, W. (2006). Designer T cells by T cell receptor replacement. European Journal of Immunology, 36(11), 3052–3059.

Sommermeyer, D., & Uckert, W. (2010). Minimal Amino Acid Exchange in Human TCR Constant Regions Fosters Improved Function of TCR Gene-Modified T Cells. The Journal of Immunology, 184(11), 6223–6231.

Song, D. G., Ye, Q., Carpenito, C., Poussin, M., Wang, L. P., Ji, C., Figini, M., June, C. H., Coukos, G., & Powell, D. J. (2011). In vivo persistence, tumor localization, and antitumor activity of CAR-engineered T cells is enhanced by costimulatory signaling through CD137 (4-1BB). Cancer Research, 71(13), 4617–4627.

Song, H., Wu, Y., Ren, G., Guo, W., & Wang, L. (2015). Prognostic factors of oral mucosal melanoma: histopathological analysis in a retrospective cohort of 82 cases. Histopathology, 67(4), 548–556.

Spindler, M. J., Nelson, A. L., Wagner, E. K., Oppermans, N., Bridgeman, J. S., Heather, J. M., Adler, A. S., Asensio, M. A., Edgar, R. C., Lim, Y. W., Meyer, E. H., Hawkins, R. E., Cobbold, M., & Johnson, D. S. (2020). Massively parallel interrogation and mining of natively paired human TCRαβ repertoires. Nature Biotechnology, 38(5), 609–619.

Spranger, S., Spaapen, R. M., Zha, Y., Williams, J., Meng, Y., Ha, T. T., & Gajewski, T. F. (2013). Up-regulation of PD-L1, IDO, and Tregs in the melanoma tumor microenvironment is driven by CD8+ T cells. Science Translational Medicine, 5(200), 200ra116.

Srivastava, S., & Riddell, S. R. (2015). Engineering CAR-T cells: Design concepts. Trends in Immunology, 36(8), 494-502.

Steinbrink, K., Jonuleit, H., Müller, G., Schuler, G., Knop, J., & Enk, A. H. (1999). Interleukin-10-treated human dendritic cells induce a melanoma-antigen- specific anergy in CD8+ T cells resulting in a failure to lyse tumor cells. Blood, 93(5), 1634–1642.

Stone, J. D., Harris, D. T., & Kranz, D. M. (2015). TCR affinity for p/MHC formed by tumor antigens that are self-proteins: Impact on efficacy and toxicity. Current Opinion in Immunology, 33, 16-22.

Sudo, T., Nishida, R., Kawahara, A., Saisho, K., Mimori, K., Yamada, A., Mizoguchi, A., Kadoya, K., Matono, S., Mori, N., Tanaka, T., & Akagi, Y. (2017). Clinical Impact of Tumor-Infiltrating Lymphocytes in Esophageal Squamous Cell Carcinoma. Annals of Surgical Oncology, 24(12), 3763–3770.

Tan, M. P., Gerry, A. B., Brewer, J. E., Melchiori, L., Bridgeman, J. S., Bennett, A. D., Pumphrey, N. J., Jakobsen, B. K., Price, D. A., Ladell, K., & Sewell, A. K. (2015). T cell receptor binding affinity governs the functional profile of cancer-specific CD8+ T cells. Clinical and Experimental Immunology, 180(2), 255–270.

Tan, Q., Zhang, C., Yang, W., Liu, Y., Heyilimu, P., Feng, D., Xing, L., Ke, Y., & Lu, Z. (2019). Isolation of T cell receptor specifically reactive with autologous tumour cells from tumour-infiltrating lymphocytes and construction of T cell receptor engineered T cells for esophageal squamous cell carcinoma. Journal for ImmunoTherapy of Cancer, 7(1), 232.

Tang, H., Wang, Y., Chlewicki, L. K., Zhang, Y., Guo, J., Liang, W., Wang, J., Wang, X., & Fu, Y. X. (2016). Facilitating T Cell Infiltration in Tumor Microenvironment Overcomes Resistance to PD-L1 Blockade. Cancer Cell, 29(3), 285–296.

Tavera, R. J., Forget, M. A., Kim, Y. U., Sakellariou-Thompson, D., Creasy, C. A., Bhatta, A., Fulbright, O. J., Ramachandran, R., Thorsen, S. T., Flores, E., Wahl, A., Gonzalez, A. M., Toth, C., Wardell, S., Mansaray, R., Radvanyi, L. G., Gombos, D. S., Patel, S. P., Hwu, P., Amaria, R. N., Bernatchez, C., & Haymaker, C. (2018). Utilizing T-cell Activation Signals 1, 2, and 3 for Tumor-infiltrating Lymphocytes (TIL) Expansion: The Advantage over the Sole Use of Interleukin-2 in Cutaneous and Uveal Melanoma. Journal of Immunotherapy, 41(9), 399–405.

Teulings, H. E., Limpens, J., Jansen, S. N., Zwinderman, A. H., Reitsma, J. B., Spuls, P. I., & Luiten, R. M. (2015). Vitiligo-like depigmentation in patients with stage III-IV melanoma receiving immunotherapy and its association with survival: A systematic review and meta-analysis. Journal of Clinical Oncology, 33(7), 773–781.

Theaker, S. M., Rius, C., Greenshields-Watson, A., Lloyd, A., Trimby, A., Fuller, A., Miles, J. J., Cole, D. K., Peakman, M., Sewell, A. K., & Dolton, G. (2016). T-cell libraries allow simple parallel generation of multiple peptide-specific human T-cell clones. Journal of Immunological Methods, 430, 43–50.

Thomas, R., Al-Khadairi, G., Roelands, J., Hendrickx, W., Dermime, S., Bedognetti, D., & Decock, J. (2018). NY-ESO-1 based immunotherapy of cancer: Current perspectives. Frontiers in Immunology, 9

Topalian, S. L., Sznol, M., McDermott, D. F., Kluger, H. M., Carvajal, R. D., Sharfman, W. H., Brahmer, J. R., Lawrence, D. P., Atkins, M. B., Powderly, J. D., Leming, P. D., Lipson, E. J., Puzanov, I., Smith, D. C., Taube, J. M., Wigginton, J. M., Kollia, G. D., Gupta, A., Pardoll, D. M., Sosman, J. A., & Hodi, F. S. (2014). Survival, durable tumor remission, and long-term safety in patients with advanced melanoma receiving nivolumab. Journal of Clinical Oncology, 32(10), 1020–1030.

Tran, K. Q., Zhou, J., Durflinger, K. H., Langhan, M. M., Shelton, T. E., Wunderlich, J. R., Robbins, P. F., Rosenberg, S. A., & Dudley, M. E. (2008). Minimally cultured tumor-infiltrating lymphocytes display optimal characteristics for adoptive cell therapy. Journal of Immunotherapy, 31(8), 742–751.

Tsao, A. S., Wistuba, I., Roth, J. A., & Kindler, H. L. (2009). Malignant pleural mesothelioma. Journal of Clinical Oncology, 27(12), 2081-2090.

Turchaninova, M. A., Britanova, O. V., Bolotin, D. A., Shugay, M., Putintseva, E. V., Staroverov, D. B., Sharonov, G., Shcherbo, D., Zvyagin, I. V., Mamedov, I. Z., Linnemann, C., Schumacher, T. N., & Chudakov, D. M. (2013). Pairing of T-cell receptor chains via emulsion PCR. European Journal of Immunology, 43(9), 2507–2515.

Turtle, C., Hanafi, L., Berger, C., Gooley, T., Chaney, C., Cherian, S., Soma, L., Chen, X., Yeung, C. S., Loeb, K., Wood, B. L., Hudecek, M., Sommermeyer, D., Li, D., Hay, K. A., Heimfeld, S., Riddell, S. R., & Maloney, D. (2016). Rate of durable complete response in ALL, NHL, and CLL after immunotherapy with optimized lymphodepletion and defined composition CD19 CAR-T cells. Journal of Clinical Oncology, 34(15), 102.

Tzifi, F., Kanariou, M., Tzanoudaki, M., Mihas, C., Paschali, E., Chrousos, G., & Kanaka-Gantenbein, C. (2013). Flow cytometric analysis of the CD4+ TCR Vβ repertoire in the peripheral blood of children with type 1 diabetes mellitus, systemic lupus erythematosus and age-matched healthy controls. BMC Immunology, 14(1), 1–12.

Ueda, T., Oji, Y., Naka, N., Nakano, Y., Takahashi, E., Koga, S., Asada, M., Ikeba, A., Nakatsuka, S-I., Abeno, S., Hosen, N., Tomita, Y., Aozasa, K., Tamai, N., Myoui, A.,

Yoshikawa, H., & Sugiyama, H. (2003). Overexpression of the Wilms' tumor gene WT1 in human bone and soft-tissue sarcomas. Cancer Science, 94(3), 271–276.

Valmori, D., Fonteneau, J.-F., Lizana, C. M., Gervois, N., Liénard, D., Rimoldi, D., Jongeneel, R., Jotereau, F., Cerottini, J-C., & Romero, P. (1998). Immunodominant Peptide Analogues CTL In Vitro by Selected Melan-A/MART-1 Enhanced Generation of Specific Tumor-Reactive. J Immunol References, 160, 1750-1758.

Van den Beemd, R., Boor, P. P. C., van Lochem, E. G., Hop, W. C. J., Langerak, A. W., Wolvers-Tettero, I. L. M., Hooijkaas, H., & van Dongen, J. J. M. (2000). Flow cytometric analysis of the Vβ repertoire in healthy controls. Cytometry, 40(4), 336–345.

Van Raamsdonk, C. D., Bezrookove, V., Green, G., Bauer, J., Gaugler, L., O'Brien, J. M., Simpson, E. M., Barsh, G. S., & Bastian, B. C. (2009). Frequent somatic mutations of GNAQ in uveal melanoma and blue naevi. Nature, 457(7229), 599–602.

Van Raamsdonk, C. D., Griewank, K. G., Crosby, M. B., Garrido, M. C., Vemula, S., Wiesner, T., Obenauf, A. C., Wackernagel, W., Green, G., Bouvier, N., Sozen, M. M., Baimukanova, G., Roy, R., Heguy, A., Dolgalev, I., Khanin, R., Busam, K., Speicher, M. R., O'Brien, J., & Bastian, B. C. (2010). Mutations in GNA11 in uveal melanoma. New England Journal of Medicine, 363(23), 2191–2199.

Vinay, D. S., & Kwon, B. S. (1998). Role of 4-1BB in immune responses. Seminars in Immunology, 10(6), 481–489.

Wang, X., Lang, M., Zhao, T., Feng, X., Zheng, C., Huang, C., Hao, J., Dong, J., Luo, L., Li, X., Lan, C., Yu, W., Yu, M., Yang, S., & Ren, H. (2017). Cancer-FOXP3 directly activated CCL5 to recruit FOXP3 + Treg cells in pancreatic ductal adenocarcinoma. Oncogene, 36(21), 3048–3058.

Wang, Z., & Cao, Y. J. (2020). Adoptive Cell Therapy Targeting Neoantigens: A Frontier for Cancer Research. Frontiers in Immunology, 11, 176.

Ward-Hartstonge, K. A., & Kemp, R. A. (2017). Regulatory T-cell heterogeneity and the cancer immune response. Clinical & Translational Immunology, 6(9), e154.

Weide, B., Pascolo, S., Scheel, B., Derhovanessian, E., Pflugfelder, A., Eigentler, T. K., Pawelec, G., Hoerr, I., Rammensee, H-G., & Garbe, C. (2009). Direct Injection of

Protamine-protected mRNA: Results of a Phase 1/2 Vaccination Trial in Metastatic Melanoma Patients. Journal of Immunotherapy, 32(5), 498–507.

Weiss, A., & Stobo, J. D. (1984). Requirement for the coexpression of T3 and the T cell antigen receptor on a malignant human T cell line. Journal of Experimental Medicine, 160(5), 1284–1299.

Wickström, S. L., Lövgren, T., Volkmar, M., Reinhold, B., Duke-Cohan, J. S., Hartmann, L., Rebmann, J., Mueller, A., Melief, J., Maas, R., Ligtenberg, M., Hansson, J., Offringa, R., Seliger, B., Poschke, I., Reinherz, E. L., & Kiessling, R. (2019). Cancer Neoepitopes for Immunotherapy: Discordance Between Tumor-Infiltrating T Cell Reactivity and Tumor MHC Peptidome Display. Frontiers in Immunology, 10, 2766.

Wolf, B. J., Choi, J. E., & Exley, M. A. (2018). Novel approaches to exploiting invariant NKT cells in cancer immunotherapy. Frontiers in Immunology, 9, 384.

Wolfl, M., Kuball, J., Ho, W. Y., Nguyen, H., Manley, T. J., Bleakley, M., & Greenberg, P. D. (2007). Activation-induced expression of CD137 permits detection, isolation, and expansion of the full repertoire of CD8+ T cells responding to antigen without requiring knowledge of epitope specificities. Blood, 110(1), 201–210.

Wooldridge, L., Ekeruche-Makinde, J., Van Den Berg, H. A., Skowera, A., Miles, J. J., Tan, M. P., Dolton, G., Clement, M., Llewellyn-Lacey, S., Price, D. A., Peakman, M., & Sewell, A. K. (2012). A single autoimmune T cell receptor recognizes more than a million different peptides. Journal of Biological Chemistry, 287(2), 1168–1177.

Wucherpfennig, K. W., Gagnon, E., Call, M. J., Huseby, E. S., & Call, M. E. (2010). Structural biology of the T-cell receptor: insights into receptor assembly, ligand recognition, and initiation of signaling. Cold Spring Harbor Perspectives in Biology, 2(4), a005140.

Xia, Y., Tian, X., Wang, J., Qiao, D., Liu, X., Xiao, L., Liang, W., Ban, D., Chu, J., Yu, J., Wang, R., Tian, G., & Wang, M. (2018). Treatment of metastatic non-small cell lung cancer with NY-ESO-1 specific TCR engineered-T cells in a phase I clinical trial: A case report. Oncology Letters, 16(6), 6998–7007.

Yasumoto, K. I., Watabe, H., Valencia, J. C., Kushimoto, T., Kobayashi, T., Appella, E., & Hearing, V. J. (2004). Epitope mapping of the melanosomal matrix protein gp100

(PMEL17). Rapid processing in the endoplasmic reticulum and glycosylation in the early Golgi compartment. Journal of Biological Chemistry, 279(27), 28330–28338.

Yazici, Y., & Paget, S. A. (2000). Elderly-onset rheumatoid arthritis. Rheumatic Disease Clinics of North America, 26(3), 517–526.

Ye, Q., Loisiou, M., Levine, B. L., Suhoski, M. M., Riley, J. L., June, C. H., Coukos, G., & Powell, D. J. (2011). Engineered artificial antigen presenting cells facilitate direct and efficient expansion of tumor infiltrating lymphocytes. Journal of Translational Medicine, 9(1).

Ye, Q., Song, D.-G., Poussin, M., Yamamoto, T., Best, A., Li, C., Coukos, G., & Powell, D. J. (2014). CD137 Accurately Identifies and Enriches for Naturally Occurring Tumor-Reactive T Cells in Tumor. Clinical Cancer Research, 20(1), 44–55.

Zbytek, B., Carlson, J. A., Granese, J., Ross, J., Mihm, M., & Slominski, A. (2008). Current concepts of metastasis in melanoma. Expert Review of Dermatology, 3(5), 569-585.

Zeng, D. Q., Yu, Y. F., Ou, Q. Y., Li, X. Y., Zhong, R. Z., Xie, C. M., & Hu, Q. G. (2016). Prognostic and predictive value of tumor-infiltrating lymphocytes for clinical therapeutic research in patients with non-small cell lung cancer. Oncotarget, 7(12), 13765–13781.

Zhang, L., Davies, J. S., Serna, C., Yu, Z., Restifo, N. P., Rosenberg, S. A., Morgan, R. A., & Hinrichs, C. S. (2020). Enhanced efficacy and limited systemic cytokine exposure with membrane-anchored interleukin-12 T-cell therapy in murine tumor models. Journal for ImmunoTherapy of Cancer, 8(1).

Zhang, L., Morgan, R. A., Beane, J. D., Zheng, Z., Dudley, M. E., Kassim, S. H., Nahvi, A. V., Ngo, L. T., Sherry, R. M., Phan, G. Q., Hughes, M. S., Kammula, U. S., Feldman, S. A., Toomey, M. A., Kerkar, S. P., Restifo, N. P., Yang, J. C., & Rosenberg, S. A. (2015). Tumor-infiltrating lymphocytes genetically engineered with an inducible gene encoding interleukin-12 for the immunotherapy of metastatic melanoma. Clinical Cancer Research, 21(10), 2278–2288.

Zhu, C., Anderson, A. C., Schubart, A., Xiong, H., Imitola, J., Khoury, S. J., Zheng, X. X., Strom, T. B., & Kuchroo, V. K. (2005). The Tim-3 ligand galectin-9 negatively regulates T helper type 1 immunity. Nature Immunology, 6(12), 1245–1252.

Zhu, Y., Smith, D. J., Zhou, Y., Li, Y. R., Yu, J., Lee, D., Wang, Y. C., Di Biase, S., Wang, X., Hardoy, C., Ku, J., Tsao, T., Lin, L. J., Pham, A. T., Moon, H., McLaughlin, J., Cheng, D., Hollis, R. P., Campo-Fernandez, B., Urbinati, F., Wei, L., Pang, L., Rezek, V., Berent-Maoz, B., Macabali, M. H., Gjertson, D., Wang, X., Galic, Z., Kitchen, S. G., An, D. S., Hu-Lieskovan, S., Kaplan-Lefko, P. J., De Oliveira, S. N., Seet, C. S., Larson, S. M., Forman, S. J., Heath, J. R., Zack, J. A., Crooks, G. M., Radu, C. G., Ribas, A., Kohn, D. B., Witte, O. N., & Yang, L. (2019). Development of Hematopoietic Stem Cell-Engineered Invariant Natural Killer T Cell Therapy for Cancer. Cell Stem Cell, 25(4), 542-557.e9.

Zou, W. (2006). Regulatory T cells, tumour immunity and immunotherapy. Nature Reviews Immunology, 6(4), 295-307.